PNNL-11694
UC-350

Desiccant Dehumidification and Cooling Systems Assessment and Analysis

R. K. Collier, Jr.[a]

September 1997

Prepared for
the U.S. Department of Energy
under Contract DE-AC06-76RLO 1830

Pacific Northwest National Laboratory
Richland, Washington 99352

(a) Collier Engineering, Reno, Nevada.

DISCLAIMER

Collier Engineering
995 Mirror Lake Dr.
Reno, NV 89511

Desiccant Dehumidification And Cooling Systems:

Assessment And Analysis

Prepared by
R. K. Collier, Jr.
President

for

Battelle Pacific Northwest Laboratories
370 L'Enfant Promenade, S.W.
901 D St., S.W., Suite 900
Washington, DC 20024-2115

November 19, 1996

EXECUTIVE SUMMARY

The objective of this report is to provide a preliminary analysis of the principles, sensitivities, and potential for national energy savings of desiccant cooling and dehumidification systems. The report is divided into four sections. Section I deals with the maximum theoretical performance of ideal desiccant cooling systems. Section II looks at the performance effects of non-ideal behavior of system components. Section III examines the effects of outdoor air properties on desiccant cooling system performance. Section IV analyzes the applicability of desiccant cooling systems to reduce primary energy requirements for providing space conditioning in buildings.

A basic desiccation process performs no useful work (cooling). That is, a desiccant material drying air is close to an isenthalpic process. Latent energy is merely converted to sensible energy. Only when heat exchange is applied to the desiccated air is any cooling accomplished. This characteristic is generic to all desiccant cycles and critical to understanding their operation.

The analyses of Section I show that desiccant cooling cycles can theoretically achieve extremely high thermal CoP's (>2). The configurations investigated are as follows: ventilation cycle, modified ventilation cycle (vent-vent), recirculation cycle, Dunkle cycle, and liquid desiccant recirculation cycle. The ventilation cycle processes outdoor air that is then introduced to the building. Rejected indoor air is used for desiccant regeneration. The modified ventilation cycle also processes outdoor air to the building, but uses outdoor air for desiccant regeneration. This cycle is appropriate for applications where the building exhaust of room air is not centralized or is not located in a convenient location for co-processing of outside air. The recirculation cycle processes indoor air and returns it to the building and uses outdoor air for desiccant regeneration. The Dunkle cycle is similar to the recirculation cycle, except that an additional heat exchanger is added to create a cooler "sink" temperature than outdoor air can provide. The liquid desiccant system is similar in air flow and processing characteristics to the recirculation system described earlier.

The main difference between all of the previous cycles (solid desiccants) and the liquid desiccant cycle is that latent processes (water transport) with solid desiccant cycles are adiabatic while the liquid desiccant cycle is near-isothermal. The major ramification of this difference is that isothermal systems produce drier air for a given regeneration temperature, while adiabatic systems allow preheat of regeneration air from the desiccant sorption energy. This preheating capability generally allows solid desiccant systems to reach higher thermal efficiencies liquid systems unless an advanced regeneration scheme (requiring less than the heat of sorption for water removal) is employed by the liquid system.

Very high CoP's are possible with all of the desiccant cycles examined when utilizing ideal components. The values of CoP ranged from a high of 2.6 to a low of 1.1. The main difference between the performance capabilities of the various cycles was the concept of vent credit. If the outdoor air that is conditioned and directed to the building space is required by the building, then cooling capacity can be calculated relative to outdoor air rather than indoor air as is normally the case. This situation results in the best performance for either of the ventilation cycles. If outdoor air is not required, cooling capacity must calculated relative to indoor air. Under this condition, the systems performed similarly at much lower values of CoP. The Dunkle cycle was devised for recirculation applications in very humid climates. For the simulated conditions, (ARI indoor and outdoor) the performance of this cycle does not justify the added complexity. The liquid desiccant

system with ideal components performed similarly to the solid desiccant systems (CoP = 1.2). However, the number of components required is larger and the degree of idealization is quite large compared to the other cycles examined.

Because desiccant systems are open-cycle (i.e., the working fluids are open to the atmosphere), their performance is strongly dependent upon the thermodynamic state of the air being processed. Analyses showed that the effects of ambient air temperature and humidity on desiccant system performance depends upon the cycle. For ventilation applications (outdoor air required by the building), desiccant system performance increases with increasing ambient air temperature and humidity. However, for the recirculation cycle, performance decreases. These results indicate that desiccant cycles are very appropriate for applications where conditioning outside air is required by the application. For desiccants, performance increases as outside air enthalpy increases. This is quite the antithesis to heat pumps, for example, whose performance decreases with increasing load.

The analyses of Section II examine the effects of non-ideal behavior in the sensible heat exchanger, evaporative cooler and desiccant wheel. The parameters examined include component effectiveness, desiccant matrix heat of sorption, heat capacity and isotherm shape. The results of these investigations reveal that all of the parameters investigated negatively affect the performance except for the desiccant heat of sorption. Evaporative cooler effectiveness has the least negative effect on performance (<5%). However, reducing heat exchanger effectiveness to values commonly encountered in practical hardware reduced efficiency up to 50%. The desiccant matrix effectiveness (also a function of isotherm shape) can have a similar effect; however, no numerical comparison to existing hardware was made. Another effect that was not quantified analytically was the desiccant matrix heat capacity. The analyses show that heat capacity within the desiccant matrix causes the dehumidification air stream to become hotter and more humid while increasing the requirements for regeneration air flow rates, both of these effects being detrimental to system performance.

The use of low regeneration temperatures, <65°C (150°F) is most often associated with sources of waste heat as the regeneration energy source. The main desiccant design ramification of waste heat sources, besides the low regeneration temperature, is that thermal CoP will not have the significance that it did when the regeneration energy had a per unit cost associated with it. Analyses performed showed that besides the obvious conclusion that the amount of moisture removal by the desiccant decreases proportionally with reductions in regeneration temperature, these analyses also showed that many other parameters that strongly influence dehumidification performance at higher regeneration temperatures, such as matrix effectiveness, heat capacity, etc., exhibit minor effects at low regeneration temperatures. The major conclusion from this work is that desiccant equipment sizes will increase significantly when low regeneration temperatures are used. To be viable, this equipment must be much lower in cost ($/cfm) than that used at higher regeneration temperatures.

Desiccants can also be used in devices that exchange the total enthalpy (temperature and water content) between two adjacent air streams. Analyses showed that the phenomenon that makes enthalpy exchange possible is the interaction between desiccant sorption and the heat capacity of the desiccant matrix. Latent and sensible effectiveness of enthalpy exchange devices can be different, but with proper consideration of desiccant uptake, matrix heat capacity, and rotational speed, the overall effectiveness can approach 80% with no differences between the latent and sensible components.

The general conclusion from Section II is that ventilation air processing is the most viable

application for the solid desiccant equipment analyzed. The attractively high performance of desiccant cycles with ideal components soon dwindled when simulated with more practical component performance. Even with the severe performance penalties associated with these components, the ventilation cycle with "vent credit" is still capable of thermal CoP's significantly greater than 1.0.

The seasonal simulations performed in Section III included five cities; Atlanta, GA, New York City, NY, Houston, TX, Chicago, IL, and Phoenix, AZ. The results from this section indicate that, generally , the seasonal performance of the desiccant system does not change significantly from that predicted for ARI outdoor conditions, except when variable regeneration temperature operation is used. Moreover, this advantage in system efficiency with variable regeneration temperature is reduced significantly as less than ideal component efficiencies are included. In addition, the latent cooling capacity of the desiccant system is significantly reduced with variable regeneration temperature. This effect would require building latent control to be performed by the building AC unit. The major exception to these general findings is the performance in Phoenix, AZ. Utilizing the variable regeneration temperature scheme, the hot, dry climate provides ample hours of operation with no desiccant regeneration required to meet the load. Cooling is provided by the evaporative coolers combined with the sensible heat exchanger under these conditions. This operational mode results in superior performance, regardless of component efficiency, for the variable regeneration temperature scheme in Phoenix.

Section IV predicts primary energy (thermal energy required for desiccant regeneration and thermal energy required by the electric power plant to operate the air moving equipment) use for desiccant systems compared to conventional vapor-compression equipment. The configurations and methodologies included a commercially available silica gel system, an advanced desiccant material, and an enthalpy exchanger.

Results from these analyses show that the enthalpy exchange device requires the least primary energy of any of the devices simulated. Of course, the use of an enthalpy exchange device requires that the building entering and exiting air streams exist at the same location. None of the active desiccant types regardless of configuration or operational mode approached the energy performance of the enthalpy exchange device. Among the active desiccant devices, the advanced desiccant with the advanced control strategy achieved the best performance. Regionally, the cities with the most adverse climate (highest enthalpy), achieved the highest energy efficiency.

For the commercially-available silica gel system, the efficiency differences between the constant and variable regeneration techniques essentially vanish when primary energy is calculated, with Phoenix, AZ, being the exception. CoPs based on primary energy ranged from 1.7 (Phoenix) to 0.57 (New York City) depending upon regeneration mode and the air face velocities chosen. For all of the climates simulated, excepting Phoenix, face velocities of 300 fpm will yield a seasonal CoP based on primary energy of about 1.0, while face velocities of 500 fpm will reduce that to about 0.9. These flow velocities compare favorably to vapor compression systems which typically operate from 300 to 400 fpm. The primary energy CoP of vapor-compression equipment is 0.8 and 1.0 for assumed seasonal energy efficiency ratios (SEER's) of 10 and 12 respectively.

Incorporating an advanced desiccant material enhanced the desiccant wheel effectiveness by about 15%. Seasonal CoP's generally increase about 10% for the advanced material for all of the

cities simulated except Phoenix, AZ. Phoenix showed no significant improvement. SEER increased about 20% for all of the cities simulated, again with the exception of Phoenix. For this case, however, Phoenix improved about 10%. The same improvements in primary energy consumption were also observed.

The advanced control strategy simulated does not operate the desiccant wheel if the sensible heat exchanger and evaporative cooler sections of the system can supply building air at or below the indoor air enthalpy. Results showed that, with the new control strategy, in cities that generally experience hot humid weather, Atlanta and Houston, the improvement in thermal efficiency is minimal at best. New York experienced about a 10% increase (similar to the advanced desiccant), Chicago about a 15% increase, and Phoenix a 100% increase. The results for a system using this control strategy and the advanced desiccant material did not significantly improve performance. However, the percentage increase in performance achieved by the advanced desiccant material is reduced as the amount of evaporative cooling increases (Phoenix). That is, there is less incentive to increase desiccant dehumidifier performance for hot, dry climates.

Operating the commercially available silica gel desiccant system in the full ventilation mode generally increased performance compared to the advanced desiccant material operating with the modified ventilation cycle. For example, for the hot, humid climates of Atlanta and Houston, the increase in thermal CoP was approximately 30%. This improvement closely matched that for the hot, dry climate, Phoenix. The least improvement was shown by the two mild climate cities, New York City and Chicago. The improvement in thermal CoP for these cities was approximately 20%. However, as with the enthalpy exchange device, building ventilation and exhaust air must be located in close proximity to one another.

The annual cooling load required by the ventilation of commercial buildings (excepting hotels and motels) is estimated to be approximately 0.4 quads. The amount of primary energy required to meet this load with conventional HVAC equipment (SEER=10) is 0.5 quads. The increase in building ventilation load due to ASHRAE 62-1989 is estimated to be slightly more than 0.1 quads, or 0.125 quads primary energy. The primary energy savings associated with all of the technologies and operational scenarios simulated are shown below.

Primary Energy Savings (Quads) Compared to Vapor Compression (SEER=10)

Desiccant Technology	Total Ventilation Load	Increase Due to ASHRAE 62-1989
Conventional	0.10	0.025
Advanced Desiccant Material	0.14	0.035
Advanced Control Strategy	0.17	0.043
Enthalpy Exchange	0.42	0.078
Full Ventilation Cycle	0.19	0.048

These results show that all of the candidate desiccant systems can save energy relative to standard vapor-compression systems. The conventional active desiccant system can save between 0.025 and 0.1 quad depending upon the size of the ventilation load. Significant improvements in

these numbers can be achieved by combinations of desiccant material and control strategy improvements. However, the largest energy savings are achieved by the enthalpy exchange device. These savings range from 0.078 to 0.42 quads, depending upon the size of the ventilation load.

Not addressed in this study are advanced regeneration concepts. Although mostly associated with liquid desiccant systems, these concepts are able to show quantum increases (2-6 times) in thermal CoP. All of the concepts examined in this study require that the heat of adsorption/absorption be supplied for desiccant regeneration. Advanced regeneration concepts are theoretically possible that require only a fraction of that energy for desiccant regeneration. Multiple effect boilers, vapor recompression systems, and water-miscible desiccants are examples of these advanced concepts. Up to 0.4 quads of primary energy savings are possible if all building ventilation air were conditioned by an advanced regeneration desiccant (probably a liquid) system. Unlike enthalpy exchange devices, these systems would not need building reject air in order to achieve this high level of performance.

Another area not addressed here is the lack of humidity control that would result from conditioning the outdoor air with conventional vapor-compression equipment. The very low SHR's required (as low as 0.11) could not be achieved with this equipment. Therefore, the energy consumption predictions for the vapor-compression equipment are low. The greatest advantage of desiccant-based ventilation air systems may be their ability to achieve wide operational values of SHR.

If the total building air conditioning market rather than only the ventilation air preconditioning market could be penetrated by desiccant systems, much greater primary energy savings could be achieved. Even though these analyses have shown that this goal cannot be achieved by conventional solid desiccant systems, advanced systems capable of recirculation CoPs above 1.0 could. Work by AIL Research[1] has shown that seasonal CoP's (thermal only) of from 1.5 to 2.25 are possible with liquid desiccant systems employing advanced regeneration concepts. Significant primary energy savings combined with superior latent load control could make these advanced desiccant systems a viable technology capable of national implications.

---

[1] Lowenstein, A.I. and Novosel, D., "The Seasonal Performance of a Liquid-Desiccant Air Conditioner," ASHRAE Transactions, V.101, Pt.1, 1995.

SECTION I: PERFORMANCE ANALYSIS OF IDEAL DESICCANT COOLING CYCLES

To evaluate the efficacy of claims made for the performance of various desiccant cycles and to determine the potential payoff for any research efforts to improve such performance, the Department of Energy wishes to determine the maximum possible thermodynamic efficiency for each type of desiccant cycle. This task, through computer simulation and state point analyses, determined the maximum thermodynamic performance of desiccant cycles, assuming that equilibrium conditions are achieved by all components in the cycle. The purpose of this study was to determine the maximum possible efficiency for each cycle modeled. The candidates for modeling are (1) Pennington Cycle, both recirculation and ventilation; (2) Dunkle Cycle; and (3) Non-Adiabatic Liquid Desiccant Cycles.

Basic Desiccant Cooling Cycle

As a first step, the investigation considered the thermodynamic performance of a basic desiccant cooling cycle that conditions saturated air. This cycle with saturated air demonstrates a "worst case" scenario for the technology. In addition, the heat of sorption for the desiccation process was assumed to be equal to the latent heat for water in air and also assumed that no heat capacity exists, other than that of water, in the desiccant material. This dehumidification process is shown psychrometrically in Figure 1-1. The thermodynamic properties of the air to be cooled and dehumidified (called the process or dehumidification air) are represented by any point along the saturation line of the psychrometric chart. This arbitrary point is designated as A. Dehumidifying the process air will result in air at state point B. The slope of the line A-B will be determined by the energetics of the process. If the heat of sorption of the desiccant is equal to the latent heat of water in air, the slope will be a constant enthalpy line on the psychrometric chart. This is a consequence of the definition of the enthalpy of water and air mixtures. The location of point B along the constant enthalpy line will be determined by the desiccant regeneration condition, which will be discussed in more detail in the next section.

Notice that at this stage of the cycle, no useful work has been accomplished because the enthalpy of the air has remained constant. Only a conversion of latent to sensible heat has occurred. To provide cooling, the enthalpy of the air must be reduced. One method of accomplishing this is to cool the air at state point B using a naturally-occurring cold sink. If the air at point A represents outdoor air, then there is essentially a limitless supply for this cycle. Therefore, this air can be used to cool the process air. This heat exchange will cool the process air from point B to C. The enthalpy difference between points C and A is defined as the cooling capacity of the cycle. The cooling capacity for this process is defined by:

$$CC = PROCMASSFLOW * (H_{A-B} - H_C) \qquad 1.0$$

where: CC = Cooling Capacity
PROCMASSFLOW = Mass Flow Rate of Process Air
H_{A-B} = Specific Enthalpy of Air at State Points A and B
H_C = Specific Enthalpy of Air at State Point C

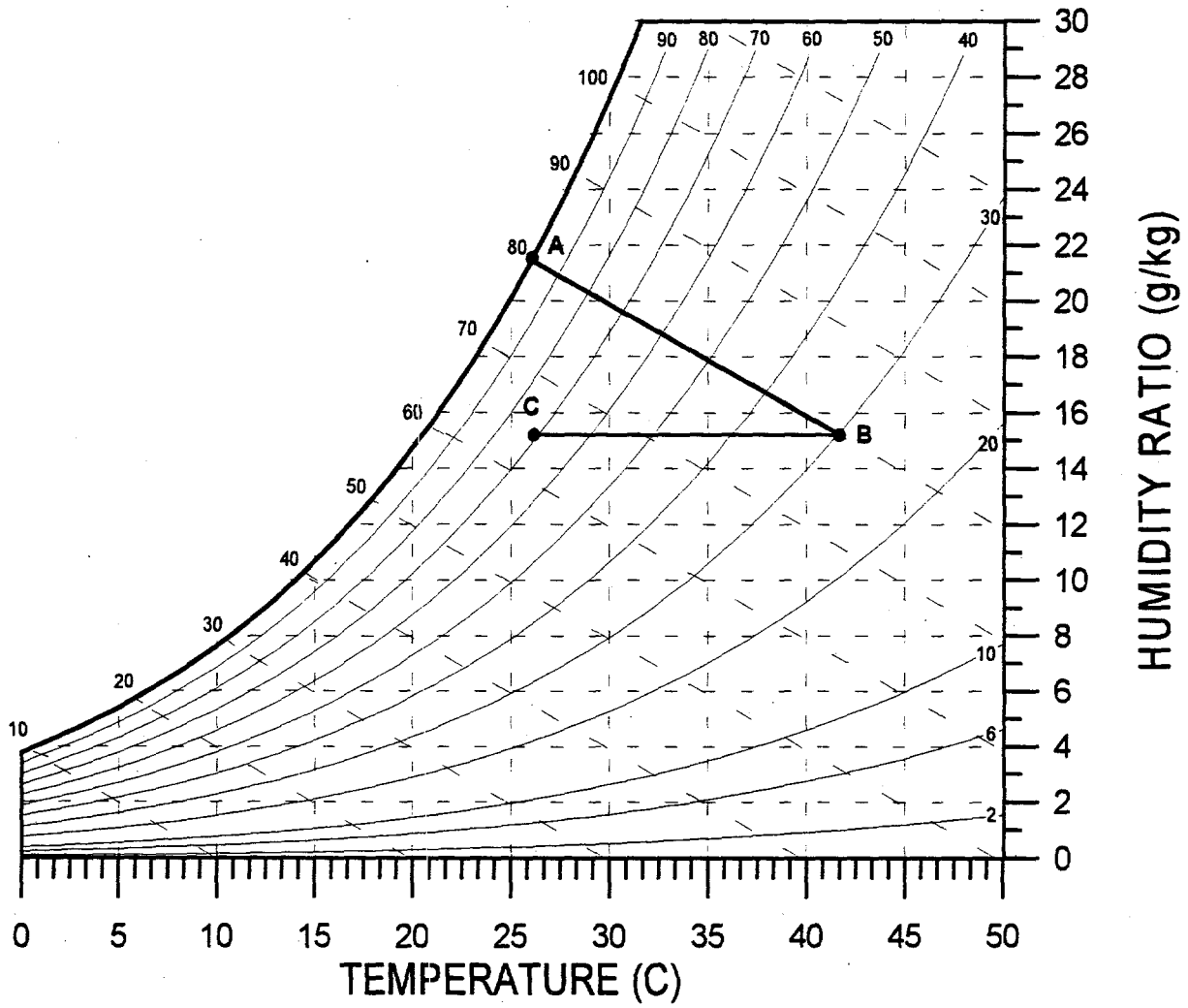

Figure 1-1. Basic desiccant dehumidification and cooling of saturated air.

For 100% effective heat exchange between the cold sink at state point A and the process air at state point B, an alternative expression for the cooling capacity becomes:

$$CC = WATERADS * HVAP \qquad 2.0$$

where: WATERADS = Mass Rate of Water Sorbed by the Desiccant
HVAP = Latent Heat of Water

Recalling that the binding energy of the water to the desiccant is equal to the latent heat of water (HVAP), the minimum energy required to remove the sorbed water from the desiccant and back into the vapor phase will be exactly the same as the cooling capacity (Eqn. 2.0). Therefore, if

all of the energy required for regeneration comes from a source external to the cycle, the maximum Coefficient of Performance (CoP) for this desiccant cycle is 1.0. All of the regeneration energy for this example is supplied by an external energy source. As will be shown later, some of this regeneration energy may be supplied with heat sources inherent to the cycle.

Consider now, a different situation with process air not at the saturation condition. Figure 1-2 shows a similar cycle, except that the beginning air state point A is not saturated. As in the previous example, air at state point A is dehumidified to state point B. Now, instead of a heat exchange with additional air at state point A, the air at state point B is now heat exchanged with air at condition D. State point D is created by evaporatively cooling the additional air at state point A. The cooling capacity for this process is defined exactly the same as in Equation 1.0; however, for this cycle Equation 2.0 becomes:

$$CC = PROCMASSFLOW*(WATERADS + WATEREVAP)*HVAP \qquad 3.0$$

where: WATEREVAP = Mass Rate of Water Evaporated from A to D

For this process, the energy required to remove the sorbed water from the desiccant is still defined exactly the same as it was in Equation 2.0. However, the CoP of the cycle, with 100% of the regeneration energy supplied by an source external to the cycle, will be:

$$CoP = 1.0 + WATEREVAP/WATERADS \qquad 4.0$$

As is readily apparent, the maximum CoP of the basic desiccant cycle is markedly increased by processing less than saturated air. This increase is due to taking advantage of the temperature depression created by evaporative cooling. However, it is important to notice that CoP alone is not the only important consideration. Examination of Equation 4.0 will reveal that the maximum CoP is achieved when the amount of water sorbed by the desiccant is zero. This cycle then becomes an indirect evaporative cooler with infinite CoP. However, if the condition of the output air (state point C) is not in the human comfort zone, the CoP is moot. Therefore, some water sorption is required by the cycle if an indirect evaporative cooling cycle is not sufficient to meet a particular cooling load.

Regeneration Conditions: Solid Desiccants

To this point in the analysis, we have considered only the energetics of regeneration, not the mechanism. If the desiccant is to be regenerated, the rate at which water molecules leave the desiccant surface must exceed the rate at which they attach to the surface. This condition must be satisfied, regardless of the desiccant type, for regeneration to take place. In the case of solid desiccants, this means that the water vapor pressure of the desiccant must exceed the water vapor pressure of the regeneration air. In addition, for solid desiccants, the desiccant is not heated directly.

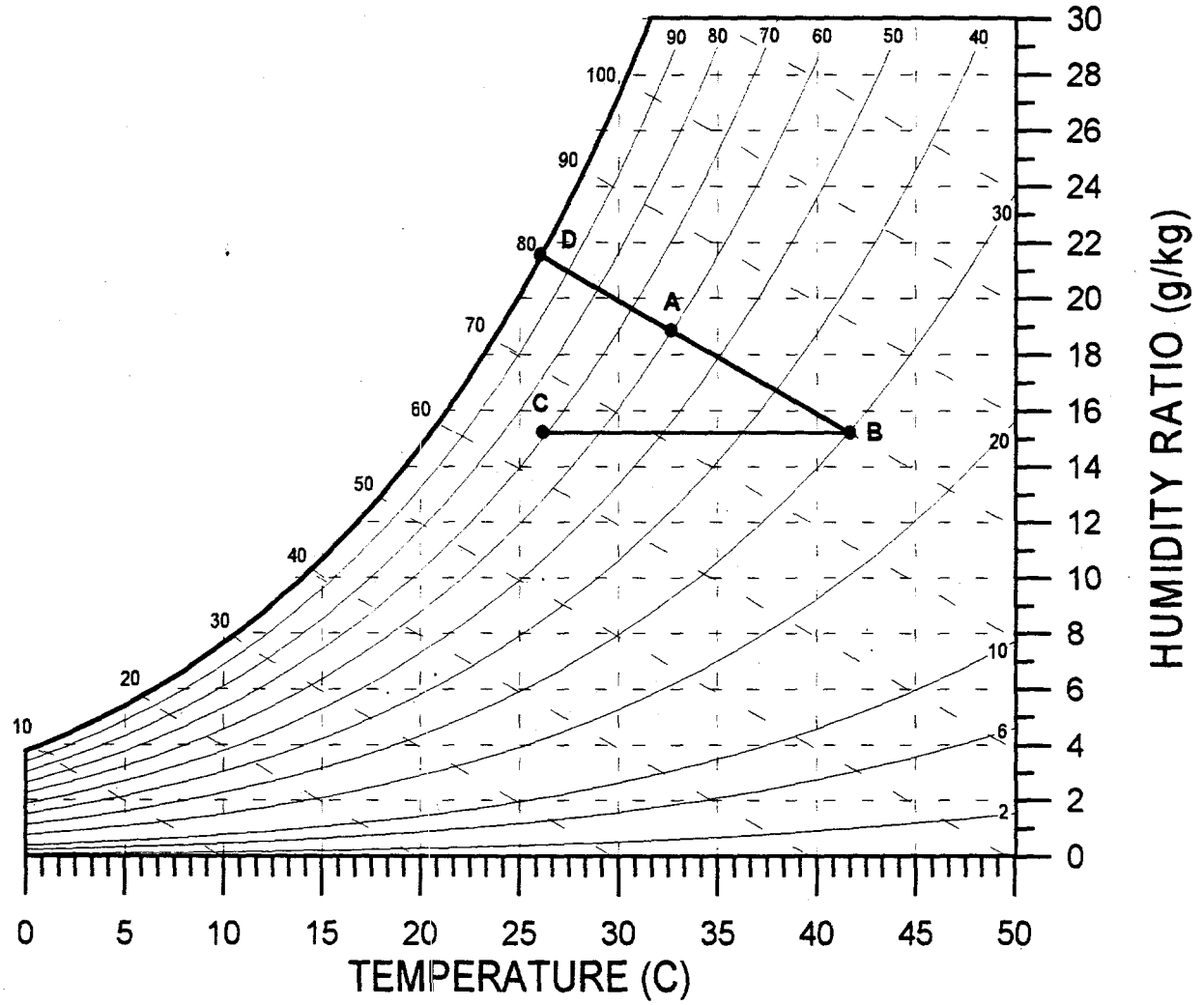

Figure 1-2. Basic desiccant dehumidification and cooling of unsaturated air.

An intermediate heat transfer fluid (air) is heated, and this fluid is then used to heat the desiccant. Moreover, the intermediate heat transfer fluid must also be the ultimate receptor of the water that is attached to the desiccant. Therefore, the regeneration air must serve as both a heat and mass transfer medium for the cycle. This aspect is distinctly different from conditions for liquid desiccant regeneration. This difference will be explained further in the next section on liquid desiccants.

When air regenerates the desiccant, the regeneration air must be capable of producing a desiccant moisture loading that is compatible with the maximum dew point depression achieved during the dehumidification process. This is a very important aspect of any desiccation cycle. To fully understand this concept, it is important to appreciate the wave nature of heat and mass transfer within the desiccant matrix. Conceptually, this means that a moisture gradient within the desiccant matrix must exist if a desiccation cycle is to be possible. The purpose of the desiccant in any useful cycle is to convert moist air into dry air. Under equilibrium conditions, this means that one end of

the desiccant will be in equilibrium with the moist, entering air, and the other end of the desiccant will be in equilibrium with the dry, outlet air. This creates the necessity for a moisture gradient within the desiccant between the high moisture loading of the inlet air to the low moisture loading of the outlet air. Figure 1-3 shows an idealized representation of how the desiccant moisture loading changes during the adsorption (dehumidification) and desorption (regeneration) processes. If moisture cycling of the desiccant is to take place, then the regeneration air must be able to produce the moisture loading in the desiccant that is in equilibrium with the dehumidified outlet air. This will be, to a first approximation, the minimum moisture loading existing in the desiccant matrix. Thermodynamically, this means that the minimum regeneration temperature for a particular cycle is that which produces a moisture loading in the desiccant that is capable of achieving the minimum process air outlet humidity. The minimum energy input will be that required to heat a specified amount of regeneration air to this minimum required temperature.

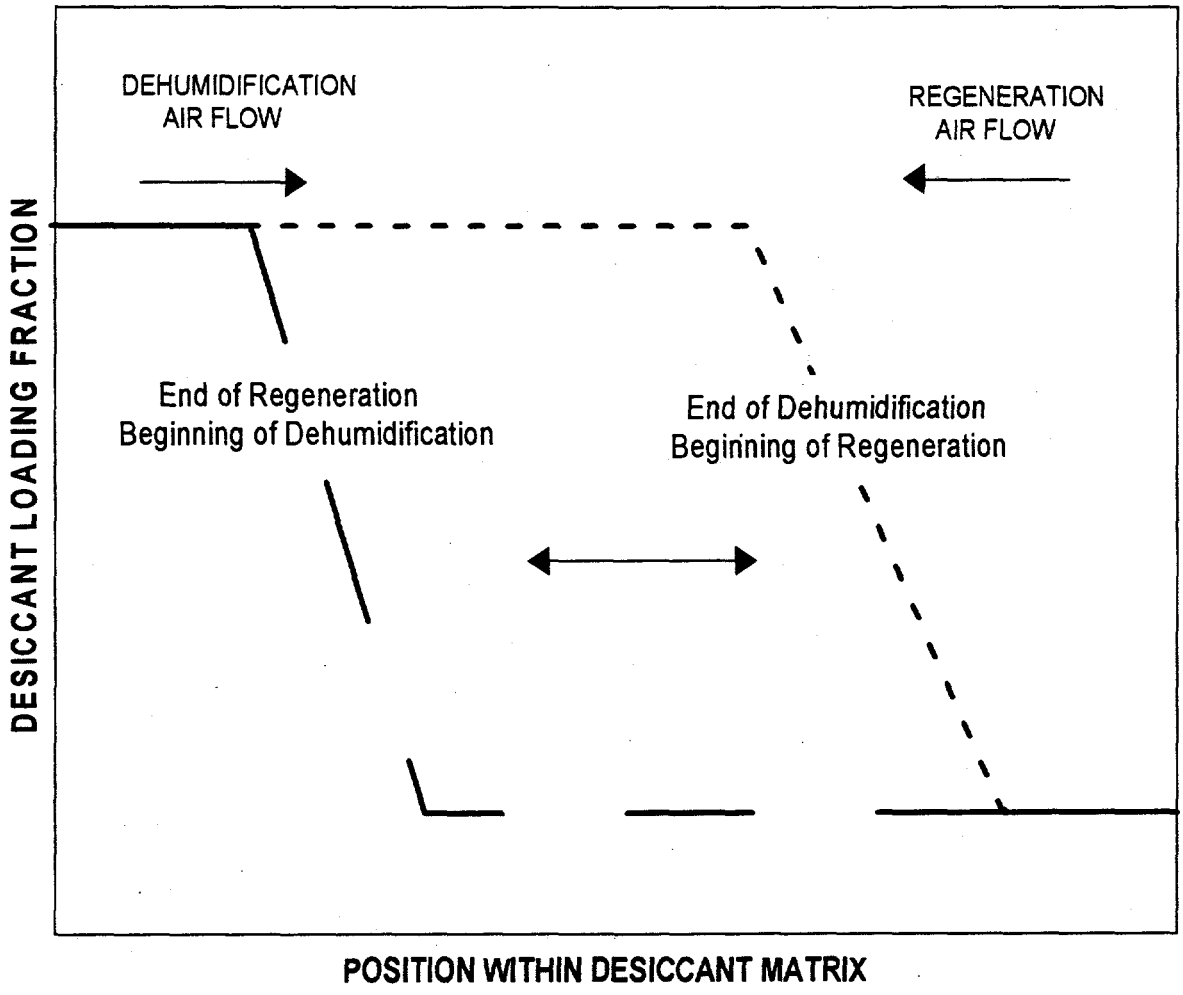

Figure 1-3. Loading Profiles Within Desiccant Matrix Between Dehumidification and Regeneration Processes

For the cooling processes depicted in Figures 1-1 or 1-2, the regeneration air must be heated to a value such that the desiccant loading in equilibrium with point B is also the desiccant loading achieved by the regeneration air. Figure 1-4 shows a desiccant cooling cycle with regeneration included. A schematic representation of the components used to create this cycle are also shown for illustrative purposes. Outdoor air at state point A is assumed to be saturated as in Figure 1-1. As in the previous examples, the process air cycle is defined as A, B, and C. The regeneration air cycle is defined as A, D, E, and F. State point E is defined as the regeneration air. This is the regeneration air condition that can create the desiccant loading that allows the desiccant to convert air at state point A to air at state point B. To determine state point E, the desiccant moisture loading associated with state point B must be determined. For a desiccant with a heat of sorption equal to the latent heat for water, lines of constant desiccant loading are also lines of constant relative humidity. A proof of this statement is as follows:

A generalized expression for defining the isotherm of any desiccant can be formulated from the Second Law of Thermodynamics in the following manner:

$$RELDESLOAD = (CONST*PVE/PSAT)*FACTOR \qquad 5.0$$

where: RELDESLOAD = Relative desiccant loading (actual loading/maximum loading)
CONST = Numerical constant that defines isotherm shape
PVE = Vapor pressure of water at the given loading and temperature
PSAT = Water saturation pressure at the given temperature
FACTOR = Modifying parameter to allow for the desiccant heat of sorption (if heat of sorption equal water latent heat, FACTOR =1)

Recognizing that PVE/PSAT is the same thing as relative humidity, equation 5 demonstrates that constant relative desiccant loading will also be constant equilibrium relative humidity.

For the cycle depicted in Figure 1-4, state point E is determined by the intersection of the constant relative humidity line (6% RH) associated with state point B and the humidity ratio of the regeneration air (13 g/kg). Before heating to state point E, the regeneration air can be preheated to state point D by heat exchange with the process air at state point B. Air at state point D will be at the humidity ratio of state point A and temperature equal to state point B if the heat exchange is 100% effective. The regeneration air must then be heated by an external energy source from state point D to the regeneration state point E. The amount of regeneration energy required by the cycle will be:

$$REGEN = REGMASSFLOW*(H_E - H_D) \qquad 6.0$$

where: REGEN = Regeneration Energy Rate (Power) Required
REGMASSFLOW = Mass Flow Rate of Regeneration Air
H = Enthalpy of Air

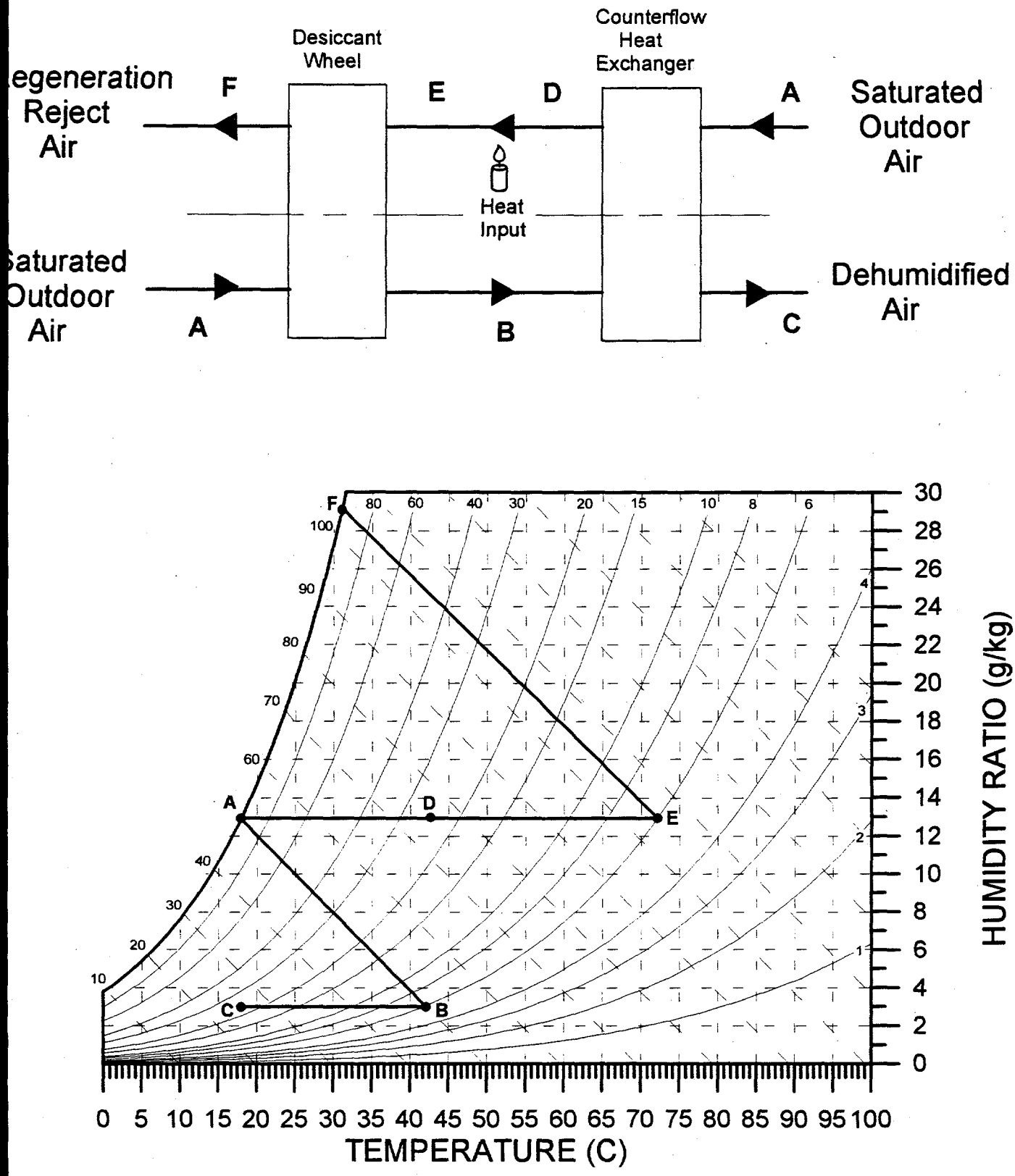

Figure 1-4. Basic desiccant cooling cycle processing saturated air

In order to mathematically determine the enthalpy of air at state point E, one must be able to determine the air temperature, knowing the humidity ratio and the relative humidity. This requires solving for temperature knowing the saturation pressure. Since the temperature dependence of saturation pressure is a higher order, mixed polynomial, it is not possible to obtain a "closed form" solution for temperature. An iterative solution is required. Therefore, an algebraic expression for "REGEN" is not possible. However, as we have seen from the previous example, it is quite straightforward to obtain these values graphically with the aid of a psychrometric chart. Knowing the regeneration air enthalpy (through either graphical or numerical means), one more parameter is needed to calculate the total regeneration energy (REGEN). That parameter is the mass flow rate of air required (REGMASSFLOW). To determine this parameter, the condition of the regeneration reject air is required. From thermodynamics, the cycle efficiency is maximized when the thermodynamic availability of the air rejected to the environment is minimized. The technique used to determine the minimum regeneration temperature is also applicable to predicting the minimum thermodynamic availability of the rejected air.

Minimizing the thermodynamic availability of the reject air requires minimizing the temperature and maximizing the moisture content of this air. Any air rejected by the cycle that is capable of doing useful work (thermodynamically speaking) represents a cycle inefficiency. The minimum air temperature and maximum water content rejected, will be that which is in thermodynamic equilibrium with that portion of the desiccant that is also in equilibrium with the process inlet air. This means that the regeneration air exiting the desiccant (rejected to the environment) cannot thermodynamically remove water from any desiccant particle that participates in the cycle. This air temperature and humidity will be that represented by an intersection of the constant desiccant loading line commensurate with the inlet air, (for this example the water saturation line), and the enthalpy of the regeneration air. Therefore, the minimum temperature and maximum humidity for the air rejected by the cycle will be created by an intersection of the enthalpy line associated with state point E and the saturation line. This air condition is shown in Figure 1-4 as F.

A close examination of Figure 1-4 reveals an inconsistency. If a moisture balance between process and regeneration air streams is to occur (a requirement for a true cycle) the regeneration air flow rate must be different than the process flow rate. This is because the humidity ratio difference between F and E is greater than that between A and B. However, if air at state points C and D are to be achieved, the regeneration and process air flow rates must be the same. To alleviate this inconsistency, two possibilities exist. One is to reduce the regeneration flow rate until a water balance exists. If this happens, then air at state point C will not be achieved and the cooling capacity of the cycle will be reduced. The other possibility is to split the regeneration flow after the heat exchanger. Part of the flow is heated (enough to ensure a mass balance) and the other part is rejected. If this happens, then the potential cycle efficiency is reduced because some air was rejected (at state point D) that could perform some useful work. That is, air rejected to the environment at state point D could still regenerate some desiccant in this cycle, although it could not regenerate to the minimum moisture loading required.

To illustrate this principle, Figure 1-5 shows the relationship between regeneration air conditions, process air conditions, and desiccant loading. As was shown earlier, the minimum desiccant loading (the loading that ultimately determines cooling capacity) for the cycle requires a specific regeneration temperature. As shown in Figure 1-5, regeneration temperatures lower than that specified for the cycle can still regenerate the desiccant relative to the inlet air (the maximum loading); however, these lower temperatures cannot create the lowest loading required to support the cycle as shown.

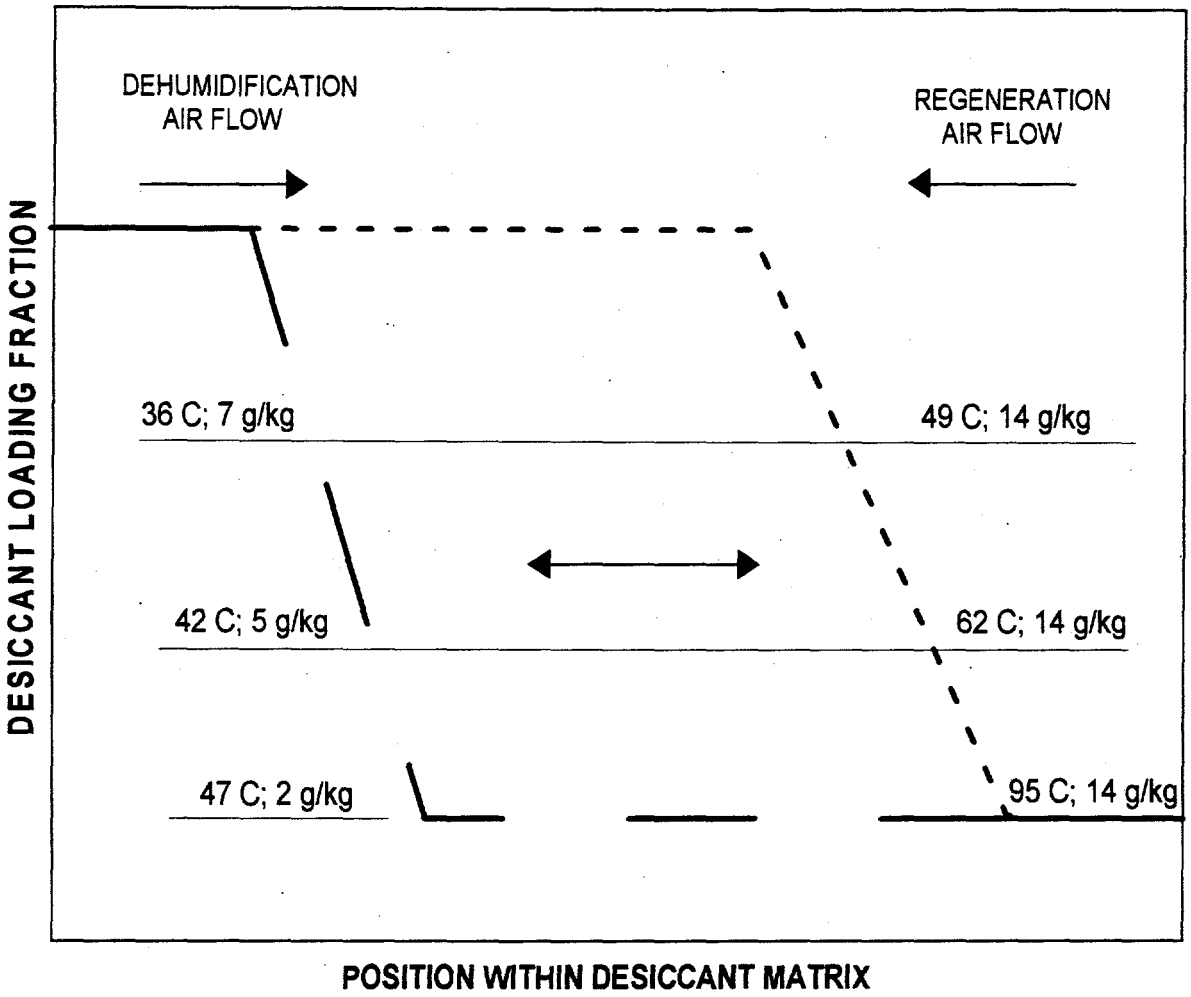

Figure 1-5. Loading Profile Within Desiccant Matrix Between Dehumidification and Regeneration Processes

The mismatch between energy and mass balances that we have just described is fundamental to open-cycle desiccant systems where air is the regeneration medium. It would appear to be a "second law" phenomenon. That is, recuperating the heat of sorption yields more low-temperature energy than can effectively be used to regenerate the desiccant to the minimum loading required by the cycle.

The results of the cycle analysis for the system shown in Figure 1-4 are given in Table 1-1. Recalling that the definition of CoP is the ratio of the cooling capacity to the regeneration energy, the cycle CoP will be defined as the ratio of more general forms of Equations 1.0 and 6.0 as given below;

$$CoP = PROCMASSFLOW * (\Delta H_{cooling}) / REGMASSFLOW*(\Delta H_{regeneration}) \quad 7.0$$

where: $\Delta H_{cooling}$ = Enthalpy difference between inlet and outlet process air.
$\Delta H_{regeneration}$ = Enthalpy difference between inlet and outlet of externally-heated regeneration air.

TABLE 1-1: State Points for the Desiccant Process Depicted in Figure 1-4.

State Point	A	B	C	D	E	F
Enthalpy (kJ/kg)	50.0	50.0	25.5	74.9	105.7	105.7
Relative Humidity (%)	100.0	6.0	24.3	24.7	6.0	100.0
Humidity Ratio (g/kg)	12.7	3.0	3.0	12.7	12.7	29.1
Dry Bulb Temp ©	17.7	41.9	17.7	41.9	71.7	31.1

Ratio of Regeneration to Process Air Flow Rates = 0.59
CoP (minimum heat input) = 1.35
CoP (heat all regeneration air) = 0.80
CoP (no regeneration preheat) = 0.75

It is interesting to compare the CoP's presented in Table 1-1 with the "regeneration independent" value (1.0) from the previous section. If regeneration preheat is combined with splitting the regeneration air flow and only the minimum amount of air is heated, the external energy required for regeneration is less than the total heat of sorption associated with the water adsorbed. In addition, without evaporative cooling credit (Eqn. 4.0), a solid desiccant cycle can achieve a CoP of greater than 1.0. This is a significant finding because it justifies using heated air as the regeneration mechanism rather than direct heating of the desiccant. Also notice that both of the other options, heating all the air and achieving no regeneration preheat, result in requiring more external energy for regeneration than the total heat of sorption for the water adsorbed.

Ideal Desiccant Cycles

Solid Desiccants

The modeling of system performance for this section will be performed using the commonly accepted ARI (Air conditioning and Refrigeration Institute) air conditions:

Indoor: 80 F (26.7 C); 50% RH
Outdoor: 95 F (35 C); 40% RH

Ventilation Cycle

The ventilation cycle for the ARI air conditions assumed is shown schematically and psychrometrically in Figure 1-6. The process air cycle is as follows: Outdoor air at state point A is dehumidified to state point B. This air is then heat exchanged with room air that is adiabatically humidified to state point F to create air at state point C. This air is then humidified to state point D. This later process, (humidifying from C to D) is usually employed to control the Sensible Heat Ratio (SHR) of the cycle.

The regeneration air cycle is as follows: Indoor air at state point E is humidified to state point F. This air is then heat exchanged with the process air at state point B to produce air at state point G. This air is then heated to the regeneration state point at "H". After regenerating the desiccant, air at state point I is then exhausted back to the outdoors.

The ventilation cycle results are shown in Table 1-2. Notice that results are shown for two regeneration air temperatures, 75 and 100 C, and for two definitions of cooling capacity (crediting and not crediting for vent air). This latter effect is quite significant in specifying system results. For building loads where ventilation air is required, many investigators will report performance using the enthalpy of outdoor air as the reference for defining cooling capacity (Equation 7.0). For these conditions, CoP and cooling capacity are termed to be given vent credit. However, many cooling loads do not require that outdoor air be the source of system return air. For these cases, using outdoor air as the reference is not appropriate. The more usual baseline enthalpy chosen is the indoor air enthalpy. Under these conditions, the CoP and cooling capacity do not receive ventilation credit.

Also shown in Table 1-2 is another important parameter in determining cooling system performance, is specific cooling capacity (SCC). This is defined as the cooling capacity per unit mass of air processed. This parameter will give an indication of the relative size of the components needed for a given cooling capacity. It is generally desirable to achieve the highest possible cooling output for each unit of air processed. This is because the physical size of components will generally be determined by the amount of air required.

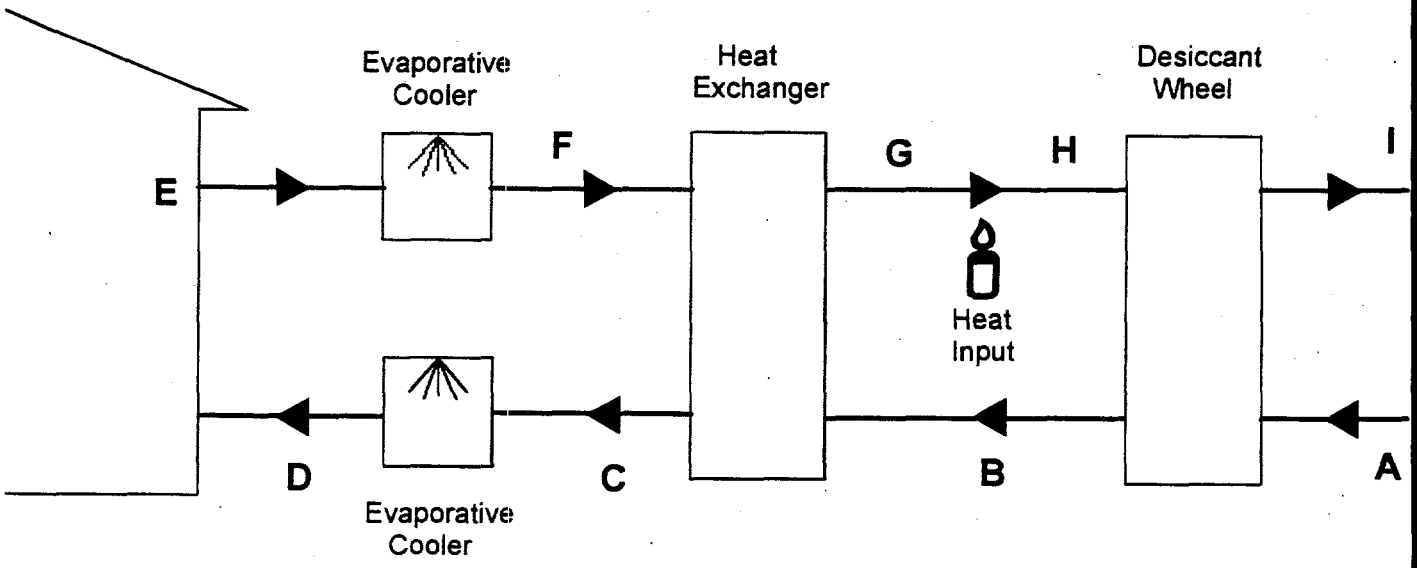

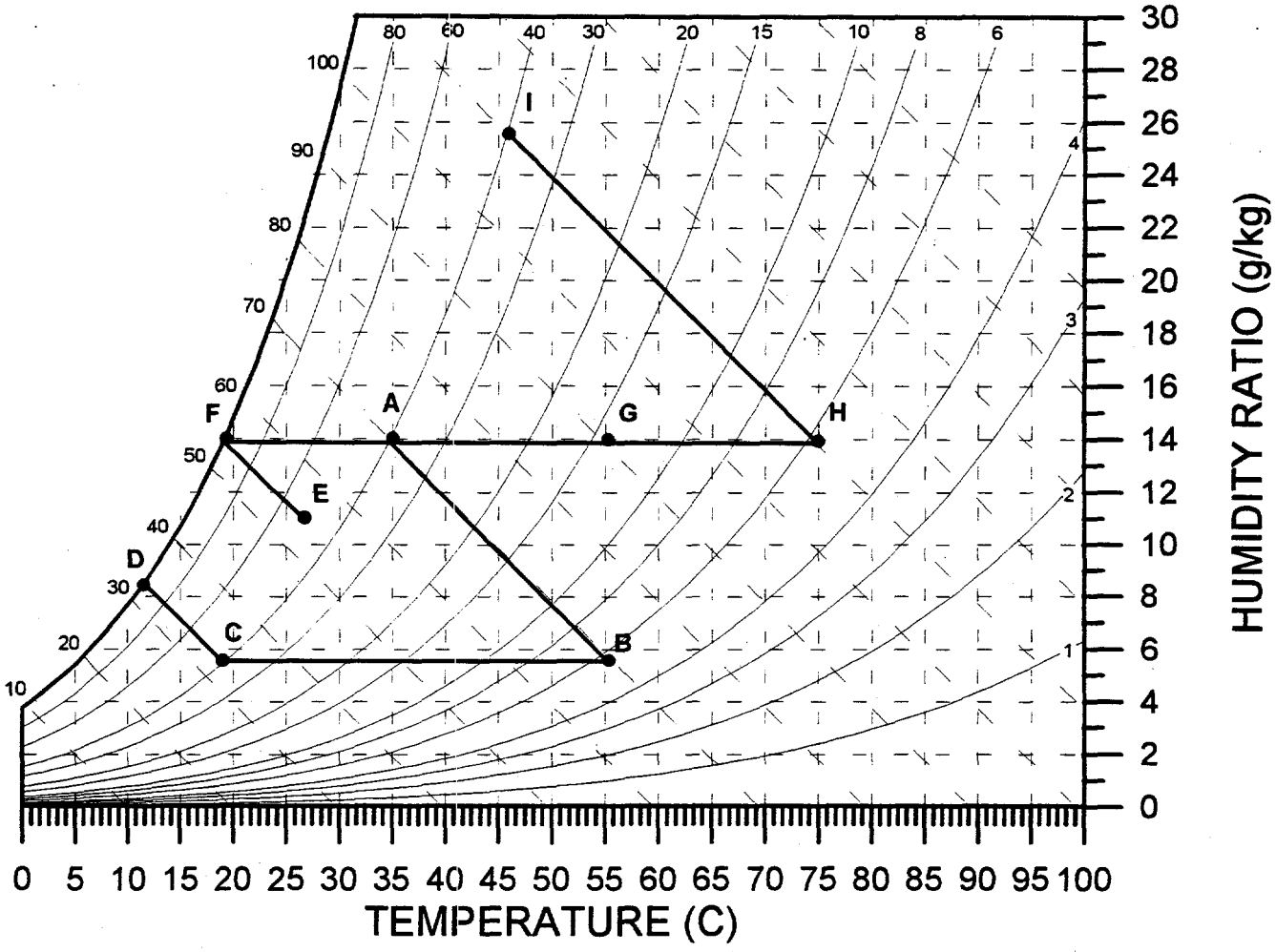

Figure 1-6. Ventilation Mode Operation

TABLE 1-2: State Points for Ventilation Cycle Depicted in Figure 1-6 for Two Regeneration Temperatures

75°C Regeneration

Air Condition	A	B	C	D	E	F	G	H	I
Enthalpy (kJ/kg)	71.1	71.1	34.2	34.2	55.0	55.0	97.2	112.8	112.8
Relative Humidity (%)	39.5	5.8	41.9	100.0	50.1	100.0	13.8	5.8	39.5
Humidity Ratio (g/kg)	14.0	5.8	5.8	8.8	11.0	14.1	14.1	14.1	25.7
Dry Bulb Temp ©	35.0	55.6	19.3	12.0	26.7	19.3	55.6	75.0	46.1

100°C Regeneration

Air Condition	A	B	C	D	E	F	G	H	I
Enthalpy (kJ/kg)	71.1	71.1	27.2	27.2	55.0	55.0	100	138.7	138.7
Relative Humidity (%)	39.5	2.2	22.2	100	50.1	100	9.9	2.2	39.5
Humidity Ratio (g/kg)	14	3.1	3.1	7.2	11.0	14.1	14.1	14.1	33.5
Dry Bulb Temp ©	35	62.7	19.3	9.1	26.7	19.3	62.7	100	51.1

Regeneration Temp ©	With Vent Credit		Without Vent Credit		
	CoP	SCC[1]	CoP	SCC	Flow Ratio[2]
75	2.6	36.9	1.5	20.7	0.71
100	2.0	43.9	1.3	27.7	0.56

[1] Specific Cooling Capacity (kJ of cooling/kg of process air)
[2] Ratio of Regeneration to Process Air Flow Rates

The results of Table 1-2 reveal three important conclusions. They are:

1. CoP decreases for increasing regeneration temperature.
2. Specific Cooling Capacity (SCC) increases with regeneration temperature.
3. Very high CoP's are possible if vent air is desired.

One significant reason for the very high CoP's obtained from the ventilation cycle is that humidified room air is the cold sink. However, there is a hidden "catch" to this situation. If this source of air is readily available, then other, even more attractive technologies could be employed. For example, a total enthalpy exchanger could be placed between the incoming outdoor air and the outgoing room air. Under ARI conditions, 16.2 kJ/kg of vent air cooling could be performed with no energy input whatsoever. In order to make a more credible analysis of the vent cycle, consider the cycle shown in Figure 1-7. With this cycle, exhausted indoor air is not available either for the desiccant cycle or a total enthalpy exchanger. All sources of air are outdoor. Outdoor air at state point A, is dehumidified to state point B. At this point, it is heat exchanged with humidified outdoor air at state point E to produce air at state point C where it is humidified to produce air at state point D. On the regeneration side, outdoor air is humidified to create state point E where it is heat exchanged with the process air at state point B to create air at state point F. This air is then heated by an external heat source to create regeneration air at state point G. Upon regenerating the desiccant, the air is rejected to the environment at state point "H".

The results for this cycle are shown in Table 1-3. Notice that both the CoP and SCC have been markedly reduced when compared to the standard ventilation cycle with vent credit. However, when compared to the recirculation cycle (Table 1-4), they are still significantly higher. It is also interesting to note that the reduction in performance relative to the standard vent cycle is proportionally less for higher regeneration temperatures.

Recirculation Cycle

The recirculation cycle operating with the ARI air conditions assumed is shown in Figure 1-8. The process air cycle is as follows: Room air at state point A is dehumidified to state point B. This air is then heat exchanged with outdoor air that is adiabatically humidified to state point F to create air at state point C. This air is then humidified to state point D.

The regeneration air cycle is as follows: Outdoor air at state point E is humidified to state point F. This air is then heat exchanged with the process air at state point B to produce air at state point G. This air is then heated to the regeneration state point at "H". After regenerating the desiccant, air at state point I is then released back to the outdoors. The recirculation cycle results are shown in Table 1-4. As with the ventilation mode, the results are shown for two regeneration conditions, 75° and 100°C. However, unlike the ventilation cycle, there are no ambiguities involving cooling capacity. It will always be evaluated relative to room conditions. Notice that for the ARI

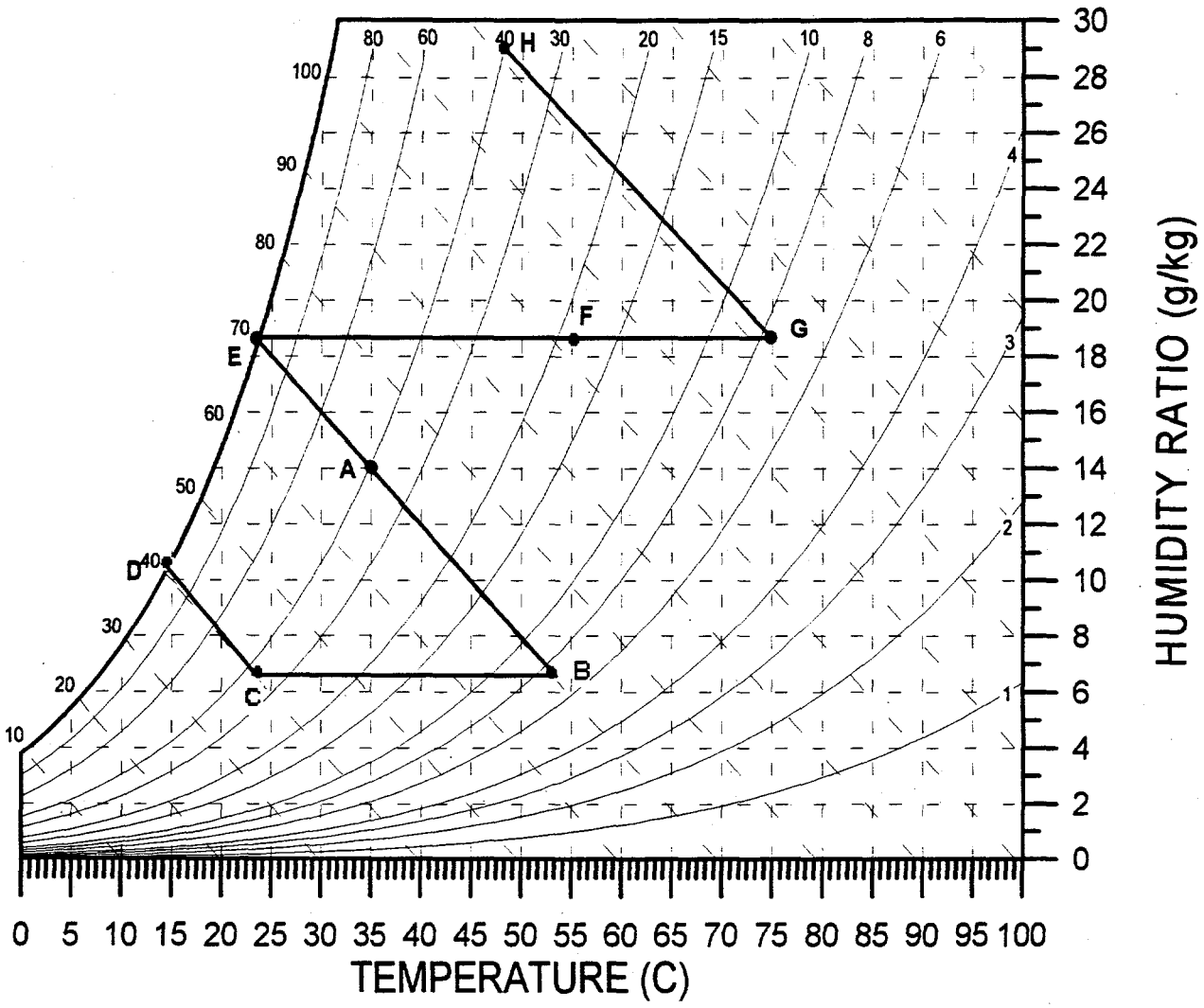

Figure 1-7. Psychrometric representation of a modified ventilation cycle

conditions assumed, the recirculation mode results in lower CoP's and specific cooling capacities than for the ventilation mode, regardless of the baseline. Also note that CoP does not drop off with increasing regeneration temperature for the recirculation mode as it does in the ventilation mode. However, specific cooling capacity does not increase as rapidly with regeneration temperature for the recirculation mode as it does in the ventilation mode.

Dunkle Cycle

The Dunkle cycle operating with the ARI air conditions assumed is shown in Figure 1-9. It is a combination of the recirculation and ventilation cycles. The idea behind it is to be able to achieve the cold sink temperatures of the ventilation cycle while processing indoor air as in the recirculation cycle. Room air at state point A is humidified to state point B. This air is then

TABLE 1-3: State Points for the 100% Ventilation Cycle Depicted in Figure 1-7 for Two Regeneration Temperatures

75°C Regeneration

Air Condition	A	B	C	D	E	F	G	H
Enthalpy (kJ/kg)	71.1	71.1	41.1	41.1	71.1	101.8	124.6	124.6
Relative Humidity (%)	39.5	7.6	37.2	100.0	100.0	20.3	7.6	39.5
Humidity Ratio (g/kg)	14.0	6.8	6.8	10.4	18.6	18.6	18.6	29.2
Dry Bulb Temp ©	35.0	53.1	23.7	14.7	23.7	53.1	75.0	48.5

100°C Regeneration

Air Condition	A	B	C	D	E	F	G	H
Enthalpy (kJ/kg)	71.1	71.1	33.3	33.3	71.1	110.0	150.7	150.7
Relative Humidity (%)	39.5	2.9	20.5	100.0	100.0	14.0	2.9	39.5
Humidity Ratio (g/kg)	14.0	3.7	3.7	8.6	18.6	18.6	18.6	37.4
Dry Bulb Temp ©	35.0	61.0	23.7	11.7	23.7	61.0	100.0	53.2

Regeneration Temp ©	CoP	SCC[1]	Flow Ratio[2]
75	1.9	30.07	0.68
100	1.7	37.87	0.55

[1] Specific Cooling Capacity (kJ of cooling/kg of process air)
[2] Ratio of Regeneration to Process Air Flow Rates

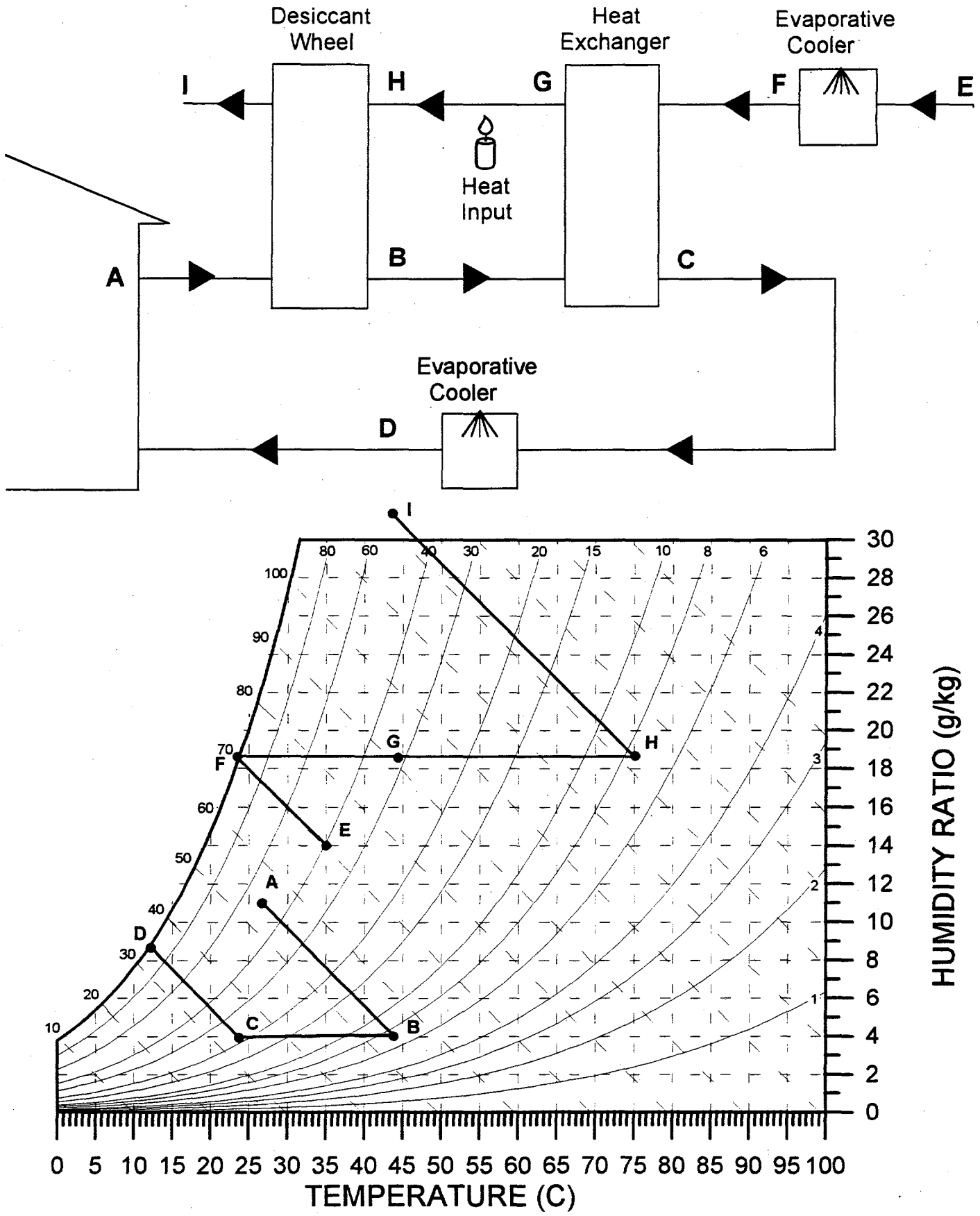

Figure 1-8. Recirculation Mode Operation

TABLE 1-4: State Points for Recirculation Cycle Shown in Figure 1-8 for Two Regeneration Temperatures

75°C Regeneration

Air Condition	A	B	C	D	E	F	G	H	I
Enthalpy (kJ/kg)	54.9	54.9	34.8	34.8	71.1	71.1	92.3	125	125
Relative Humidity (%)	50.1	7.6	23.2	100	39.5	100	32.9	7.6	50.1
Humidity Ratio (g/kg)	11	4.2	4.2	8.9	14	18.7	18.7	18.7	30.9
Dry Bulb Temp ©	26.7	43.7	23.8	12.3	35	23.8	43.7	75	44.9

. 100°C Regeneration

Air Condition	A	B	C	D	E	F	G	H	I
Enthalpy (kJ/kg)	54.9	54.9	29.3	29.3	71.1	71.1	98.0	151.1	151.1
Relative Humidity (%)	50.1	2.9	11.6	100.0	39.5	100.0	24.9	2.9	50.1
Humidity Ratio (g/kg)	11.0	2.1	2.1	7.6	14.0	18.7	18.7	18.7	39.1
Dry Bulb Temp ©	26.7	49.1	23.8	10.0	35.0	23.8	49.1	100.0	49.3

Regeneration Temp ©	CoP	SCC[1]	Flow Ratio[2]
75	1.1	20.2	0.56
100	1.1	25.6	0.44

[1] Specific Cooling Capacity (kJ of cooling/kg of process air)
[2] Ratio of Regeneration to Process Air Flow Rates

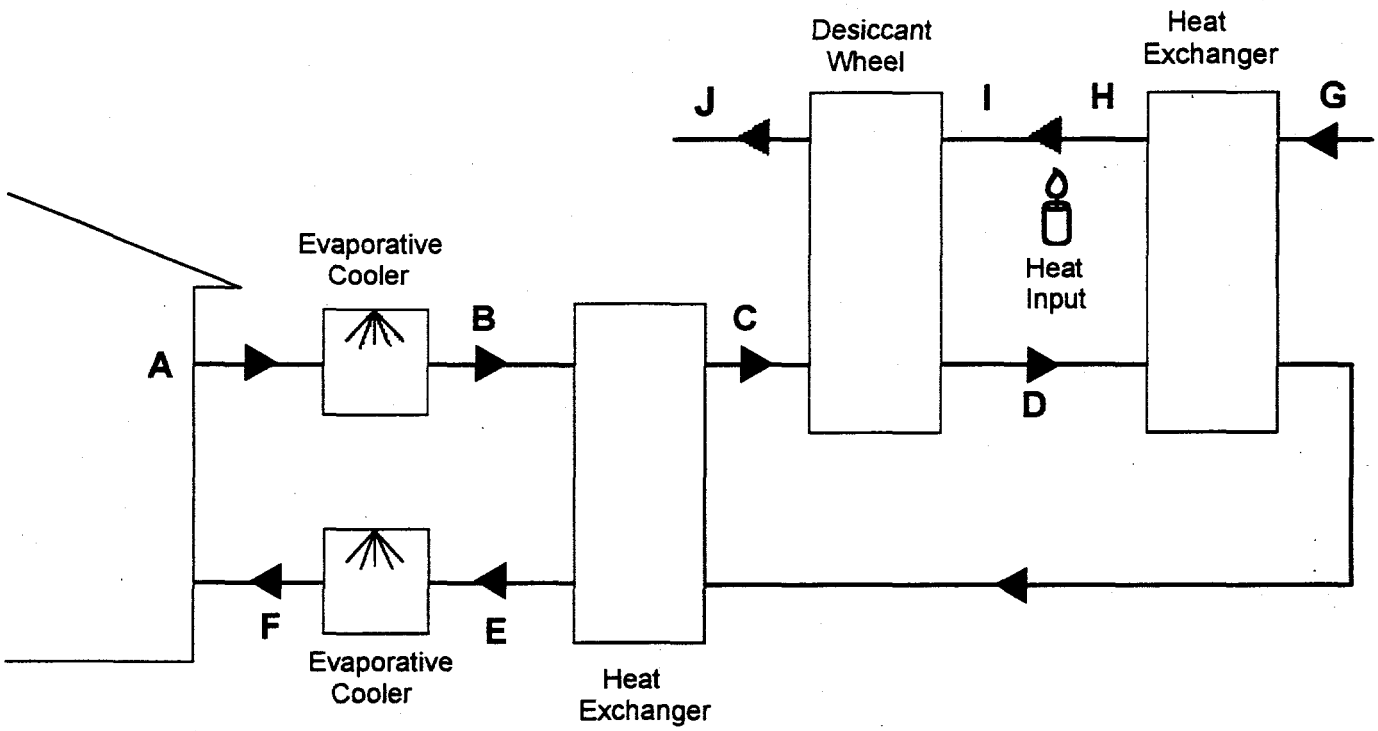

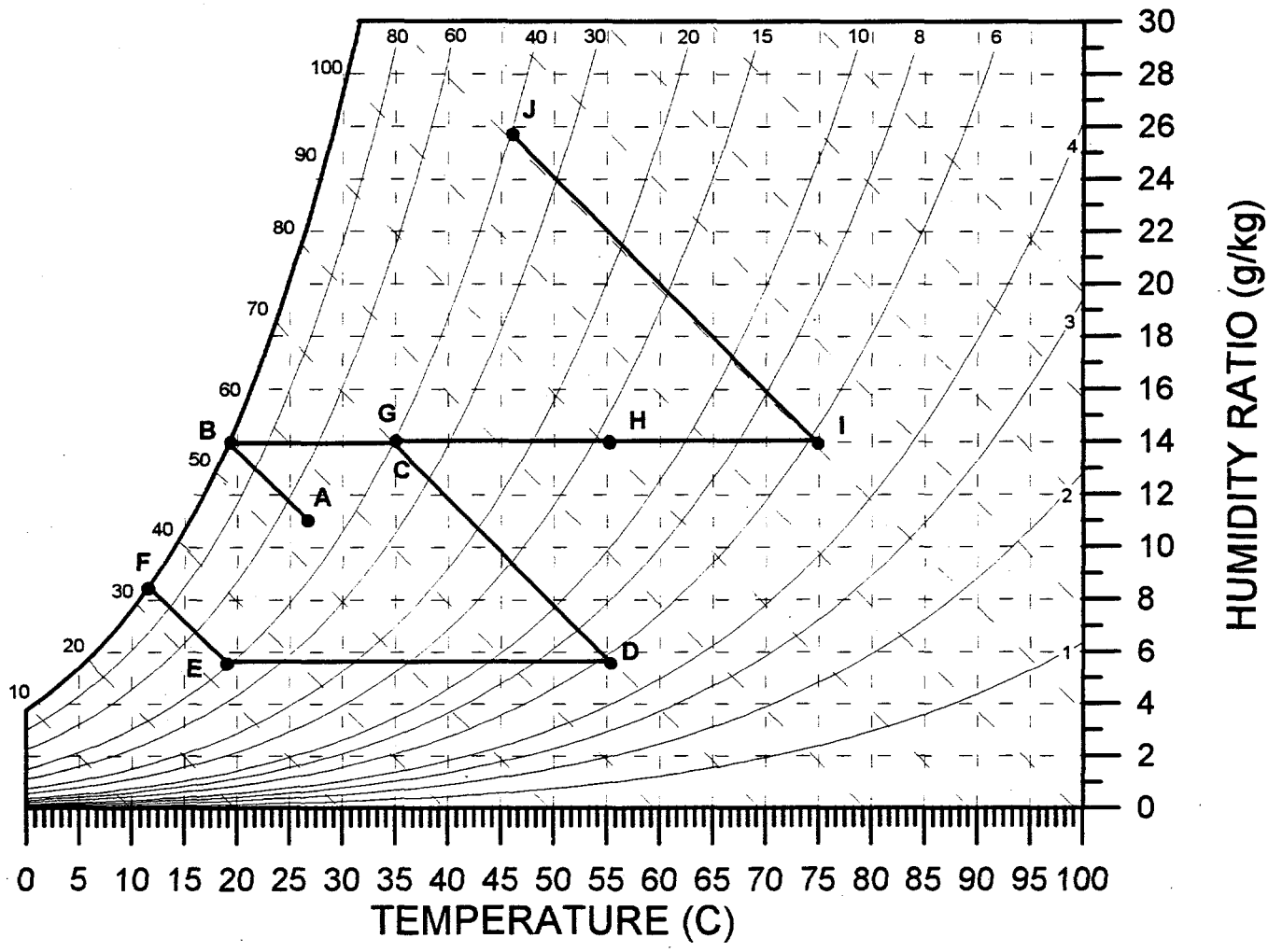

Figure 1-9. Dunkle Cycle

heat exchanged with process air that has been heat exchanged with outdoor air at state point G. This creates air at state point C. Notice that for this example, air state points C and G are identical. This would not be the case with different air starting conditions or when real effectivities were chosen for analysis. Air at state point C is then dehumidified to state point D. It is then heat exchanged with the air at state point B to create state point E. This air is then cooled by direct humidification to create the process air delivery stream at state point F. For regeneration, outdoor air at state point G is heat exchanged with the process air to create state point "H". Heat is then added to create the desiccant regeneration air at state point I. After passing through the desiccant, this air is then rejected back to the environment at state point J.

The performance results for the Dunkle cycle are shown in Table 1-5. Because the air conditions at C and G are identical, the results for this cycle are exactly the same as the ventilation cycle with no vent air credit for cooling. This tends to penalize this cycle because it requires an extra heat exchanger when compared with the other two cycles.

Liquid Desiccants: Non-Adiabatic Cycle

This cycle, which can be either ventilation or recirculation, is most often associated with liquid desiccants because the implementation is much more straightforward than for solid desiccants. The liquid-desiccant, non-adiabatic recirculation cycle is shown in Figure 1-10. Two aspects about this cycle are different from the previous examples:

1. The entire dehumidification process is conducted at the cold sink temperature.

2. Regeneration is accomplished by heating the desiccant directly.

In Figure 1-10, room air at state point A is dehumidified non-adiabatically to state point B. The heat of sorption is removed by cooling the liquid desiccant with a heat transfer medium that is at the cycle cold sink temperature, E. In this example, it is the ambient wet bulb temperature created in the cooling tower shown in Figure 1-10. State point B is determined by the regeneration state point F and the cold sink temperature, state point E using the same criterion used when analyzing solid desiccant systems. However, for a non-adiabatic system, state point B will be the intersection of the relative humidity line of state point F with the constant dry bulb temperature line of the cold sink, state point E. This air is then adiabatically humidified to state point C. The regeneration side is much the same as the dehumidification side. First, ambient air at state point D is adiabatically humidified to create the cold sink for the cycle at state point E. Second, ambient air at state point D is heated by the desiccant to state point F.

Calculating the system performance for this cycle is much different than that for the previous examples. In this example, the regeneration process is isothermal. This is accomplished by adding

TABLE 1-5: State Points for the Dunkle Cycle Depicted in Figure 1-9 for Two Regeneration Temperatures

75°C Regeneration

Air Condition	A	B	C	D	E	F	G	H	I	J
Enthalpy (kJ/kg)	54.9	54.9	71.1	71.1	34.2	34.2	71.1	92.7	112.8	112.8
Relative Humidity (%)	50.1	100.0	39.5	5.8	41.9	100.0	39.5	13.8	6.8	39.5
Humidity Ratio (g/kg)	11.0	14.0	14.0	5.8	5.8	8.8	14.0	14.0	14.0	25.7
Dry Bulb Temp ©	26.7	19.3	35.0	55.6	19.3	12.0	35.0	55.6	75.0	46.1

100°C Regeneration

Air Condition	A	B	C	D	E	F	G	H	I	J
Enthalpy (kJ/kg)	54.9	54.9	71.1	71.1	27.2	27.2	77.1	100.0	138.7	138.7
Relative Humidity (%)	50.1	100.0	39.5	2.2	22.2	100.0	39.5	9.9	2.2	39.5
Humidity Ratio (g/kg)	11.0	14.0	14.0	3.1	3.10	7.21	14.0	14.1	14.1	33.5
Dry Bulb Temp ©	26.7	19.3	35.0	62.7	19.3	9.1	35.0	62.7	100.0	51.1

Regeneration Temp ©	CoP	SCC[1]	Flow Ratio[2]
75	1.5	20.7	0.71
100	1.3	27.7	0.56

[1] Specific Cooling Capacity (kJ of cooling/kg of process air)
[2] Ratio of Regeneration to Process Air Flow Rates

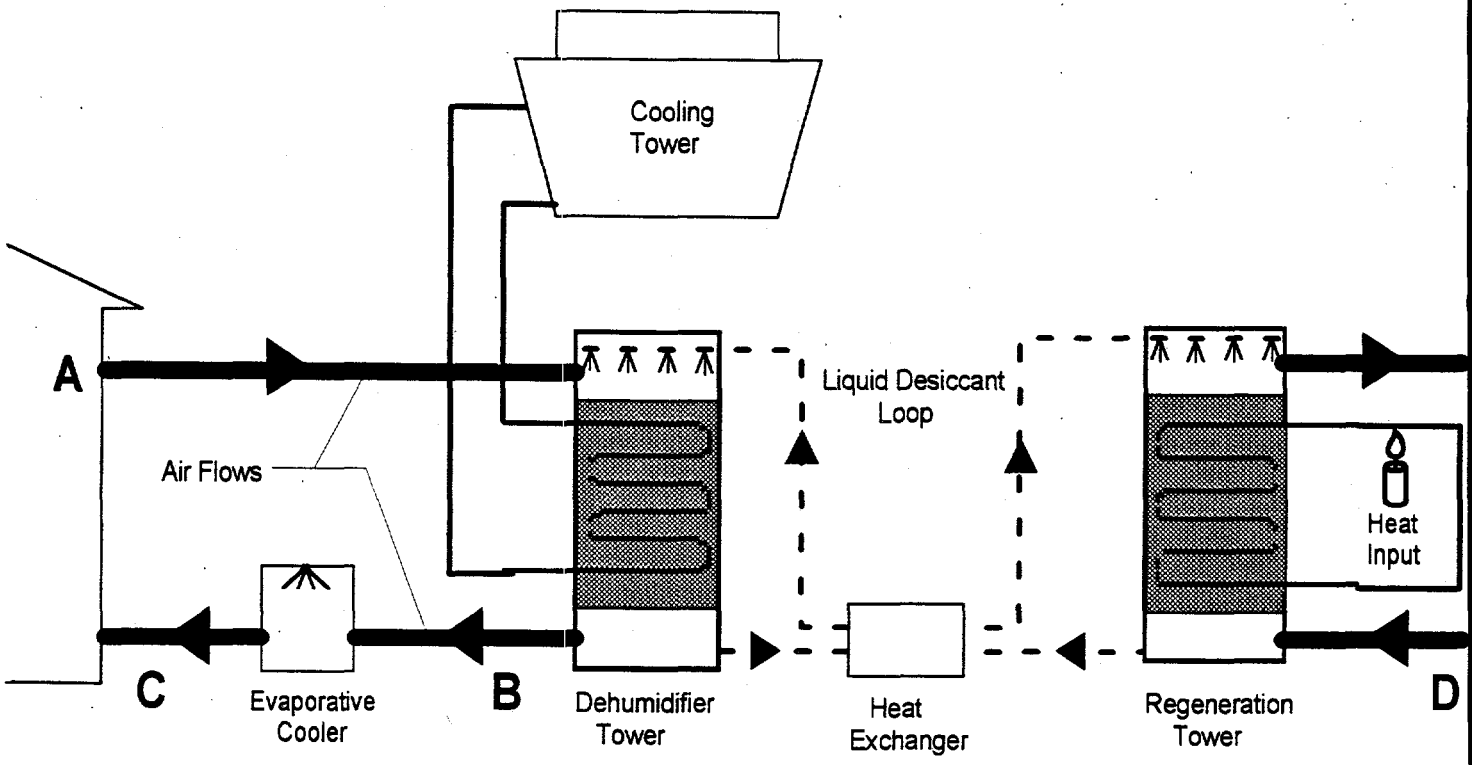

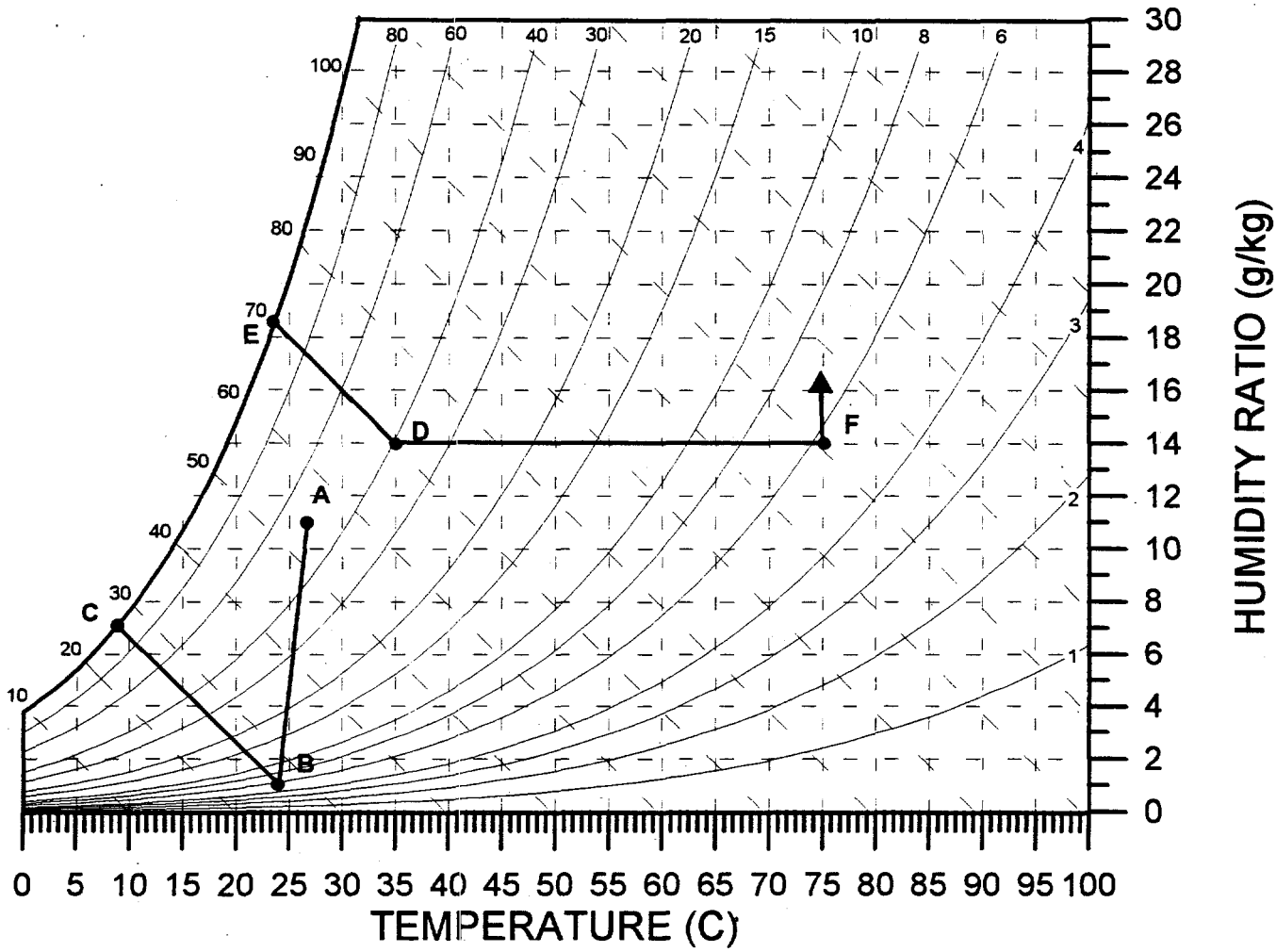

Figure 1-10. Non-Adiabatic Liquid Desiccant Cycle

heat directly to the desiccant in close proximity to the desiccant-air interface for mass transport. The air condition leaving the regenerator is not shown on Figure 1-10 because it will depend on the flow rate of air. It will take on whatever value is required to create a mass balance for water with the dehumidification side. Under the ideal conditions depicted here, there are no theoretical boundaries determining this flow rate as there were in the previous examples. This is because thermal energy is added directly to the desiccant rather than the regeneration air. Therefore, the only energy required to regenerate the desiccant (considering that the heated air can be heat exchanged with itself to create no net air heating requirements) is the heat of sorption for that water absorbed during dehumidification. This then creates a situation identical to that proposed in the initial analyses. That is, the limiting CoP will be that specified by Equation 4.0. The sensible cooling between state points A and B is "free", but the latent cooling is not. For the ARI conditions assumed in these analyses, the performance of this idealized liquid desiccant system is as follows:

CoP = 1.2
SCC = 33.5

The main difference between the performance of liquid and solid desiccant cycles is the trade-off between cooling capacity and CoP. The liquid desiccant cycle rejected the heat of sorption in order to achieve a much lower dew point for a given regeneration temperature. This lowered the CoP relative to solid desiccant cycles because the effect of the energy lost for regeneration preheat was greater than the increase in cooling capacity achieved. However, the degree of idealization for this liquid desiccant cycle is considerably greater than that for the previous solid desiccant cycles.

Another regeneration concept is theoretically possible here. For liquid desiccants, unlike solid desiccants, regeneration does not require that air be both the heat and mass transport mechanism. The previous liquid desiccant example used ambient air as the mass transport mechanism. This required that the desiccant temperature be raised to the point that its water vapor pressure equaled that of ambient air. In addition, it required that the heat of vaporization be supplied to the desiccant in order to release it. The regeneration energy required may be much less than this. Real world sorption cycles are not possible where the heat of sorption is equal to the heat of vaporization for water. If they were equal, there would be no driving potential for the process. However, in practical terms the actual heat of sorption is not much different than the heat of vaporization and is often calculated as equal in order to simplify the analyses. The heat of sorption is actually made up of two components. One is the heat of vaporization for water and the other is called the heat of solution (or the heat of wetting in the case of solid desiccants). The heat of solution is the added energy required for the water the seek the desiccant rather than the air.

For liquid desiccant systems where air is not required to be the heat and mass transport mechanism, only the heat of solution need be expended in order to separate the sorbed water from the desiccant. For the above example, where the heat of solution is zero, the CoP will be infinite, which of course is not possible. However, it can typically be one tenth that of the heat of vaporization which would yield a maximum CoP of 10. Of course, this extremely idealized performance requires at least three infinite effectiveness heat exchangers to achieve. Nonetheless,

this is still an exciting possibility for high-performance systems.

Two possible mechanisms for such a regeneration scheme have been suggested. One is to use a vapor compressor to regenerate the desiccant. In this scheme the vapor pressure over the desiccant is reduced by a compressor and the heat of condensation of the rejected water vapor is recuperated into the desiccant by the pressure difference across the compressor. The other is to develop a desiccant where the water absorbed becomes miscible at some threshold temperature. Under these conditions the water can be removed from the desiccant by skimming rather than evaporation and the only external energy required would be the heat of solution added during the separation process.

Effects of Ambient Air Conditions on System Performance

Because these desiccant systems are open-cycle (i.e., the working fluids are open to the atmosphere), their performance will be dependent upon the thermodynamic state of the air being processed. Many factors will influence how changing air conditions affect performance. Indoor conditions are relatively fixed by standardized definitions of comfort. However, outdoor air conditions, both temperature and humidity, can fluctuate a great deal while the system still maintains constant indoor air conditions. This section of the report will examine the effects of outdoor air conditions (temperature and humidity) on the maximum theoretical performance of several solid desiccant cooling cycles

Ambient Air Temperature

Figure 1-11 shows psychometrically, the effect of lowering outdoor air temperature. For this example, the modified ventilation cycle is shown. Instead of the process ABCD for the dehumidification process, the process A'B'C'D' results when the outdoor air temperature drops from A to A'. Also, instead of regeneration process AEFGH, A'E'F'G'H' results from the same change in outdoor air temperature. An overall view of Figure 1-11 shows that as outdoor air temperature drops, the dehumidification air stream becomes drier and cooler, all other conditions being equal.

Figures 1-12 though 1-19 (in Appendix A) show the effects of ambient temperature on CoP and specific cooling capacity for the ventilation cycle (with and without vent credit), the modified ventilation cycle, and the recirculation cycle. Each of these configurations is presented for two regeneration temperatures, 75° and 100°C. An interesting result is that there is no consistent effect on performance for all cycles simulated. These results show that if outside air is not required for the building load (i.e., the recirculation and ventilation with no vent credit cycles), cooling capacity is always reduced with increasing ambient temperature. In addition, this effect is more pronounced as regeneration temperature decreases. CoP, on the other hand, is minimally influenced in the vent cycle, whereas it is significantly reduced in the recirculation cycle as ambient air temperature increases.

When outside air is required for the application, increases in ambient air temperature increase both cooling capacity and CoP. Both the ventilation cycle with vent credit and the modified ventilation cycle show significantly improved performance as ambient air temperature increases and

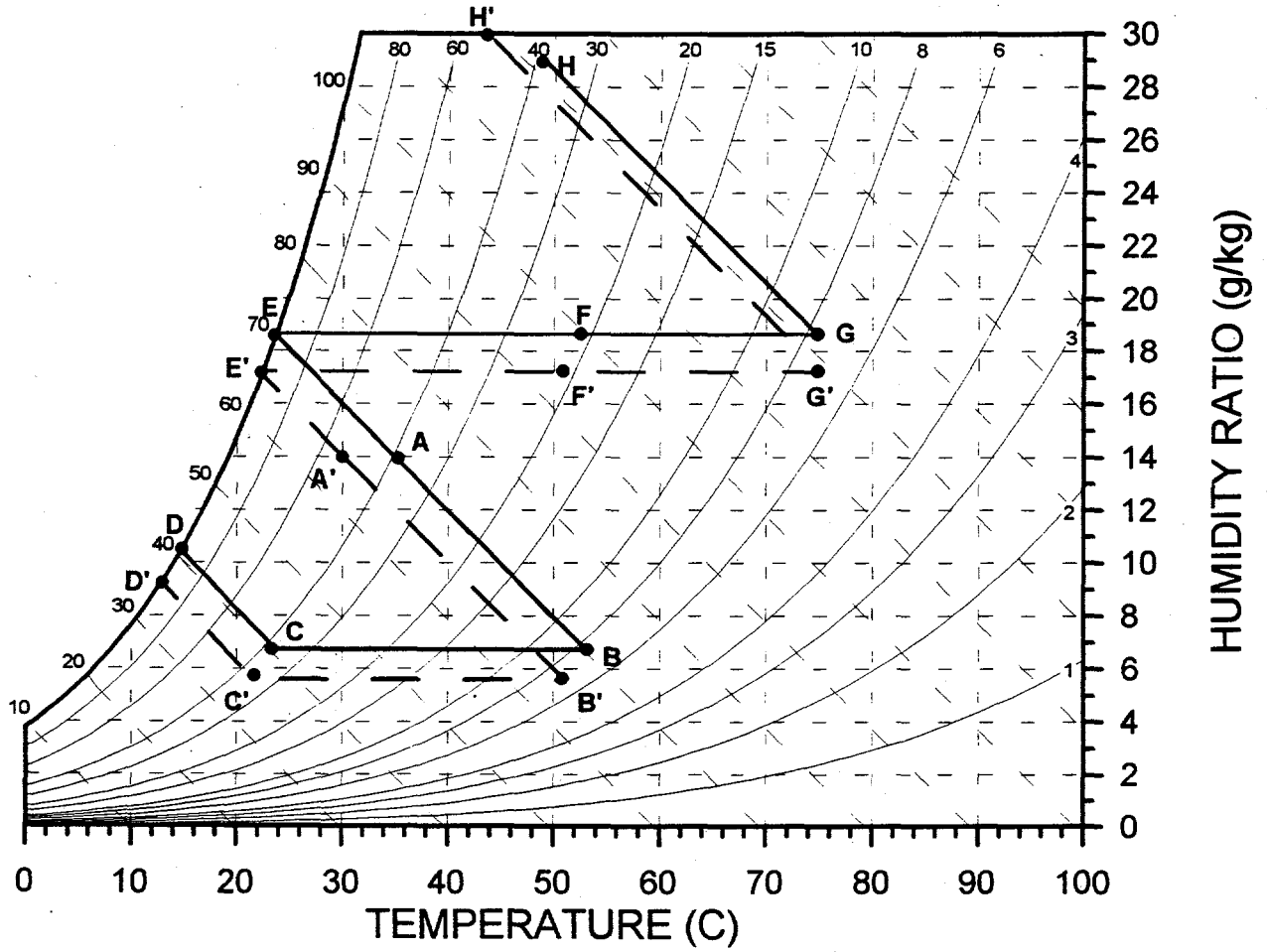

FIGURE 1-11. Modified vent cycle as a function of dry bulb temperature.

decreased performance as ambient air temperature decreases.

Ambient Air Humidity

Figure 1-20 shows, psychrometrically, the effect of increasing outdoor air humidity. For this example, the modified ventilation cycle is again shown. Instead of the process ABCD for the dehumidification process, the process A'B'C'D' results when the outdoor air humidity increases from A to A'. Also, instead of regeneration process AEFGH, A'E'F'G'H' results from the same change in outdoor air humidity. An overall view of Figure 1-20 shows that as outdoor air humidity increases, the dehumidification air stream becomes moister and warmer, all other conditions being equal.

Figures 1-21 through 1-28 (in Appendix A) show the effects of ambient humidity ratio on CoP and Specific Cooling Capacity for the same cycles simulated in the previous section. The same general results were obtained for ambient air humidity as were obtained for ambient air temperature. That is, as outdoor air humidity increases, performance is generally reduced when dealing with cycles that relate only to indoor air. On the other hand, performance is generally improved for those cycles

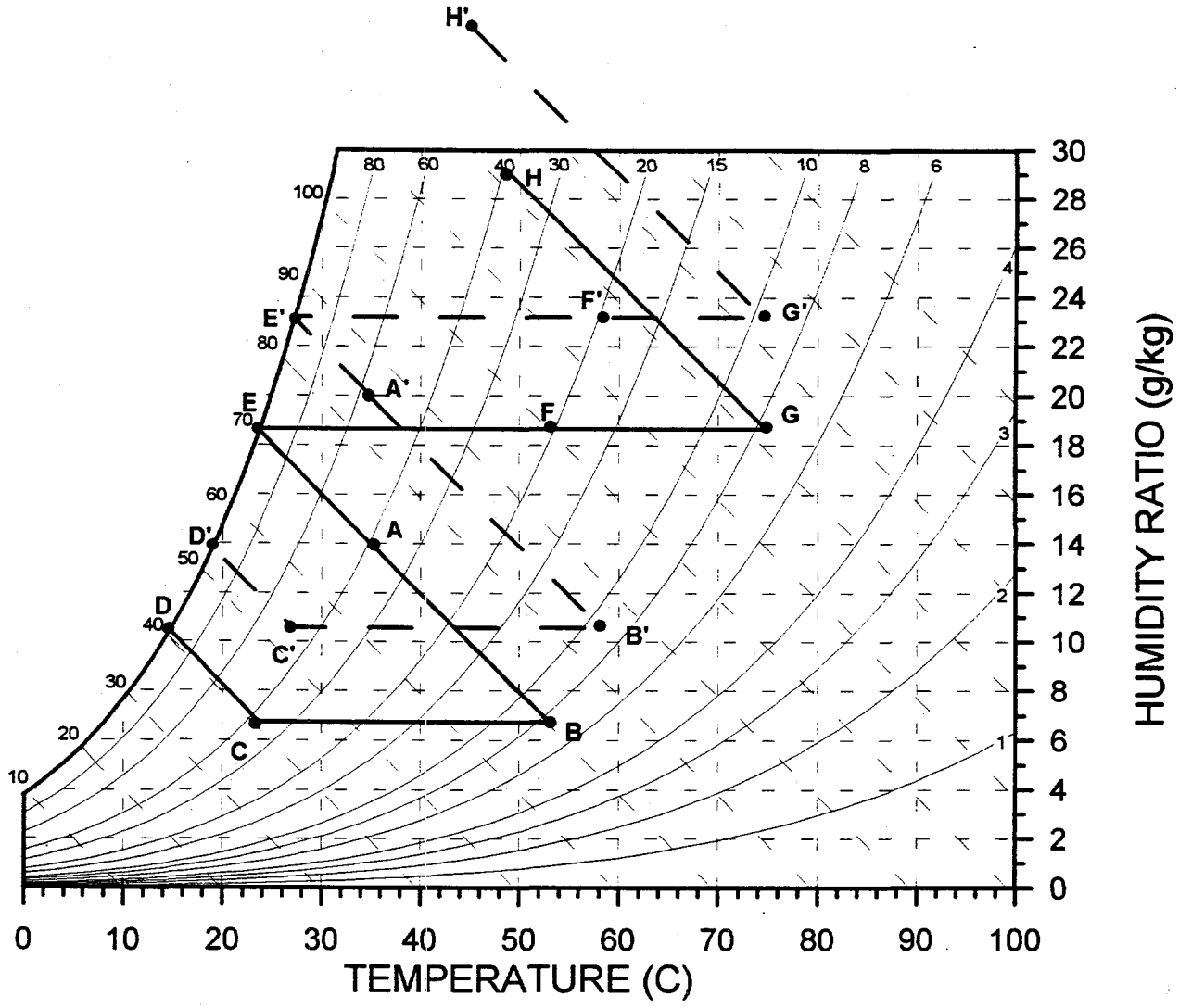

Figure 1-20. Modified vent cycle as a function of humidity ratio.

based on processing outdoor air.

Of particular note is Figure 1-23. The ventilation cycle with indoor air being available as a heat sink can yield incredibly high CoP's at the moderate regeneration temperature of 75°C. This is because the dehumidification process line almost coincides with the regeneration process line. Regeneration preheat is very nearly the regeneration condition, so very little regeneration energy is required. In essence, the cooling capacity is generated by indirect evaporative cooling and the desiccant wheel acts as a moisture exchange device. These two processes combine to yield the incredibly high CoP shown in Figure 1-23. Of course, under these conditions, there is virtually no latent capacity to the cycle just as there would be none with an enthalpy exchange device.

Conclusions

Some very significant results concerning the basic nature of desiccant cooling cycles have been generated by this idealistic investigation. The most significant are as follows:

1. CoPs greater than one are possible with desiccant cooling cycles for two major reasons:

    a. Evaporative cooling is used to reduce the cold sink temperature; this increases cooling capacity.

    b. The heat of sorption can be recouped and used as preheat for the regeneration process.

2. The regeneration and dehumidification processes are inherently unbalanced. This creates the situation that not all of the heat of sorption is available as preheat for the regeneration process. It is most efficient, for the ideal conditions assumed, to heat only that air required for regeneration and reject the excess sorption energy.

3. Desiccant cooling systems achieve higher performance when processing outdoor air than indoor air. This higher performance is significant if the outdoor air is required by the application.

4. Liquid desiccant cycles are inherently different from solid desiccant cycles in that air is not required as a heat and mass transfer mechanism for regeneration. This creates several scenarios for performance differences:

    a. For conventional desiccants, liquid systems will achieve higher specific cooling capacities at a lower thermal CoP.

    b. Extremely high thermal CoPs are possible with liquid desiccants if a system is employed to decouple air from regeneration.

5. Desiccant cycles are most appropriate where outside air is required by the application. As ambient temperature and humidity increase, desiccant cycles based on room air conditions degrade in performance. However, those cycles which use outdoor air as the basis of operation increase in performance as outside air temperature and humidity increase.

SECTION II: DETERMINATION OF THE EFFECTS OF PHYSICAL PROPERTIES ON SYSTEM PERFORMANCE

Important determinants of the thermodynamic performance of desiccant cooling and dehumidification systems are the sensitivity to finite heat and mass transfer rates, and physical parameters such as heat capacity and sorption heats. All of these phenomena will deleteriously affect the performance predicted in the previous analyses. The specific parameters that will be examined here are:

1. Heat exchanger effectiveness.
2. Evaporative cooler effectiveness.
3. Desiccant wheel effectiveness.
4. Desiccant heat of sorption.
5. Desiccant wheel heat capacity.

In addition, two other subjects of interest concerning the use of desiccants are included in this section. The first is to examine the ramifications of low regeneration temperatures on system performance as well as its effect on system design. The second is to examine the use of desiccants in systems that exchange enthalpy between adjacent air streams. This technology is important for building applications requiring ventilation air.

Heat Exchanger Effectiveness

The performance of the sensible heat exchanger is critically import to the successful operation of the desiccant cooling system. The heat exchanger not only cools the process air stream, thereby providing cooling capacity, but also preheats the regeneration air stream, thereby reducing external energy inputs and increasing CoP. Figure 2-1 shows graphically the effect of heat exchanger effectiveness. This is the ventilation mode operating with ARI air conditions as depicted in Figure 1-6. As the heat exchanger effectiveness decreases, the process air outlet changes from C-D to C'-D', and C"-D". Notice how this change affects the cooling capacity of the cycle. As explained in Section 1, the cooling capacity will be proportional to the enthalpy difference between the processes air outlet and the indoor air (or the outdoor air if ventilation air is required). As the heat exchanger outlet on the process side moves to the right (shown as C' and C") with decreasing heat exchanger effectiveness, this enthalpy difference decreases and hence so does cooling capacity.

On the regeneration side, as the heat exchanger outlet on the regeneration side moves to the left (shown as G' and G") with decreasing heat exchanger effectiveness, the externally-supplied energy required to achieve air condition H (the regeneration condition) increases and hence decreases CoP.

Figures 2-2 through 2-17 (in Appendix B) quantify the effect that heat exchanger effectiveness has on system performance. Figures 2-2 through 2-5 depict the ventilation cycle, Figures 2-6 through 2-9 depict the recirculation cycle, Figures 2-10 through 2-13 compare the ventilation and recirculation cycles, and Figures 2-14 through 2-17 depict the vent-vent cycle.

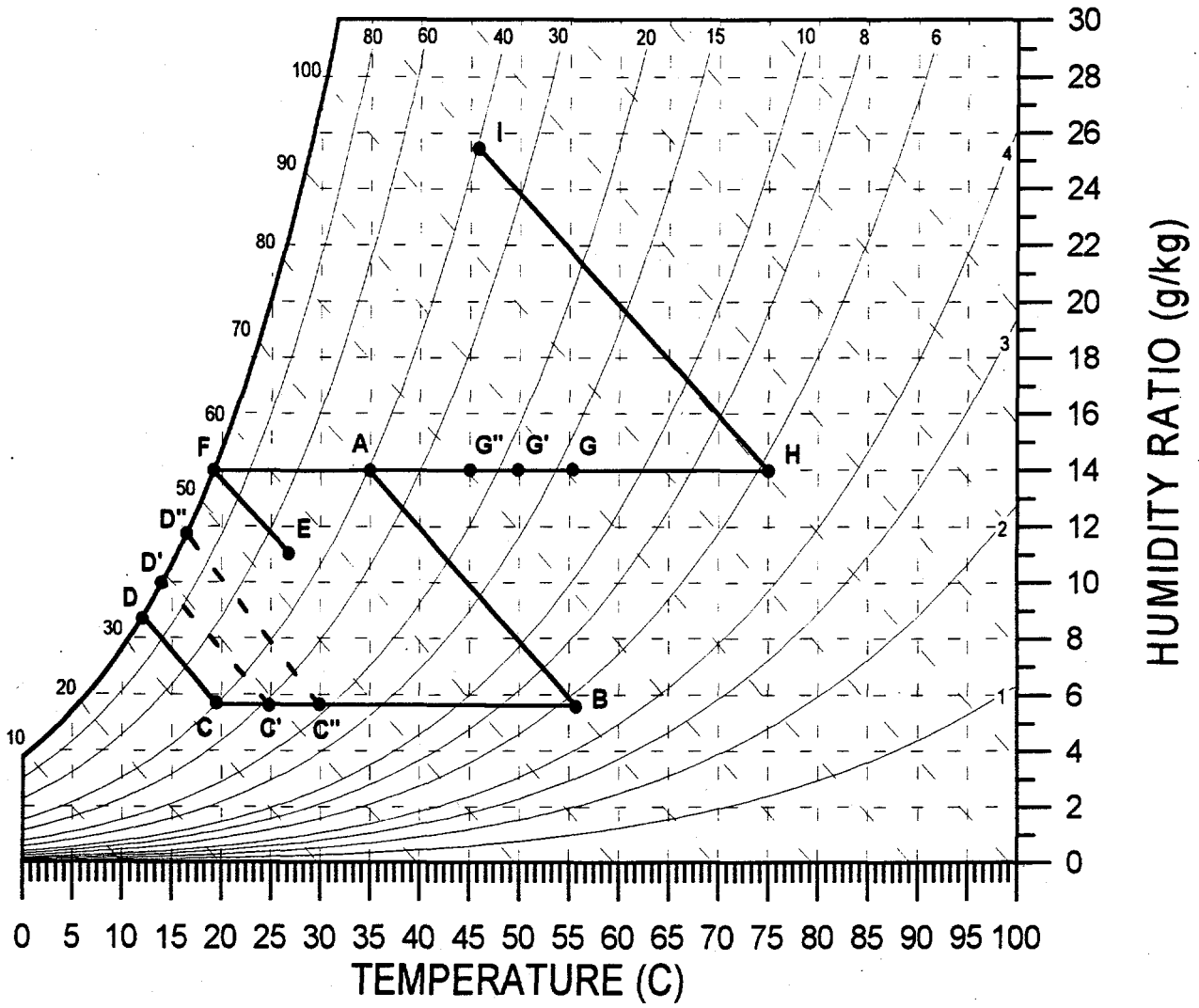

Figure 2-1. Psychrometric representation of the effect of heat exchanger effectiveness.

The major observations to be made from these figures are as follows:

1. The reduction in performance is significant when heat exchangers of reasonable effectiveness are incorporated.

2. The CoP is always affected more than specific cooling capacity regardless of the cycle chosen. This is because the heat exchanger performance affects not only cooling capacity, but also the energy required for regeneration. Therefore, the numerator of CoP decreases while the denominator increases.

3. The ventilation cycle is more sensitive to heat exchanger effectiveness than the recirculation cycle.

4. The vent-vent cycle is less sensitive than the ventilation cycle, but slightly more than the recirculation cycle.

5. For the ventilation cycle, regeneration temperature is a significant variable in relation to heat exchanger effectiveness, which is less affected by higher temperatures than lower temperatures. The effects on the recirculation cycle do not seem to be functions of regeneration temperature.

6. The performance of the recirculation cycle equals that of the ventilation cycle at a heat exchanger effectiveness between 0.90 and 0.85, regardless of regeneration temperature. The one exception is cooling capacity at 75°C regeneration, where the break-even effectiveness was over 0.95.

7. The high performance offered by the ventilation cycle (when vent air is not required) requires a heat exchanger with very high effectiveness.

In reality, achieving air-to-air heat exchanger efficiencies over 90% has proven to be impractical. The equipment becomes enormously large for two reasons. One is the surface area required; the other is the very low air face velocities required. Presently, efficiencies in the range of 85 to 87% appear feasible; however, heat exchangers are still the most problematical area of open-cycle desiccant cooling systems.

Evaporative Cooler Effectiveness

Two evaporative coolers are generally employed in all of the solid desiccant cycles shown (see Section 1). One is used to cool the process air adiabatically and the other is used to create a cold sink for the cycle. Notice that the evaporative cooler used to cool the process air does not significantly change its enthalpy. Therefore, the effectiveness of this evaporative cooler will have a negligible effect on both CoP and Specific Cooling Capacity. It will serve only to determine the Sensible Heat Ratio (SHR) of the system. If this effectiveness is 1.0, then the SHR will be a maximum (maximum sensible cooling). If this effectiveness is 0.0, then the SHR will be a minimum (maximum latent cooling).

Figure 2-18 shows a psychrometric representation of the effect of the cold sink evaporative cooler effectiveness on desiccant cooling system performance. This figure shows the same cycle and environmental parameters as Figure 2-1. Notice as the evaporative cooler effectiveness decreases, air at condition E is only humidified to condition F' instead of F. This change to the cycle effects both the process and regeneration cycles. Because the regeneration air is drier, air condition H' results in a slightly lower relative humidity than air condition H at the same regeneration temperature. This allows the process air to become drier and hotter (B' vs. B). Because B' is hotter, the regeneration preheat (G') is also hotter. On the negative side, because the reduced evaporative cooler effectiveness results in a lower cold sink temperature (F'), the process outlet, C'-D', has a higher enthalpy than C-D, which results in a lower cooling capacity.

Finally, although not obvious from the chart, the change in moisture loading between H' and I' may be different than between H and I, which would change the amount of regeneration air required and hence affect CoP. Only quantitative analyses will determine if this effect is significant.

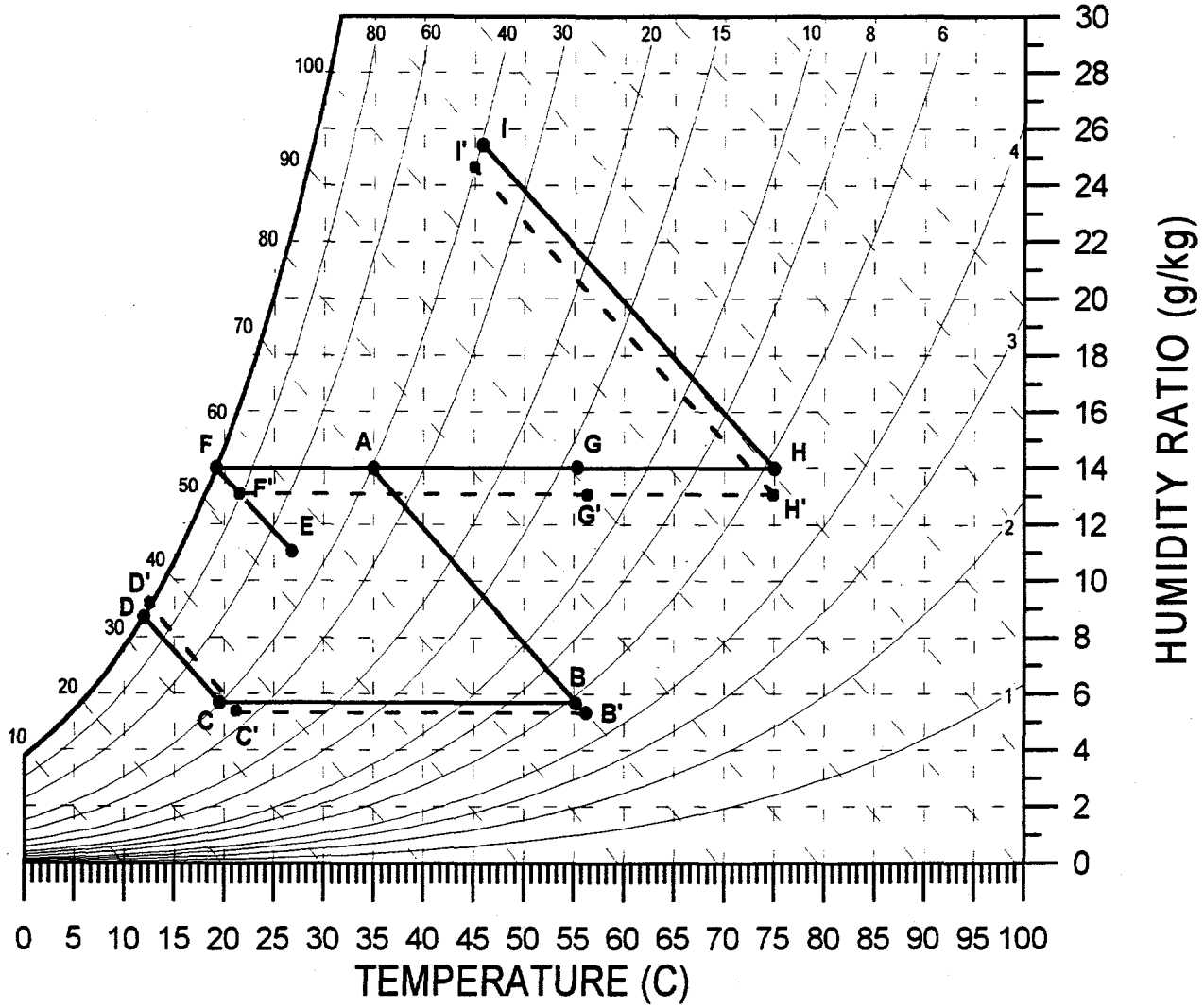

Figure 2-18. Psychrometric representation of the effect of evaporative cooler effectiveness.

Figures 2-19 through 2-34 (in Appendix B) quantify the effect of evaporative cooler effectiveness on system performance for two regeneration temperatures and three cycles described in Section 1. Figures 2-19 through 2-22 show the ventilation cycle, Figures 2-23 through 2-26 show the recirculation cycle, Figures 2-27 through 2-30 compare the ventilation and recirculation cycles, and Figures 2-31 through 2-34 show the vent-vent cycle.

The major observations to be made are as follows:

1. The effect of evaporative cooler effectiveness on system performance is much less than that of the sensible heat exchanger, regardless of cycle or regeneration temperature.

2. The recirculation cycle is affected much more than either the ventilation or vent-vent cycles.

3. The effect of regeneration temperature is not strong, although there may be some differences below an effectiveness of 0.75. For almost all practical applications, an effectiveness of 0.75 would be easily attainable.

Table 2-1 shows the performance of the ventilation cycle described in Table 1-2 from the previous section with the cold sink evaporative cooler effectiveness equal to 90%. Comparing Tables 1-2 and 2-1 yields the following conclusions:

1. The results agree with those ascertained by examining the psychrometric chart of effectiveness.

2. Quantitatively, diminished cold sink evaporative cooler effectiveness reduces cooling capacity for both regeneration temperatures. However, only CoP is reduced at the 75°C regeneration temperature. At 100°C, CoP remained the same (within one decimal point). The flow ratio (regeneration to process) stayed the same regardless of regeneration temperature.

Desiccant Matrix Effectiveness

Figure 2-35 shows the effect of desiccant matrix effectiveness on the desiccant psychrometric process. The desiccant matrix effectiveness can influence both the dehumidification and regeneration processes. For the dehumidification process, air is now dehumidified to condition B' instead of condition B. Air condition C' still attains the same temperature as C, but is of higher humidity because of the desiccant matrix ineffectiveness. The end result is that process C'-D' has a higher enthalpy than process C-D so cooling capacity is reduced.

On the regeneration side, regeneration condition H is still required to produce condition B'. However, because of the lower temperature of B', condition G' has a lower temperature than G. This results in more energy required to produce the regeneration condition H so CoP is lowered. Also, the regeneration exit condition, I', has a lower humidity and higher temperature than condition I. The lower humidity may change the ratio of air flows between regeneration and dehumidification, and the higher temperature will lower CoP as discussed in the thermodynamic availability arguments presented in the previous section.

TABLE 2-1: State Points for Ventilation Cycle of Table 1-2 for a Cold Sink Evaporative Cooler Effectiveness of 90%.

75°C Regeneration

Air Condition	A	B	C	D	E	F	G	H	I
Enthalpy (kJ/kg)	71.1	71.1	34.7	34.7	55.0	55.0	91.9	111.8	111.8
Relative Humidity (%)	39.5	5.6	49.5	100.0	50.1	100.0	13.3	5.6	39.5
Humidity Ratio (g/kg)	14.0	5.7	5.7	8.9	11.0	14.0	14.0	14.0	25.4
Dry Bulb Temp ©	35.0	55.8	20.0	12.2	26.7	20.0	55.8	75.0	45.8

100°C Regeneration

Air Condition	A	B	C	D	E	F	G	H	I
Enthalpy (kJ/kg)	71.1	71.1	27.7	27.7	55.0	55.0	99.2	138.4	138.4
Relative Humidity (%)	39.5	2.1	20.8	100	50.1	100	9.6	2.1	39.5
Humidity Ratio (g/kg)	14.0	3.0	3.0	7.3	11.0.	14.0	14.0	14.0	33.3
Dry Bulb Temp ©	35.0	62.8	20.0	9.3	26.7	20.0	62.8	100.0	51.0

Regeneration Temp ©	With Vent Credit		Without Vent Credit		
	CoP	SCC[1]	CoP	SCC	Flow Ratio[2]
75	2.5	36.4	1.4	20.3	0.71
100	2.0	43.4	1.3	27.3	0.56

[1] Specific Cooling Capacity (kJ of cooling/kg of process air)
[2] Ratio of Regeneration to Process Air Flow Rates

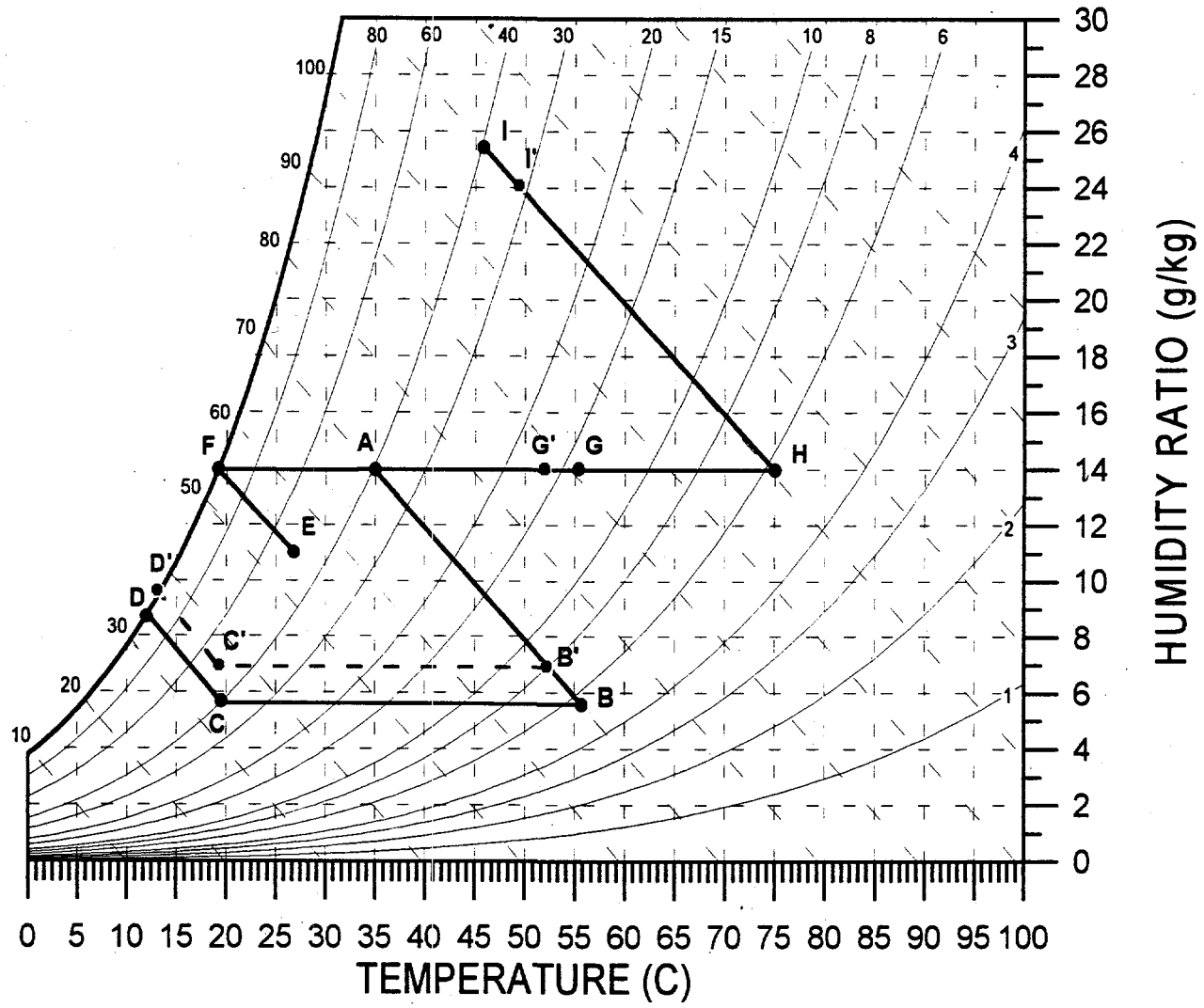

Figure 2-35. Psychrometric representation of the effect of desiccant matrix effectiveness.

The concept of desiccant matrix effectiveness is not limited to only heat and mass transfer considerations. Although this is one aspect to the phenomenon, a much more important one is the effect of isotherm shape. As has been previously shown by this author, attaining the output of a desiccant matrix that is equivalent to the thermodynamic optimum is directly tied to the desiccant matrix's ability to contain heat and mass transfer wavefronts during both dehumidification and regeneration processes. Figure 2-36 is an idealized picture of a desiccant sorption process with no heat capacity other than the air and water. Shown is the air humidity as a function of internal desiccant matrix position. During any sorption process, the air must make a transition from the thermodynamic properties of the entering air to those of the exiting air. If the desiccant has been preconditioned by a previous process (either dehumidification or regeneration), the exiting air will be at a significantly different temperature and humidity than that entering. In the case of the dehumidification process, the outlet air condition should be the driest possible for the regeneration conditions of the desiccant. An important aspect of this transition in air properties is called the mass

transfer zone (MTZ). As shown in Figure 2-36, the MTZ is the length of desiccant matrix required for the air to transist between its inlet and outlet conditions. This is important for desiccant cooling and dehumidification applications because the MTZ can be a significant fraction of the overall desiccant matrix length.

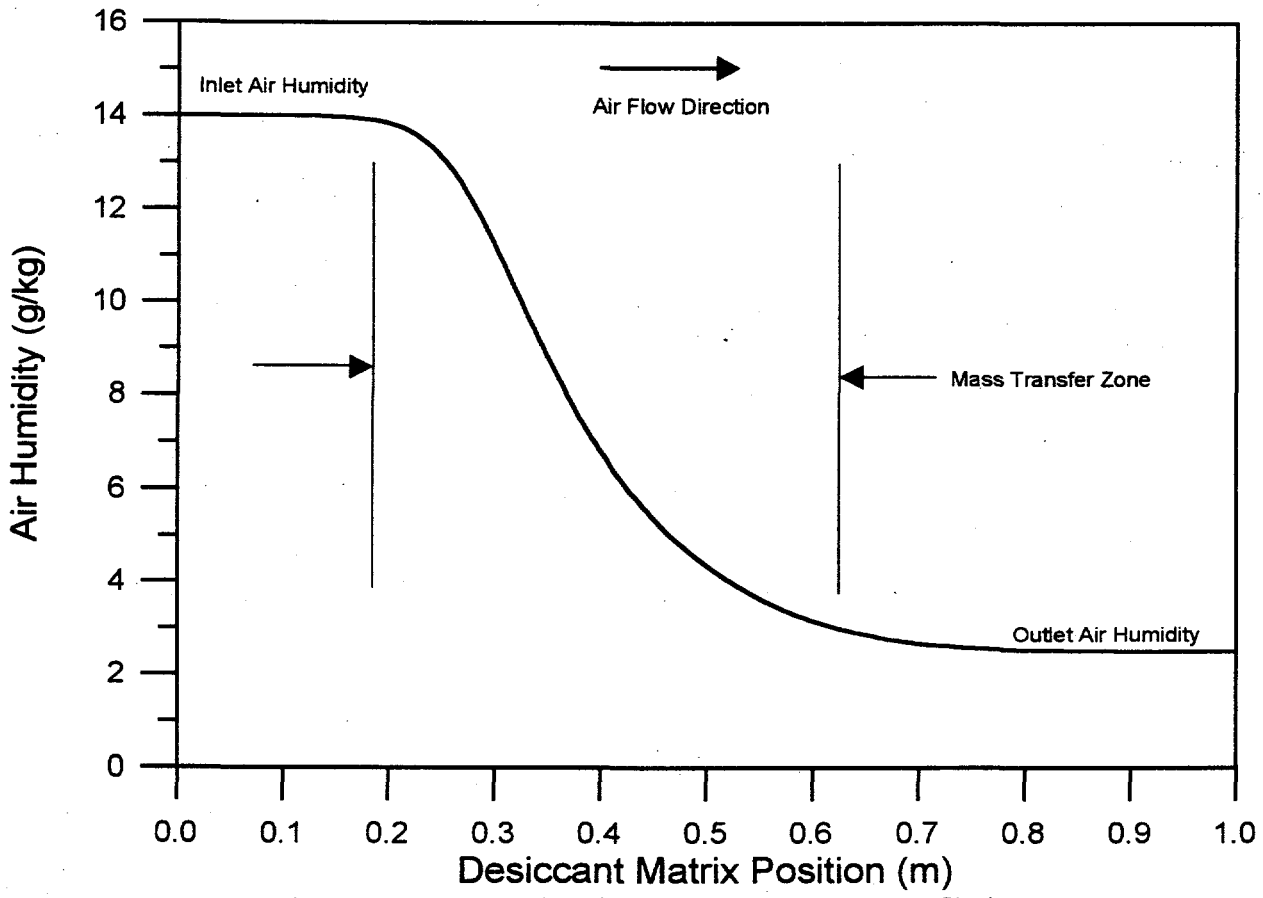

Figure 2-36. Internal desiccant matrix humidity profile.

Figures 2-37 and 2-38 demonstrate this principle. Figure 2-37 shows the air humidity as a function of position within the desiccant matrix for a typical dehumidification process for two common desiccants, silica gel and molecular sieve. Figure 2-38 shows the regeneration process for the same two desiccants. With silica gel in the dehumidification mode and with molecular sieve in regeneration mode, the MTZ is extremely wide. Unlike the chemical processing industry, where desiccant beds can be three meters thick or more, space conditioning applications require much smaller desiccant depths because the electrical consumption of the equipment must be controlled within very stringent limits. This is because every function of a desiccant used for space conditioning can also be accomplished by electric vapor-compression equipment. Therefore, the electrical consumption of a desiccant-based system must be much smaller (by at least a factor of three) than that of an equivalent electric vapor-compression system. This limits packed bed desiccant matrices to about 5 centimeters in depth and laminar flow channel matrices to between 15 and 30 centimeters. As can be seen in Figures 2-37 and 2-38, the MTZ for both silica gel and molecular sieve exceeds the

entire desiccant matrix length (one meter in this example) for either the regeneration or dehumidification processes. The end result is that even with no heat or mass transfer resistance the effectiveness of the desiccant matrix for commercially-available desiccants cannot be 100%.

The preceding example is the impetus behind the development of the Type 1M desiccant concept. Figure 2-39 shows the normalized air humidity profiles for a Type 1M desiccant in both dehumidification and regeneration modes. Notice that the MTZ for the Type 1M can fit nicely within the confines of a reasonable desiccant matrix depth for both the dehumidification and regeneration processes. This desiccant can, therefore, theoretically achieve a desiccant matrix effectiveness of 100%.

Table 2-2 shows the desiccant cooling cycle state points and performance parameters for the cycle shown in Table 1-2 for a desiccant matrix efficiency of 90% for both the dehumidification and the regeneration processes. For these analyses, the desiccant matrix effectiveness is defined by the approach to the maximum attainable relative humidity. Another approach could be to define effectiveness relative to humidity ratio. The proper definition is relative humidity because the desiccant isotherm, and therefore the mass transport potential, is a nearly singular function of relative humidity. This definition makes desiccant matrix effectiveness non-linear with respect to temperature and humidity ratio. This non-linearity results in some rather interesting results that will be discussed in detail later in this section.

Comparing Tables 1-2 and 2-1 yields the following conclusions:

1. The results agree with those ascertained by examining the psychrometric chart of effectiveness.

2. For the ventilation cycle depicted, achieving the vent credit is extremely important when dealing with finite desiccant matrix effectiveness. This effect is exacerbated by lower regeneration temperatures.

Figures 2-40 through 2-55 (in Appendix B) quantify the effect of desiccant matrix effectiveness on system performance for two regeneration temperatures and three cycles described in Section 1. Figures 2-40 through 2-43 show the ventilation cycle, Figures 2-44 through 2-48 show the recirculation cycle, Figures 2-49 through 2-51 compare the ventilation and recirculation cycles, and Figures 2-52 through 2-55 show the vent-vent cycle.

The major observations to be made from these figures are as follows:

1. Recirculation cycle performance is more influenced by desiccant matrix effectiveness than the ventilation cycle.

2. System performance at higher regeneration temperatures is more adversely affected regardless of the cycle configuration.

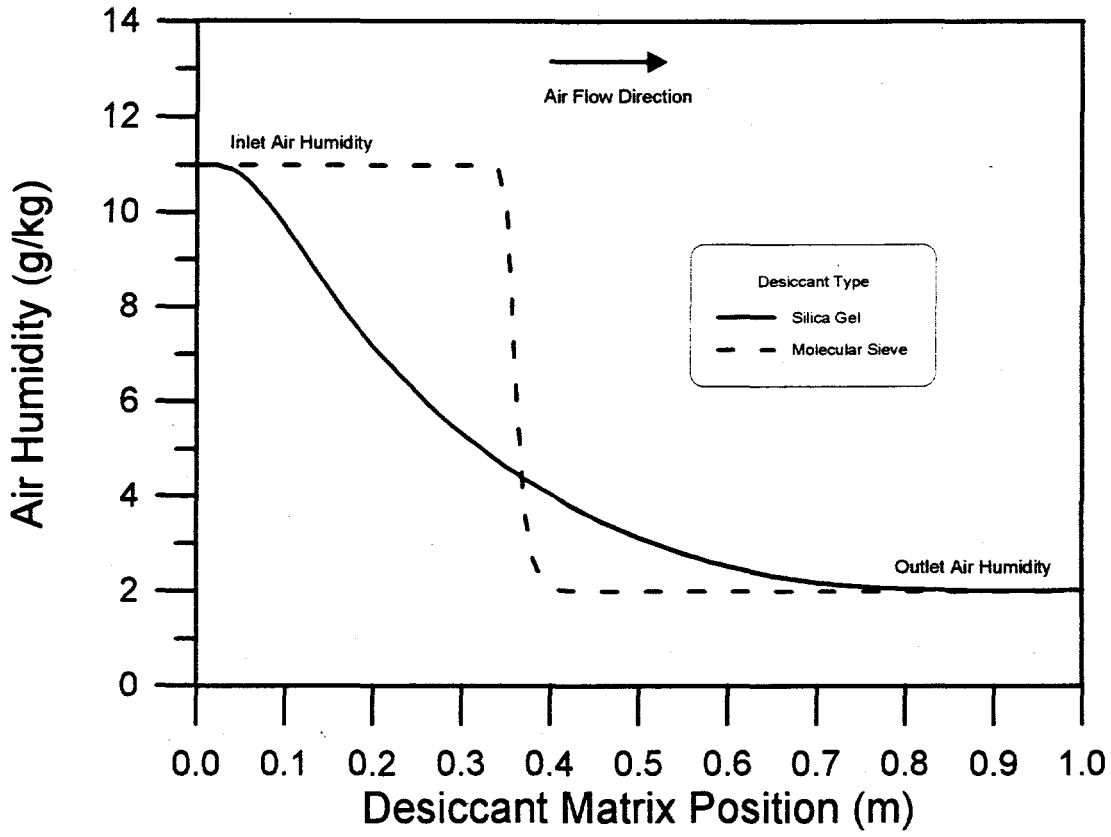

Figure 2-37. Internal desiccant matrix humidity profiles; dehumidification

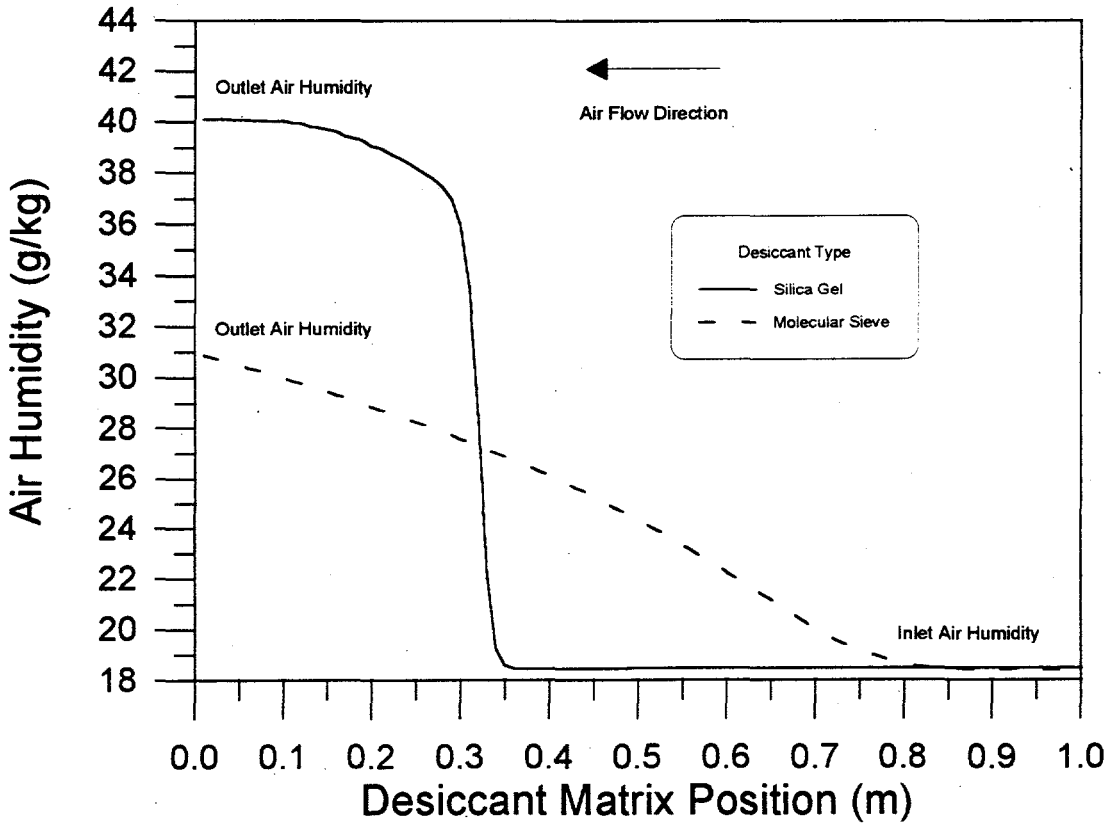

Figure 2-38. Internal desiccant matrix humdity profiles; regeneration

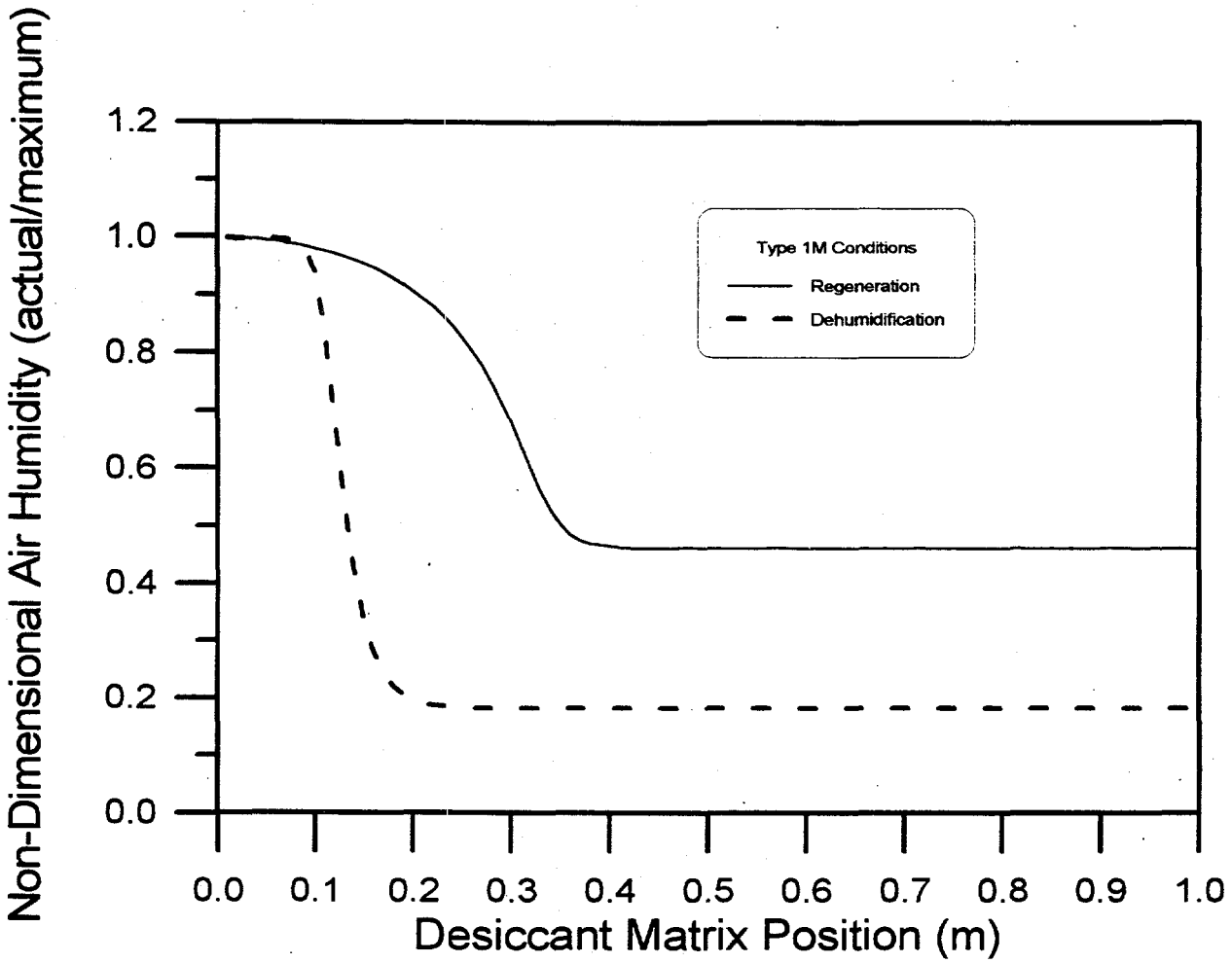

Figure 2-39. Internal desiccant matrix humidity profiles; Type 1M desiccant.

3. Specific cooling capacity is generally affected more than CoP, with the recirculation cycle affected more than the ventilation cycle.

4. The vent-vent cycle reacts generally between the recirculation and ventilation cycles.

5. Desiccant matrix effectiveness has a major effect on system performance.

The preceding analyses have dealt with the situation where both the dehumidification and regeneration processes exhibit the same desiccant matrix effectiveness. As was shown previously, the effect of isotherm shape is generally not the same for both the dehumidification and regeneration processes. To examine this behavior in more detail, Figures 2-56 through 2-58 show the effects on system performance where regeneration and dehumidification processes are varied independently of one another. Figure 2-56 shows the thermal CoP of the ventilation cycle, Figure 2-57 shows the CoP of the recirculation cycle, and Figure 2-58 shows the vent-vent cycle. The recirculation cycle shows

equal sensitivity to both the dehumidification and regeneration desiccant matrix effectiveness. However, the ventilation cycle exhibits a much greater sensitivity to the dehumidification effectiveness than does the regeneration process. This is because the relative humidity lines are further apart as the air temperature increases. Therefore, there is a greater effect on humidity ratio than when these lines are closer together. The really interesting behavior is exhibited by the vent-vent cycle in Figure 2-58. System CoP actually increases after an initial decrease in desiccant dehumidification effectiveness. The cause of this seemingly irrational behavior is mostly a function of the definition of the desiccant matrix effectiveness.

Table 2-3 lists the state points for the conditions shown in Figures 2-56 through 2-58. Comparison of the data for the ventilation and recirculation cycles shows that the specific cooling capacity of the ventilation cycle is reduced much more as dehumidification effectiveness decreases. This is consistent with the explanation discussed earlier concerning the spacing between relative humidity lines. For the vent-vent cycle, the phenomenon taking place with respect to dehumidification effectiveness is the relationship between the fractional air flows required between the dehumidification and regeneration processes and the reduction in specific cooling capacity. As the dew point of the dehumidification outlet air condition increases (less dry air), the amount of regeneration air required to achieve a mass balance also decreases. For this particular cycle, the flow ratio shown in Table 2-3 is reduced more than the loss in specific cooling capacity. Hence, the CoP increases. Another important note is the difference in the definition of specific cooling capacity between the ventilation and the vent-vent cycle. For these examples, no ventilation air credit is used in determining the specific cooling capacity for the ventilation cycle. In the vent-vent cycle, outdoor air is the basis for determining cooling capacity.

Heat of Sorption Effects[2*]

The preceding examples have all assumed that the desiccant heat of sorption is equal to the latent heat of water. As discussed earlier, this assumption is generally accepted as valid because many desiccants have values close to that for water alone. These include silica gel and lithium chloride. However, some desiccants (molecular sieves) have quite large heats of sorption. Figure 2-59 shows psychrometrically the effect of the heat of sorption on desiccant cooling system performance. There are two major psychrometric effects due to changes in the desiccant heat of sorption. One is that process lines are no longer constant enthalpy lines. The other is that constant desiccant loading lines are no longer constant relative humidity lines.

---

[2]The heat of sorption is the difference in enthalpy between water vapor and water sorbed on or in the desiccant. It can also be expressed as the sum of the latent heat for water plus a term called the heat of wetting.

TABLE 2-2: State Points for Ventilation Cycle of Table 1-2 for a Desiccant Matrix Effectiveness of 90% for Both Dehumidification and Regeneration Processes.

75°C Regeneration

Air Condition	A	B	C	D	E	F	G	H	I
Enthalpy (kJ/kg)	71.1	71.1	38.5	38.5	55.0	55.0	88.1	112.6	112.6
Relative Humidity (%)	39.5	9.2	54.1	100.0	50.1	100.0	17.0	5.8	36.1
Humidity Ratio (g/kg)	14.0	7.5	7.5	9.8	11.0	14.1	14.1	14.1	25.1
Dry Bulb Temp ©	35.0	51.2	19.3	13.7	26.7	19.3	51.2	75.0	47.4

100°C Regeneration

Air Condition	A	B	C	D	E	F	G	H	I
Enthalpy (kJ/kg)	71.1	71.1	34.4	34.4	55.0	55.0	92.3	138.5	138.5
Relative Humidity (%)	39.5	5.9	42.6	100.0	50.1	100.0	13.9	2.2	35.8
Humidity Ratio (g/kg)	14.0	5.9	5.9	8.8	11.0	14.1	14.1	14.1	32.9
Dry Bulb Temp ©	35.0	55.3	19.3	12.1	26.7	19.3	55.3	100.0	52.8

Regeneration Temp ©	With Vent Credit		Without Vent Credit		
	CoP	SCC[1]	CoP	SCC	Flow Ratio[2]
75	2.3	32.7	1.1	16.5	0.59
100	1.9	36.7	1.0	20.6	0.43

[1] Specific Cooling Capacity (kJ of cooling/kg of process air)
[2] Ratio of Regeneration to Process Air Flow Rates

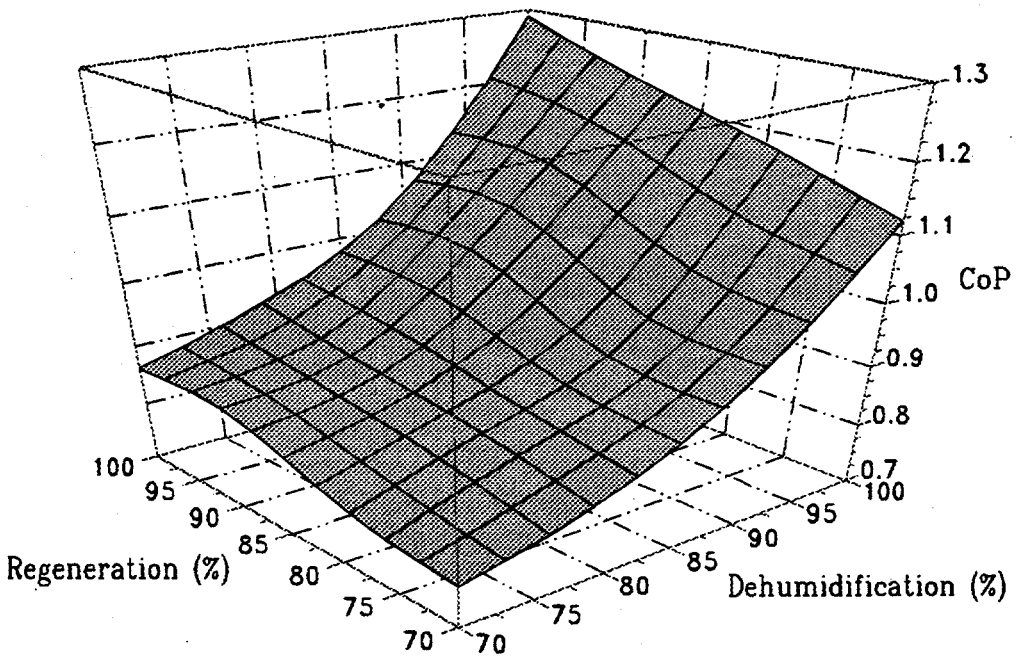

Figure 2-56. Effect of desiccant matrix effectiveness on thermal CoP. Independent variation of regeneration and dehumidification processes. Ventilation mode; 100C regeneration.

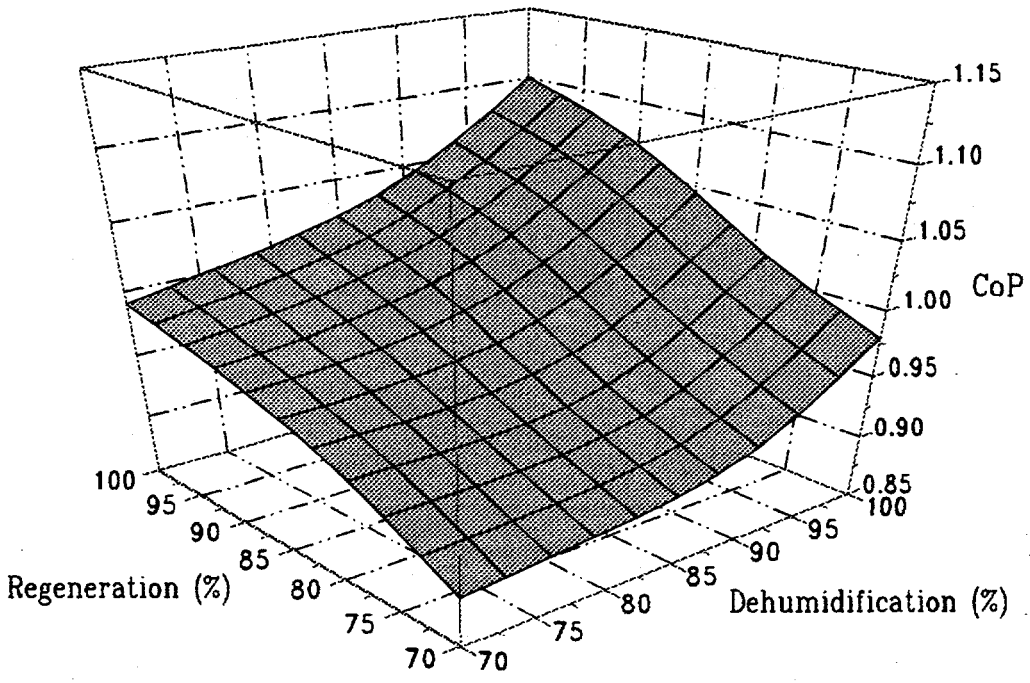

Figure 2-57. Effect of desiccant matrix effectiveness on thermal CoP. Independent variation of regeneration and dehumidification processes. Recirculation mode; 100C regeneration.

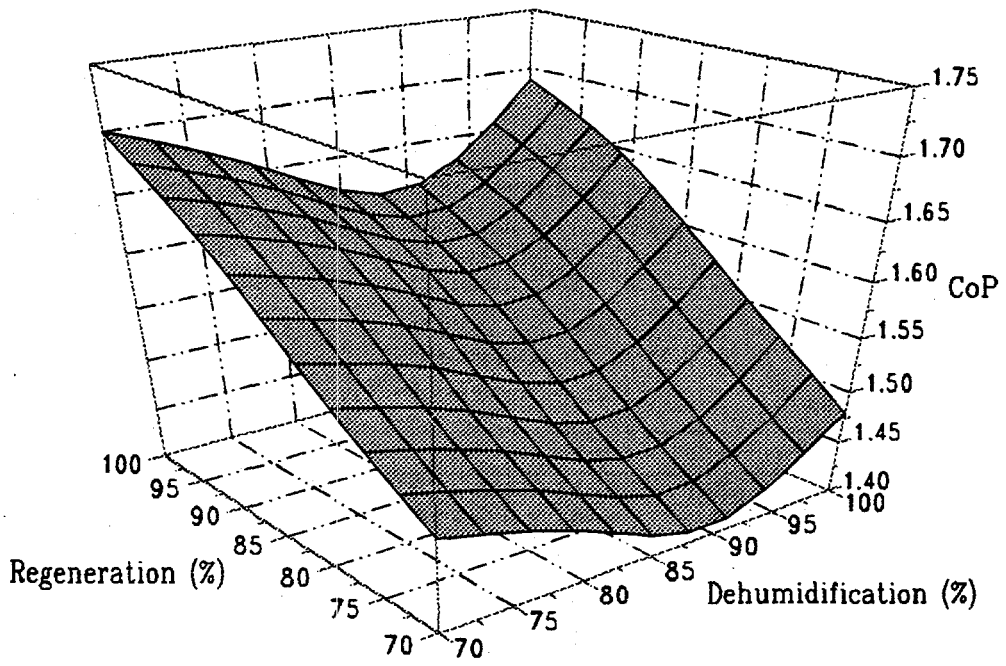

Figure 2-58. Effect of desiccant matrix effectiveness on thermal CoP. Independent variation of regeneration and dehumidification processes. Vent-vent mode; 100C regeneration.

Table 2-3: State Points for Figures 2-56 through 2-58.

Effectiveness %		Ventilation Cycle			Vent-Vent Cycle			Recirculation Cycle		
Regen	Dehumid	COP[1]	SCC[2]	FR[3]	COP	SCC	FR	COP	SCC	FR
100	100	1.29	27.5	0.56	1.69	37.8	0.55	1.1	25.5	0.44
100	90	1.05	20	0.42	1.61	31.4	0.41	1.04	20.2	0.33
100	80	0.93	15.4	0.33	1.65	27.6	0.32	1.01	16.5	0.26
100	70	0.86	12	0.26	1.7	23.9	0.26	0.99	13.7	0.21
90	100	1.23	27.3	0.59	1.64	37.8	0.57	1.07	25.6	0.45
90	90	1.05	20.7	0.44	1.56	31.4	0.42	1.01	20.2	0.34
90	80	0.9	15.4	0.34	1.6	27.6	0.33	0.98	16.5	0.27
90	70	0.86	12.6	0.27	1.64	23.9	0.26	0.97	13.7	0.21
80	100	1.18	27.3	0.62	1.56	37.8	0.6	1.02	25.6	0.47
80	90	0.96	20	0.46	1.48	31.4	0.45	0.96	20.2	0.36
80	80	0.87	15.4	0.35	1.52	27.6	0.35	0.94	16.5	0.28
80	70	0.8	12	0.28	1.56	12.9	0.28	0.94	13.7	0.22
70	100	1.12	27.8	0.64	1.48	37.8	0.63	0.98	25.6	0.49
70	90	0.94	20	0.48	1.41	31.4	0.47	0.92	20.2	0.37
70	80	0.83	15.4	0.37	1.45	27.6	0.37	0.9	16.5	0.29
70	70	0.77	12	0.29	1.49	23.9	0.29	0.89	13.7	0.23

[1]Coefficient of Performance; [2]Specific Cooling Capacity; [3]Flow Ratio (regeneration/dehumidification)

The enthalpy of water and air mixtures is defined as:

$$ENTH = C1*T + W*(C2 + C3*T) \qquad 8.0$$

where: ENTH = Air/water enthalpy
T = Temperature
W = Air humidity ratio
C1 = heat capacity of air
C2 = latent heat for water
C3 = heat capacity of water

Recognizing that the term C3*T is small compared to C2, the slope of a constant enthalpy line is approximately:

$$SLOPE = \Delta W/\Delta T = C1/C2 \qquad 9.0$$

For a desiccant system, neglecting heat capacity, the enthalpy will be modified by replacing C2, the latent heat for water, with the heat of sorption of the desiccant. The slope of this new "constant enthalpy" line will be smaller (shallower slope) as the value of C2 increases. The psychrometric representation of constant desiccant loading will also change with adsorption energy. From the preceding section, equation 5.0 defined the isotherm shape.

$$RELDESLOAD = (CONST*PVE/PSAT)*FACTOR \qquad 5.0$$

where: RELDESLOAD = Relative desiccant loading (actual loading/maximum loading)
CONST = Numerical constant that defines isotherm shape
PVE = Vapor pressure of water at the given loading and temperature
PSAT = Water saturation pressure at the given temperature
FACTOR = Modifying parameter to allow for the desiccant heat of sorption

The term FACTOR is defined as:

$$FACTOR = (PSAT/PSAT(TREF))**(HSHV-1) \qquad 10.0$$

where: PSAT(TREF) = Water saturation pressure at the reference temperature that defines the isotherm shape.
HSHV = Ratio of the heat of sorption to the latent heat for water. Note: The term (HSHV-1) is the heat of wetting discussed earlier.

As noted in the previous section, when the heat of sorption and the latent heat for water are equal (HSHV=1), FACTOR equals 1.0 and desiccant loading is linearly related to relative humidity. When these terms are not equal, psychrometric lines of constant loading are no longer equal to constant relative humidity lines because the term, FACTOR, is non-linear with temperature (PSAT).

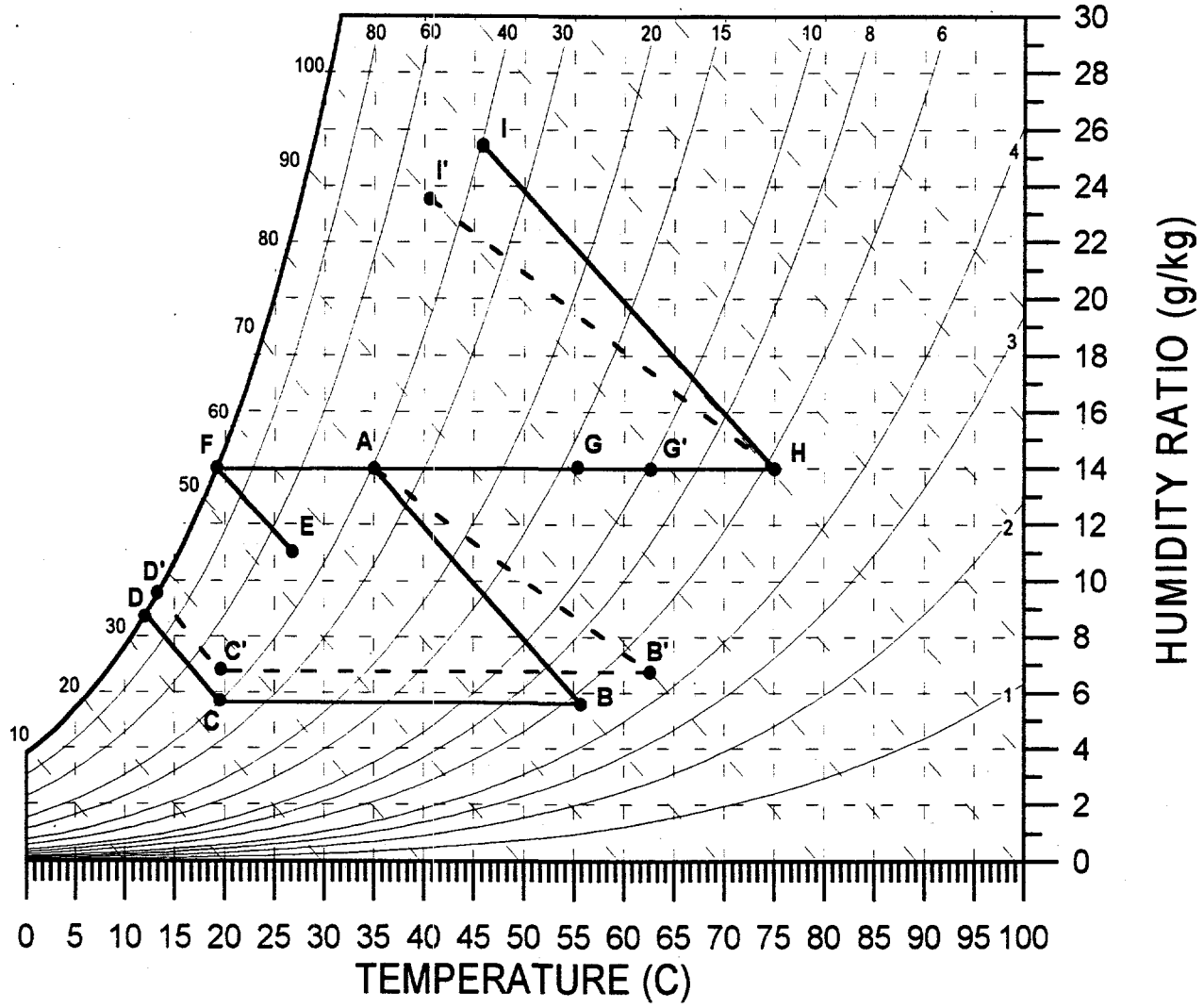

Figure 2-59. Psychrometric representation of the effect of desiccant heat of sorption.

Determining the slope of the constant loading line by differentiating equation 5.0 is quite complex because PVE is a function of both W and T, and PSAT is a very complicated function of T. To simplify understanding the effect of sorption energy on the relative slope of constant loading lines, equation 5.0 can be rewritten in the form:

$$RH = f(RELDESLOAD)*FACTOR \qquad 11.0$$

where: RH = Relative humidity in equilibrium with the desiccant at a particular loading.
f(RELDESLOAD) = Function that defines isotherm shape.
FACTOR = Same as before.

As noted earlier, when FACTOR equals one, desiccant loading and relative humidity are the same. If the temperature increases, FACTOR will be greater than one because PSAT at the higher value of temperature will be larger than that of the reference temperature. Therefore, for a constant desiccant loading, the relative humidity in equilibrium with this loading will increase as temperature increases and will decrease as temperature decreases. Therefore, for heats of sorption greater than the latent heat of water, lines of constant desiccant loading will be steeper than constant relative humidity lines on a psychrometric chart.

Referring back to Figure 2-59, the dehumidification process A-B' will have a shallower slope than the conventional process A-B. Dehumidification outlet condition B' will be hotter and less dry than condition B. This is because of the intersection of the shallower process line (Eqn. 9.0) with a more vertical constant loading line (qualitative argument earlier). The result of this is that the enthalpy of C'-D' is higher than that of C-D, thereby lowering cooling capacity. On the regeneration side, again the process line H-I' is shallower than H-I. The regeneration outlet condition I' will again be less dry, but cooler due to the intersection of the shallower process line with more vertical constant loading line. The drier regeneration outlet will result in more regeneration air requirement, lowering CoP, but the lower outlet temperature would indicate that the reject air contains less thermodynamic availability, thereby increasing CoP. Also, because the regeneration preheat G' is hotter than G, less regeneration energy is required which would again increase CoP. The ramification of desiccant sorption energy cannot be totally ascertained without a quantitative analysis.

As stated earlier, because of the complex nature of the equation defining saturation pressure, a closed form mathematical solution for predicting cooling system performance as a function of sorption energy is not possible. However, an iterative solution is. The dehumidification process line can be determined by applying equation 9.0 with the appropriate value of C2. The outlet air condition for the dehumidification process will be the intersection of this process line with the constant loading line from the regeneration condition. To predict this constant loading line, equation 5.0 is required. To begin, the regeneration air condition is taken as the reference condition. PVE and PSAT(REF) are known, and FACTOR becomes 1.0 (from equation 10.0). Recalling from Section I that relative humidity is equivalent to PVE/PSAT, yields the following:

$$RH(B) = RH(H)/FACTOR \qquad 12.0$$

where: RH(B) = relative humidity at condition B on the psychrometric chart.
RH(H) = relative humidity at condition H on the psychrometric chart.
FACTOR = defined in equation 10.0

The solution procedure is to assume an outlet temperature associated with the dehumidification process outlet (lies on the line AB). Next, the temperature is used to calculate the water saturation pressure. If equation 12.0 is satisfied (the water vapor pressure at conditions B and H are the same), then the problem is solved. If not, then new guesses for temperature must be made until equation 12.0 is satisfied. Figure 2-60 demonstrates the results of this iterative procedure. The

heat of sorption ratio is shown in parentheses next to the appropriate desiccant matrix outlet air conditions. They are B' through B''' for the dehumidification process, and I' through I''' for the regeneration process. Of course, conditions B and I refer to a heat of sorption ratio of 1.0. An important consequence of Figure 2-60 concerns the changes in humidity ratio as B progresses to B''' and I progresses to I'''. The humidity ratio on the dehumidification process is not increasing as fast as the humidity ratio on the regeneration process is decreasing. This would indicate that the reduction in cooling capacity is not as great as the reduction in the quantity of regeneration air required. A more detailed analysis follows.

Figures 2-61 through 2-76 (in Appendix B) quantify the effect of desiccant heat of sorption on system performance for two regeneration temperatures and the three cycles described earlier. Figures 2-61 through 64 show the ventilation cycle, Figures 2-65 through 68 show the recirculation cycle, and Figures 2-69 through 72 show the vent-vent cycle. Figures 2-73 through 76 compare the ventilation and recirculation cycles.

The results from these graphics generally reinforce the original qualitative observations made earlier. Specific cooling capacity generally decreases as sorption energy increases. However, thermal CoP always increases with sorption energy. The tradeoff between lower cooling capacity and higher regeneration preheat combined with lower regeneration air flow rates is decidedly in favor of the latter. The most unexpected result is the slight increase in specific cooling capacity for the recirculation cycle. This is a consequence of the nature of air and water properties. The dehumidification process outlet condition for the recirculation cycle is lower in temperature and humidity ratio than either the ventilation or vent-vent cycles. In this range of temperatures and humidities, the relative humidity lines (and hence the constant loading lines) are more horizontal. Therefore, in this regime of psychrometrics, the outlet of the dehumidification process will actually occur at a lower humidity ratio as sorption energy increases. As can be seen in Figures 2-65 through 68, this phenomenon is not a strong one and only results in a minor increase in cooling capacity for a narrow range of heat of sorption ratios.

Other significant observations are:

1. The increase in CoP with sorption energy is quite dramatic. Its positive effect is as great as the negative effect associated with the sensible heat exchanger. However, this increase in performance is achieved with a 100% effective heat exchanger. It is not obvious from these analyses how the results would differ with reduced heat exchanger effectiveness.

2. For all of the cycles examined, the improvement in thermal CoP with increasing sorption heat diminishes with regeneration temperature.

3. The reduction in specific cooling capacity is very modest. Under the conditions examined, the overall system performance is definitely enhanced by increasing the sorption energy of the desiccant.

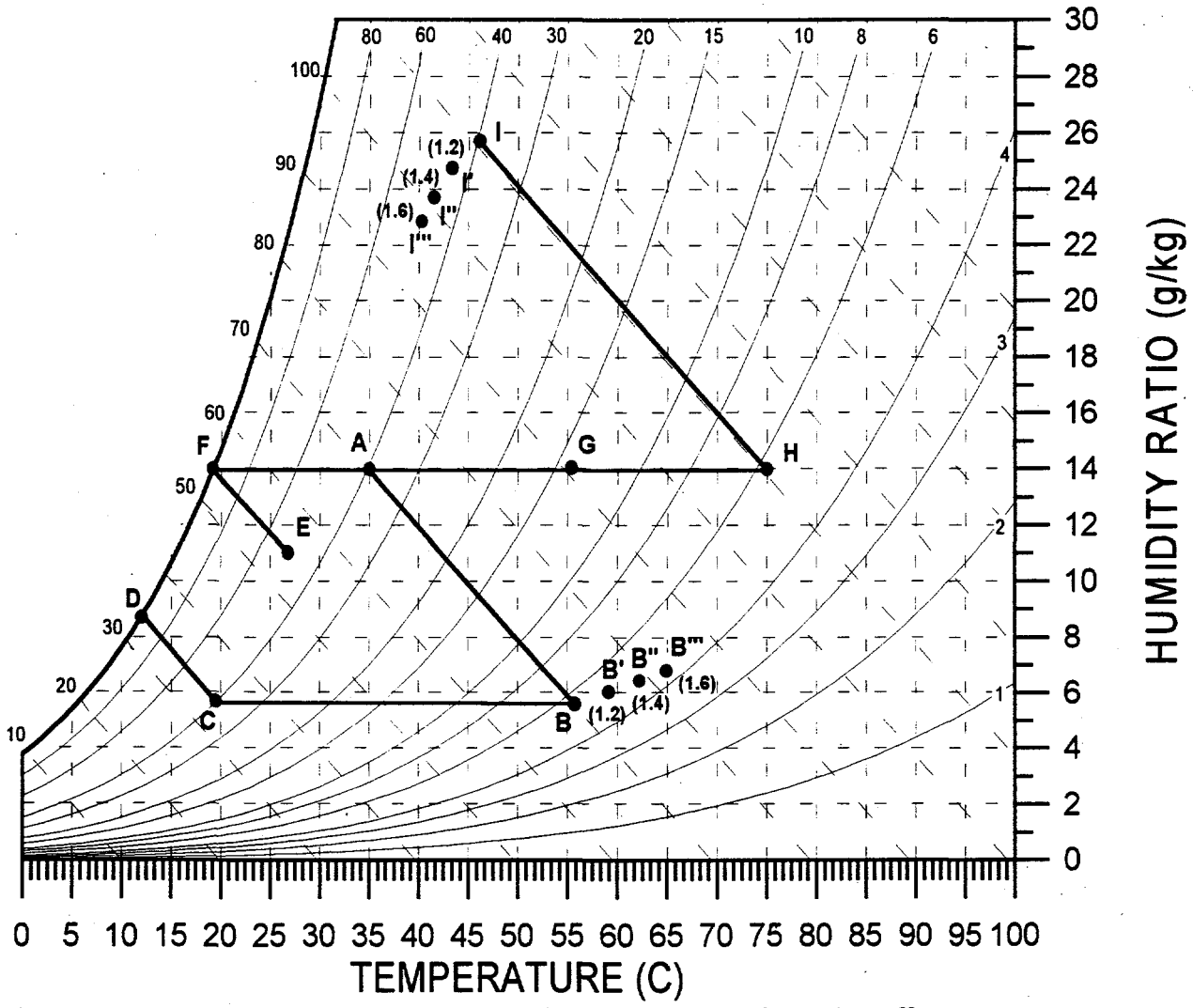

Figure 2-60. Psychrometric representation of quantified heat of sorption effects.

Desiccant Matrix Heat Capacity

No parameter associated with desiccant cooling systems has generated more controversy than the sensible heat capacity of the desiccant matrix. The reasons for this controversy and the references to the sources of information are detailed in a paper by Collier and Cohen[3]. The following is a general overview of the phenomenon.

---

[3]Collier, R.K., and B.M. Cohen, "An Analytical Examination of Methods for Improving the Performance of Desiccant Cooling Systems", Journal of Solar Energy Engineering, V.113, August 1991.

One of the most important aspects of the effects of heat capacity is the additional wavefront that becomes part of the process. Figures 2-77 and 2-78 demonstrate this additional wavefront for the dehumidification process. Figure 2-77 shows the internal humidity profile of the desiccant matrix, and Figure 2-78 shows the dehumidification outlet air conditions as a function of time. Notice that the main effect of heat capacity is the addition of a wavefront that precedes the main concentration wavefront. As shown in Figure 2-78, it is a relatively fast-moving front. The so-called "middle zone" shown in both figures is the desirable output of the desiccant. Hopefully, the middle zone is the desiccant exit condition that was predicted for the case with no heat capacity. As will be shown later, this is regrettably not the case.

To more fully understand this phenomenon, it is beneficial to examine the desiccant loading profiles within the desiccant matrix. Figure 2-79 shows this for a dehumidification process, and Figure 2-80 shows this for a regeneration process. Notice that for the dehumidification process, the exit end of the desiccant matrix is actually further regenerated by the dehumidification air stream. This is the source of moisture that makes up the additional wavefront observed earlier. For the regeneration process, the exit end of the desiccant matrix actually adsorbs moisture from the regeneration air stream. The manifestation of these heat capacity-related processes on desiccant cooling system performance is unfortunately deleterious.

Figure 2-81 shows psychrometrically the effect that heat capacity has on the process lines of a cooling cycle. For viewing and analyzing this graph, it is important to realize that the graph shows both the effect of heat capacity and the effect of desiccant matrix effectiveness. For the later case, this results mostly from the effect of isotherm shape rather than heat and mass transfer considerations. Shown in Figure 2-81 are the outlet conditions for both the regeneration and dehumidification processes of a linear (silica gel) desiccant matrix without heat of sorption effects. One case considers only the heat capacity associated with the desiccant itself. This would be close to that displayed by a packed bed configuration. The other case is considered to be similar to a laminar flow channel design where an inert substrate is deployed to support the desiccant and form channels. The multiple points are shown to indicate that the outlet air conditions of the desiccant matrix are not constant. Each symbol represents the desiccant matrix outlet air condition as a function of rotational position (if the system is a wheel or drum), or as a function of time (if the system is a fixed bed). The regeneration air condition for both systems is 95°C and 14 g/kg humidity. The entering dehumidification air condition for both systems is 35°C and 14 g/kg humidity.

On the dehumidification side, the outlet states transist from the regeneration air condition to a point that represents the middle zone condition and then towards the inlet condition. Because we have chosen a linear desiccant, wavefront breakthrough occurs with the dehumidification wavefront. On the regeneration side, the outlet states transistion from the dehumidification inlet condition to a point that represents the middle zone and then towards the regeneration air condition. Because the regeneration wavefront is contained extremely well, the departure of air states from the middle zone condition towards the regeneration air condition is extremely small. On the dehumidification side, the actual outlet air humidity is lower than that used as the benchmark in the idealized analyses. The so-called "thermodynamic optimum" would be the intersection of the relative humidity line of the regeneration air (approx. 2.5%) with the constant enthalpy line of the dehumidification inlet air (approx. 70 kJ/kg). This is because of the additional regeneration of the desiccant by the process air

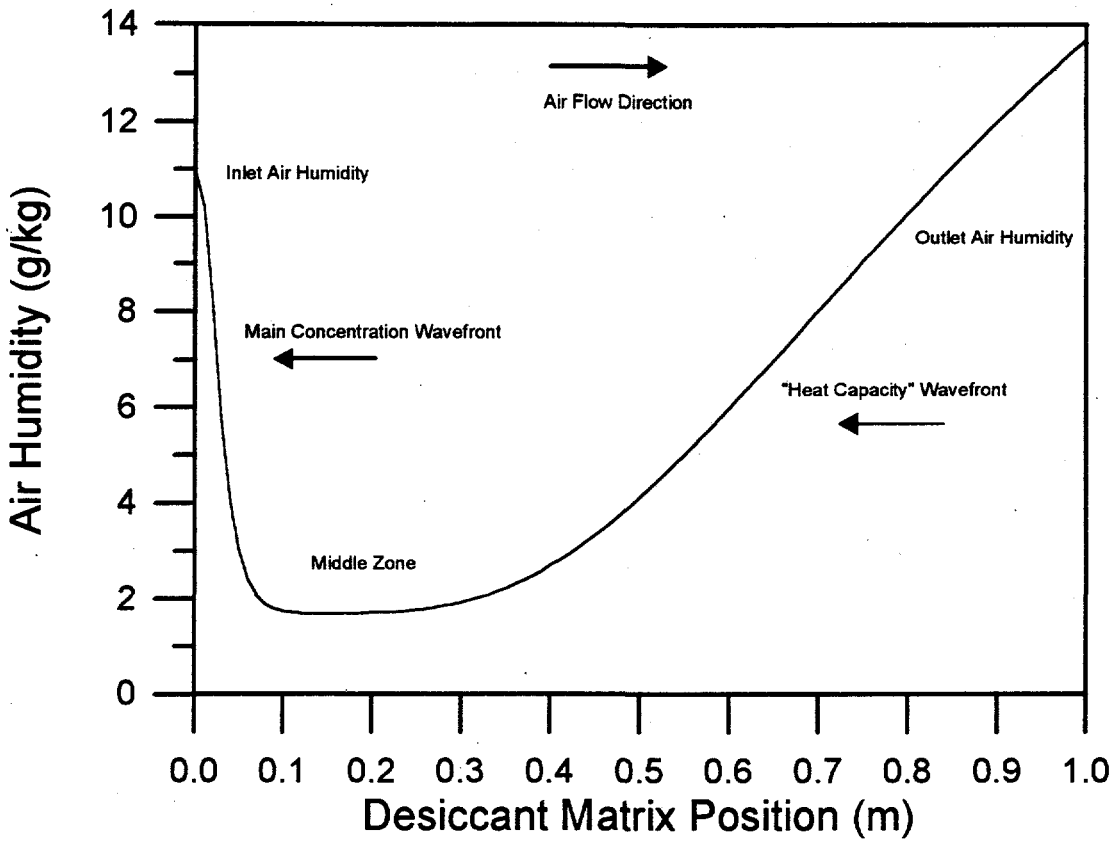

Figure 2-77. Internal desiccant matrix air humidity profiles with heat capacity effects.

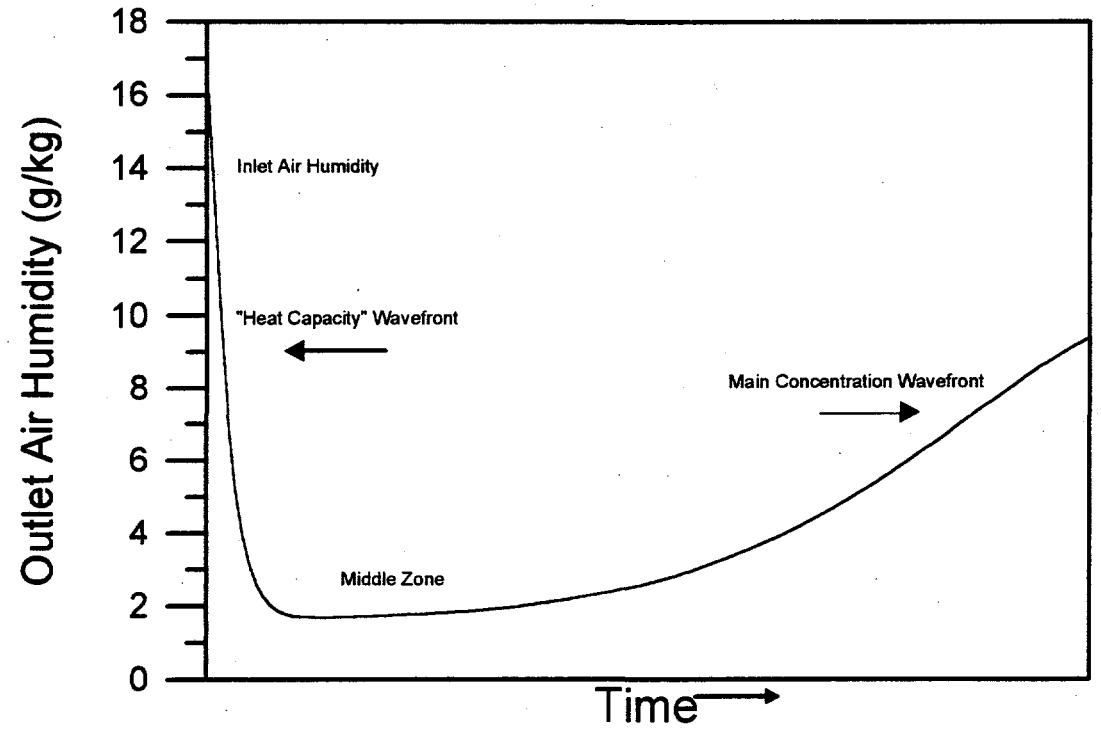

Figure 2-78. Desiccant matrix outlet humidity conditions with heat capacity effects.

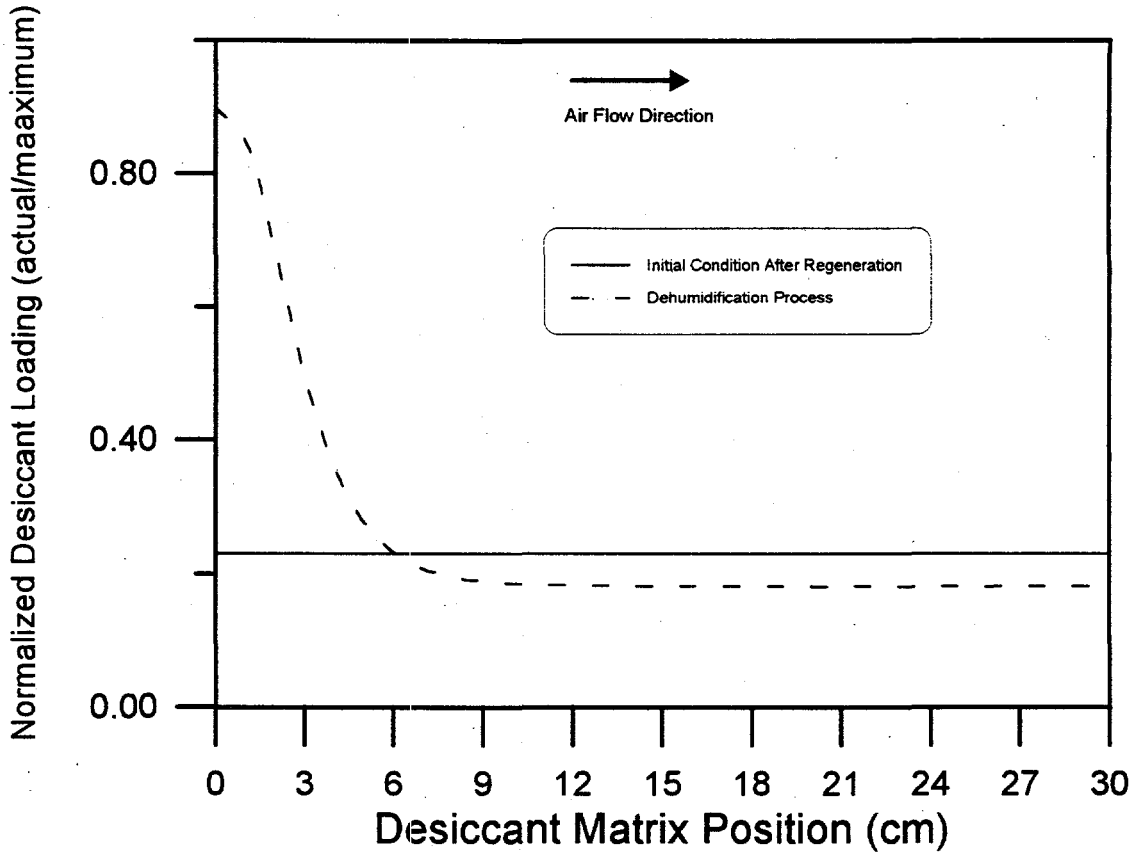

Figure 2-79. Internal desiccant matrix dehumidification loading profiles with heat capacity effects.

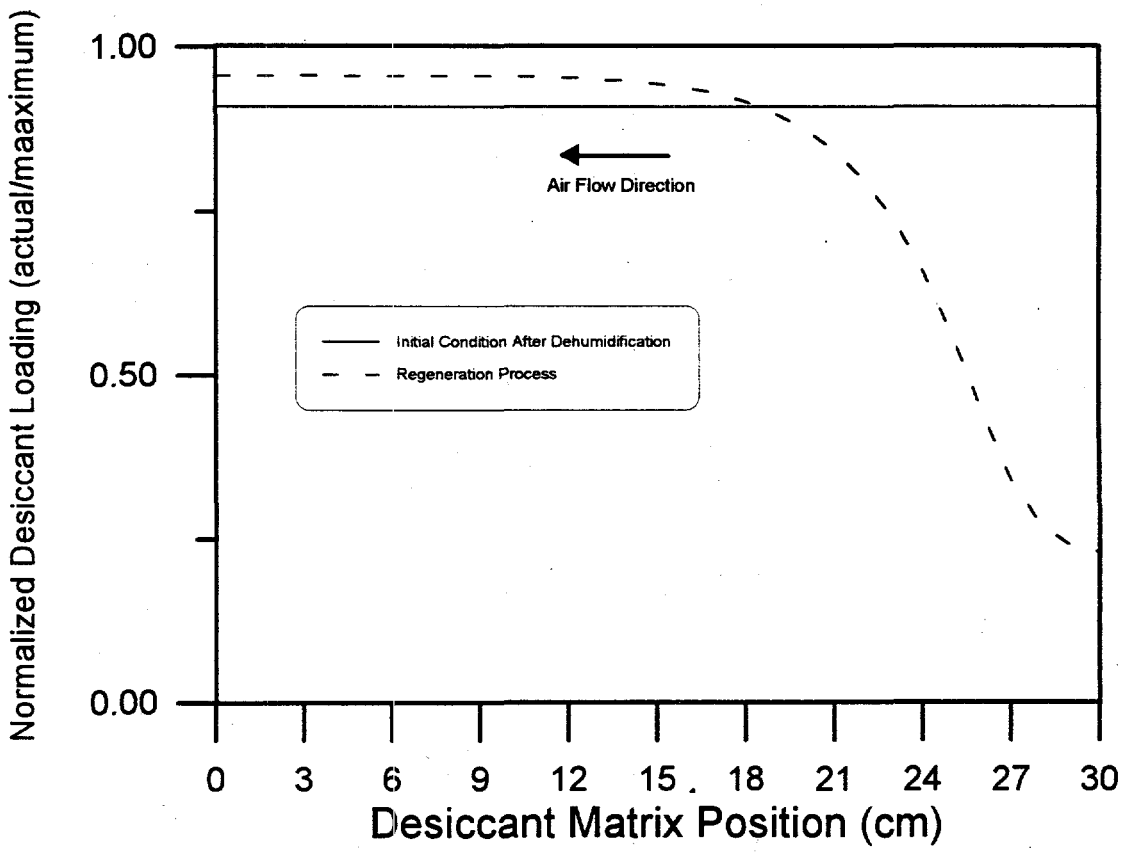

Figure 2-80. Internal desiccant matrix regeneration loading profiles with heat capacity effects.

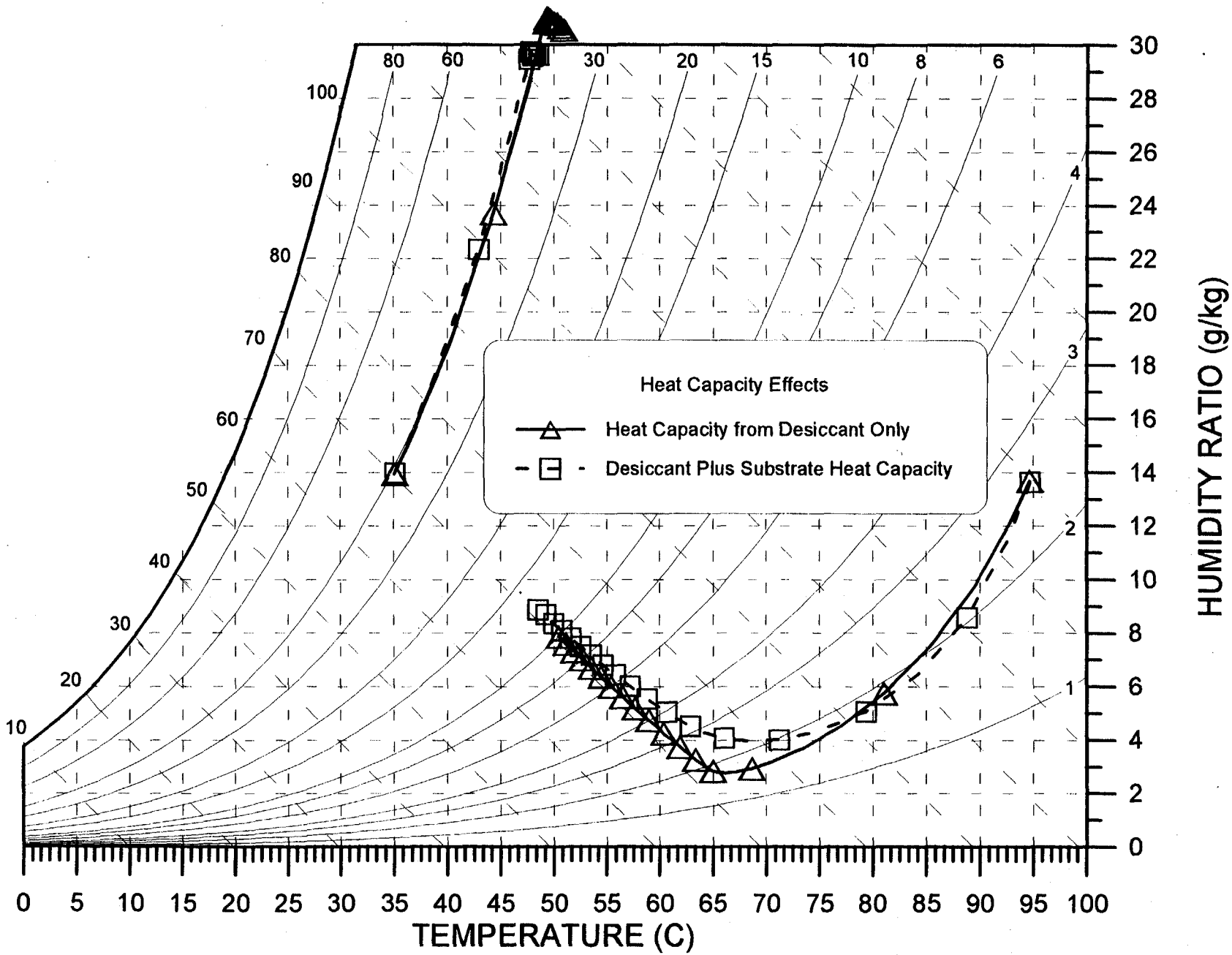

Figure 2-81. Psychrometric representation of heat capacity effects on desiccation processes.

that was shown earlier.

Table 2-4 quantifies the effect of heat capacity and wavefront breakthrough for the example chosen. On the regeneration side, where wavefront breakthrough is negligible, the effect of heat capacity is to reduce the average outlet humidity for all cases. This results in more regeneration air being required to move a given mass of water, which will reduce CoP. On the dehumidification side, where wavefront breakthrough is appreciable, the effect of heat capacity increases the average outlet humidity for all cases. This results in less cooling capacity for a given regeneration condition, which also reduces CoP. Generally speaking, on the dehumidification side, the role of heat capacity is to increase average outlet temperature and increase average outlet humidity. On the regeneration side, the role is to reduce average outlet temperature and decrease average outlet humidity. The minimum dehumidification outlet humidity occurs at higher temperatures as heat capacity increases. The maximum regeneration outlet humidity occurs at lower temperatures as heat capacity increases. These results from computer simulation agree with the generalized analyses presented earlier.

Table 2-4: State Points for Heat Capacity Effects Shown in Figure 2-81.

Heat Capacity	Average Temperature (°C)	Average Humidity (g/kg)	Min/Max Humidity (g/kg)	Temperature at Min/Max Humidity
Desiccant Only (Dehumidification)	60.7	5.7	2.8	66.2
Desiccant Only (Regeneration)	48.4	29.1	30.6	48.9
Desiccant Plus Substrate (Dehumidification)	61.5	6.9	4.0	68.3
Desiccant Plus Substrate (Regeneration)	46.1	27.1	29.7	47.9
None (Dehumidification)	61.6	3.5	3.5	61.6
None (Regeneration)	46.4	33.5	34	46.4

Interestingly, heat capacity actually reduces the minimum value of air humidity on the dehumidification side and increases the maximum humidity on the regeneration side when compared to no heat capacity. This is a result of the effect noted earlier where the desiccant is regenerated by the initial wavefront during dehumidification and where the regeneration air is dehumidified by the initial wavefront during the regeneration process.

Low Temperature Regeneration

The incorporation of low regeneration temperatures, <65°C (150 °F) is most often associated with sources of waste heat as the regeneration energy source. This is because most other heat sources for regeneration are inherently higher. This is true even for flat plate solar collectors. The main desiccant design ramification of waste heat sources, besides the low regeneration temperature,

is that thermal CoP will not have the significance that it did when the regeneration energy had a per unit cost associated with it. Therefore, when analyzing desiccant systems incorporating low regeneration temperatures, the amount of moisture removed from the process air stream will be the important analysis parameter rather than thermal CoP.

Figure 2-82 shows a psychrometric representation for several processes associated with desiccant regeneration temperatures of 45°, 55°, and 65°C. The processes shown are adiabatic (typical of solid desiccants) and isothermal (typical of liquid desiccants) dehumidification. Two process air conditions are shown, ARI indoor and ARI outdoor. As discussed in Section I, under ideal conditions, the interception of the process line (constant enthalpy or constant temperature) and the relative humidity line associated with the regeneration air condition will be the resultant process air outlet condition.

The amount of moisture that can be removed from the air streams described above (called humidity depression) is shown in Tables 2-5 and 2-6. Table 2-5 shows the amount of water removed in grams from each kilogram of air processed for both ARI indoor and outdoor air and various regeneration temperatures for an adiabatic dehumidification process. Table 2-6 shows the same results for an isothermal dehumidification process. These results are also plotted in Figure 2-83, where "Ratio of Humidity Depression" refers to the ratio of isothermal to adiabatic moisture removal.

Table 2-7 shows the optimized humidity depression for a typical commercially available solid desiccant wheel. The results shown assume that the mass fraction of the desiccant matrix that is active desiccant (some of the desiccant wheel will consist of moisture inert material) is 0.8, that the air face velocity is 1.5 m/sec (300 ft/min), and that the air entering the desiccant is ARI outdoor air. Four different desiccants are shown against three regeneration temperatures. The desiccant simulated are silica gel and three hypothetical materials. The hypothetical materials are linear (separation factor = 1.0), a Brunauer Type 1 (separation factor = 0.1, called Type 1M in the literature), and another Brunauer Type 1 (separation factor = 0.5).

Table 2-8 depicts the same solid desiccant wheel and process air with only silica gel desiccant present, the same 1.5 m/sec air face velocity, and the same regeneration temperatures. Humidity depressions are shown for three values of desiccant mass fraction. They are the 0.8, 0.6, and 0.4 assumed for the results shown in Table 2-7.

Table 2-9 again depicts the silica gel desiccant wheel with 0.8 desiccant mass fraction. Humidity depressions are shown for varying desiccant wheel face velocities as a function of regeneration temperature.

Results

Besides the obvious results that moisture removal from air decreases with regeneration temperature, these analyses show that some operational and design parameters are very significant while others are not. The most dramatic effects modeled are between adiabatic and isothermal dehumidification. Figure 2-83 shows this relationship very clearly. As regeneration temperature decreases, the benefits of isothermal dehumidification become very significant. Recalling the discussion in Section I, the major negative effect with isothermal dehumidification is the regeneration

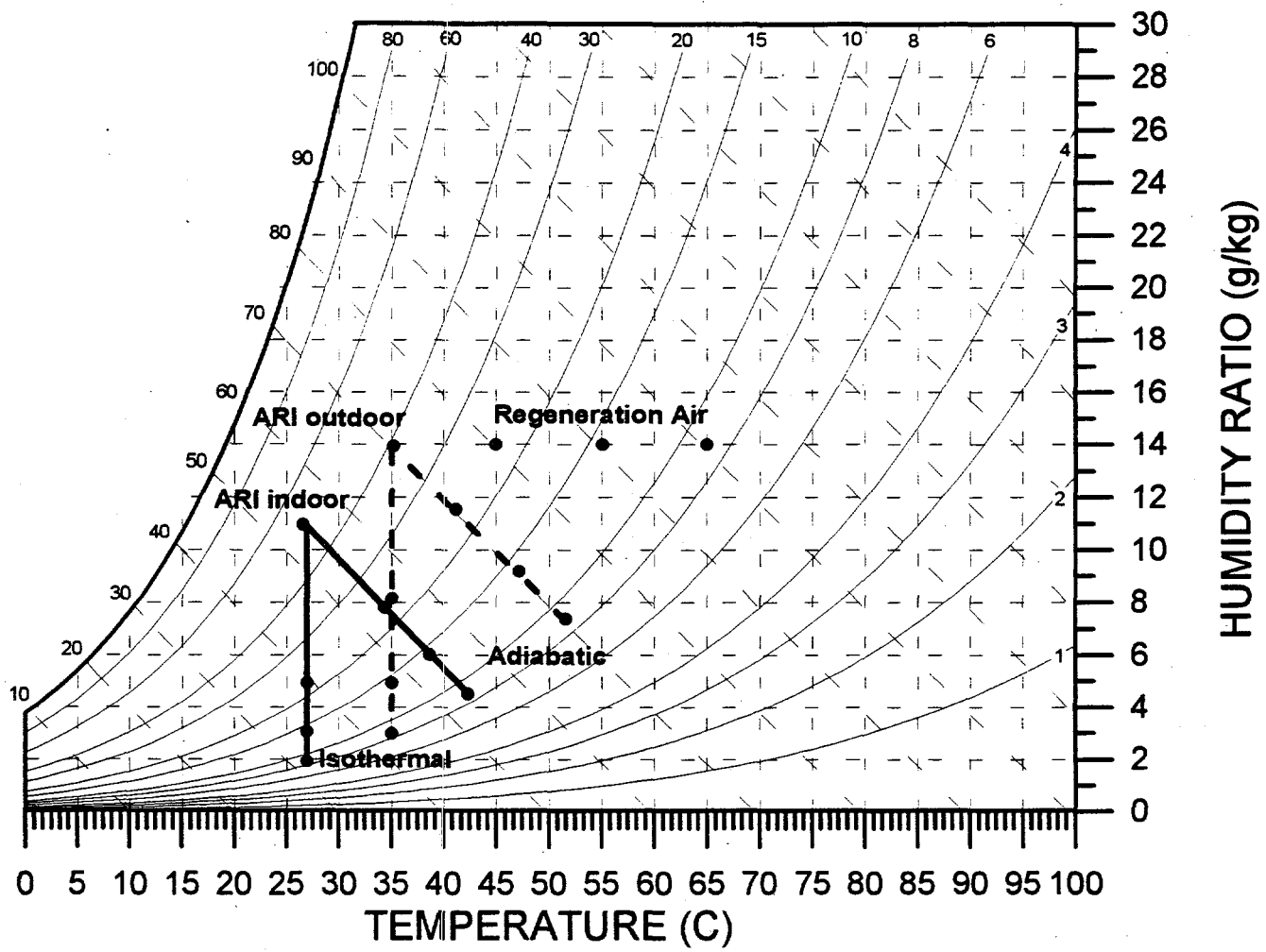

Figure 2-82. Adiabatic and isothermal dehumidification for regeneration temperatures of 45, 55, and 65C.

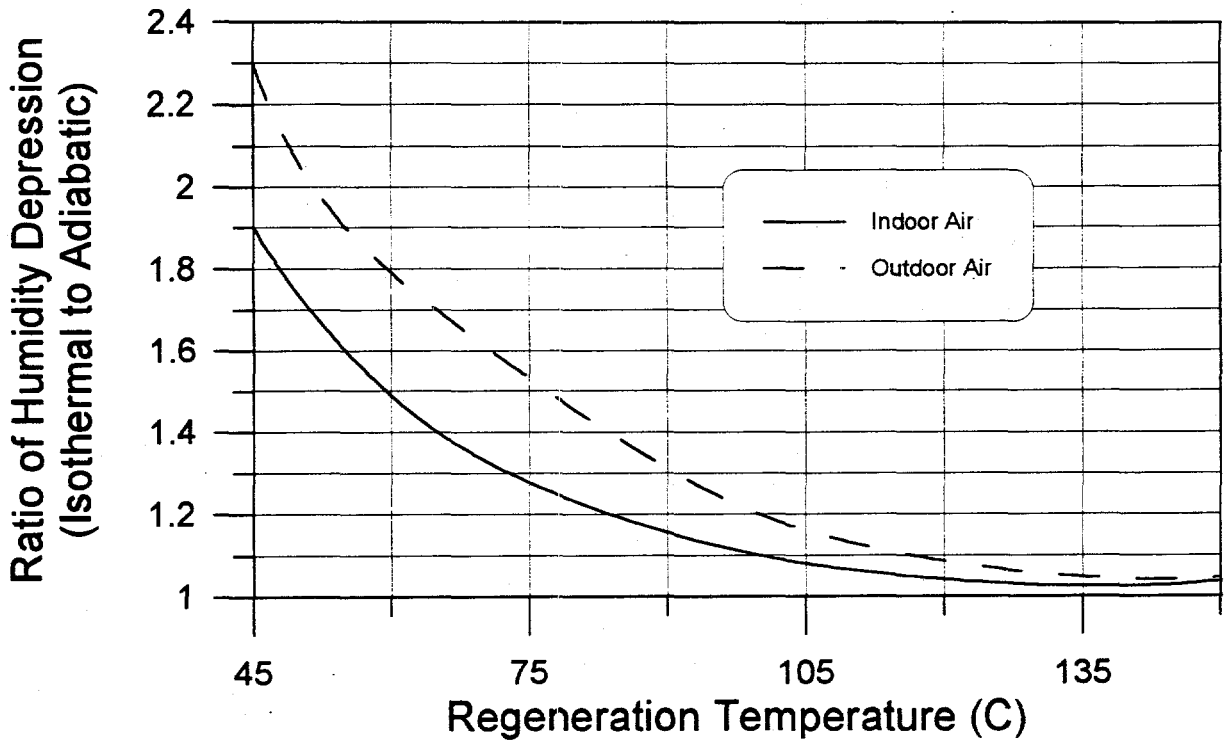

Figure 2-83. Ratio of humidity depression for isothermal and adiabatic processes.

Table 2-5. Ideal moisture depression (g/kg of air) for adiabatic dehumdification.

Regeneration Temperature (°C)	45	55	65	100	150
Indoor Air	3.1	4.9	6.3	9.3	10.6
Outdoor Air	2.5	4.7	6.6	10.9	13.2

Table 2-6. Ideal moisture depression (g/kg of dry air) for isothermal dehumdification

Regeneration Temperature (°C)	45	55	65	100	150
Indoor Air	6.0	8.0	9.1	10.5	11.0
Outdoor Air	5.9	9.1	10.9	13.2	13.8

Table 2-7. Moisture depression for various desiccant materials (adiabatic).

Regeneration Temperature	Silica Gel	Linear Sep Factor = 1	Type 1M Sep Factor = 0.1	Type 1 Sep Factor = 0.5
45°C	2	2	1.8	1.8
55°C	3.9	3.9	3.7	3.9
65°C	5.5	5.5	5.5	5.7

Table 2-8. Moisture depression of silica gel with varying active desiccant mass fractions (adiabatic).

	Mass Fraction of Active Desiccant Material		
Regeneration Temperature	0.80	0.60	0.40
45°C	2	1.9	1.9
55°C	3.9	3.7	3.6
65°C	5.5	5.4	5.1

Table 2-9. Moisture depression of silica gel with varying face velocities (adiabatic).

	Face Velocity		
Regeneration Temperature	1.5	2.5	4.0
45°C	2	2	1.9
55°C	3.9	3.8	3.8
65°C	5.5	5.5	5.4

preheat energy is lost. In the case of waste heat applications, the loss of regeneration preheat is of minor consequence. Also notice that as regeneration temperatures approach more common values (>100 °C) the advantages in humidity depression for isothermal operation are negligible.

Another significant result of these analyses is to show that factors that are significant in determining the performance of systems incorporating higher regeneration temperatures are not significant when dealing with these low regeneration temperatures. Tables 2-7 through 2-9 are an attempt to quantify these factors. Desiccant type, desiccant mass fraction and face velocity are not significant in determining system performance. This observation is important because it shows that desiccant system design parameters that have a strong influence on cost (desiccant deployment, system size, etc.) can be relaxed without compromising performance. Admitedly, system sizes will be quite large regardless of other design parameters simply because the regeneration temperature, and hence the moisture transport potential, is reduced. This is especially true for the 45°C regeneration temperature. Two grams of water per kilogram of processed air will probably never make sense economically. Depending upon the ratio of pressure drop to air mass flow rate, the cost of electricity for the fan may exceed this modest amount of dehumidification.

Enthalpy Exchange Devices

Desiccants can also be used in devices that exchange the total enthalpy (temperature and water content) between two adjacent air streams. The physical mechanisms employed and the sensitivity of performance on the physical properties of the desiccant matrix are explained.

A full understanding of the operating principles of enthalpy exchange devices requires understanding the relationship between desiccant moisture transport and thermal heat capacity within the desiccant matrix. Figure 2-78 shows that the air humidity conditions associated with the "Heat Capacity" wavefront are closely matched by the regeneration air stream. This condition is further amplified in Figure 2-81. For both the dehumidification and regeneration processes, the initial condition of the air exiting the desiccant matrix closely matches that of the air associated with the previous process. That is, the initial condition of the air exiting the desiccant matrix during the dehumidification process closely matches the air conditions associated with the regeneration process, and vice versa. Also, as the thermal heat capacity increases relative to the amount of desiccant in the matrix, the more pronounced this effect becomes over time. Understanding why this situation exists is demonstrated in Figures 2-79 and 2-80.

As discussed in the previous section, heat capacity creates a situation where during the initial stages of a given process, the opposite process actually occurs. That is, regeneration of the desiccant occurs during the initial stages of the dehumidification process, and dehumidification of the air occurs during the initial stages of the regeneration process. The explanation of this phenomenon is that the heat capacity that is part of the desiccant itself, as well as that associated with a desiccant support matrix, interacts with the sorption process to create thermodynamic conditions that are not in equilibrium with the rest of the desiccant matrix. For example, thermal heat capacity that is present at the regeneration air temperature increases the air temperature more than the sorption process would have without this thermal effect. This increased temperature coupled with the lower humidity of the process air creates the potential for regeneration of the desiccant downstream. Without this

heat capacity available at an elevated temperature relative to the process air, no further regeneration of the desiccant is possible and therefore no moisture source capable of creating a transition region in the outlet air.

From this discussion, it is clear that the initial interaction between desiccant sorption, thermal heat capacity, and changing air conditions in an adiabatic process makes an enthalpy exchange device possible. The rotational speed of the desiccant matrix clearly must be much higher for enthalpy exchange relative to air dehumidification. This higher speed must be incorporated in order to remain in the initial transition region of the overall process and keep the full dehumidification and regeneration processes from occurring.

The effectiveness of an enthalpy exchange device is defined similarly to that of other exchange devices. It is the fraction (or percentage) of the maximum theoretical enthalpy exchange between two air streams of differing enthalpy. For building applications, where rejected indoor air is exchanged with entering outdoor air, the maximum theoretical enthalpy exchange would be for the entering outdoor air to achieve the same enthalpy as the exiting indoor air. The complicating factor for enthalpy exchange relative to other exchange devices is that air enthalpy consists of two components, latent and sensible. Because human comfort relies on both latent and sensible components, it is important to know not only the effectiveness for enthalpy, but it is also important to know the effectiveness for the latent and sensible components as well.

Figures 2-84 and 2-85 demonstrate the effect of rotational desiccant wheel speed and its performance as an enthalpy exchange device. Figure 2-84 shows qualitatively the effect of rotating a standard desiccant dehumidification wheel at increasing rotational speed. Notice that as the rotational speed increases, the process lines for both dehumidification and regeneration deviate from constant enthalpy lines to direct transfer of temperature and humidity conditions. Figure 2-85 is a plot of enthalpy exchange effectiveness versus rotational speed for a commercially-available desiccant matrix configured for desiccant dehumidification. By definition, efficient adiabatic dehumidification of process air will result in process air conditions that exhibit extremely low effectiveness as an enthalpy exchanger. This is shown in Figure 2-85 by the extremely low enthalpy exchange effectiveness at low rotational speeds. The latent effectiveness actually becomes less than zero for rotational speeds below about 1 rpm. As the rotational speed increases, both sensible and latent effectiveness increase. This situation continues until a critical rotational speed is reached. At this critical rotational speed, effectiveness reaches a maximum and does not change with further increasing rotational speed. For this example, the speed at which both latent and sensible effectiveness reach a maximum appears to be the same. This is an effect of the logarithmic axis and the desiccant matrix chosen. This will be shown in more detail later in this section.

Figure 2-86 shows the relationship between the sensible and latent exchange effectiveness and the number of transfer units (NTU) of a typical desiccant dehumidification matrix that is rotated at the critical speed required for maximum effectiveness. NTU is a non-dimensional parameter that defines the ability of a surface to achieve equilibrium conditions (both thermal and moisture) with air that is adjacent to it. The higher the NTU, the closer to equilibrium that is possible. Infinite NTU

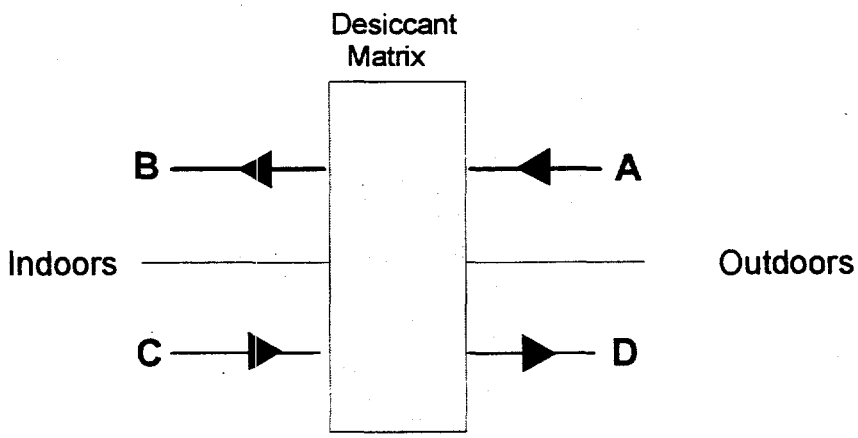

High Rotational Speed

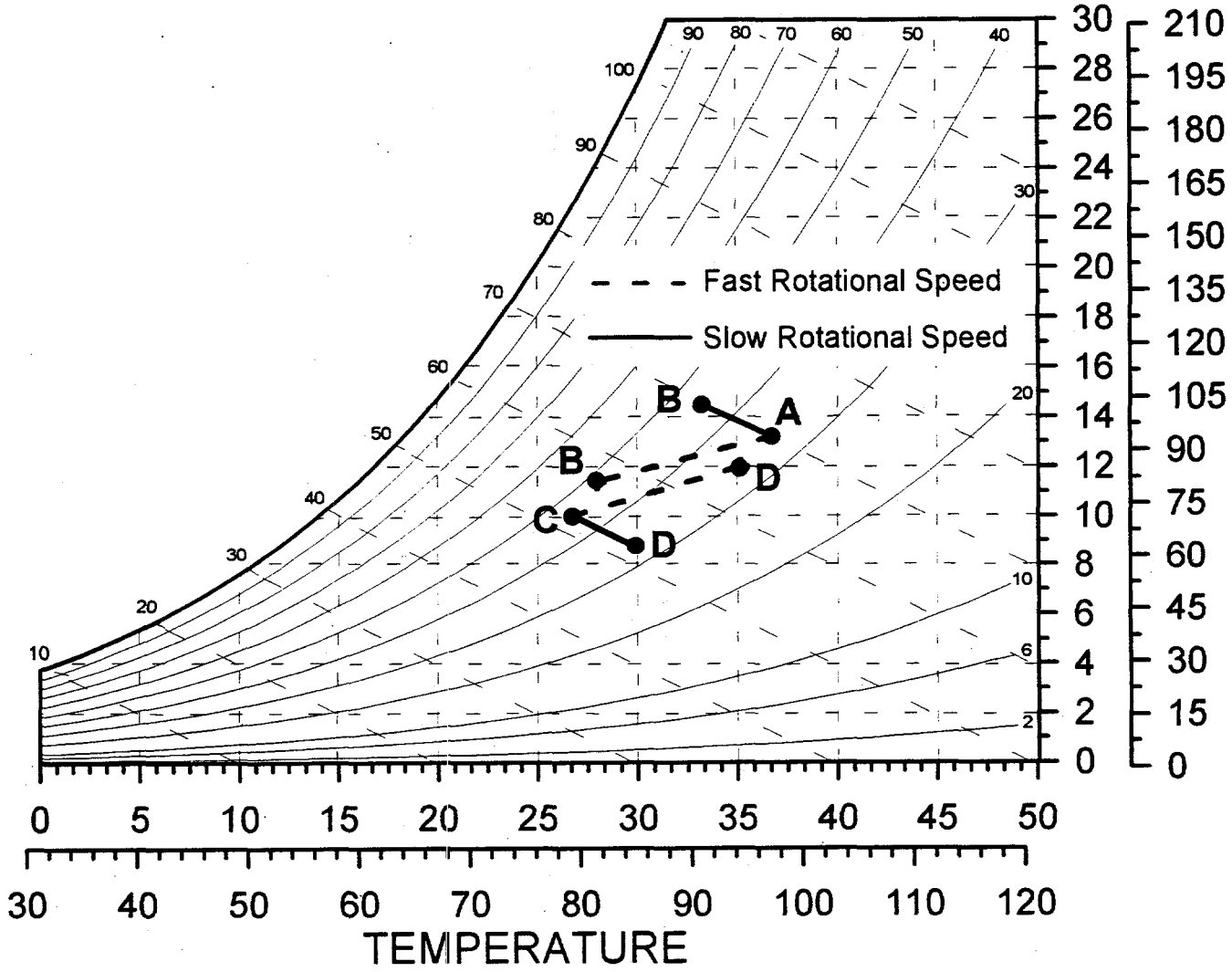

Figure 2-84. Enthalpy Exchanger for Ventilation Applications

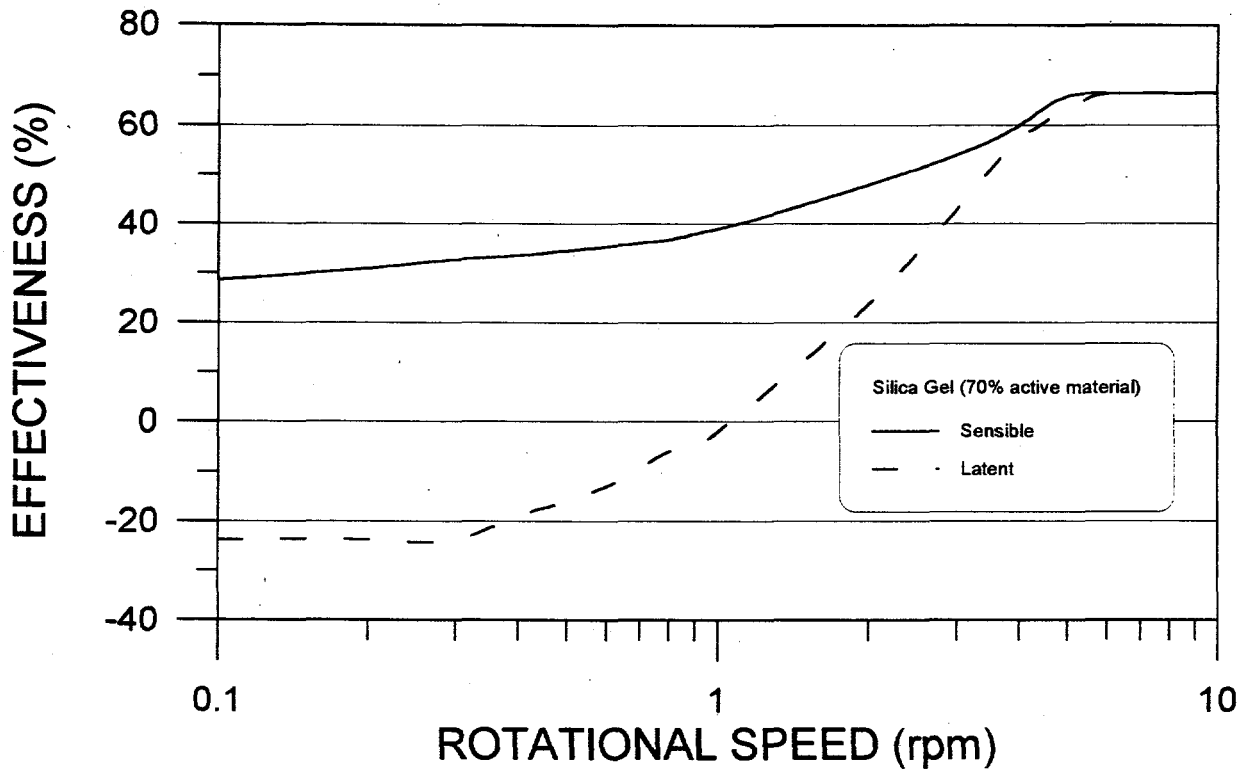

Figure 2-85 . Effectiveness as a function of rotational speed; Silica Gel

will achieve total equilibrium. The simulation depicted in Figure 2-86 is performed assuming that a typical desiccant dehumidification wheel is rotated at about 7 to 10 rpm. The air streams are assumed to be ARI standard indoor (26.7°C, 11 g/kg) and outdoor (35°C, 14 g/kg) conditions. The amount of active desiccant within this matrix is assumed to be 70% by dry mass. As a reference, a typical value of NTU for a commercially available honeycomb silica gel desiccant drying wheel is about 17, depending largely on air face velocity. Figure 2-86 demonstrates that both the latent and sensible effectiveness for a desiccant matrix designed for dehumidification are mostly equivalent. As one would expect, the overall effectiveness decreases as NTU decreases. Only moderate differences between the latent and sensible effectiveness are observed for NTU less than about 8.

Figure 2-87 shows the relationship between effectiveness and the desiccant mass ratio. The desiccant mass ratio is the fraction of the total matrix mass that is desiccant. In this figure, molecular sieve (4A) is also shown with silica gel. For this simulation, the NTU assumed was 17 and ARI air conditions were again used. Notice that silica gel will maintain equivalent latent and sensible effectiveness for a wide range of desiccant mass loadings. On the other hand, molecular sieve requires a certain mass fraction (0.5 for the conditions shown in Figure 2-87) in order to achieve equivalency. Below this value, latent capacity falls off markedly as desiccant mass fraction decreases. This is probably a consequence of the isotherm shapes for silica gel and molecular sieve. In the relative humidity range of 40 to 50%, silica gel is able to cycle considerably more moisture than molecular sieve.

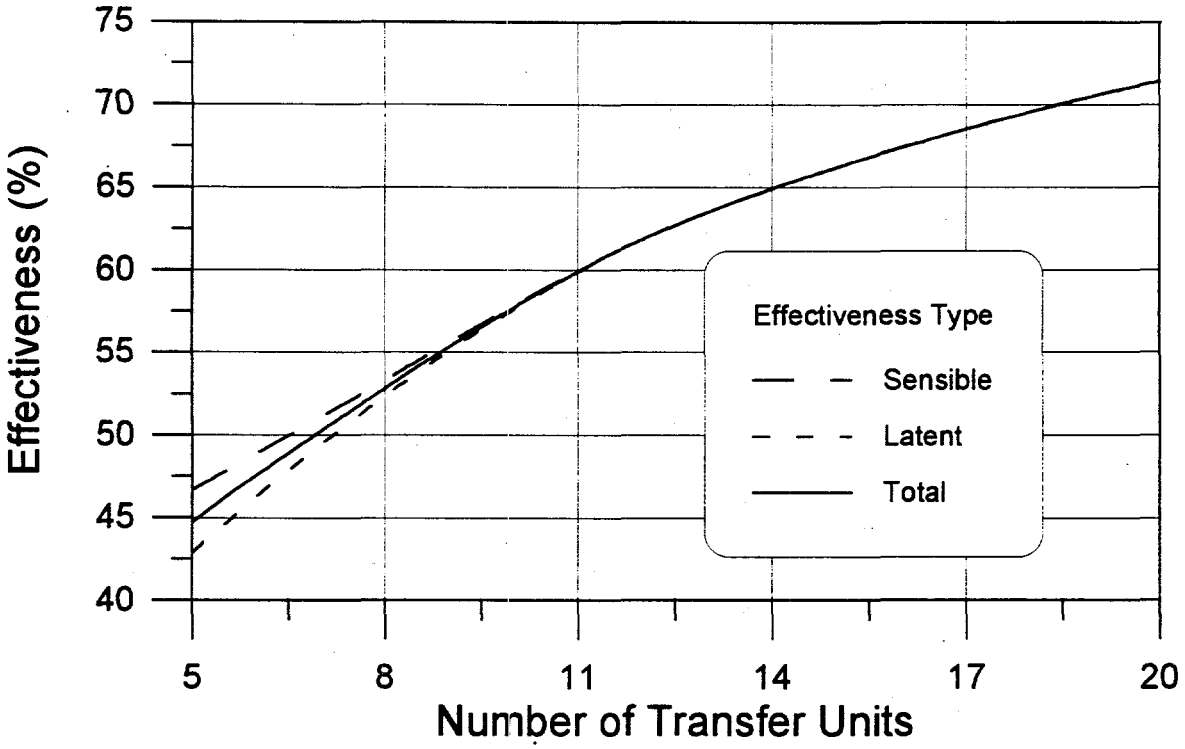

Figure 2-86. Effectiveness as a function of desiccant matrix NTU.

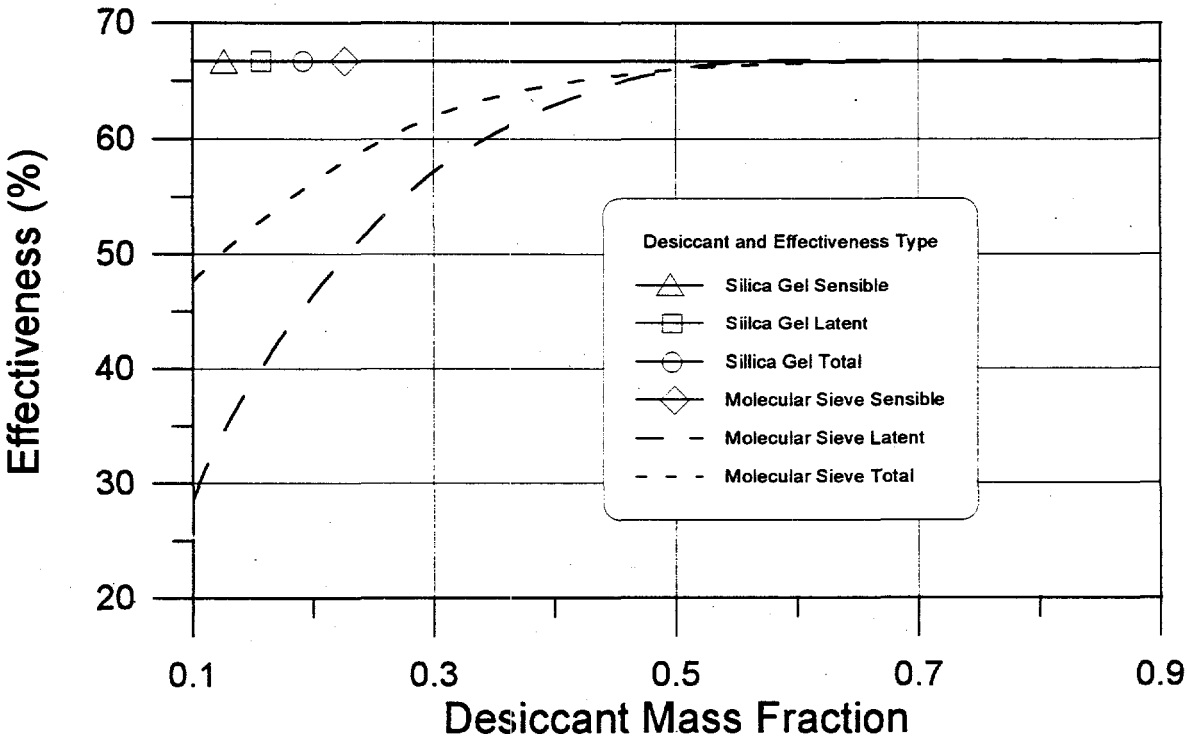

Figure 2-87. Effectiveness as a function of desiccant type and mass fraction.

Figure 2-88 shows the relationship between effectiveness and the outdoor air humidity. As in Figure 2-87, both silica gel and molecular sieve were simulated with an NTU of 17. However, for this simulation, a desiccant mass fraction of 0.5 was assumed. Figure 2-88 verifies that the humidity ratio of outside air influences the latent performance of both silica gel and molecular sieve-based matricies. As one would expect, the sensible performance of both matricies simulated is unchanged by outdoor air humidity ratio. However, as outdoor air humidity ratio increases from ARI conditions, the silica gel latent effectiveness increases while the molecular sieve effectiveness decreases. The magnitude of these effects is fairly small, roughly 5% for the silica gel and 10% for the molecular sieve. Again, this effect is thought to result from the higher sorption cycling capacity of silica gel between the 50 to 60% relative humidities simulated here.

Figures 2-89 and 2-90 show the relationship between latent and sensible effectiveness as a function of rotational wheel speed and two values of desiccant mass fraction for silica gel and molecular sieve respectively. Examination of these two figures shows that achieving the proper rotational speed is important in determining the ultimate performance, both latent and sensible, for any given desiccant type. Furthermore, a specific speed exists for a given wheel type, both desiccant and mass fraction, above which no further improvement is observed. This minimum critical speed can be different for maximum latent and sensible effectiveness.

Conclusions

The simplified analyses presented in Section I showed that desiccant systems are theoretically capable of very high cooling efficiencies. However, analyses in this section have shown that the physical parameters commonly neglected in theoretical analyses contribute to a very significant loss in performance, in both cooling capacity and thermal CoP. The most significant negative effects that were quantified were the sensible heat exchanger and the desiccant matrix effectiveness. To a much lesser degree, the evaporative cooler effectiveness also negatively affected performance. Surprisingly, the desiccant heat of sorption actually improved the CoP of all cycles examined, dramatically. The negative effect on cooling capacity was generally minor. Because much of the cycle efficiency improvement was due to the increase regeneration preheat temperature, it would be advisable to further examine the combined effect of sorption energy and heat exchanger effectiveness. Although not generally quantified in this report, desiccant matrix heat capacity is also significant in reducing system performance.

Also demonstrated in this section was the dependence of system configuration and regeneration temperature on the deleterious effects of these physical parameters. Although not all configurations and regeneration temperatures reacted equally, it was generally shown that the ventilation or vent-vent cycle with high regeneration temperatures is desirable when ventilation air is required and system performance can be measured against outdoor air as the baseline rather than indoor air.

The analyses of enthalpy exchangers presented here show that the ability of a desiccant matrix to perform enthalpy exchange between air streams is a consequence of the relationship between the thermal and moisture sorption capacity of the matrix. These phenomena are not independent of one

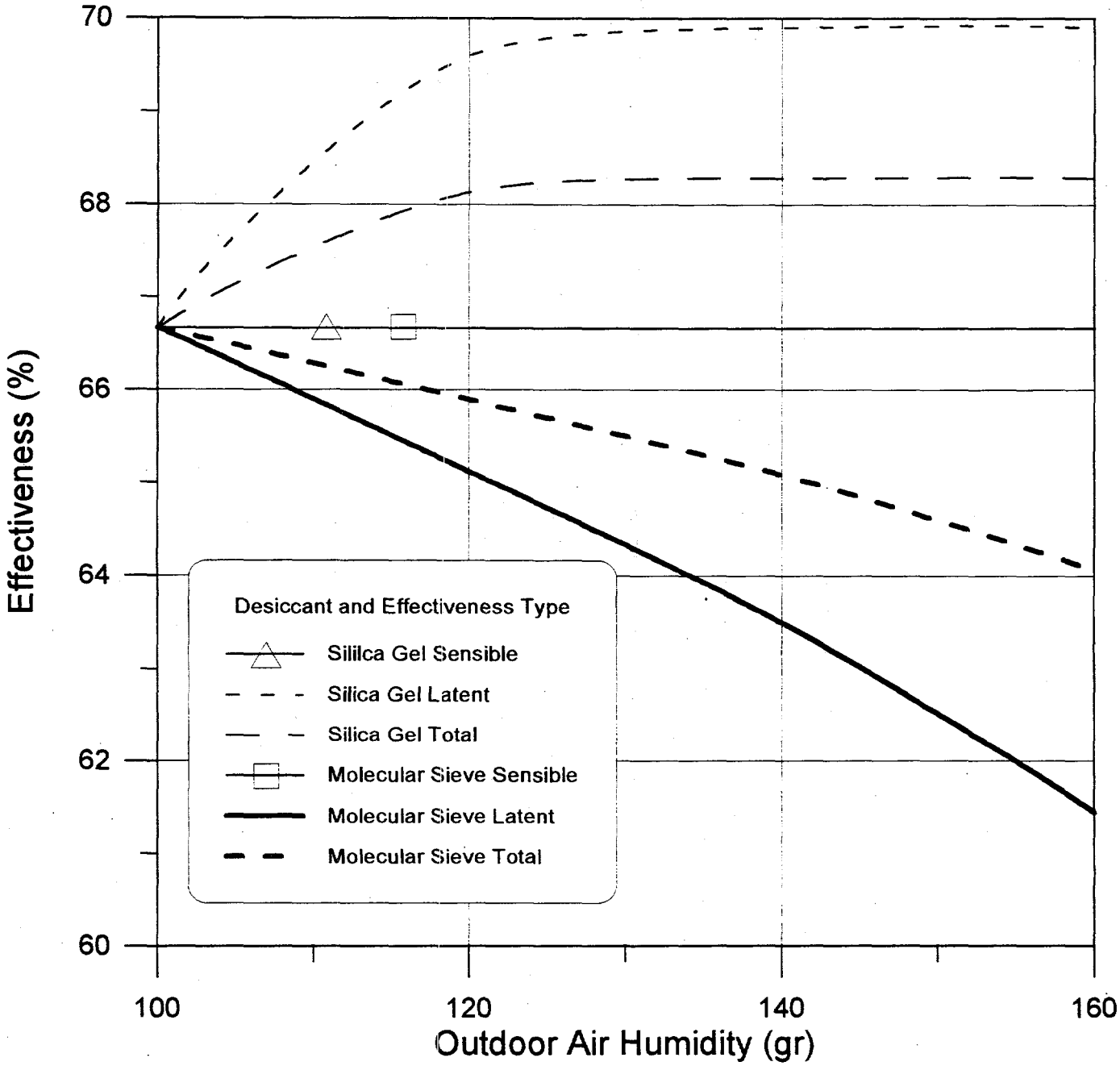

Figure 2-88. Effectiveness as a function of desiccant type and outdoor humidity ratio.

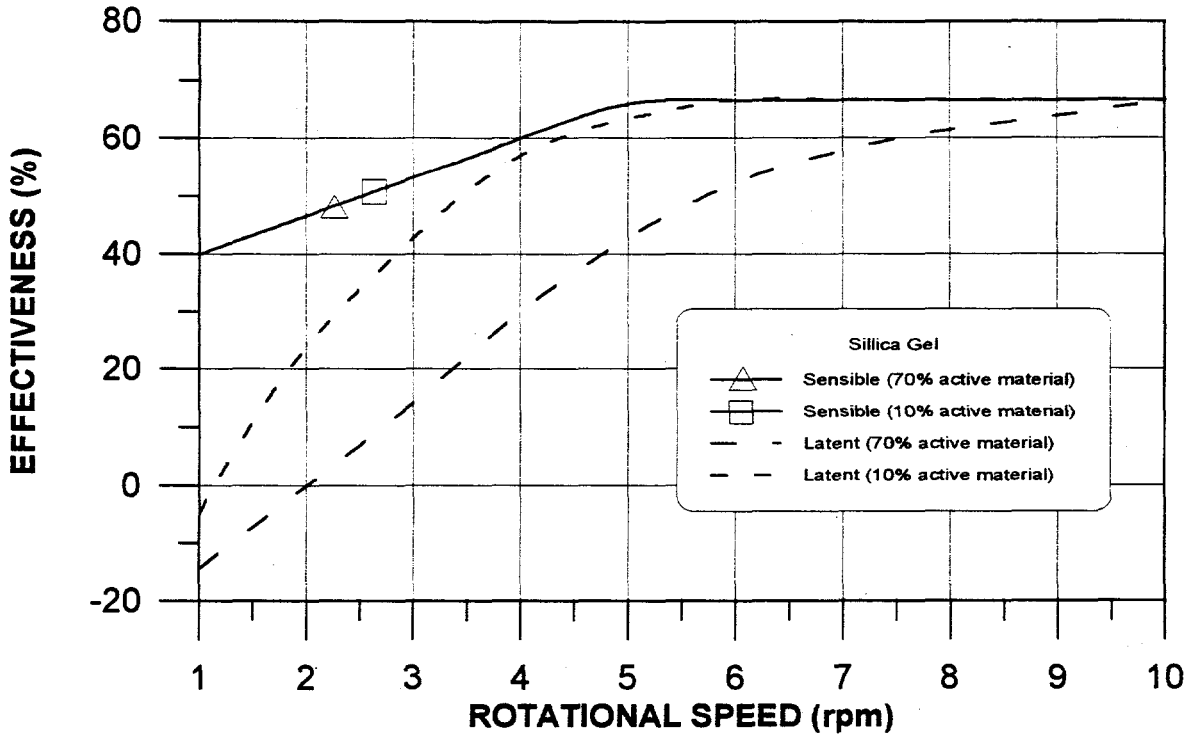

Figure 2-89. Effectiveness as a function of rotational speed; Silica Gel.

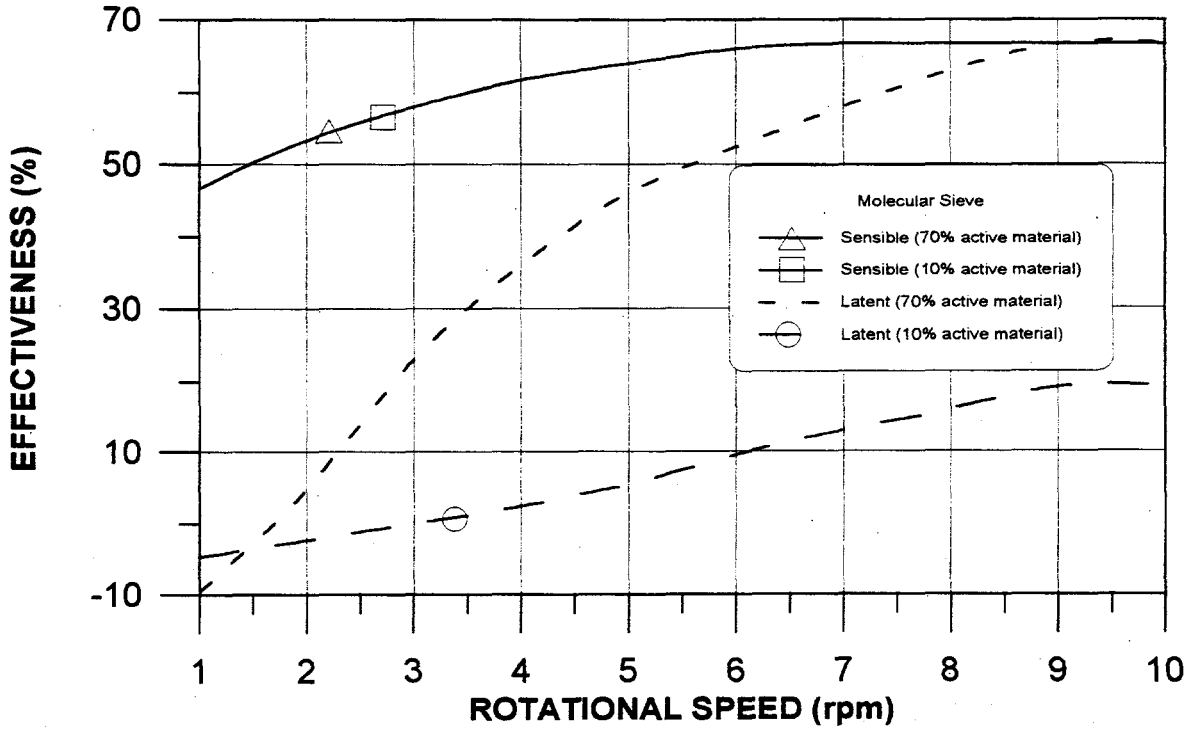

Figure 2-90. Effectiveness as a function of rotational speed; Molecular Sieve.

another. Both the latent and sensible effectiveness of a desiccant matrix will be similar as long as some minimum moisture capacity exists within the matrix for the entering air conditions. This moisture capacity will be determined by the amount of desiccant in the matrix and the desiccant moisture cycling capabilities of the desiccant between the relative humidities of the two air streams.

An efficient enthalpy exchange device consisting of a desiccant in conduction with thermal heat capacity can be designed with sufficient thermal and mass transport NTU to achieve the sensible price/performance goal needed, and sufficient moisture cycling capabilities for the air conditions encountered. More simply stated, you can't use too much desiccant, but you can use too little.

SECTION III. SEASONAL SIMULATIONS

In Section I, very high thermal CoPs were reported for desiccant cooling cycles with ideal components. In Section II, the effects of less-than-ideal component behavior were investigated. One of those cycles investigated, the ventilation cycle, resulted in the highest performance when ventilation air was required for a particular application. This allowed the cooling capacity and CoP to be based on outdoor air enthalpy rather than indoor air. The operation of the standard ventilation cycle, where indoor air is the source of the regeneration air, results in very high CoPs (up to 2.6 from Table 1-2). However, the use of vented indoor air will also improve the performance of conventional vapor-compression equipment. Adding a total enthalpy exchanger to exchange vented room air conditions with entering outdoor air allows the desiccant system and the vapor-compression system to be compared as recirculation systems. Therefore, even though the desiccant system can exhibit high thermal CoP's, the vapor compression equipment will also display higher CoP's when given credit for the enthalpy wheel. The CoP's reported for the modified ventilation (vent-vent) cycle, where ambient air is the source for both air streams, are still relatively high (up to 1.9 from Table 1-3) compared with the recirculation cycle. In this section, the modified ventilation cycle is studied further. Seasonal simulations are performed for 5 U.S. cities. Component effectiveness values are incorporated into the model to assess the effect of real components on the seasonal performance of the system. In addition, operating the modified ventilation cycle with a variable regeneration temperature is investigated.

Seasonal Simulations with Ideal Components

The modified ventilation cycle is initially modeled using ideal components to demonstrate the effects of ambient air conditions and to determine upper performance bounds. The modified ventilation cycle is shown schematically in Figure 3-1. The operational principles of the ideal components are identical to those in Section I:

1. The air passing through the evaporative coolers follows a process path of constant enthalpy and exits at a saturated state (100% relative humidity).

2. The heat exchanger has an effectiveness of 100%.

3. The air passing through the desiccant wheel follows a process path of constant enthalpy. The process air exit relative humidity is equal to the inlet regeneration relative humidity. Mass and energy balances are utilized to calculate the outlet regeneration air state.

Two desiccant system operational modes are considered:

1. The system is simulated at a constant regeneration temperature and cycled on and off as necessary to meet the total ventilation cooling load for each hour.

2. The regeneration temperature is adjusted on an hourly basis so that the system capacity equals the ventilation cooling load and the system operates continuously during each hour that a cooling load exists.

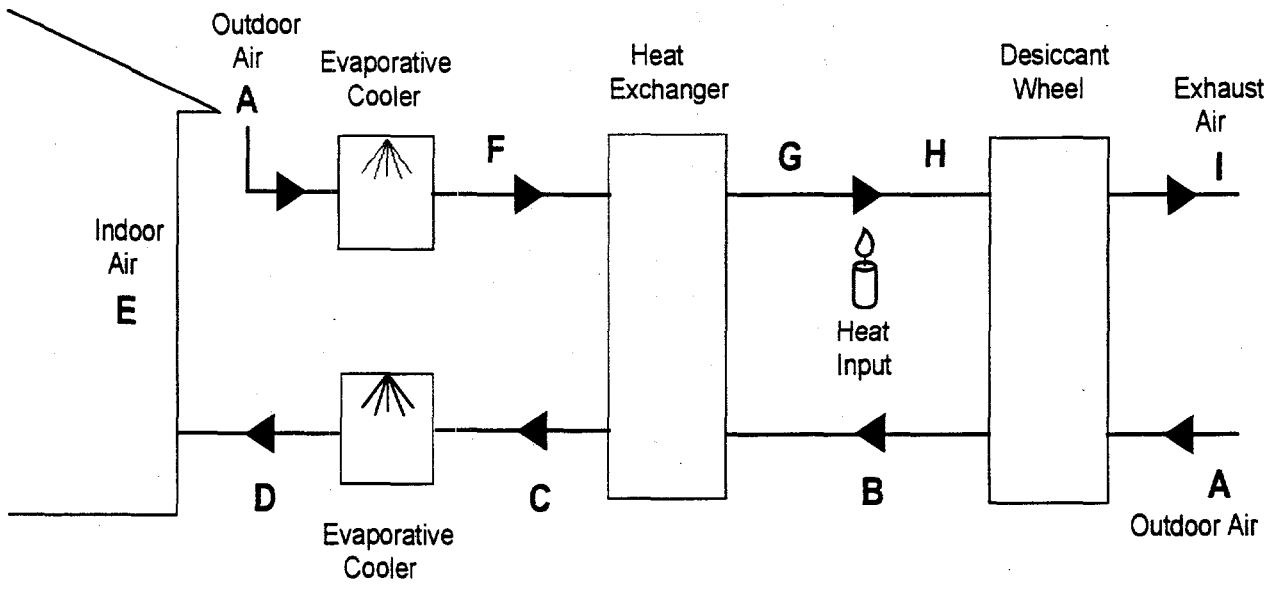

Figure 3-1. Schematic representation of the modified ventilation cycle.

Weather data used for these simulations are typical meteorological year (TMY). There were approximately 1400 hours in the annual simulation which represented the occupancy schedule for a 50,000 square foot office building modeled in a previous contract using DOE2. For all simulations, except where indicated otherwise, the ventilation cooling load is defined as the difference between the outside air enthalpy and the enthalpy of ARI indoor air (26.7°C and 50% RH). Two psychrometric representations of the modified ventilation cycle are illustrated in Figures 3-2 and 3-3. Figure 3-2 illustrates the air paths when ARI outdoor air (35°C, 40% RH) is processed and the system is operating at a predetermined regeneration temperature of 70°C. Since the reference enthalpy is that of ARI indoor air, the cooling capacity of the system exceeds the ventilation cooling load in this example. In the constant regeneration temperature mode, this mismatch is handled by operating the cooling system for a fraction of each hour simulated until the total ventilation cooling load is achieved for that hour. The CoP for the ideal cycle depicted in Figure 3-2 is 2.1. This CoP is slightly higher than the ideal modified ventilation cycle presented in Section I because the regeneration temperature is 5°C lower. This result is consistent with the results on regeneration temperature shown in that section.

Figure 3-3 is a psychrometric representation of the modified ventilation cycle when the regeneration temperature is adjusted to exactly meet the load. The CoP for this example is 2.4 and the regeneration temperature is 47.4°C. It is important to note that latent capacity is sacrificed at the lower regeneration temperature to achieve improved CoP's. Even though the enthalpy of the air supplied to the building is the same as ARI (and hence the building cooling load is unchanged), the SHR of the resultant building load will vary as outdoor conditions change. This result will require a building air conditioning (AC) system with a variable sensible heat ratio (SHR). If this situation cannot be resolved satisfactorily with the building AC system, the desiccant regeneration temperature could be increased in the event that additional latent cooling capacity is desired. The seasonal simulation results are shown in Table 3-1. Five U.S. cities were chosen: Atlanta, GA; New York

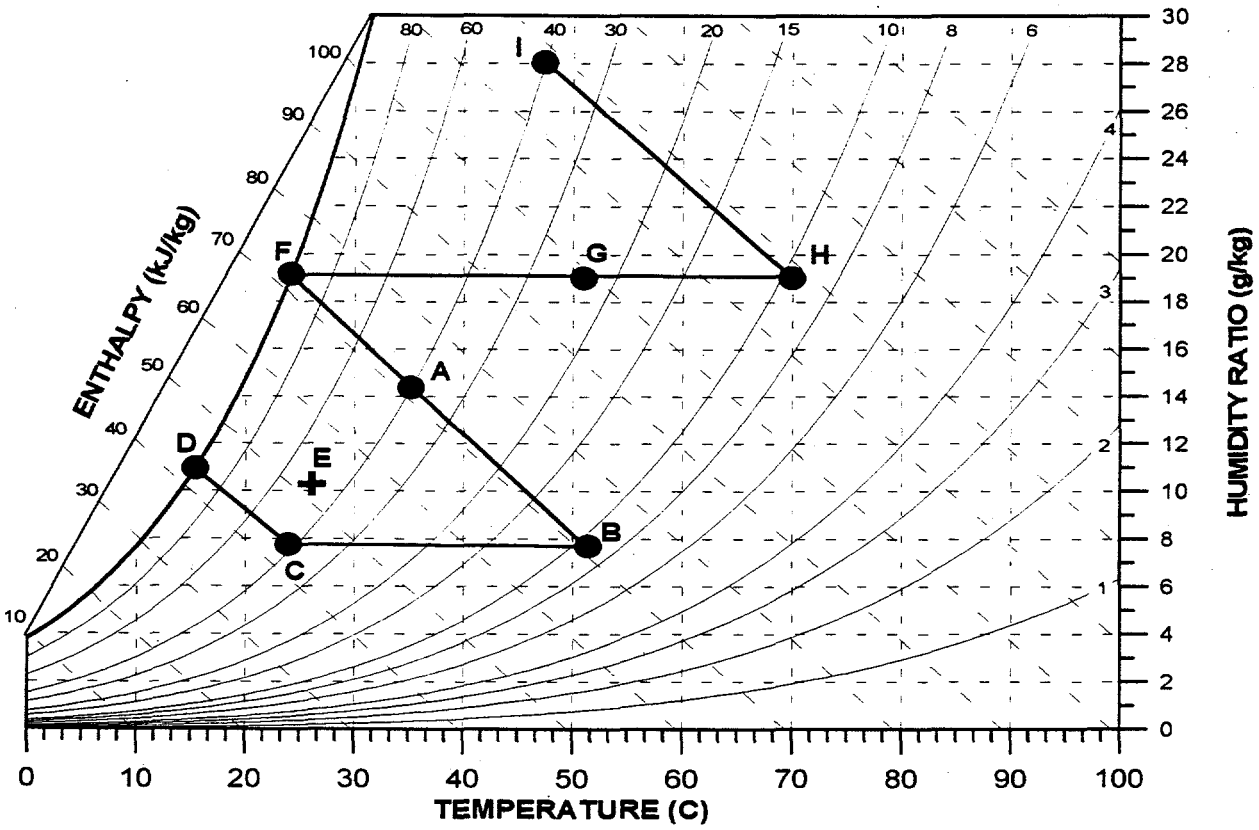

Figure 3-2. Psychrometric representation of constant regeneration temperature.

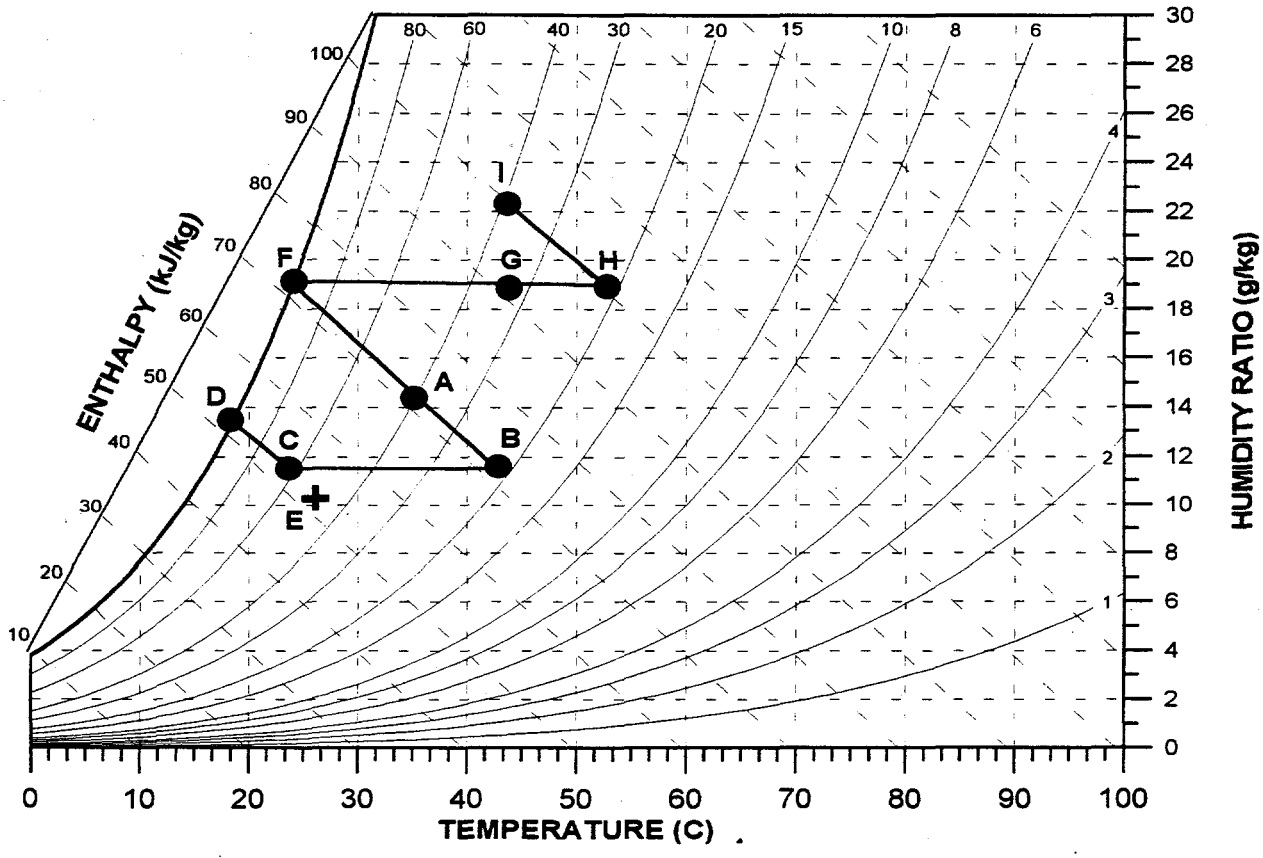

Figure 3-3. Psychrometric representation of variable regeneration temperature.

City, NY, Chicago, IL; Houston, TX; and Phoenix, AZ. The simulations performed utilize the ideal components previously described in Section I. Seasonal CoP, average SHR and average specific cooling capacity are tabulated. Cooling capacity and thermal CoP are as defined in Section I with the ventilation credit.

The two modes of operation, constant and variable regeneration temperatures, are compared. Figure 3-4 graphically compares the thermal CoP of these two modes. From these results, the following conclusions can be derived:

1. The variable regeneration temperature mode achieves higher CoP's for all the cities simulated.

2. The variable regeneration temperature mode always provides less latent cooling than the constant regeneration temperature mode.

3. The variable regeneration temperature mode allows the desiccant cooling system to operate as a regenerative evaporative cooler when possible. This is particularly evident in Phoenix, AZ, where there are many dry, hot days during the cooling season. This is the major reason for the very high seasonal CoP for the variable regeneration temperature mode in Phoenix (1.9 vs. 5.1), and the extraordinarily high SHR (0.98).

4. The seasonal CoP is not appreciably different from the ARI-assumed outdoor air conditions with constant regeneration temperature, regardless of climate. The only way CoP is appreciably improved is through the variable regeneration temperature mode.

The performance characteristics of these two operational modes are compared in more detail in Figures 3-5 through 3-8. These figures show the results of a seasonal simulation processing ventilation air to ARI indoor air enthalpy for a cooling season in Atlanta, GA. For these examples, the cooling season is defined not only by the outdoor air enthalpy, but also by the occupancy rate of the office building simulated. (There is ventilation load only when the building is normally occupied.)

Figures 3-5 through 3-8 divide the ambient conditions simulated into 5 two-degree wet-bulb bins. Only those ambient conditions for which a cooling load greater than zero exists are plotted. Figures 3-5 and 3-6 show the number of hours the ambient conditions were within a particular wet bulb bin as well as comparing the thermal CoP of the two operational modes as a function of these wet bulb bins. When the ambient wet bulb temperature is high, the CoPs for the two modes are similar because the regeneration temperatures are similar and the CoP dependency on regeneration temperature is small. The CoP of the variable regeneration temperature mode increases as the outdoor wet bulb enters a regime where the regenerative evaporative cooler is able to supply the cooling load. Figure 3-6 demonstrates that the improved CoP of the variable regeneration mode is achieved at the expense of decreased latent capacity as the outdoor wet bulb decreases. The system

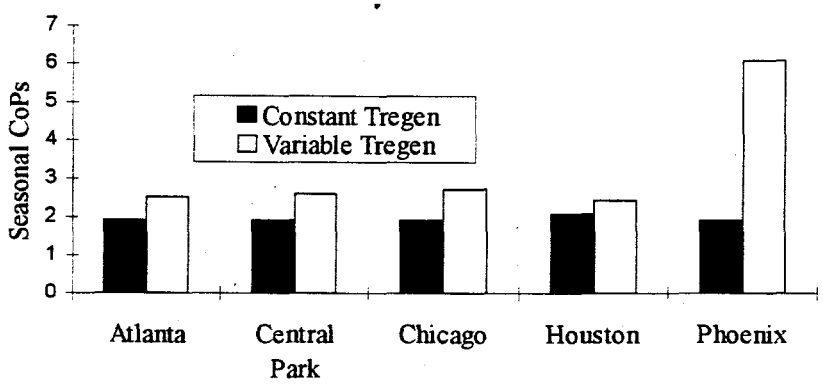

Figure 3-4. Comparison of two regeneration modes with ideal components

TABLE 3-1. Modified ventilation cycle seasonal simulation results. All components are ideal ($\varepsilon = 1$). Constant and variable regeneration temperature modes.

Location	T_{reg} (Max = 70°C)	Seasonal CoP	Average SHR	Average System SCC (kJ/kg)
Atlanta, Ga.	Constant	1.9	.53	25.4
Atlanta, Ga.	Variable	2.5	.70	11.9
New York City , NY	Constant	1.9	.62	22.8
New York City , NY	Variable	2.6	.76	12.5
Chicago, IL	Constant	1.9	.65	23.4
Chicago, IL	Variable	2.7	.80	12.8
Houston, TX	Constant	2.1	.52	26.9
Houston, TX	Variable	2.4	.64	15.8
Phoenix, AZ	Constant	1.9	.88	23.9
Phoenix, AZ	Variable	6.1	.98	15.0

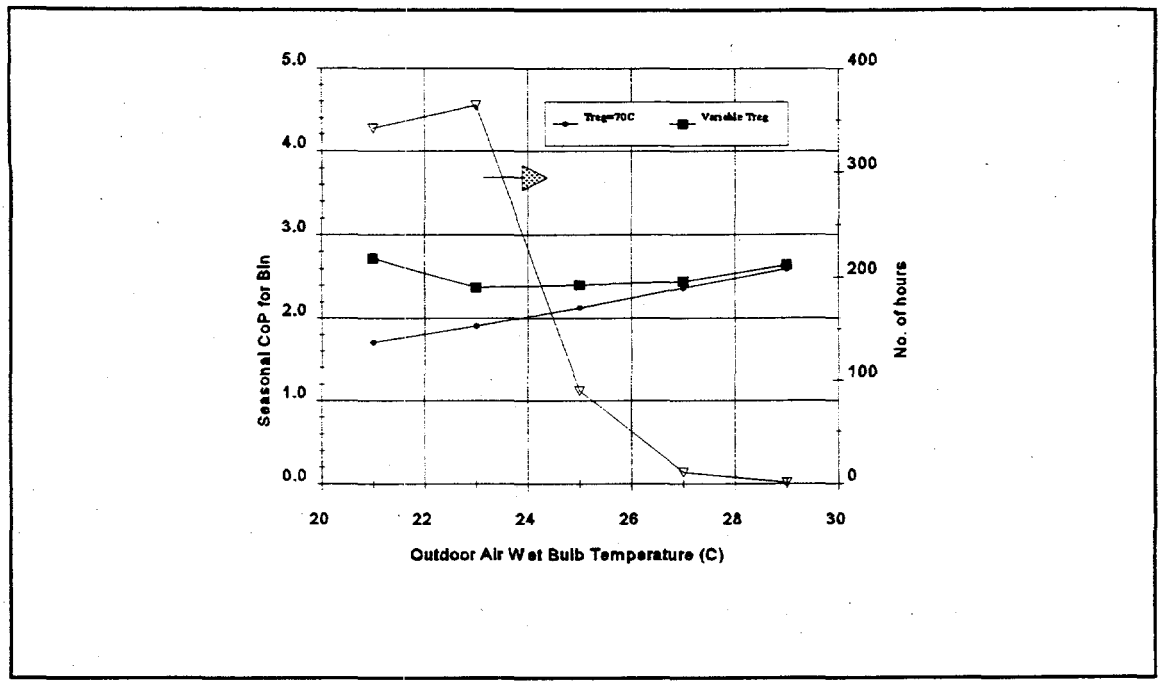

Figure 3-5. Seasonal simulation results: Constant vs. variable regeneration temperature. Average CoP; Atlanta GA

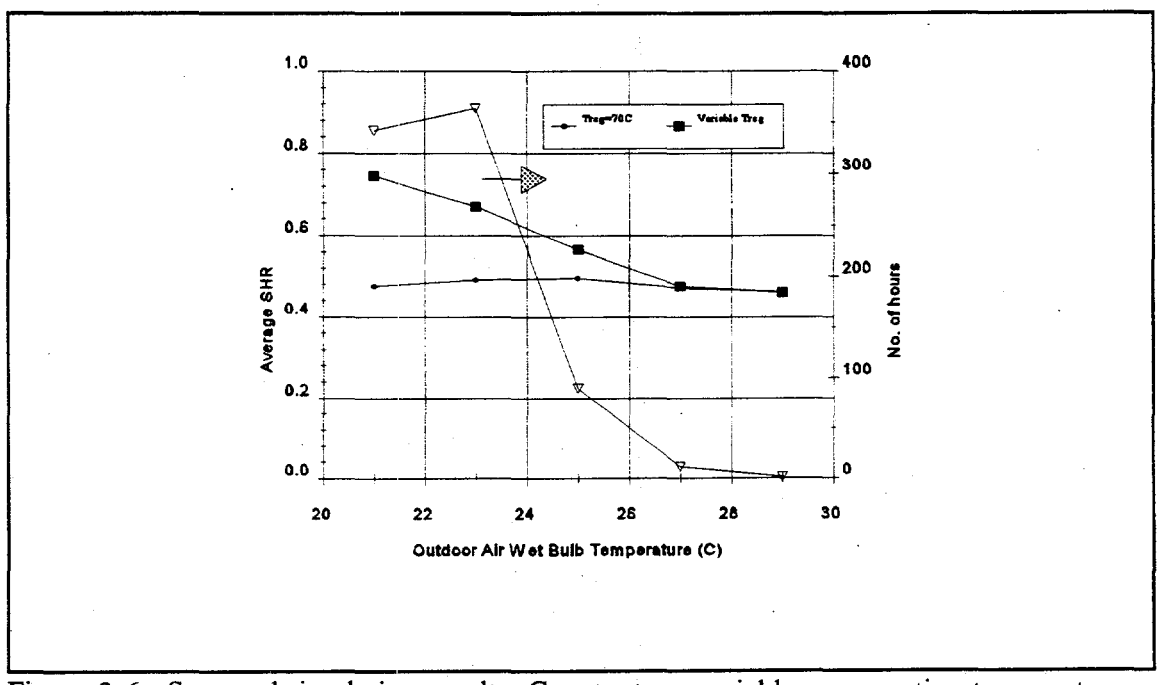

Figure 3-6. Seasonal simulation results: Constant vs. variable regeneration temperature. Average SHR; Atlanta GA

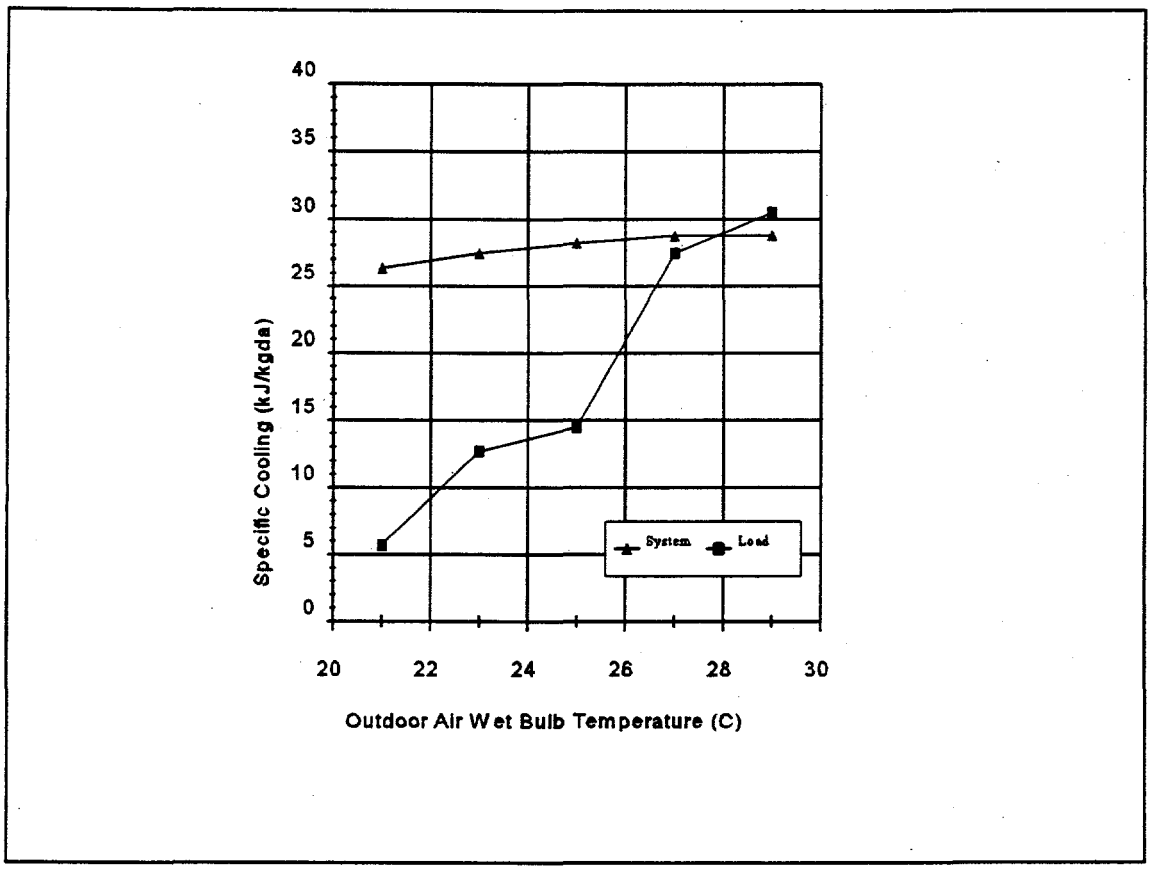

Figure 3-7. Seasonal simulation results: System SCC and building load variation, Regeneration temperature = 70 °C, Atlanta GA

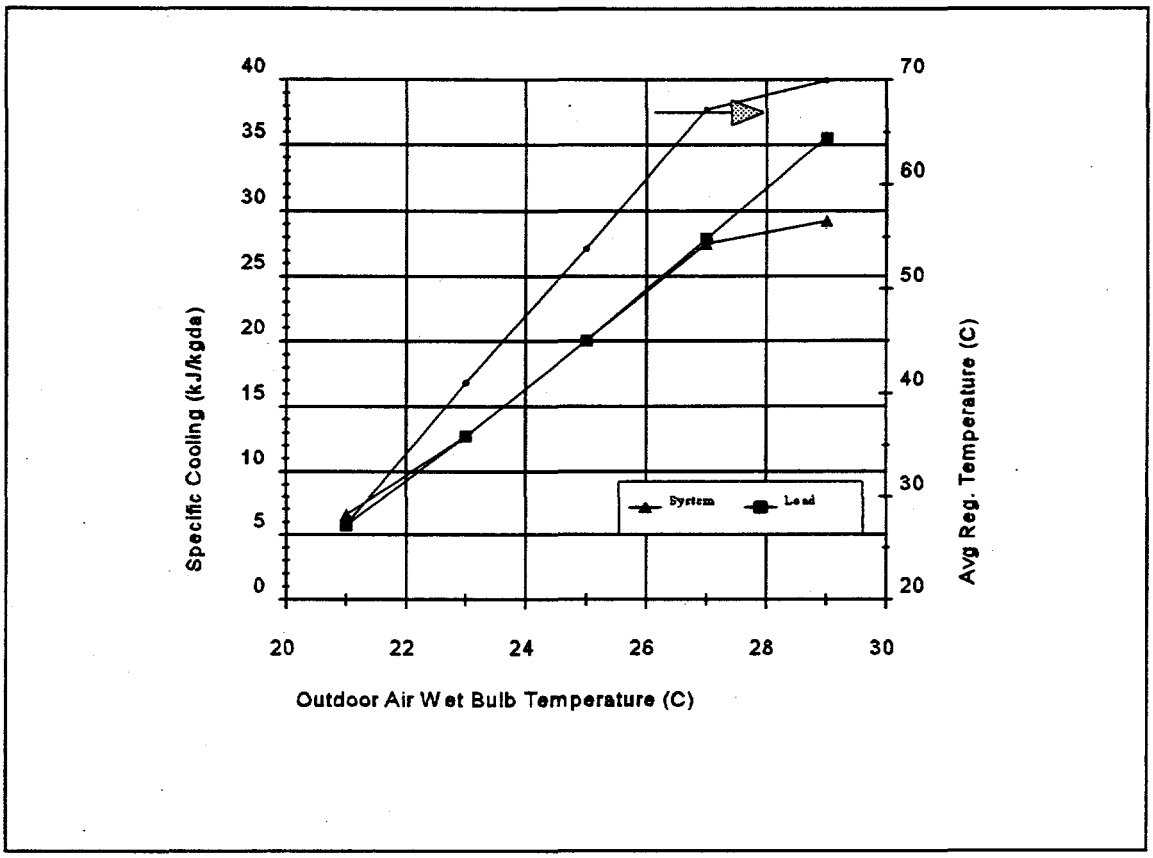

Figure 3-8. Seasonal simulation results: System SCC and building load variation, Variable regeneration temperature, Atlanta GA

SCC and the cooling load for the constant regeneration temperature mode is illustrated in Figure 3-7. For a wet bulb temperature below the 27°C wet bulb bin, the system SCC exceeds the load and the system must be cycled as necessary to meet the load. Figure 3-8 illustrates the system SCC and cooling load for the variable regeneration temperature mode. The required regeneration temperature is also shown. As the ambient wet bulb temperature increases, the cooling load increases and the regeneration energy required to meet the load is adjusted. The regeneration temperature was selected such that the system meet the load 97.5% of the time. This criterion causes the system SCC to be somewhat lower than the cooling load at high wet bulb temperatures. Although the SCC of the variable temperature mode is lower, in many cases, than the constant temperature mode, it is important to note that the system is still meeting the total cooling requirements of the load (although at a higher SHR) by operating continuously at a higher CoP.

Seasonal Simulations with Variable Component Effectiveness

The results shown in Table 3-1 are for ideal components, that is, components with maximum theoretical efficiency. The effects of more realistic components on the seasonal performance of the modified ventilation cycle are now considered. As presented in Section II, the desiccant wheel performance and the heat exchanger effectiveness have the most significant impact on the performance of open-cycle desiccant systems. Thus these two components were the focus of the following seasonal simulations.

Heat Exchanger Effectiveness

Referring to Figure 3-1, for the case of equal flow rates through each side of the heat exchanger, the heat exchanger effectiveness is defined as:

$$\varepsilon = q/q_{max} \approx (T_5-T_6)/(T_5-T_1)$$

Where:

ε = Heat exchanger effectiveness
q = Actual heat transfer
q_{max} = Maximum heat transfer
T_5 = Inlet process air temperature to heat exchanger
T_6 = Outlet process air temperature to heat exchanger
T_1 = Inlet regeneration air temperature to heat exchanger.

All other components were treated as ideal and seasonal simulations were performed for the same five locations for heat exchanger effectiveness values of 0.8, 0.85, 0.9, 0.95 and 1.0. The results of the simulations are shown in Tables 3-2 through 3-11 (in Appendix C). As expected from previous results in Section II, both seasonal CoP's and SCC's decrease with decreasing heat exchanger effectiveness. In all cases the variable regeneration temperature offers higher CoP's than the constant temperature system. However, this CoP advantage diminishes with decreasing heat exchanger effectiveness. This is because the regeneration temperature of the desiccant must increase to meet the load as system performance decreases (loss in cooling capacity as heat exchanger effectiveness decreases). As regeneration temperature increases for the variable regeneration temperature mode, that mode then becomes more like the constant regeneration temperature mode.

In particular, this advantage diminishes most in drier climates because most of the CoP advantage for the variable regeneration temperature mode depends on the regenerative evaporative cooler performance. When the hours of evaporative cooling operation are decreased, the system must operate with the desiccant more often.

Desiccant Wheel Performance

From Section II, the physical parameters that influence desiccant wheel performance are desiccant heat of sorption, thermal heat capacity, isotherm shape, and heat and mass transfer NTU. There are two physical ramifications of these parameters. One is to change the outlet air enthalpy (thermal heat capacity and heat of sorption). The other is to change the outlet air relative humidity (all of these parameters). Rather than deal with all of the desiccant wheel physical parameters separately, as in Section II, we have selected to investigate the performance effects based on the ramifications to these parameters, that is outlet air enthalpy and relative humidity.

The effects of non-isenthalpic operation are modeled by defining a ratio of entering and exiting air enthalpies. This effect is applied only to the dehumidification process because the energy and mass balances used to determine the regeneration conditions will determine the enthalpy ratio for the regeneration process. The effects of achieving less than ideal outlet air relative humidities are modeled the same way as defined in Section II.

Reasonable values for these parameters were determined from test data for real desiccant wheels and computer simulation. Two commercially available desiccant wheels were evaluated over a wide range of entering air conditions. In addition, a numerical desiccant wheel model was used to simulate the same entering air conditions. Once the efficacy of the numerical computer model was established (typical agreement about 2%), this model was then used to generate results for entering air conditions that represented the spread of outdoor air conditions encountered for the cities chosen. For a typical wheel, the enthalpy ratio varied from .93 to .96, while the RH effectiveness varied from .83 to .98 over the full range of process air inlet conditions.

Seasonal simulations were performed for the same five locations for a desiccant wheel with inlet to outlet enthalpy ratios of 1.0, 0.95 and 0.9 for the modified ventilation cycle. On the regeneration side, the specified outlet RH and a mass and energy balance is used to calculate the ratio of regeneration air flow to process air flow. As stated earlier, this energy and mass balance determines the outlet regeneration enthalpy.

These seasonal simulation results are tabulated in Tables 3-12 through 3-21 (in Appendix C). The effect of non-isenthalpic desiccant wheel operation is generally not very significant. The effect is generally a CoP reduction of 2 to 5% per 5% change in enthalpy ratio. The higher dehumidification outlet air enthalpy imparts more preheat to the regeneration stream, which tends to increase the CoP. However in order to maintain a mass balance, the calculated mass flow ratio between regeneration and dehumidification rises as the enthalpy ratio decreases. This effect tends to decrease the CoP. As the process outlet enthalpy ratio decreases, the CoP advantage of variable regeneration temperature operation is somewhat diminished for all locations.

The one exception to these general results is the variable regeneration temperature mode for Phoenix, AZ. For this climate and operational mode, the CoP reduction is approximately 13 to 23% for each 5% change in enthalpy ratio. This is because, under these hot, dry conditions, a moisture balance for the cycle requires more regeneration air flow than more humid conditions. Based on the earlier analyses of practical desiccant wheels, it appears that the desiccant wheel enthalpy ratio will remain well above 0.9 for a wide range of entering air conditions. This ratio tends to be lower as the regeneration temperature increases. Thus the value of 0.95 appears to be reasonable for most of the climates simulated, except for Phoenix, where a value of 1.0 to 0.98 is more appropriate.

Additional simulations were performed for simultaneously varying the heat exchanger effectiveness and desiccant wheel enthalpy ratio. These results are tabulated in Tables 3-22 through 3-31 (in Appendix C). In order to incorporate the effect of a more realistic process outlet relative humidity into the model, the simulations were repeated with the relative humidity effectiveness of 0.9. These results are shown in Tables 3-32 through 3-41 (in Appendix C).

Conclusions

The modified ventilation cycle was simulated for processing ventilation air to ARI indoor enthalpy during a cooling season for 5 U.S. cities. A simplified model was utilized to describe the components of the cycle. This is a preliminary study and is only designed to demonstrate the behavior of the system under changing ambient conditions and provide approximate performance information on the system. If further investigations are pursued, more detailed modeling tools should be used.

In all cases, the variable regeneration temperature operation of the ventilation cycle results in higher seasonal CoPs than the constant regeneration temperature mode. While this is accomplished at the expense of latent capacity, the system can be controlled to increase regeneration temperature if additional latent capacity is desired. For the simulations performed with ideal components, the CoP increase for the variable regeneration temperature mode ranged from 14% to 37% for four locations. For Phoenix, the CoP increase was 220%. The high CoP value for Phoenix is because an evaporative cooling system alone (without the desiccant wheel) is well suited for the desert climate in that location. For a very humid climate such as Houston, the CoP advantage is minimized because dehumidification from the desiccant wheel is needed most of the time.

The effect of component performance was modeled utilizing defined effectiveness values. Only the heat exchanger and desiccant wheel performance were considered based on results in Section II. The overall CoP and the CoP advantage of the variable regeneration temperature mode diminishes with component performance. The CoP was degraded in the range of 45 to 65% as the heat exchanger effectiveness was varied from 1 to 0.8.

Lastly, a commercially-available desiccant wheel was considered through the use of two defined parameters; relative humidity effectiveness and enthalpy ratio. For the variable regeneration temperature mode, the process enthalpy ratio caused a moderate CoP degradation (range 10 to 33%) over the range investigated (1 to 0.9). These ranges are given for the case when the other

effectiveness values are 1. The CoP degradation for varying enthalpy ratio for the constant regeneration temperature mode is only 3 to 8%. However, the 8% figure (the highest) is again for Phoenix. The desiccant wheel relative humidity effectiveness caused a moderate CoP degradation (range 9% to 23%) for the range investigated (1 to 0.9). The lowest degradation is for Phoenix, while the highest is for Houston.

SECTION IV. FIELD PERFORMANCE AND PRIMARY ENERGY COMPARISONS

The preceding analyses have determined the performance characteristics of desiccant cooling cycles, in general, and the modified ventilation cycle (shown in Figure 3-1) specifically. The intent of this section is to show the results of implementing this technology nationally. These results will include system performance (both thermal and electrical) in the field with realistic components, comparison of this performance to conventional technology, and an estimate of the implications of desiccant technology on national energy use.

Conventional Desiccant Dehumidification Technology

Description of Components

In order to quantify the electrical consumption of desiccant cooling units, the pumping power required to move air through the unit must be determined. This pumping power will be strongly influenced by the geometry of the component. Tables 4-1 through 4-3 define the details of the heat exchanger wheel, the desiccant wheel, and the evaporative cooler media used in simulating actual operational performance.

A random woven screen mesh rotary heat exchanger is the selected geometry for the heat exchanger. Rotary heat exchangers are preferred for this application as they are compact, of reasonably high effectiveness, and easily integrated into the desiccant system geometry. The selected parameters which are considered constant for this analysis include the matrix porosity, alpha (ratio of transfer area on one side to total heat exchanger volume), depth of wheel and rotary capacity rate ratio. The airflow was held constant at 15000 cfm. For this exchanger, the frontal area was varied to obtain face velocities of 300, 500 and 800 fpm. Experimental data for the selected geometry were obtained[4] to determine the Stanton number and friction factor for each case. The heat exchanger effectiveness (ε_{HX}) for each configuration considered were calculated from numerical solutions for the number of transfer units (NTU's)[1]. As the face velocity increases from 300 to 800 fpm, the heat exchanger effectiveness decreases from 0.91 to 0.87, while the size of the rotary wheel decreases from 11.2 to 4.2 square meters. The fan efficiency assumed is 55% and the motor efficiency is 90%.

A number of computer simulations were performed to determine the appropriate effectiveness values to use in the seasonal simulations. Initially the computer model used, developed by Enerscope Inc., was compared against manufacturer's data supplied by Cargocaire. The Cargocaire series HCE-20,000 wheel was selected[2]. The information supplied by the manufacturer does not allow calculation of the regeneration outlet state. In addition, there is no information about the pressure drop through the wheel. For a face velocity of 450 fpm, a silica gel wheel was simulated, using the Enercope model, over 4 different inlet process air conditions:

---

[4]Kays, W.M. and London, A.L., Compact Heat Exchangers, McGraw-Hill, 1984.
[2]Cargocaire bulletin 400, Cargocaire Corporation, Amesbury, Mass., 1978.

Table 4-1. Heat Exchanger Performance

Calculated HX values

Cmin (hot) = 8.30 kJ/kg-s
Cmax (cold) = 8.30 kJ/kg-s
Cmin/Cmax = 1
hydraulic radius = 0.0010 m

Selected Heat Exchanger Conditions

HE Type: Periodic counterflow heat exchanger
process flow = 15000 cfm
Regen. flow = 15000 cfm
surface type: random woven screen matrix
porosity = 0.832
Cr/Cmin = 3
L = 0.25 m
alpha = 800 m

Fan

fan efficiency = 0.58
motor efficiency = 0.9

Face Vel. (fpm)	U (m/s)	Afr (m2) total	Ac (m2) side	G (kg/s-m2)	Re	As (m2) side	StPr^2/3	St	h (kW/m2-K)	NTU	εHX	f	dP(Pa) side	fan kW side
300	1.52	11.17	4.65	1.77	400	1117	0.080	0.1008	0.1801	12.12	0.91	0.68	31.00	0.42
500	2.54	6.70	2.79	2.96	666	670	0.063	0.0794	0.2364	9.54	0.89	0.58	73.44	1.00
800	4.06	4.19	1.74	4.73	1066	419	0.049	0.0617	0.2942	7.42	0.87	0.52	168.55	2.29

Table 4-2. Desiccant Wheel Performance Calculations

Enerscope Model
U of Wisc fit to Silica Gel

CFM,proc =	15010	cfm	**Bed density =**	110	kg/m3
CFM,reg =	7505	cfm	**cpbed =**	921	kJ/kg-K
mproc	8.25	kg/s	**AU =**	5000	
A/V =	1.55	1/m	**mreg =**	4.12	kg/s
Trot =	1.2	min	**Depth =**	0.1	m
sigma =	0.85		**Vol =**	0.82	m3

Face Velocity =	**300**	**fpm**	**Proc. flow area =**	4.63	m2
Regen. flow area =	2.32	m2	**U air =**	1.53	m/s
Afr =	8.17	m2	**As =**	1	m2

Tpi (C)	wpi (kg/kg)	hpi (kJ/kg)	RHpi	Treg (C)	RHri	RHro	Tpo (C)	wpo (kg/kg)	hpo (kJ/kg)	RHpo	εRH Proc	εRH Reg.	hin/hout	dPproc (Pa)	dPreg (Pa)	Fan,proc (kW)	Fan, reg (kW)
35	0.0142	71.6	0.4	70	0.09	0.42	47.05	0.0107	75	0.16	0.77	1.06	0.95	49	54.6	0.66	0.37
43.3	0.011	72	0.2	70	0.09	0.22	50.6	0.0093	75	0.12	0.73	1.18	0.96	49	53.1	0.66	0.36
43.3	0.0156	83.9	0.28	70	0.11	0.3	51.7	0.0133	86.5	0.16	0.71	1.12	0.97	49	53.1	0.66	0.36
26.7	0.0156	66.7	0.7	70	0.09	0.72	43	0.0105	70.4	0.19	0.84	1.03	0.95	49	56.1	0.66	0.38
								Average values =			0.76	1.10	0.96				

Table 4-2. Desiccant Wheel Performance Calculations (continued)

Face Velocity =	**500**	**fpm**	**Proc. flow area =**	2.8	m2
Regen. flow area =	1.87	m2	**U air =**	2.54	m/s
Afr =	5.49	m2	**As =** 1	m2	

Tpi (C)	wpi (kg/kg)	hpi (kJ/kg)	RHpi	Treg (C)	RHri	RHro	Tpo (C)	wpo (kg/kg)	hpo (kJ/kg)	RHpo	εRH Proc	εRH Reg.	hin/hout	dPproc (Pa)	dPreg (Pa)	Fan,proc (kW)	Fan, reg (kW)
35	0.0142	71.6	0.4	70	0.09	0.41	46.58	0.0105	74	0.16	0.77	1.03	0.97	82	91.3	1.11	0.62
43.3	0.011	72	0.2	70	0.09	0.22	50.2	0.0091	74.1	0.12	0.73	1.18	0.97	82	88.9	1.11	0.60
43.3	0.0156	83.9	0.28	70	0.11	0.3	51.4	0.0131	85.8	0.16	0.71	1.12	0.98	82	88.9	1.11	0.60
26.7	0.0156	66.7	0.7	70	0.09	0.68	42.4	0.0103	69.2	0.2	0.82	0.97	0.96	82.1	93.9	1.11	0.64
								Average values =			0.76	1.07	0.97				

Face Velocity =	**800**	**fpm**	**Proc. flow area =**	1.75	m2
Regen. flow area =	1.16	m2	**U air =**	4.07	m/s
Afr =	3.42	m2	**As =**	1	m2

Tpi (C)	wpi (kg/kg)	hpi (kJ/kg)	RHpi	Treg (C)	RHri	RHro	Tpo (C)	wpo (kg/kg)	hpo (kJ/kg)	RHpo	εRH Proc	εRH Reg.	hin/hout	dPproc (Pa)	dPreg (Pa)	Fan,proc (kW)	Fan, reg (kW)
35	0.0142	71.6	0.4	70	0.09	0.37	45.7	0.0106	73.4	0.17	0.74	0.90	0.98	132	147	2.09	1.16
43.3	0.011	72	0.2	70	0.09	0.2	49.4	0.0092	73.6	0.12	0.73	1.00	0.98	132	144	2.09	1.13
43.3	0.0156	83.9	0.28	70	0.11	0.28	43.3	0.0156	83.9	0.16	0.71	1.00	1.00	132	144	2.09	1.13
26.7	0.0156	66.7	0.7	70	0.09	0.6	41.3	0.0105	68.5	0.21	0.80	0.84	0.97	133	152	2.09	1.20
								Average values =			0.74	0.93	0.98				

Table 4-3. Evaporative Cooler Performance Predictions

Unit selected: Cargocaire 1000 series; **Air Flow** = 15000 cfm

Face Vel. (fpm)	Ac (m2)	εEC	dP (in-H2O)	dP (Pa)	Fan kW
300	4.65	0.905	0.30	74.7	1.0
500	2.79	0.835	0.48	119.52	1.6
800	1.74	0.76	0.77	191.73	2.6

1. ARI outdoor air (35 °C, 40% RH)
2. Hot and humid air (43 °C, 50% RH)
3. Hot and dry air (43 °C, 28% RH)
4. Cool and humid air (26.7 °C, 70% RH)

The regeneration temperature for this comparison is 88°C. This is the lowest regeneration temperature data supplied by Cargocaire. The process side relative humidity effectiveness agreed within 10% and the process side enthalpy ratio agreed within 1%. The model predicted slightly poorer performance of the desiccant wheel than the manufacturer.

The model was then used to predict performance of the desiccant wheel for a regeneration temperature of 70°C. The same inlet process air states were used. This simulation was repeated for the same 3 face velocities: 300, 500 and 800 fpm. The frontal area of the desiccant wheel was varied for a constant flow of 15,000 cfm to obtain the desired face velocities. The relative humidity effectiveness values are much higher on the regeneration side than on the process side. As the face velocity increases from 300 to 800 fpm, the relative humidity effectiveness on the process side decreases from .76 to .74 and the enthalpy ratio increases from .96 to .98. On the regeneration side, the relative humidity effectiveness decreases from 1.1 to 0.93. These values are averages over the range of process air conditions modeled.

The evaporative cooler performance is based on manufacturer's data. The Cargocaire 1000 series evaporative cooler data supplies pressure drop and evaporative cooler effectiveness as a function of face velocity. For 15,000 cfm, the free flow area of the evaporative cooler is calculated to achieve the desired face velocity. As the face velocity increases from 300 to 800 fpm, the evaporative cooler effectiveness decreases from .905 to .76 and the free flow area decreases from 4.65 to 1.74 square meters.

Seasonal Simulations

Tables 4-4 and 4-5 (in Appendix D) show the detailed results of operating these components in the five climates analyzed earlier. The headings of these two tables indicate: Total hours of cooling, total cooling load supplied, the component face velocity, external energy required for regeneration, the heat exchanger effectiveness, the evaporative cooler effectiveness, the desiccant wheel relative humidity effectiveness for the dehumidification process, the desiccant wheel relative

humidity effectiveness for the regeneration process, the ratio of air enthalpies in and out of the desiccant wheel for the dehumidification process, the electrical requirements for fan power, the seasonal CoP of the system based on external regeneration energy, the sensible heat ratio of the system, the specific cooling capacity, and finally, the seasonal energy efficiency ratio (SEER) based on the fan power requirements.

Table 4-6 (in Appendix D) compares the primary energy usage for the fixed and variable regeneration temperature desiccant systems. In this table, the primary energy CoP includes the thermal energy required for desiccant regeneration as well as that required at the electrical power plant to operate the fans. The efficiency of converting primary energy at the power plant to electricity at the building is assumed to be 28%. This value is lower than the commonly assumed value of 33% for the following reason. The distribution of electricity is thought to be grossly miscalculated. Most researchers use the national average of 92% as transmission efficiency. What these researchers fail to take into account is the fact that the vast majority of electricity generated is transmitted a very short distance. An aluminum ore processing facility will use more electricity than a city and will require that electricity be transmitted across a river. Actual electrical transmission efficiency from a generating plant to a building requiring electricity for HVAC equipment is closer to 79%. We base this number on test data taken from diesel-grid systems where the distribution efficiency is 86%. We assume this to be similar to the sub-station system level of larger grid systems. This efficiency is then multiplied by a cross-country transmission efficiency of 92% to yield the overall efficiency of 79%.

Results

Tables 4-4 and 4-5 yield a number of interesting insights. The relative humidity effectiveness of the desiccant wheel for the dehumidification process is generally much lower than previously modeled (0.75 vs. 0.9). However, on the regeneration side, this effectiveness is much higher. It should be noted that an effectiveness greater than one is not a violation of physics here. Recall from the previous sections that heat capacity and adsorption energy will create equilibrium outlet relative humidities that are greater than the entering relative humidity used as a reference. The main reason these ratios are different from those modeled in Section III is because the regeneration temperature used in these analyses is lower than the data available of wheel manufacturers. However, the implications of this result for seasonal CoP does not differ considerably from those predicted in Section III.

Comparing the results from Tables 4-4 and 4-5 yields the following conclusions:

1. The CoP improvement for the variable regeneration temperature mode is much less significant when simulating real-world components. Thermal CoPs are generally greater than 1.0, but not approaching those for ideal components.

2. A performance trade-off exists between regeneration energy requirements, electrical energy requirements, and sensible heat ratio. SEERs are significantly higher for the constant regeneration mode of operation.

3. Face velocities between 300 and 500 feet per minute yield high SEERs. Face velocities of 800 fpm yield much lower SEERs.

Table 4-6 shows that electrical energy requirements are the great "equalizer" between operational modes. When primary energy is considered, the constant regeneration temperature mode gives almost identical energy efficiencies to that for variable regeneration temperature. All of the climates perform similarly except for the hot, dry climate of Phoenix, AZ. Here, operation definitely favors variable regeneration temperature. The overall primary energy CoP for Phoenix is quite impressive when compared to the generalized ARI CoP with idealized components (1.7 vs. 2.1). For all of the remaining cities, the primary energy CoP is generally 1.0 for 300 fpm component face velocities and 0.8 to 0.9 for 500 fpm. Including the primary energy needed to operate fans in the desiccant system generally reduces overall CoP anywhere from 10 to 30% depending mostly upon operational mode and component face velocity rather than climate. Variable regeneration temperature and high component face velocities result in the greatest reduction.

A conventional vapor-compression system with an SEER of 10 will yield a primary energy CoP (under the assumptions chosen) of 0.8. An SEER 12 system will be 1.0. This result shows that desiccant cooling systems with conventional components are energy competitive with vapor-compression systems in all climates. In hot, dry climates the desiccant system is vastly more efficient if the correct operational parameters are chosen. The major parameter is to operate the system with only the evaporative coolers for as much of the cooling season as possible.

Advanced Desiccant Materials

The previous section modeled the performance of conventional desiccant dehumidification equipment. This equipment is typified by desiccant wheels constructed of laminar flow passages with a form of silica gel desiccant impregnated into the walls of these passages. The critical performance parameter that can be improved by the type of desiccant chosen is the desiccant wheel effectiveness. This parameter is shown in Table 4-5 as εRH, proc. For conventional desiccant materials, this value ranges from 0.74 to 0.76, depending upon face velocity. Advanced desiccant materials have been shown to significantly improve desiccant wheel effectiveness. Simulations were performed using the Enerscope computer modeling tools described earlier to determine values for "εRH, proc" that are commensurate with a Type 1M desiccant material. These new values ranged from 0.84 to 0.86, depending upon face velocity.

Results

Table 4-7 (in Appendix D) shows the results for the same seasonal simulations as performed in Table 4-5. The only difference is that the desiccant wheel effectiveness for the process air stream is increased to reflect the improved performance of the advanced desiccant material. Seasonal CoP's generally increase about 10% for the advanced material for all of the cities simulated except Phoenix, AZ. Phoenix showed no significant improvement. SEER increased about 20% for all of the cities simulated, again with the exception of Phoenix. For this case, however, Phoenix improved about 10%.

Comparing Tables 4-5 and 4-7, show that the improved effectiveness associated with the advanced desiccant material creates more cooling for less regeneration energy. This is the source of the improvement in thermal CoP. Also notice, that the number of cooling hours are reduced for the advanced desiccant material. This, combined with the increased amount of cooling, creates the greater percentage increase in SEER that for thermal CoP.

Table 4-8 (in Appendix D) shows the effects on primary energy consumption for the advanced desiccant material. These results are computed the same as those from Table 4-6 for conventional desiccants. Comparing the results between Tables 4-8 and 4-6 shows approximately the same relative benefits for the advanced material as was achieved on thermal CoP alone. The main reason for this is that the power plant primary energy required to operate air moving equipment is very small compared to the primary energy required for desiccant regeneration.

Control Strategies

The seasonal simulations performed previously operate the desiccant cooling equipment under all outdoor conditions whenever the outdoor enthalpy is greater than the indoor enthalpy and the building is occupied. Examining the hourly results of those simulations rather than the seasonal averages presented in Tables 4-4 through 4-8 yields some interesting insights. Whenever the outdoor air is near the ARI cooling standard (35°C, 14 g/kg) the resulting thermal CoP ranges from 1.3 to 1.5 depending upon desiccant type. As the outdoor air becomes cooler, but with relatively high humidity, the thermal CoP drops significantly. This large drop combined with the high number of occurrences for cool, humid weather creates the result that seasonal CoP's are significantly lower than the CoP's for ARI air conditions.

In an effort to operate the desiccant cooling equipment in a manner that may significantly improve seasonal CoP, the seasonal simulations were repeated incorporating a different control strategy than previously used. The new control strategy does not operate the desiccant wheel if the sensible heat exchanger and evaporative cooler sections of the system can supply building air at or below the indoor air enthalpy. The rationale behind this control strategy is to avoid the hours of low thermal CoP operation for the desiccant wheel. An additional benefit is that during periods when the building load is met without using the desiccant wheel, cooling is being supplied to the building without any thermal energy input. Only electrical energy is needed to operate the fans needed for air movement.

Results

Tables 4-9 and 4-10 (in Appendix D) show the results for operating the standard commercially-available desiccant equipment with the new control strategy. For the cities that generally experience hot humid weather, Atlanta and Houston, the improvement in thermal efficiency is minimal at best. New York experienced about a 10% increase (similar to the advanced desiccant), Chicago about a 15% increase, and Phoenix a 100% increase. Obviously, as the weather becomes less humid, the greater the thermal efficiency benefit of supplying cooling with no thermal input. These simulations were repeated for equipment incorporating the advanced desiccant material described earlier. The results of these simulations are shown in Tables 4-11 and 4-12 (in Appendix

D). Similar results to those achieved using conventional technology are shown. However, the percentage increase in performance achieved by the advanced desiccant material is reduced as the amount of evaporative cooling increases. That is, there is less incentive to increase desiccant dehumidifier performance for hot, dry climates.

Enthalpy Exchange Devices

An alternative to treating outdoor air with a desiccant dehumidification device is to incorporate an enthalpy exchange device. A discussion of the differences in construction and performance between desiccant dehumidification and enthalpy exchange devices is given in Section II. Table 4-13 (in Appendix D) shows the detailed seasonal simulation results for enthalpy exchange of building ventilation air for the same building and air flow rate requirements as those shown in Tables 4-4 and 4-5. The enthalpy exchange device modeled is a commercially-available unit operating within the manufacturer's recommended conditions. The main difference between the operational conditions assumed for the desiccant systems depicted in Tables 4-4 and 4-5 and the enthalpy exchange device depicted Table 4-13, is that exhaust air from the building must exist in a central location that is located adjacent to the building ventilation air inlet for the enthalpy exchange device. As discussed earlier, this configuration is not common in existing buildings.

Because the desiccant dehumidification system can also operate using exhausted indoor air rather than outdoor air for the regeneration side of the system, simulations were conducted for the desiccant dehumidification system operating in the ventilation cycle. The results for those simulations are shown in Table 4-14 (in Appendix D).

Table 4-15 (in Appendix D) shows the primary energy results for the enthalpy exchange device modeled in Table 4-13.

Results

Because an enthalpy exchanger is a passive device, no external thermal energy is required for operation. Only electrical energy for operating fans and a small motor for wheel rotation is required. The EER's shown for the enthalpy exchanger are based on the electrical energy required to overcome the pressure drop of the enthalpy exchange wheel only. Building air circulation is not included. Extremely high seasonal EER's are shown for the enthalpy exchange device for all of the climates simulated. However, Houston TX stands out because the enthalpy differences between indoor and outdoor air are the greatest in that location. Given the fact that the power consumption of the device will be constant regardless of building energy load, only the enthalpy difference between indoor and outdoor air will determine cooling capacity, and hence, EER. Also notice that the number of hours of operation for the enthalpy exchange device equal those for the variable regeneration case for desiccant dehumidification. This is because the control strategy for these two cases is essentially the same. That is, if the outdoor enthalpy is less than the indoor enthalpy, the unit will operate for the entire hour. Therefore, the number of hours of operation shown are the total number of hours that the outdoor enthalpy exceeds the indoor enthalpy when ventilation air (occupied hours) is required for the building.

Because the EER's are extremely high and no external source of regeneration energy is required by the enthalpy exchange device, the primary energy CoP's are also extremely high. Comparing Tables 4-13 and 4-15 with Tables 4-5 and 4-6 shows that enthalpy exchange devices will provide almost identical amounts of total cooling for about half the primary energy as desiccant dehumidification devices. This observation is true for all of the cities modeled with the exception of Houston TX. In Houston, the enthalpy exchange device provided approximately 25% more cooling energy with a little less than one-third the total primary energy.

Full Ventilation Cycle Simulations

The preceding section on enthalpy exchangers showed them to achieve superior total performance when compared to desiccant dehumidifiers. However, the comparison between the two technologies was not totally equal. The enthalpy exchanger must use exhausted indoor air in order to achieve cooling or dehumidification. The desiccant dehumidifier technology was simulated without the aid of utilizing this exhausted indoor air. Therefore, the results from Tables 4-5 and 4-6 were repeated for the same system using exhausted indoor air as the regeneration air rather than outdoor air. These results are shown in Tables 4-14 and 4-16 (in Appendix D).

Results

Comparing Tables 4-5 and 4-14 shows that the ability to use exhausted indoor air with the desiccant dehumidification equipment improves performance markedly. For the hot, humid climates of Atlanta and Houston, the increase in thermal CoP was approximately 30%. This improvement closely matched that for the hot, dry climate, Phoenix. The least improvement was shown by the two mild climate cities, New York City and Chicago. The improvement in thermal CoP for these cities was approximately 20%.

Comparing Tables 4-6 and 4-16 shows that the improvement in primary energy CoPs closely matches those shown for thermal CoP. Again, Atlanta, Houston, and Phoenix show approximately 30% improvement while New York City and Chicago show only a 20% improvement.

Comparing the desiccant dehumdification technology against the enthalpy exchange technology still shows an overwhelming efficiency edge to enthalpy exchange devices. The fact that the desiccant dehumidifier provides approximately 10% more cooling hardly compensates for the factor of 1300% to 2600% increase in primary energy consumption.

Implications for National Energy Usage

Table 4-17 (in Appendix D) shows the ventilation air requirements for the U.S. by building use and by ventilation standards. ASHRAE 62-1981 and 62-1989 are compared for numerous building uses. These data are used to predict the national energy usage for commercial buildings as a consequence of ventilation standards and technologies.

Combining the data from Tables 4-6, 4-8, 4-10, 4-12, 4-15, and 4-16 with Table 4-17 allows the calculation of the energy used to condition ventilation air for the entire country given the following assumptions. In order to translate the air cfm rates given in Table 4-17 into a quantity of air, some knowledge of the times of operation required for each building type is necessary. It was assumed that the average operational hours of ventilation air for all building uses combined was equal to that of an office building. The buildings requiring the most total ventilation air flow rates are auditoriums, schools, food service , mercantile, office, and churches. Uses requiring less ventilation time than office buildings would be auditoriums and churches. Uses requiring more time would be food service, and mercantile. Education would probably be similar to office buildings in ventilation time. The time profiles for ventilation air requirements in an office building have already been determined for the seasonal simulations presented in this section. The next assumption necessary is to determine the outdoor air conditions that apply to each building use. If we can assume that the average of the five cities chosen for simulation represent the national average for all buildings (admittedly a great leap of faith), then the energy difference between the outdoor air needed to supply ventilation to all buildings and ARI indoor air is about 0.4 quads for the country. If we apply only that energy difference associated with ASHRAE 62-1989, then that amount is reduced to slightly more than 0.1 quad.

The potential primary energy savings for various desiccant technologies compared with conventional vapor-compression equipment (SEER=10) is shown in Table 4-18. The desiccant technologies chosen, conventional, advanced desiccant material, advanced control strategies, enthalpy exchange, and ventilation cycle represent the primary energy performance depicted in Tables 4-6, 4-8, 4-10, 4-12, 4-15, and 4-16. These results are based on a city average of the primary energy CoP for each of the desiccant systems being compared to a vapor-compression system with a primary energy CoP of 0.8. The primary energy savings are shown in Table 4-18 for two conditions. One is that all of the building ventilation air is processed by this equipment. The other is that only the increase in ventilation air required by ASHRAE 62-1989 is processed.

Results

The most obvious result from these analyses is the overwhelming superiority relative to primary energy savings exhibited by the enthalpy exchange device when compared to all other alternatives. Of course, these predictions are based on the assumption that building exiting air is available for exchange with the entering ventilation air. However, a potential total primary energy savings of 0.4 quads is very significant.

Another observation of note is that desiccant-based systems, even those incorporating commercially-available components can compete with conventional vapor-compression systems on a primary energy basis as long as the application of the technology is the treatment of building ventilation air. Moreover, the potential for desiccant-based systems to produce significant national energy savings (fractions of a quad) is significant if improvements in component efficiencies and/or control strategies can be implemented. Up to 0.14 quads of energy savings are possible with an improvement in the desiccant wheel and 0.17 quads could be saved with regeneration energy controls. No attempt has been made in these analyses to identify niche applications for desiccant systems where individual market energy savings could be large. The one obvious niche application would be

Table 4-18. Potential Energy Savings (Quads) Compared to Vapor Compression (SEER=10)

Desiccant Technology	Total Ventilation Load	Increase Due to ASHRAE 62-1989
Conventional	0.10	0.025
Advanced Desiccant Material	0.14	0.035
Advanced Control Strategy	0.17	0.043
Enthalpy Exchange	0.40	0.10
Full Ventilation Cycle	0.19	0.048

operation in hot, dry climates with variable regeneration control and/or an advanced control strategy. This application would require almost one-third the primary energy consumption as vapor-compression equipment.

One obvious area not addressed in this analysis is that of humidity control. All of these analyses were performed on an enthalpy basis only. The sensible heat ratios (SHRs) for the desiccant technologies using active regeneration can be as low as 0.5 (Houston). Vapor-compression equipment will generally be about 0.7 to 0.8 for SEER=10 equipment, and higher (up to 0.9) for SEER 12 to 14 equipment. The enthalpy exchange devices show the widest range in SHR of any of the devices simulated. This is because an enthalpy exchange device matches the actual SHR of the load (ventilation air relative to indoor air) as long as both the sensible and latent effectiveness are the same. Therefore, enthalpy exchange devices will have the least impact on the SHR of the building. This situation would not be true, however, if the regeneration temperature of the desiccant cycle were allowed to change with changing air conditions. The results shown here are strongly influenced by choosing a constant (low) regeneration temperature for the desiccant systems. The major ramification of not including the effects of SHR on the building is that the energy usage could be significantly higher or building comfort seriously compromised for the vapor compression equipment.

Another area not addressed in this study are unconventional desiccant cycles. Vapor-recompression cycles, and desiccants requiring only the heat of wetting for regeneration are two of these options. These kinds of advanced concepts allow theoretical thermal CoPs in the range of 8 to 10.

Appendix A

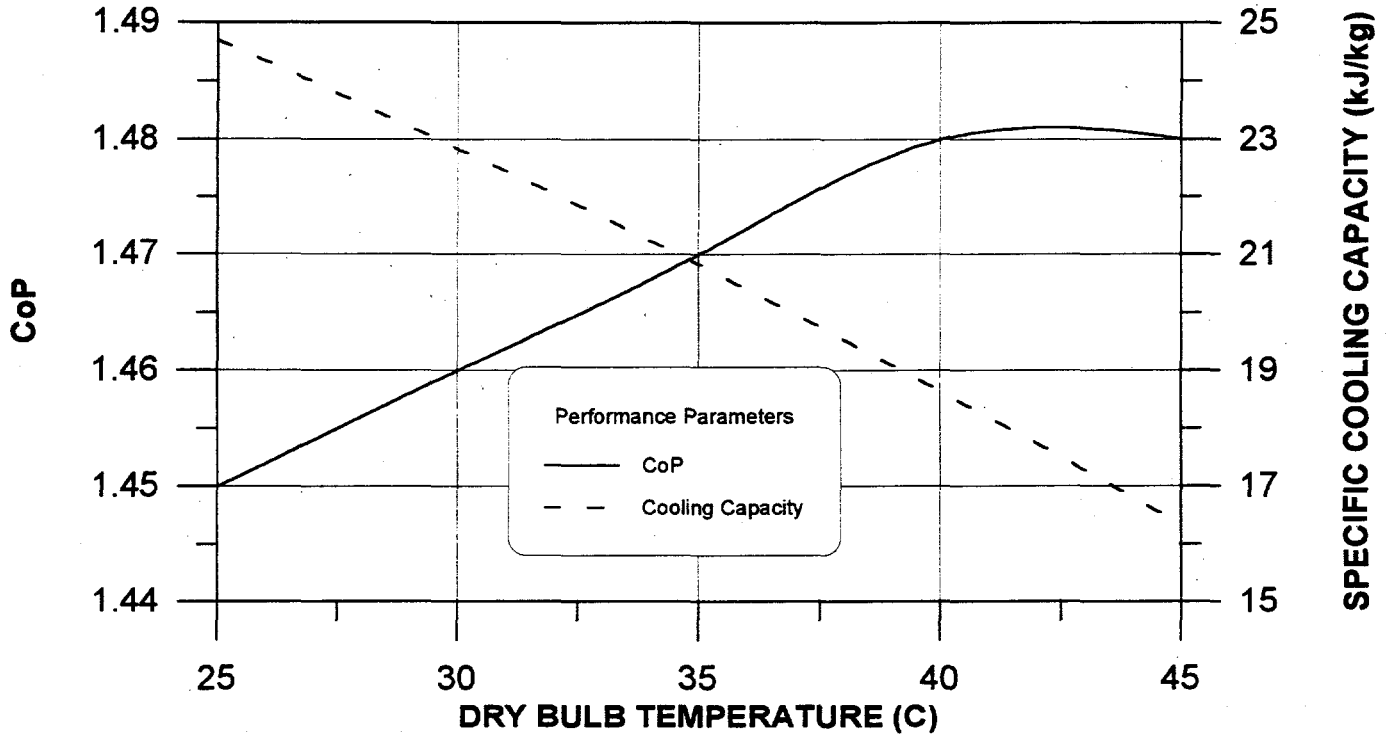

Figure 1-12. Cooling system performance as a function of dry bulb temperature. Ventilation cycle without vent credit. 75C regeneration.

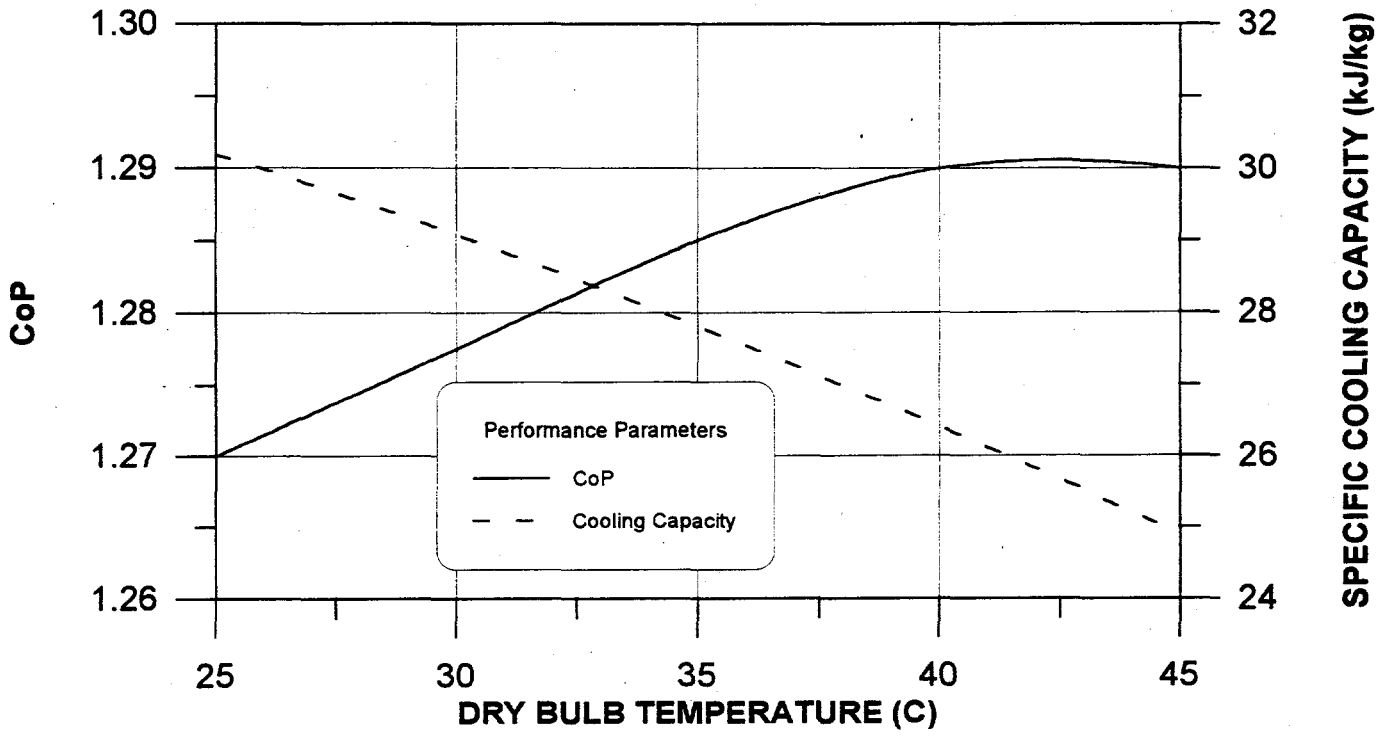

Figure 1-13. Cooling system performance as a function of dry bulb temperature. Ventilation cycle without vent credit. 100C regeneration.

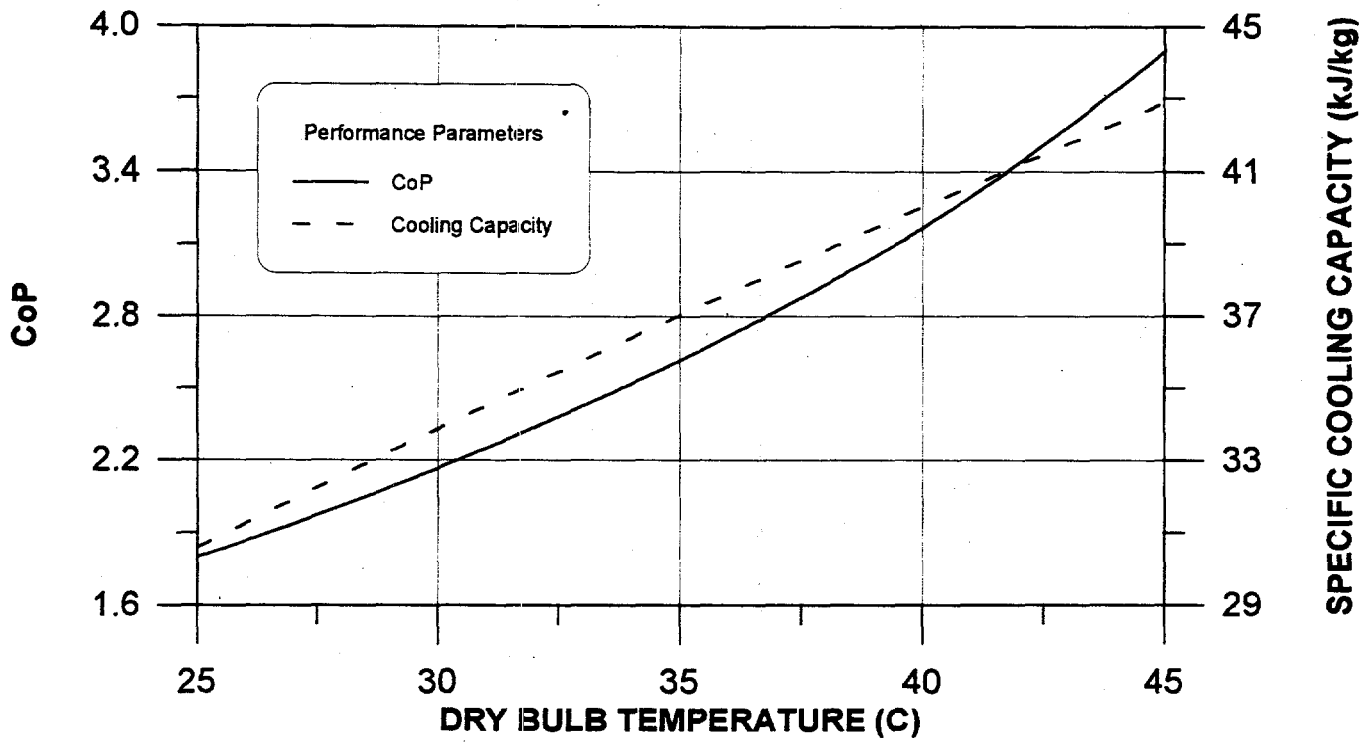

Figure 1-14. Cooling system performance as a function of dry bulb temperature. Ventilation cycle with vent credit. 75C regeneration.

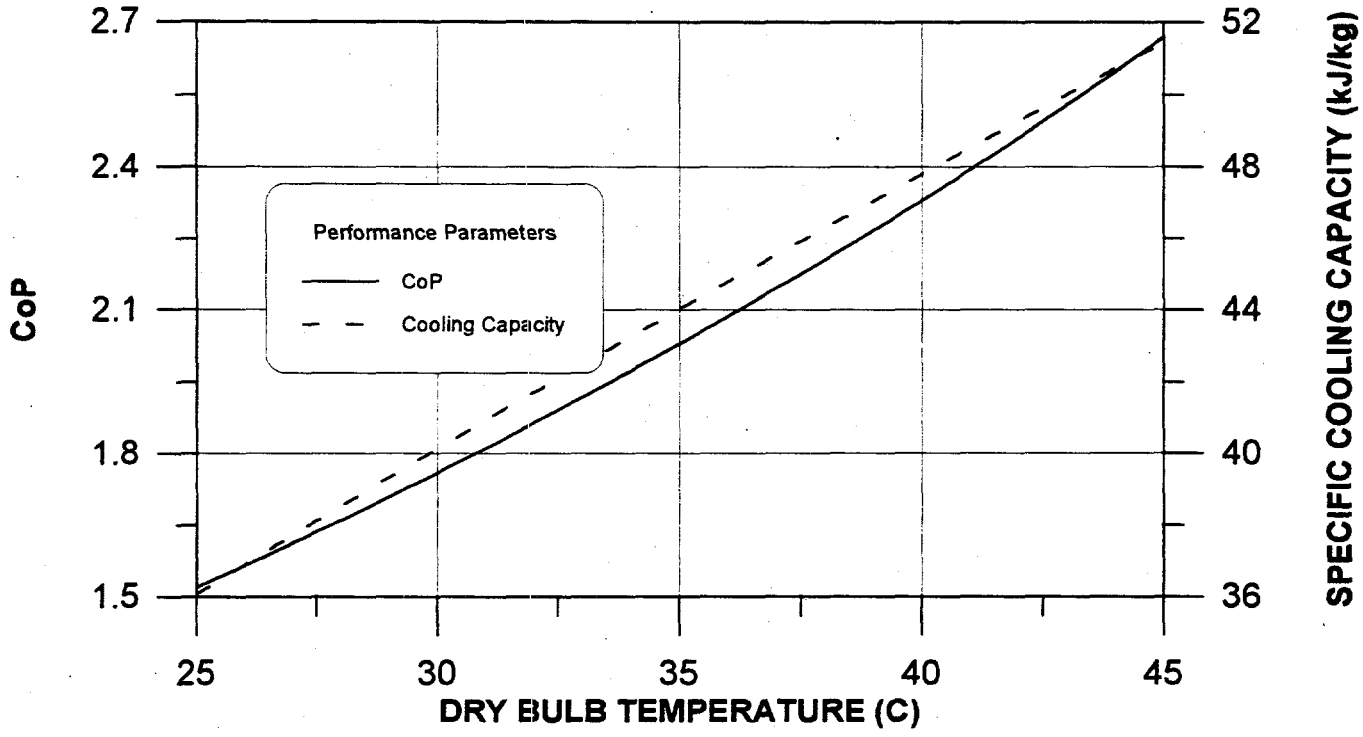

Figure 1-15. Cooling system performance as a function of dry bulb temperature. Ventilation cycle with vent credit. 100C regeneration.

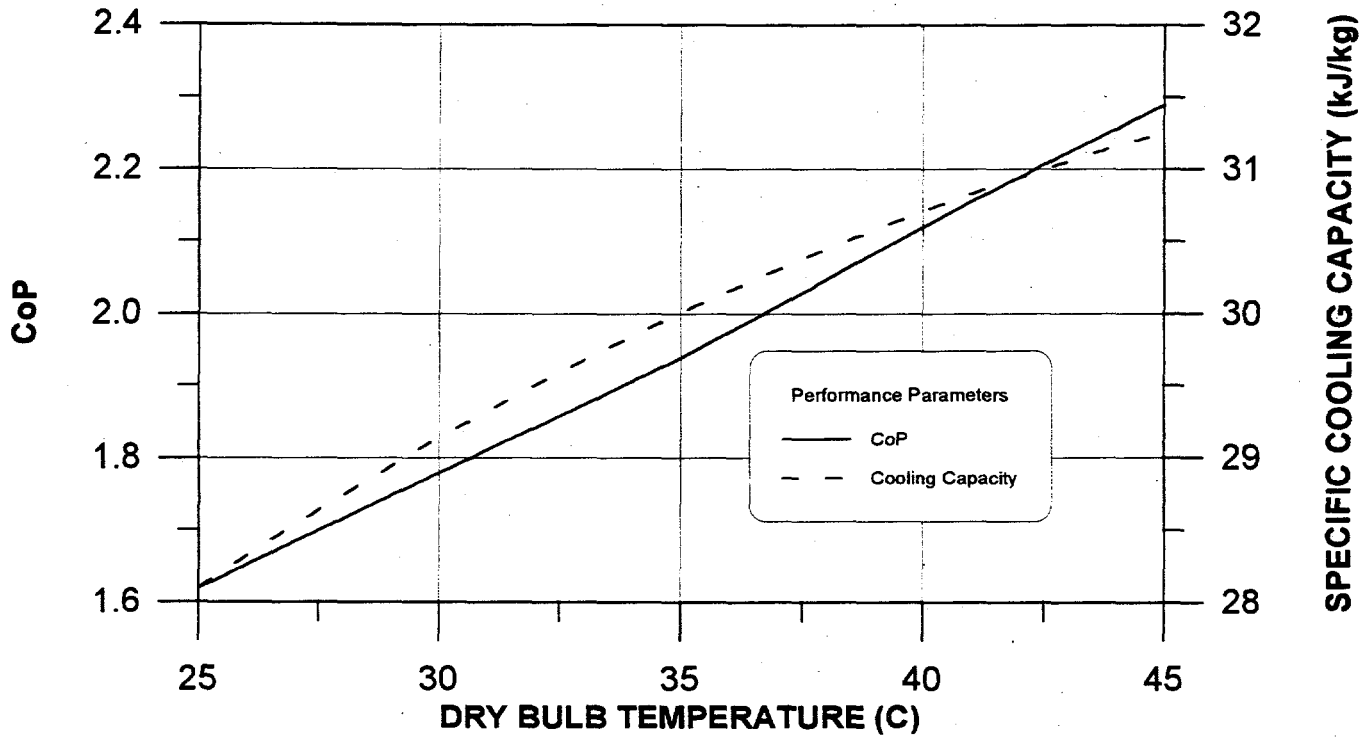

Figure 1-16. Cooling system performance as a function of dry bulb temperature. Modified vent cycle. 75C regeneration.

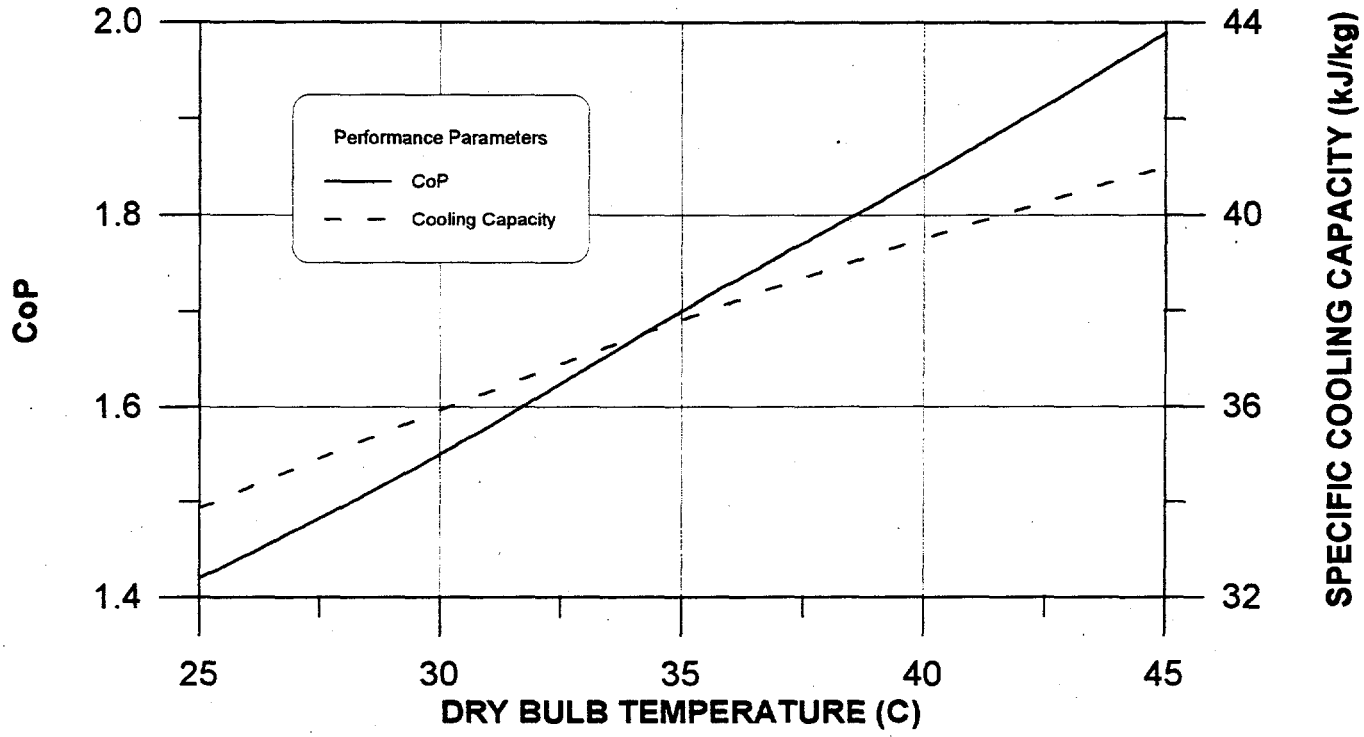

Figure 1-17. Cooling system performance as a function of dry bulb temperature. Modified vent cycle. 100C regeneration.

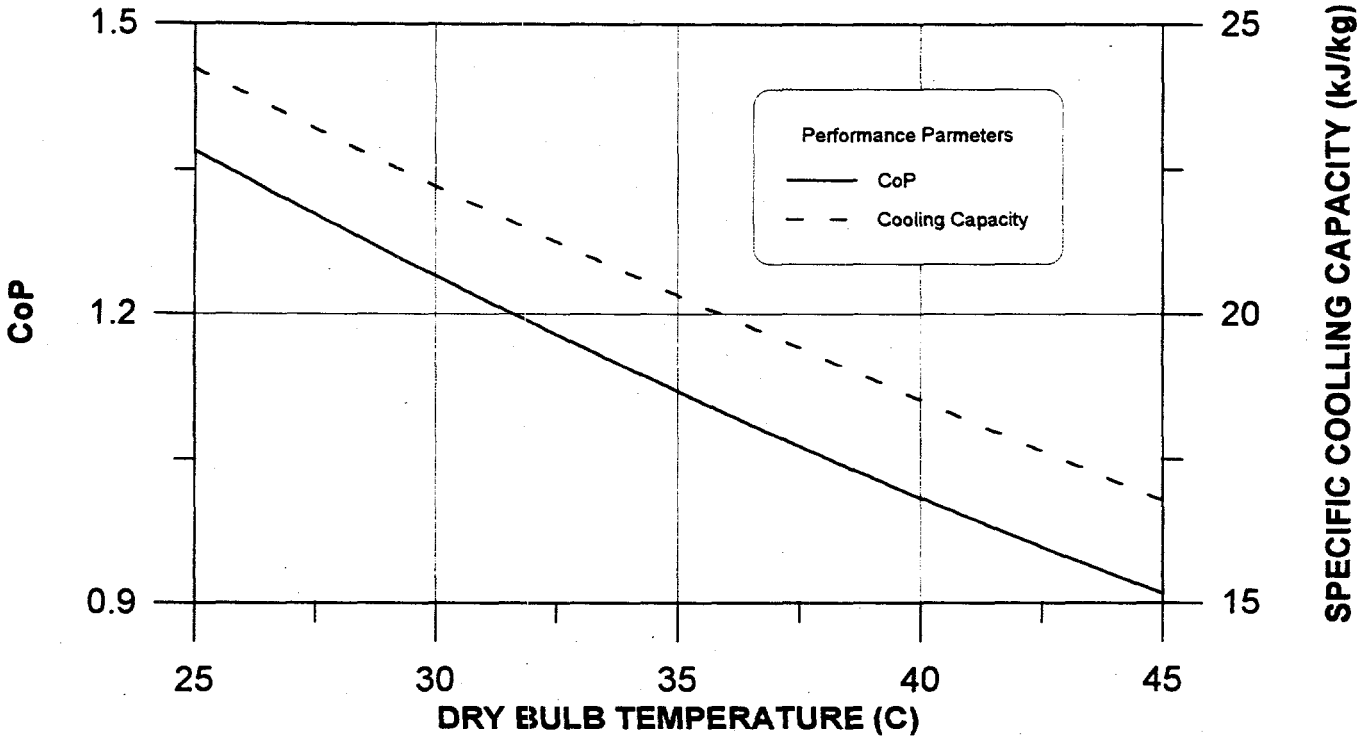

Figure 1-18. Cooling system performance as a function of dry bulb temperature. Recirculation cycle. 75C regeneration.

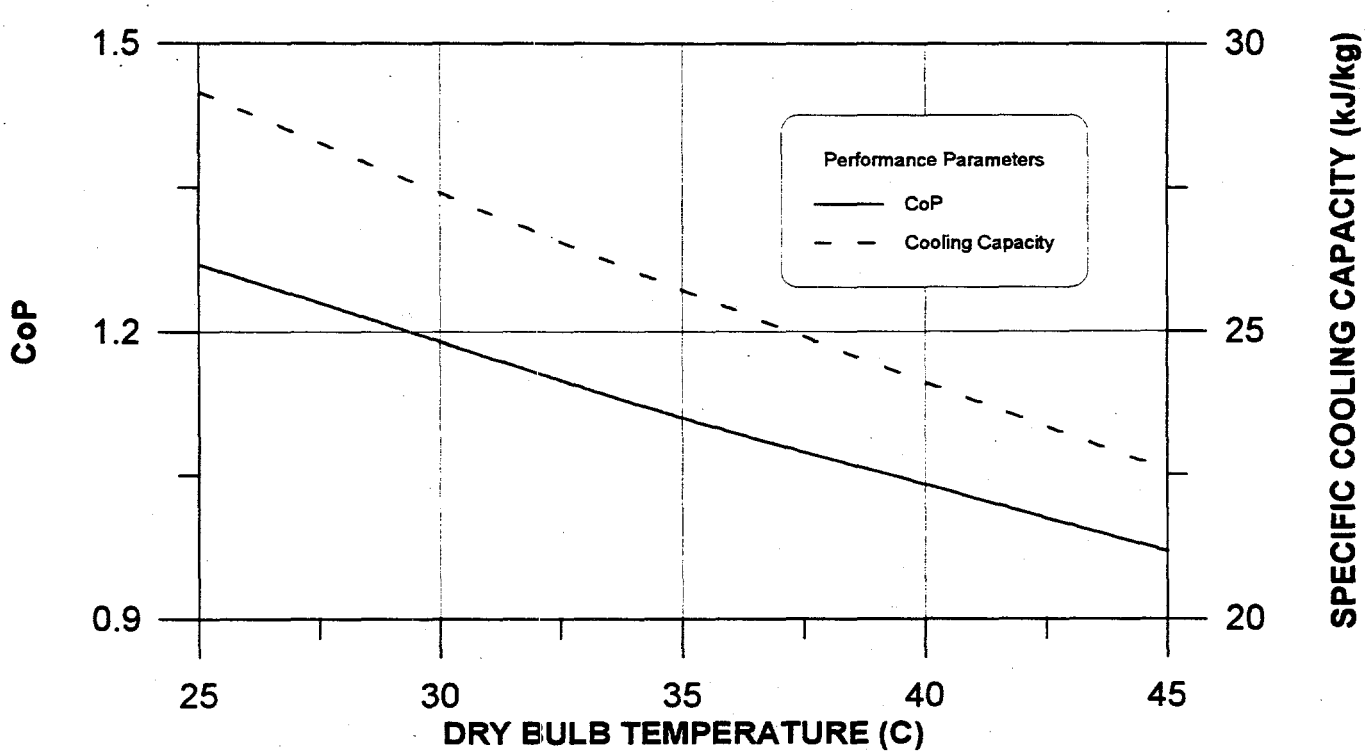

Figure 1-19. Cooling system performance as a function of dry bulb temperature. Recircullation cycle. 100C regeneration.

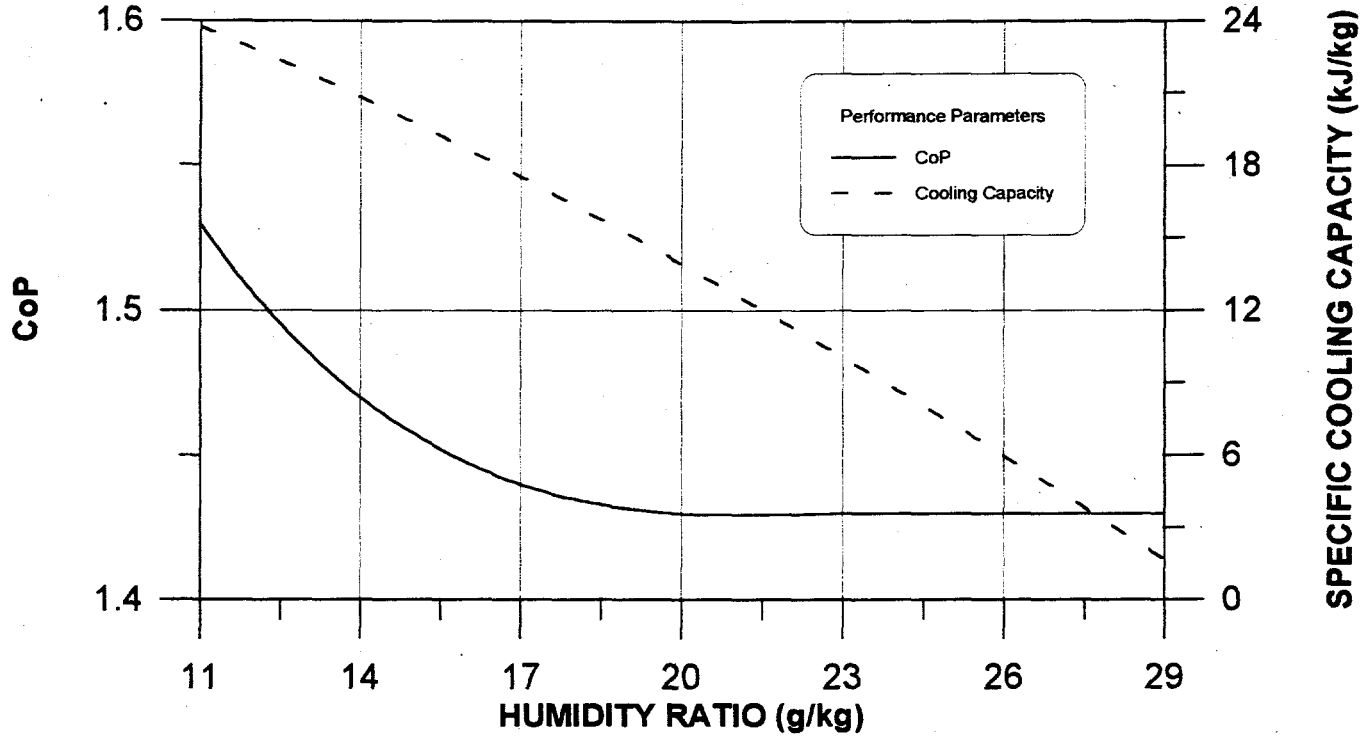

Figure 1-21. Cooling system performance as a function of humidity ratio. Ventilation cycle without vent credit. 75C regeneration.

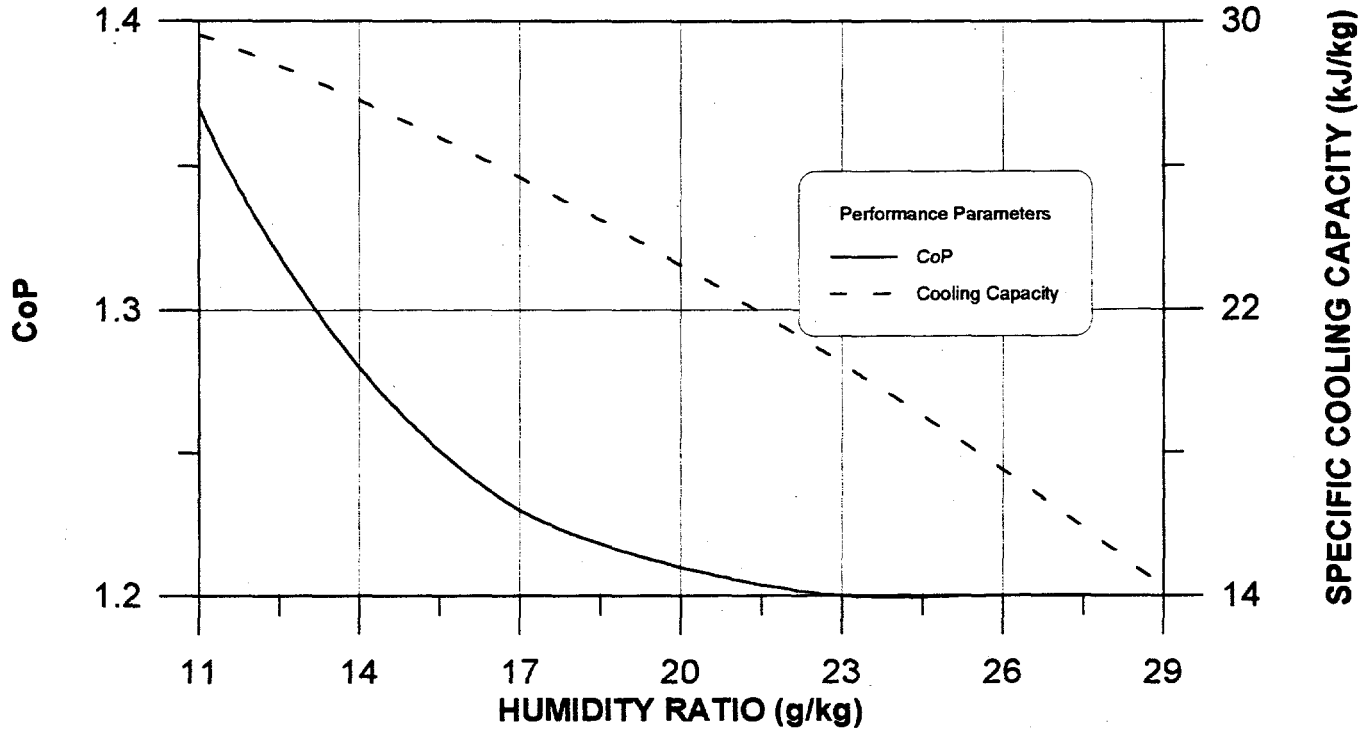

Figure 1-22. Cooling system performance as a function of humidity ratio. Ventilation cycle without vent credit. 100C regeneration.

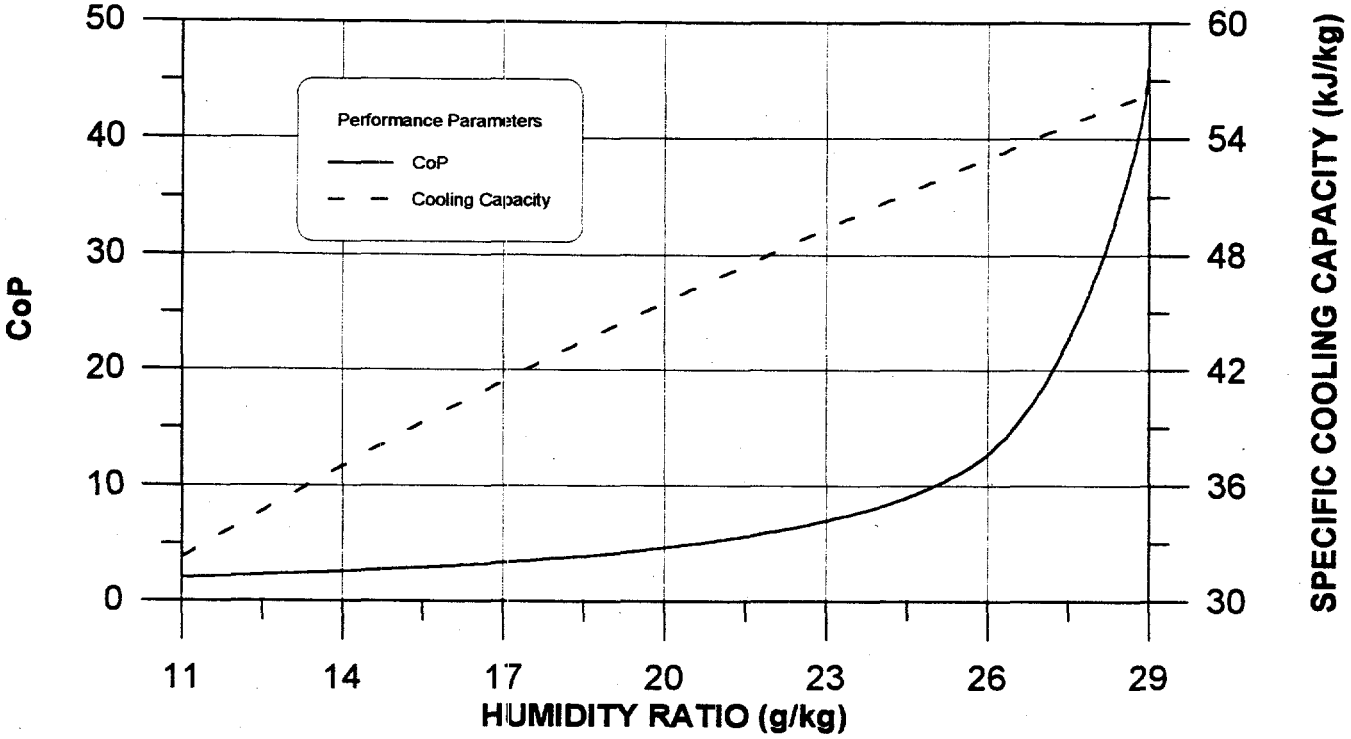

Figure 1-23. Cooling system performance as a function of humidity ratio. Ventilation cycle with vent credit. 75C regeneration.

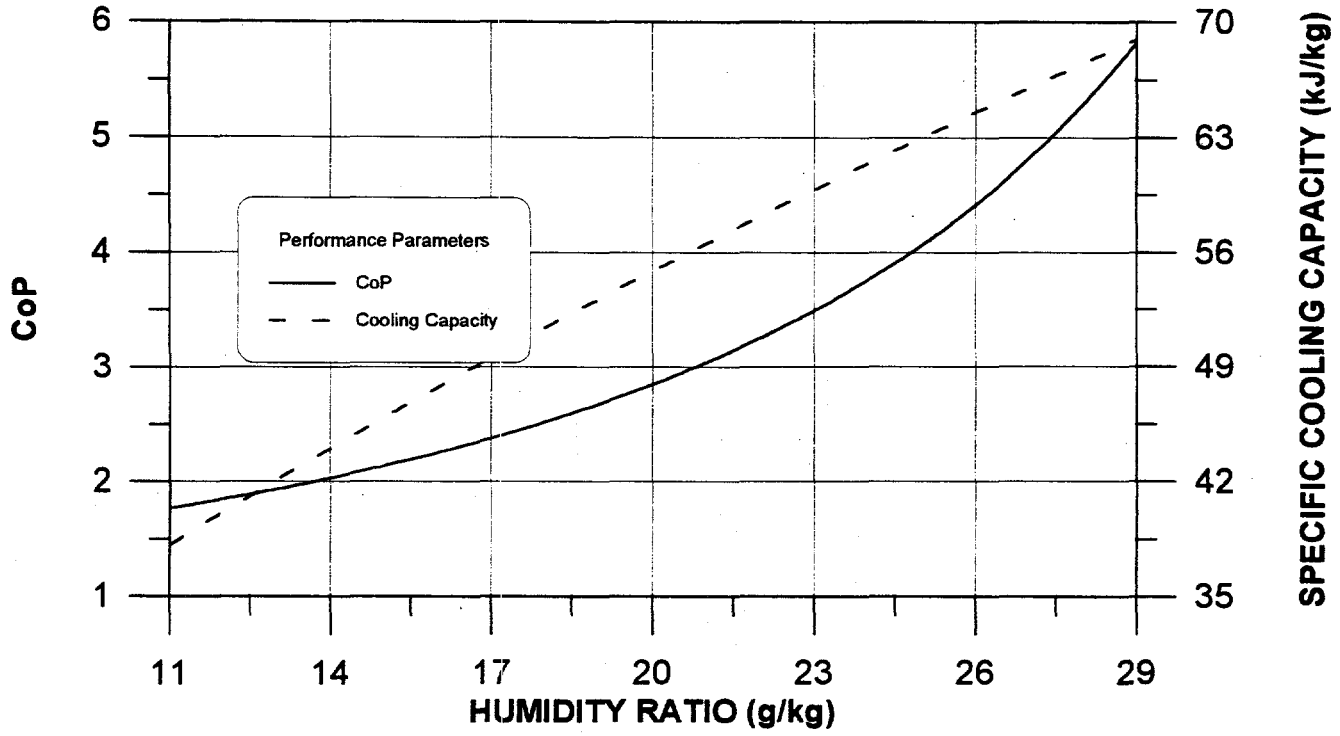

Figure 1-24. Cooling system performance as a function of humidity ratio. Ventilation cycle with vent credit. 100C regeneration.

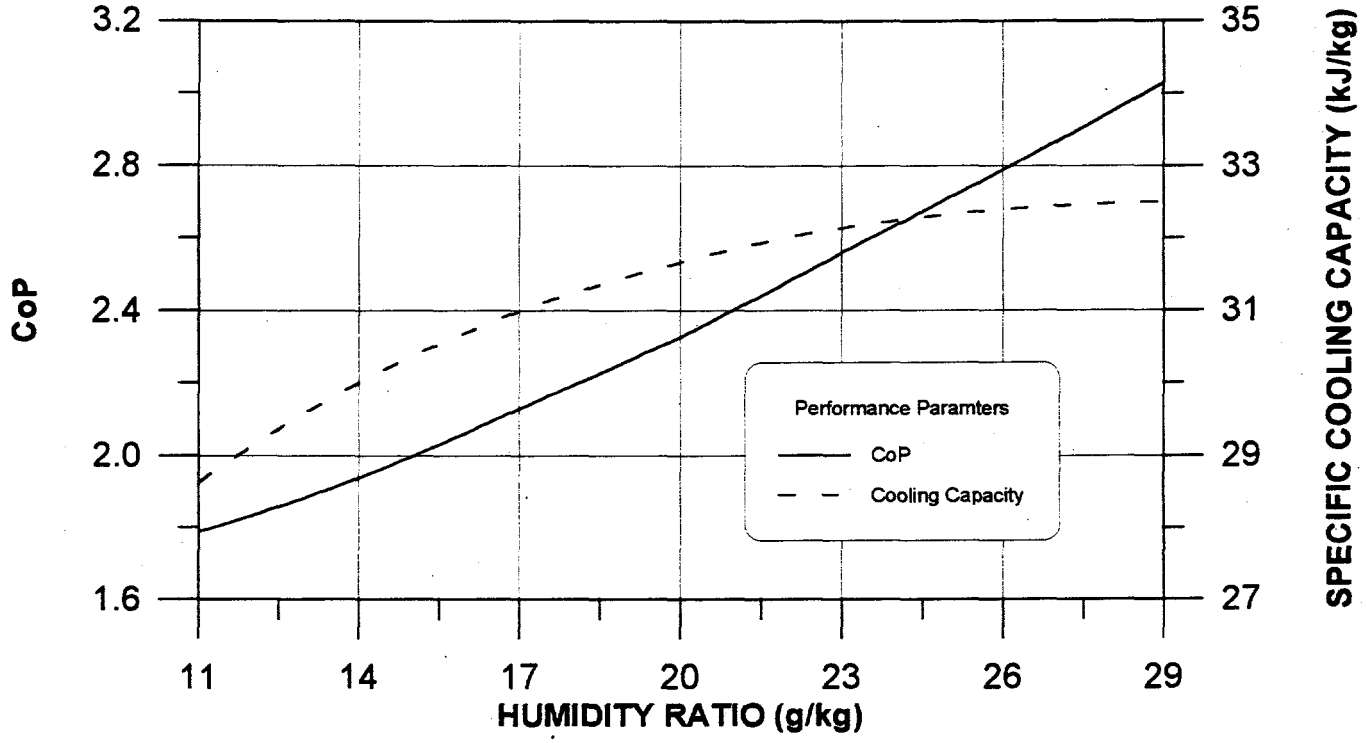

Figure 1-25. Cooling system performance as a function of humidity ratio. Modified vent cycle. 75C regeneration.

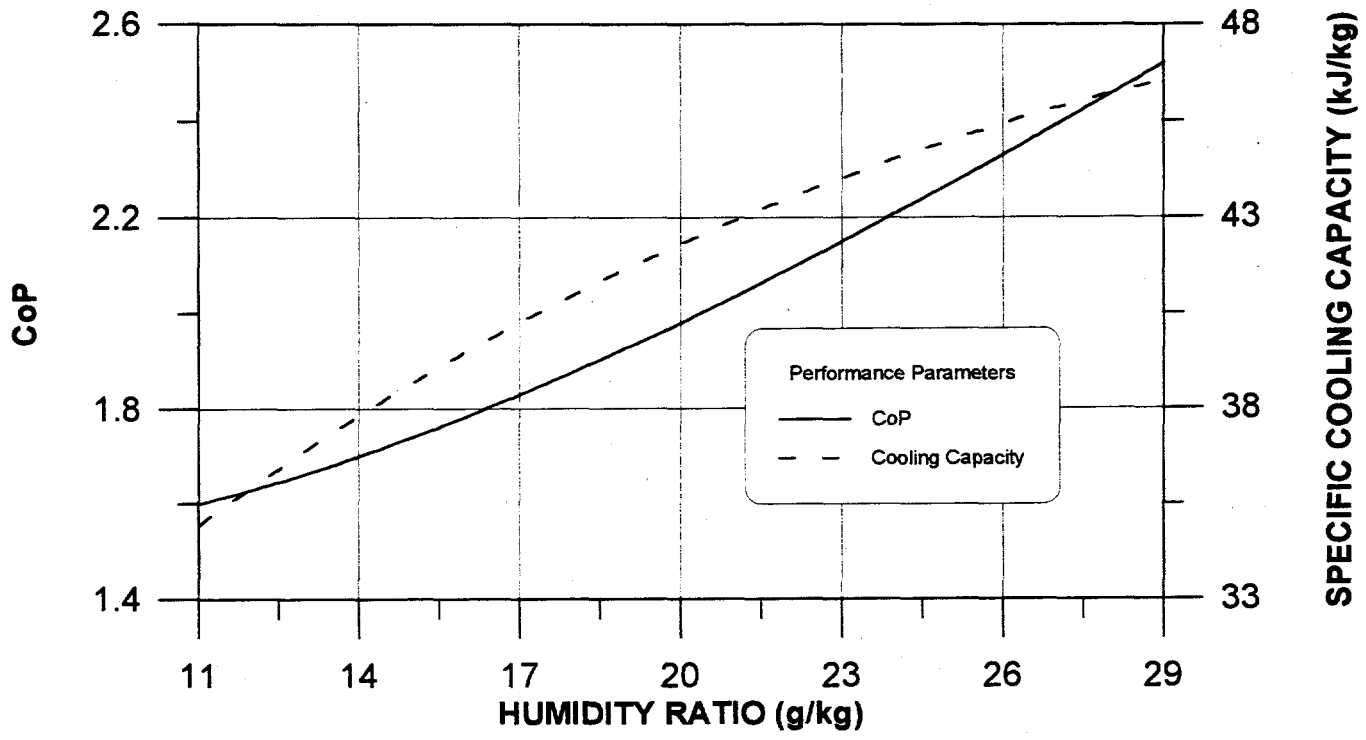

Figure 1-26. Cooling system performance as a function of humidity ratio. Modified vent cycle. 100C regeneration.

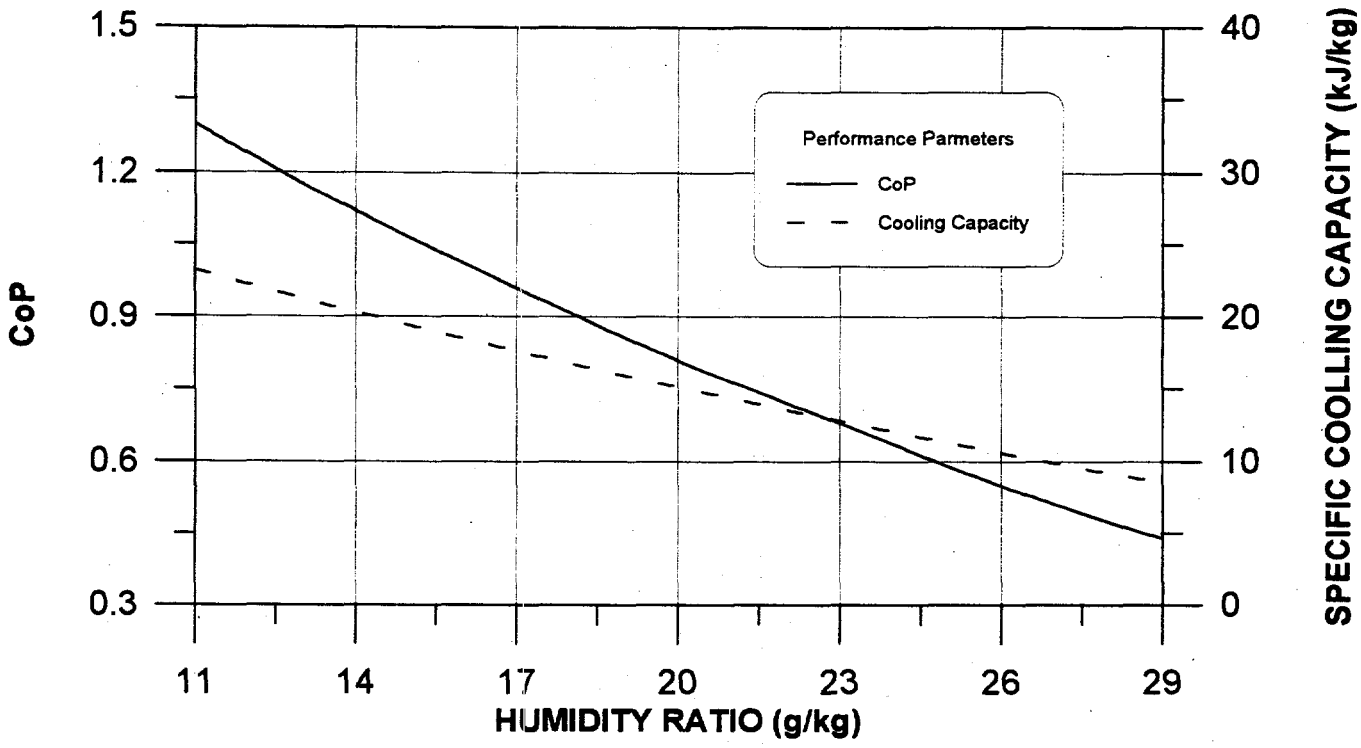

Figure 1-27. Cooling system performance as a function of humidity ratio. Recirculation cycle. 75C regeneration.

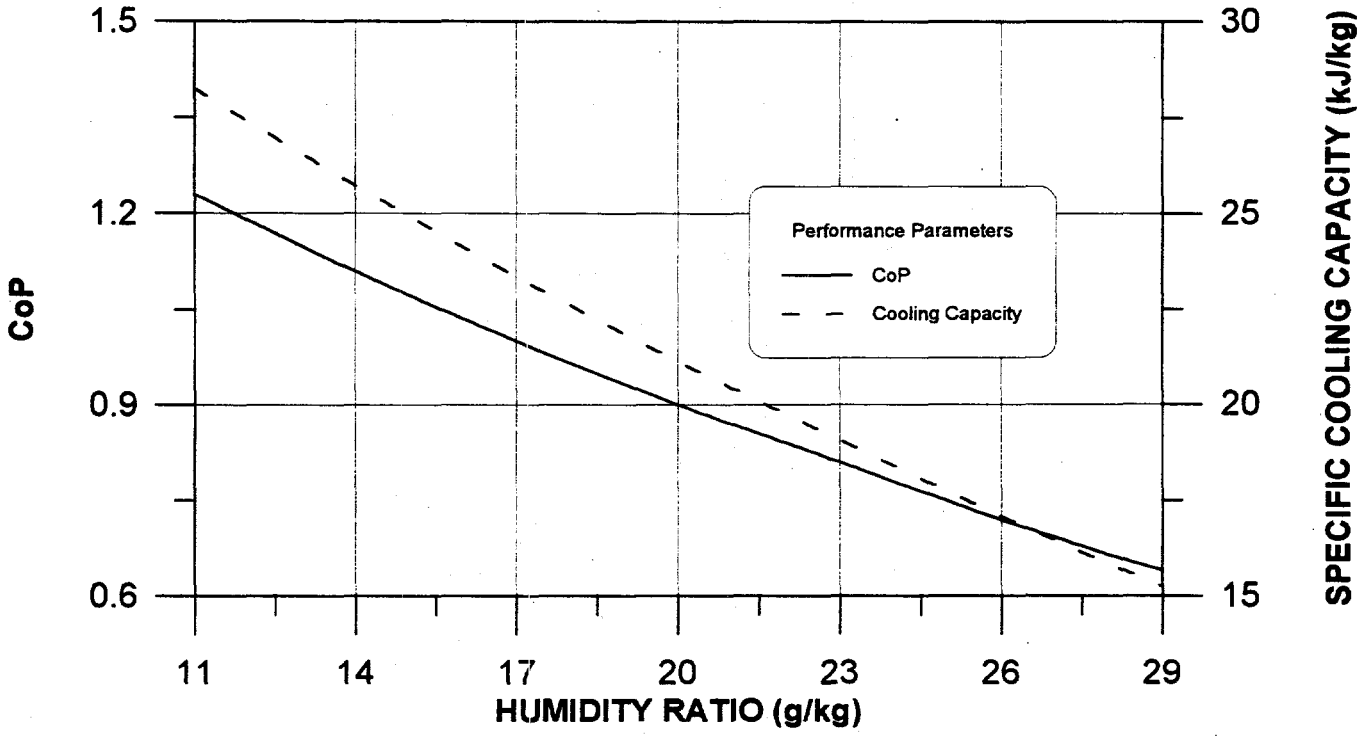

Figure 1-28. Cooling system performance as a function of humidity ratio. Recirculation cycle. 100C regeneration.

Appendix B

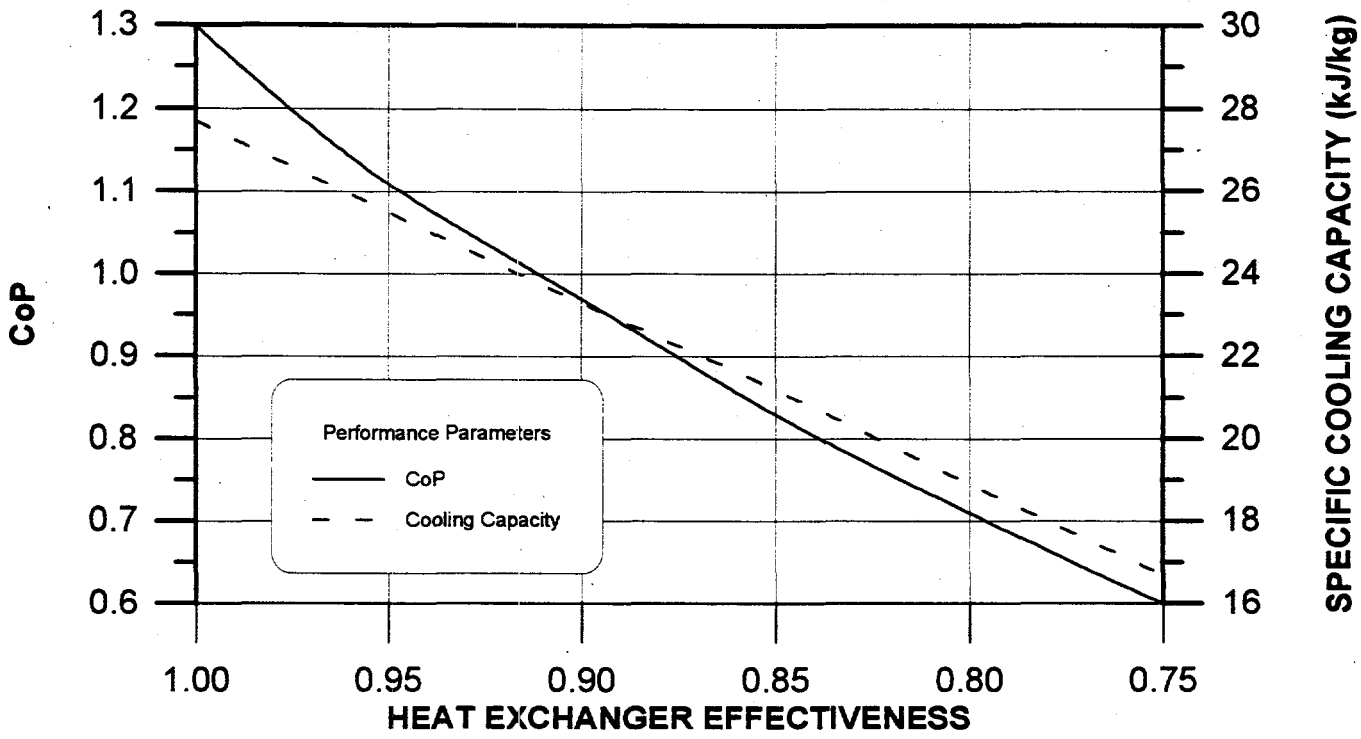

Figure 2-2. Cooling system performance as a function of heat exchanger effectiveness. Ventilation cycle; 100C regeneration.

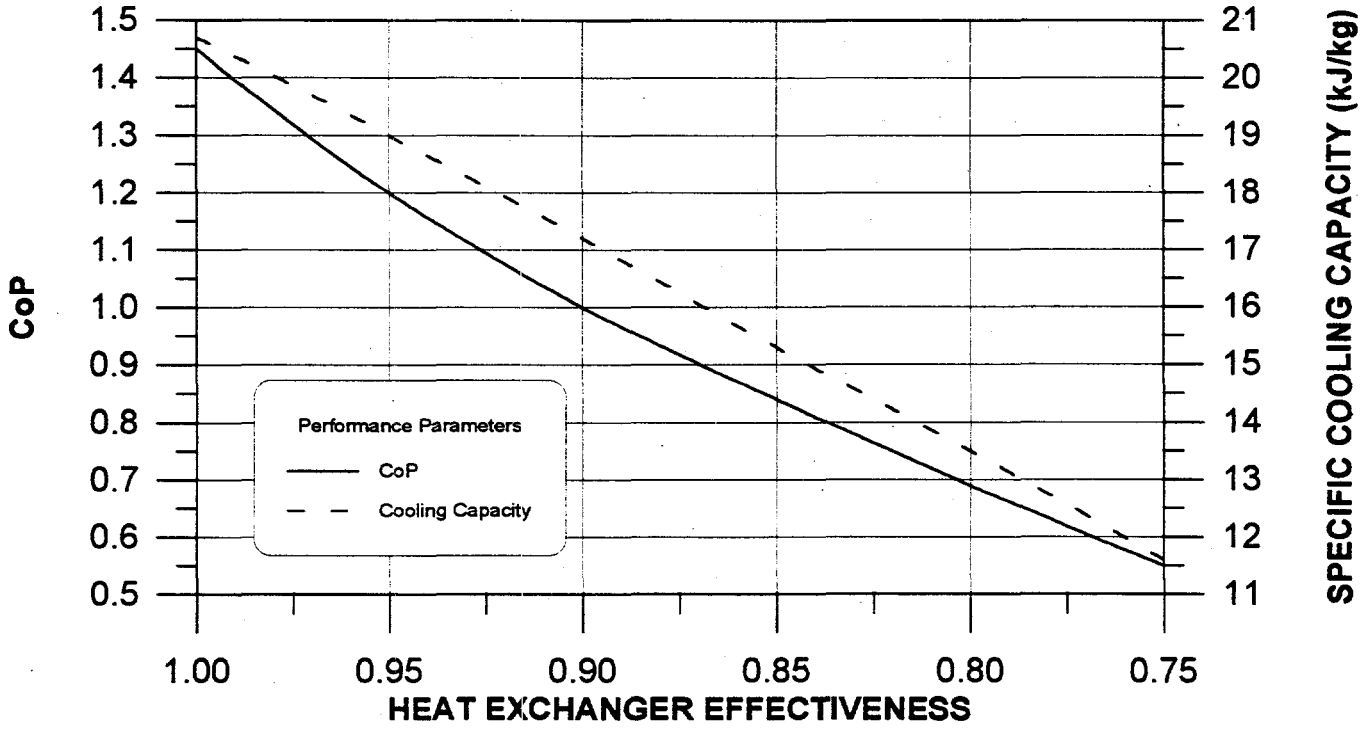

Figure 2-3. Cooling system performance as a function of heat exchanger effectiveness. Ventilation cycle; 75C regeneration.

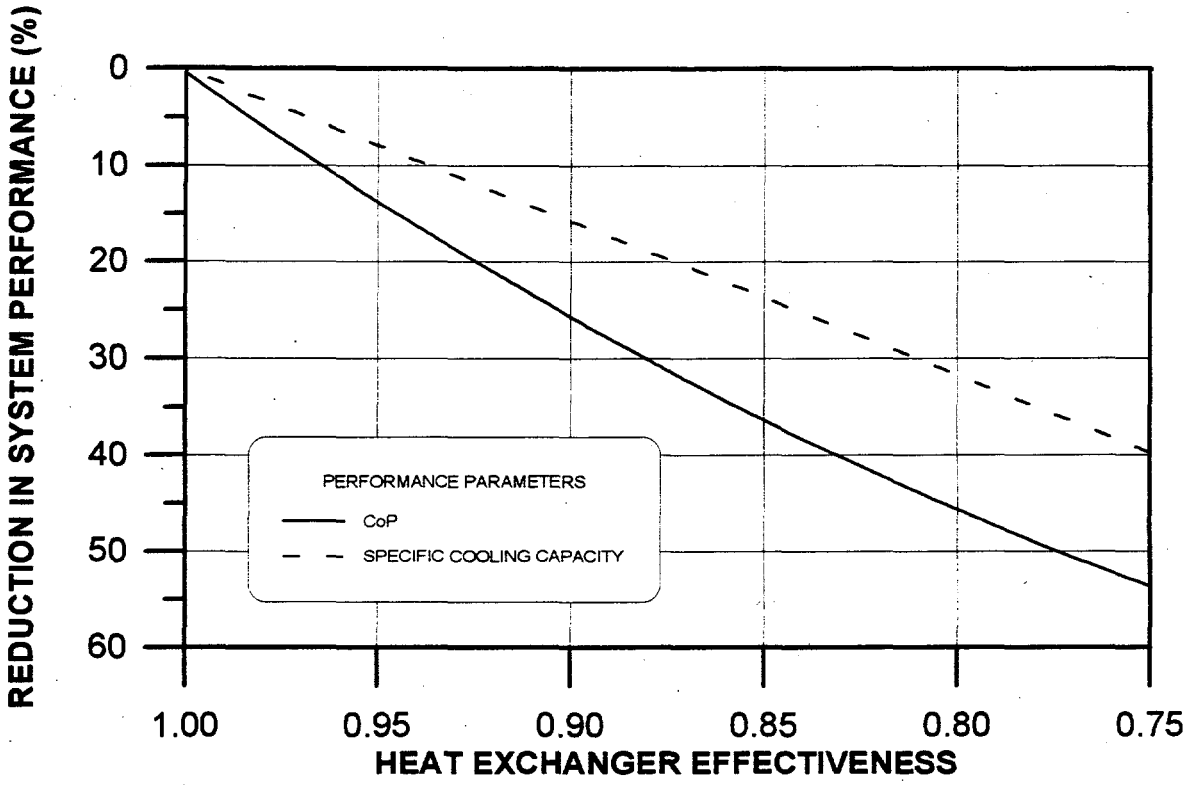

Figure 2-4. Reduction in system performance as a function of heat exchanger effectiveness. Ventilation cycle; 100C regeneration.

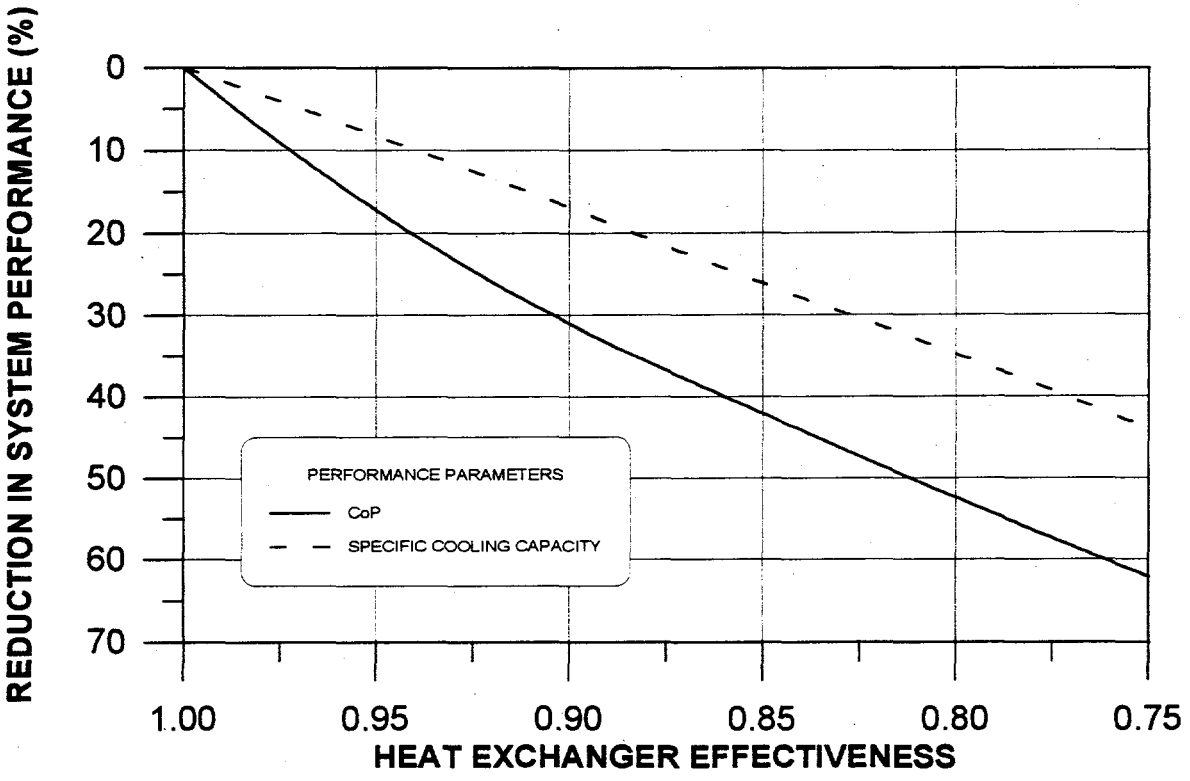

Figure 2-5. Reduction in system performance as a function of heat exchanger effectiveness. Ventilation cycle; 75C regeneration.

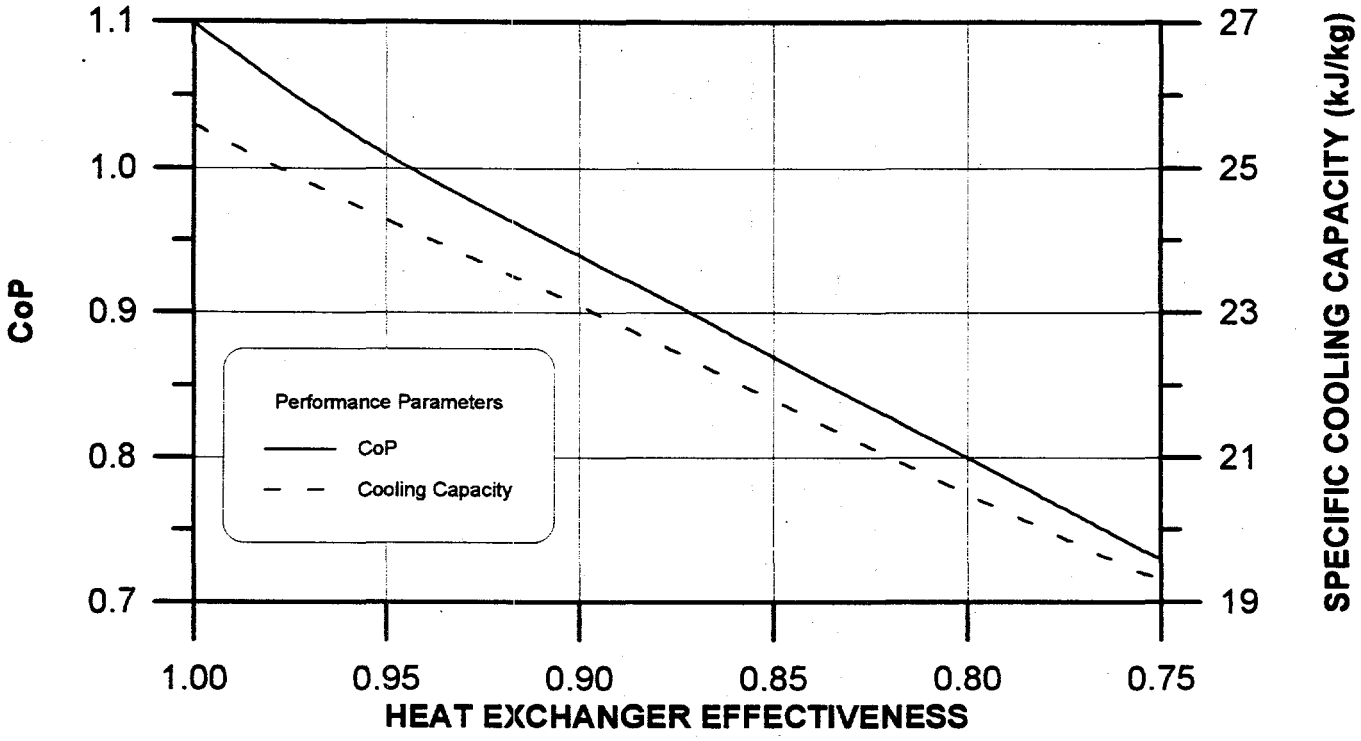

Figure 2-6. Cooling system performance as a function of heat exchanger effectiveness. Recirculation cycle; 100C regeneration.

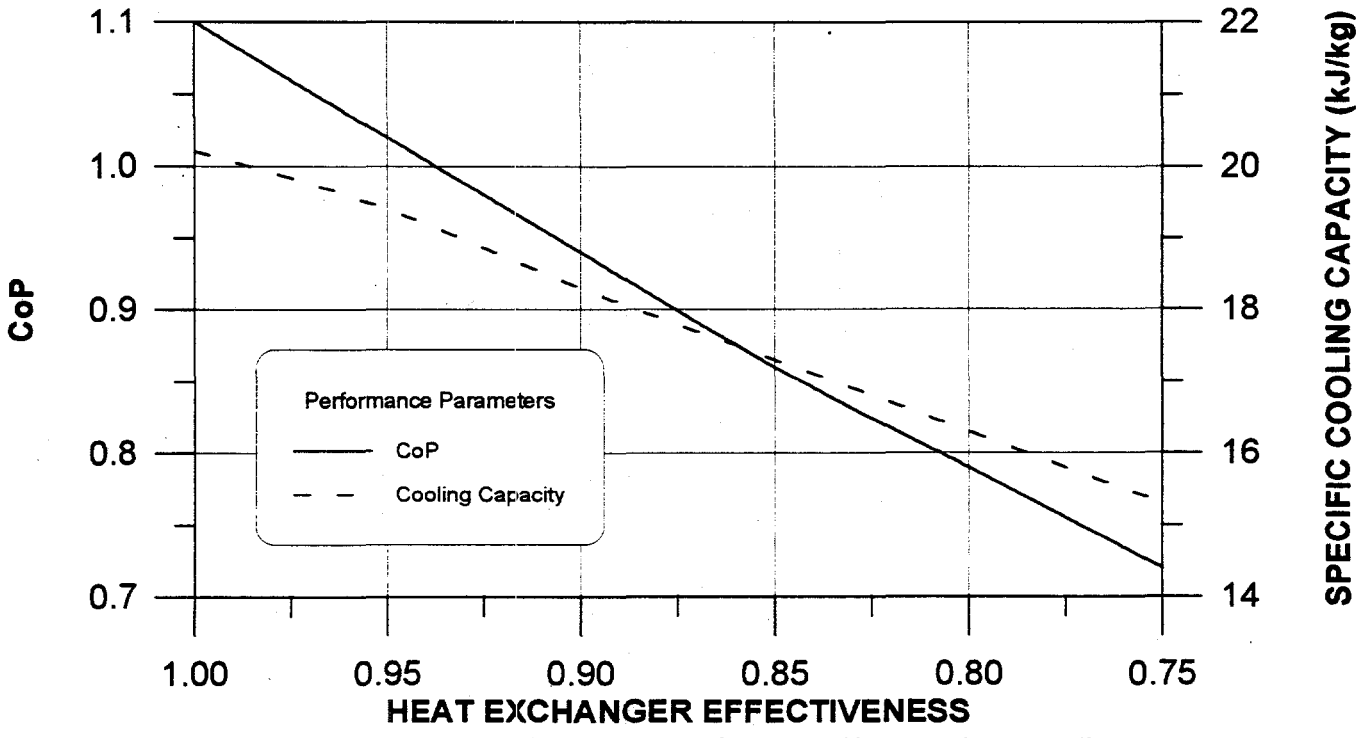

Figure 2-7. Cooling system performance as a function of heat exchanger effectiveness. Recirculation cycle; 75C regeneration.

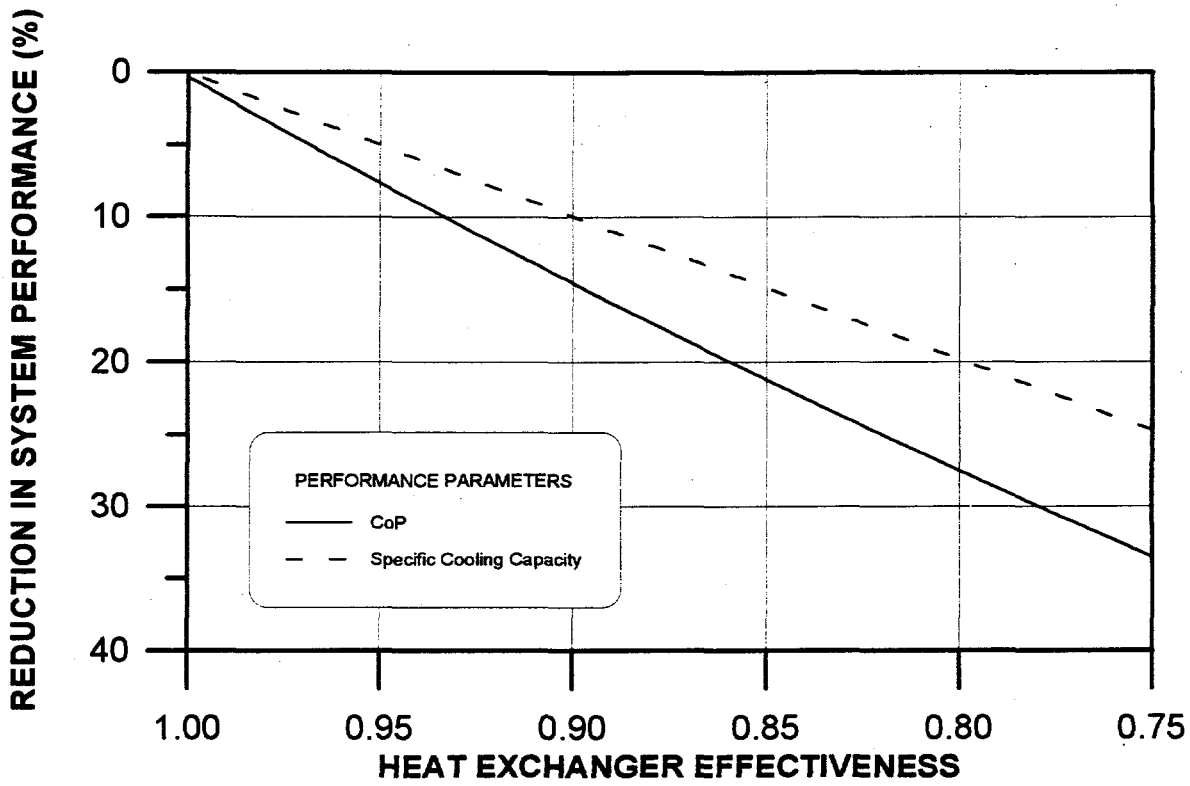

Figure 2-8. Reduction in system performance as a function of heat exchanger effectiveness. Recirculation cycle; 100C regeneration.

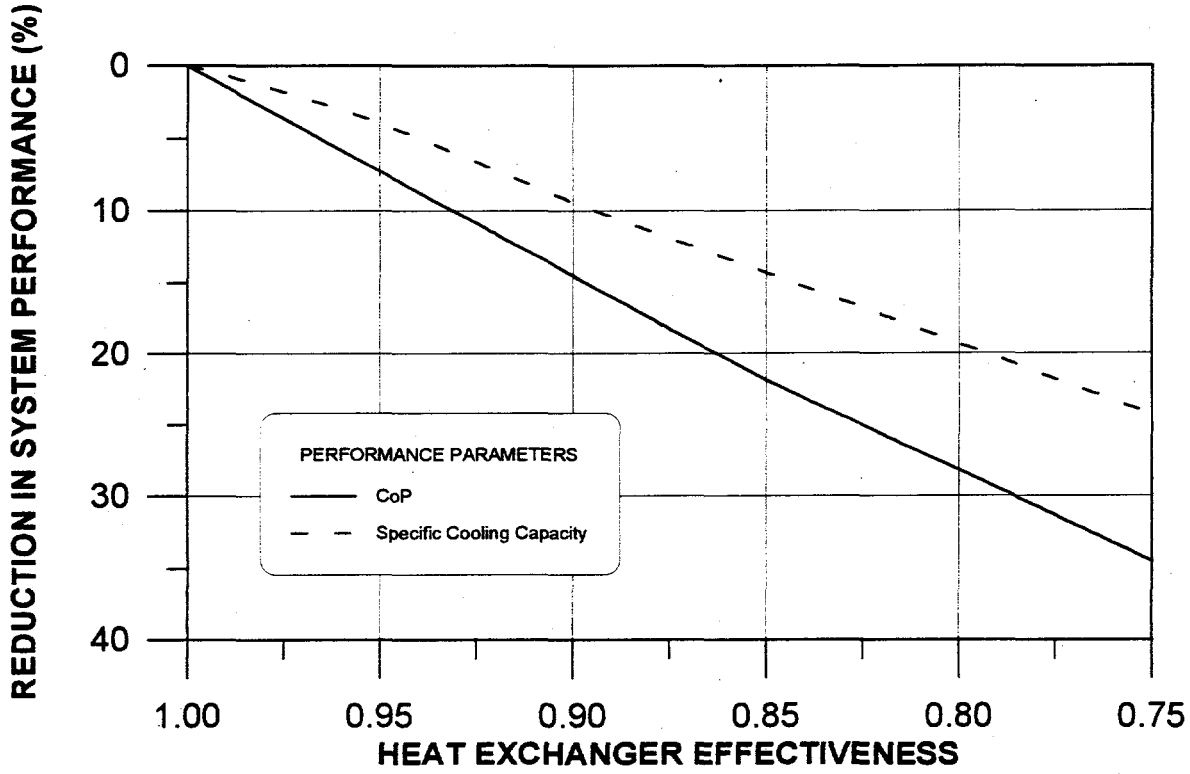

Figure 2-9. Reduction in system performance as a function of heat exchanger effectiveness. Recirculation cycle; 75C regeneration.

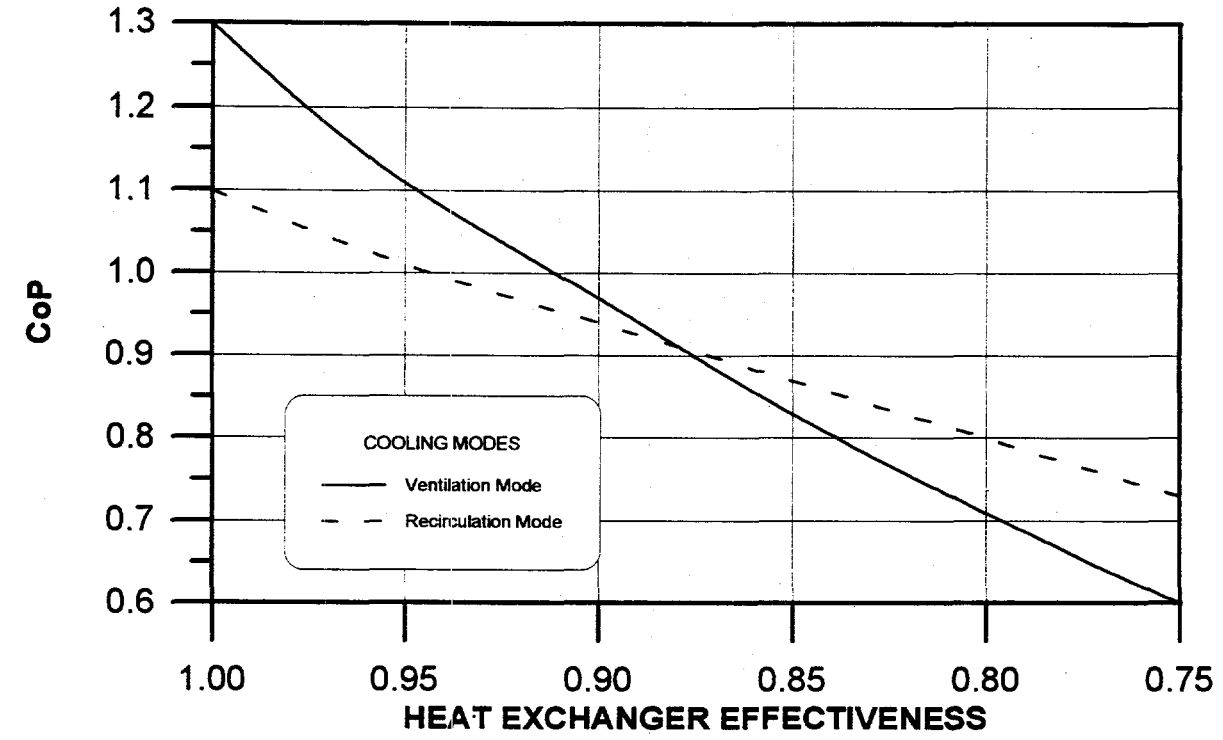

Figure 2-10. CoP comparisons for two cooling modes as a function of heat exchanger effectiveness. 100C regeneration.

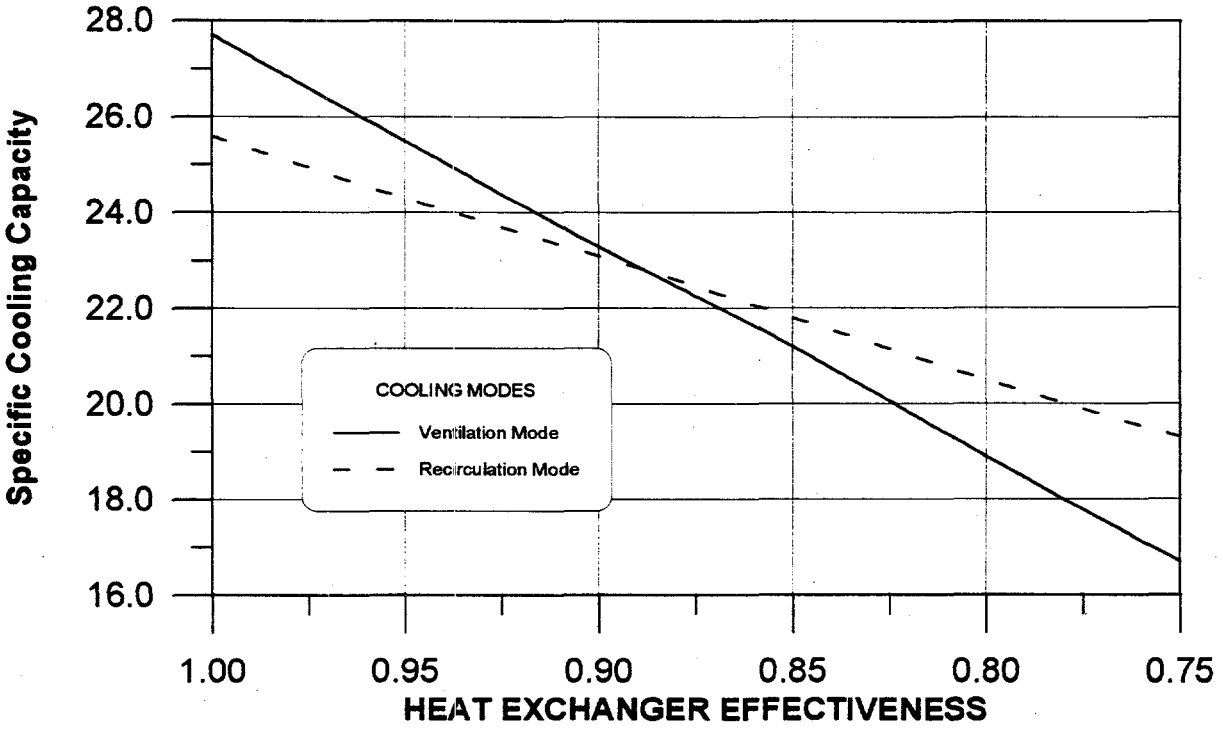

Figure 2-11. Specific Cooling Capacity comparisons for two cooling modes as a function of heat exchanger effectiveness; 100C regeneration.

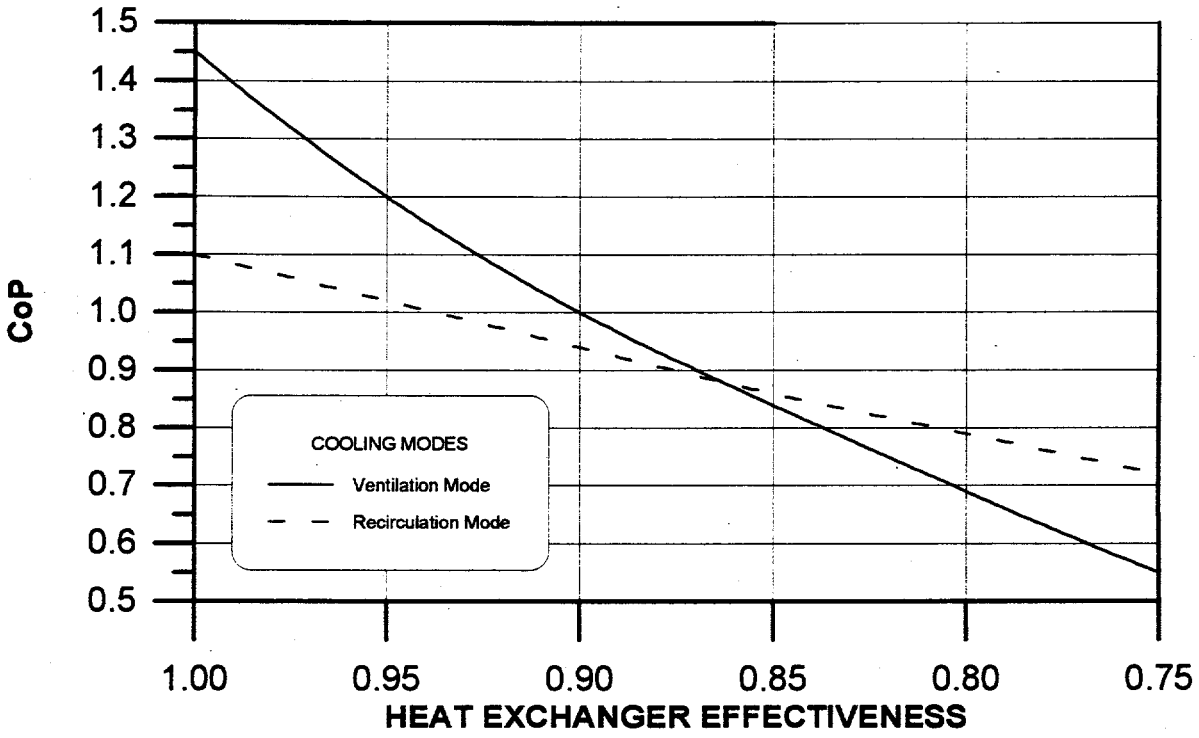

Figure 2-12. CoP comparisons for two cooling modes as a function of heat exchanger effectiveness; 75C regeneration.

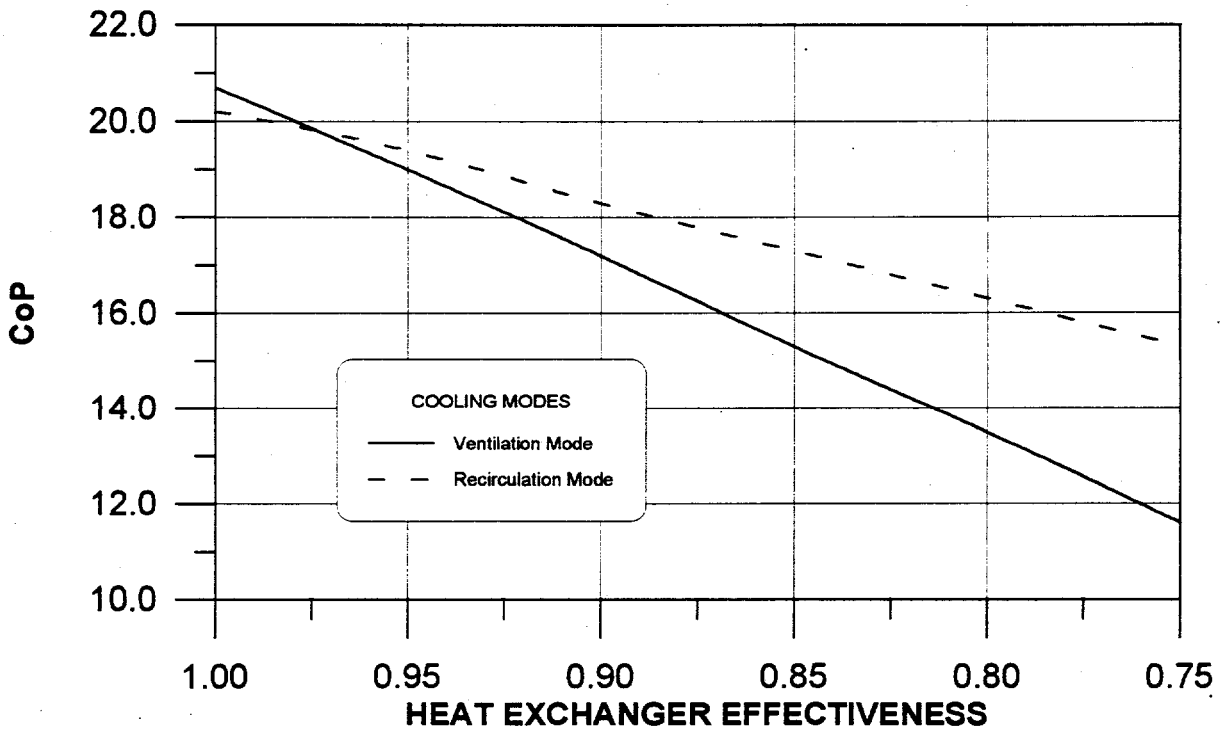

Figure 2-13. Specific Cooling Capacity comparisons for two cooling modes as a function of heat exchanger effectiveness; 75C regeneration.

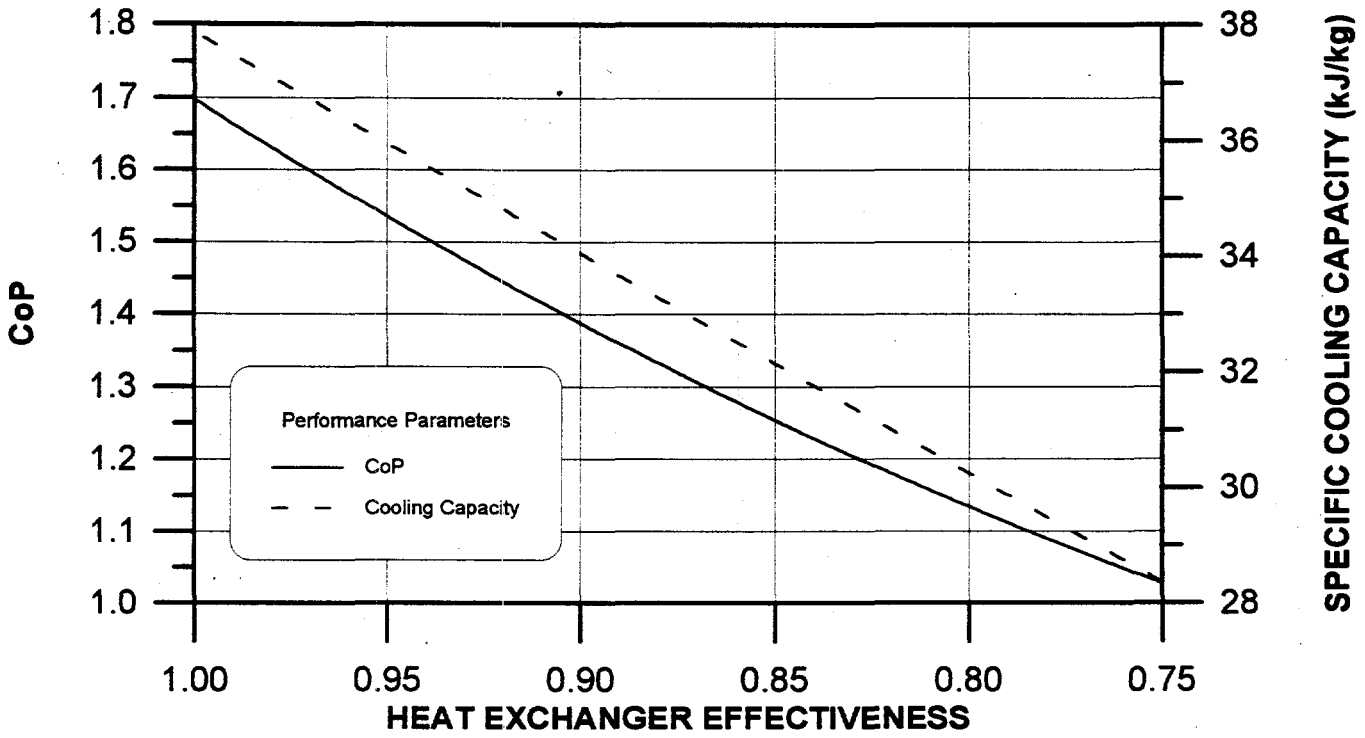

Figure 2-14. CoP and Specific Cooling Capacity as a function of heat exchanger effectiveness. Vent-vent cycle; 100 C regeneration

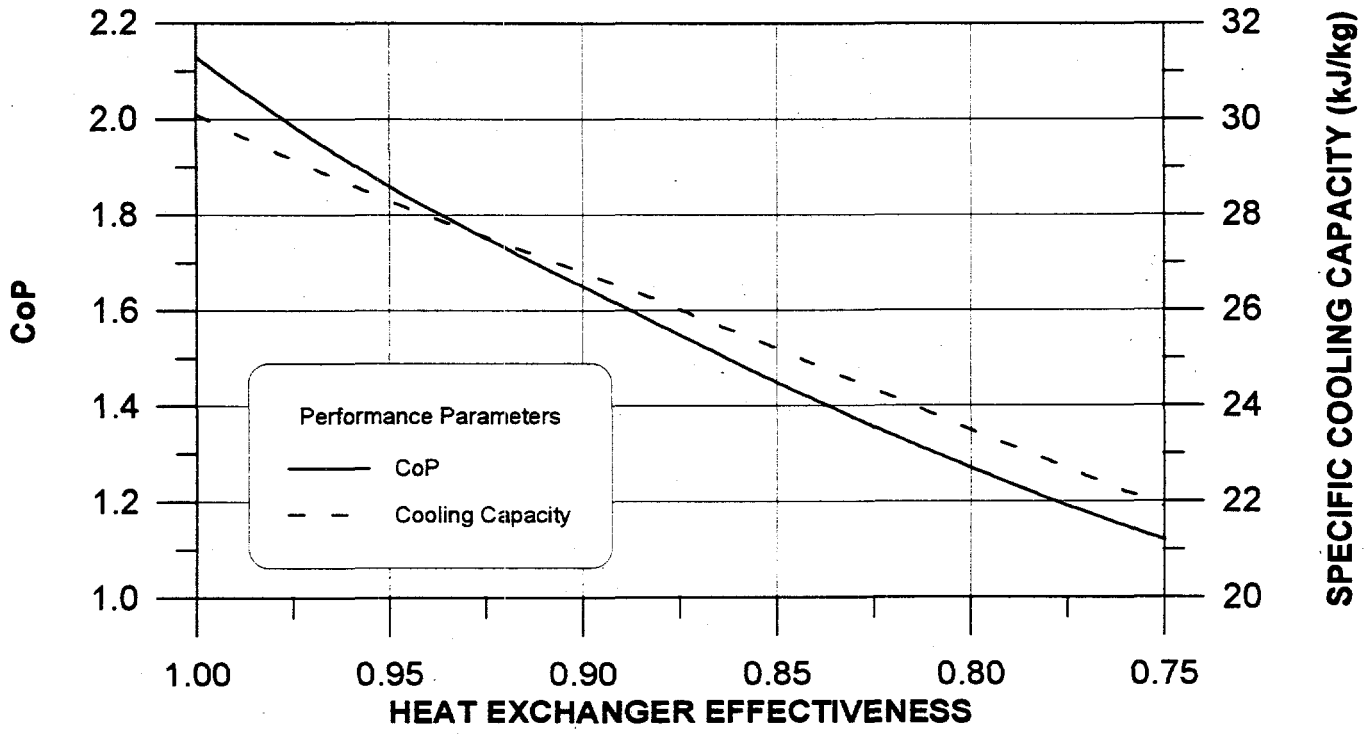

Figure 2-15. CoP and Specific Cooling Capacity as a function of heat exchanger effectiveness. Vent-vent cycle; 75C regeneration.

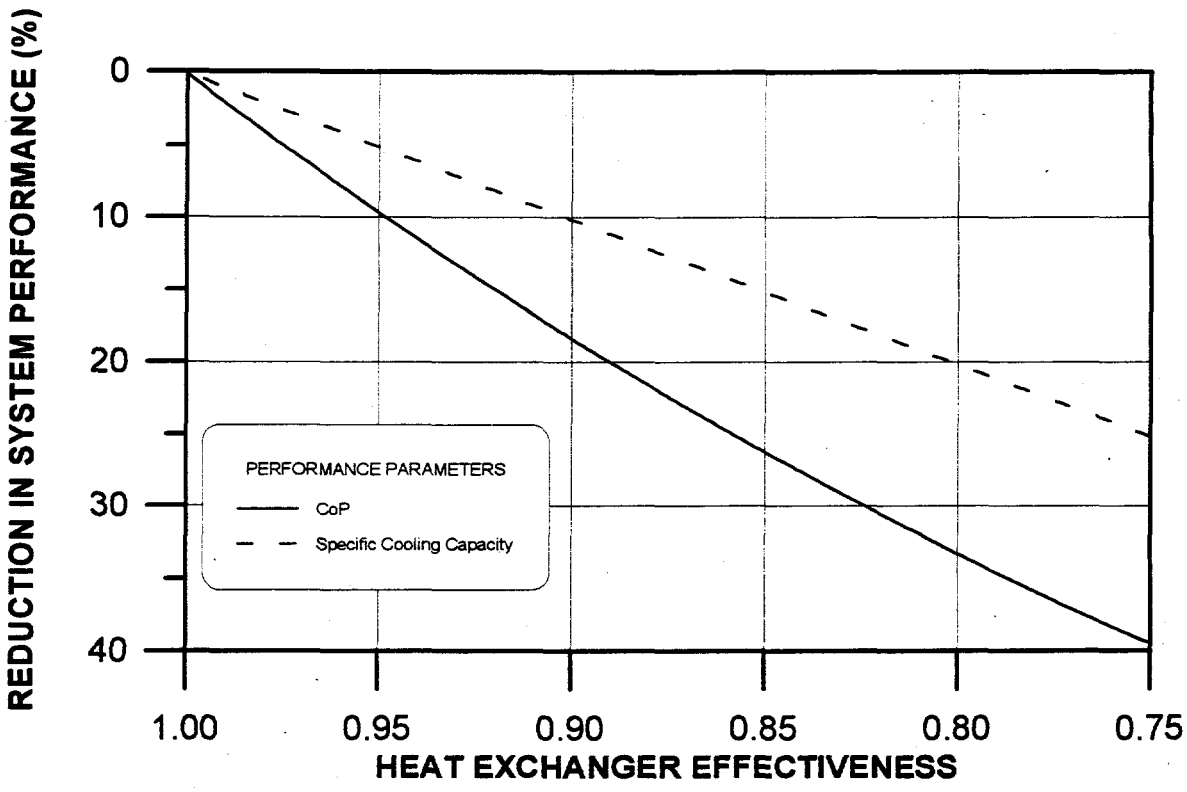

Figure 2-16. Relative reduction in system performance vs. heat exchanger effectiveness Vent-Vent Cycle; 100C regeneration.

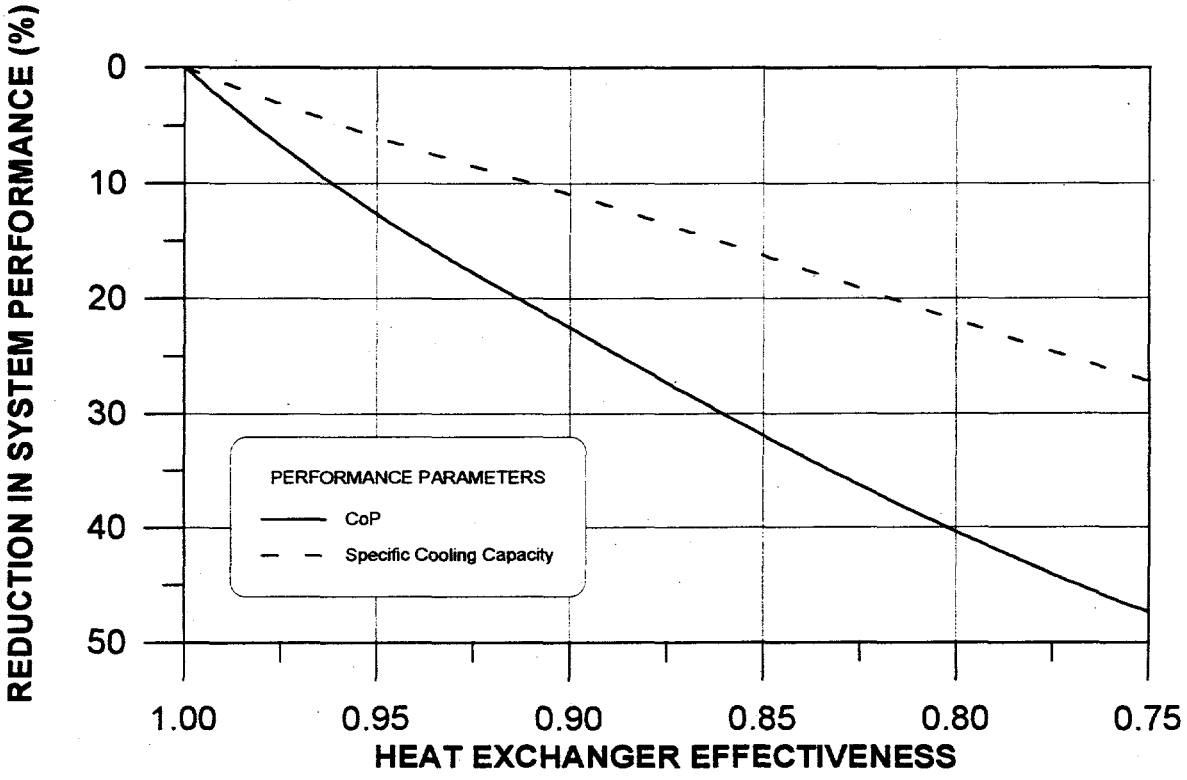

Figure 2-17. Relative reduction in system performance vs. heat exchanger effectivenss. Vent-Vent Cycle; 75C regeneration.

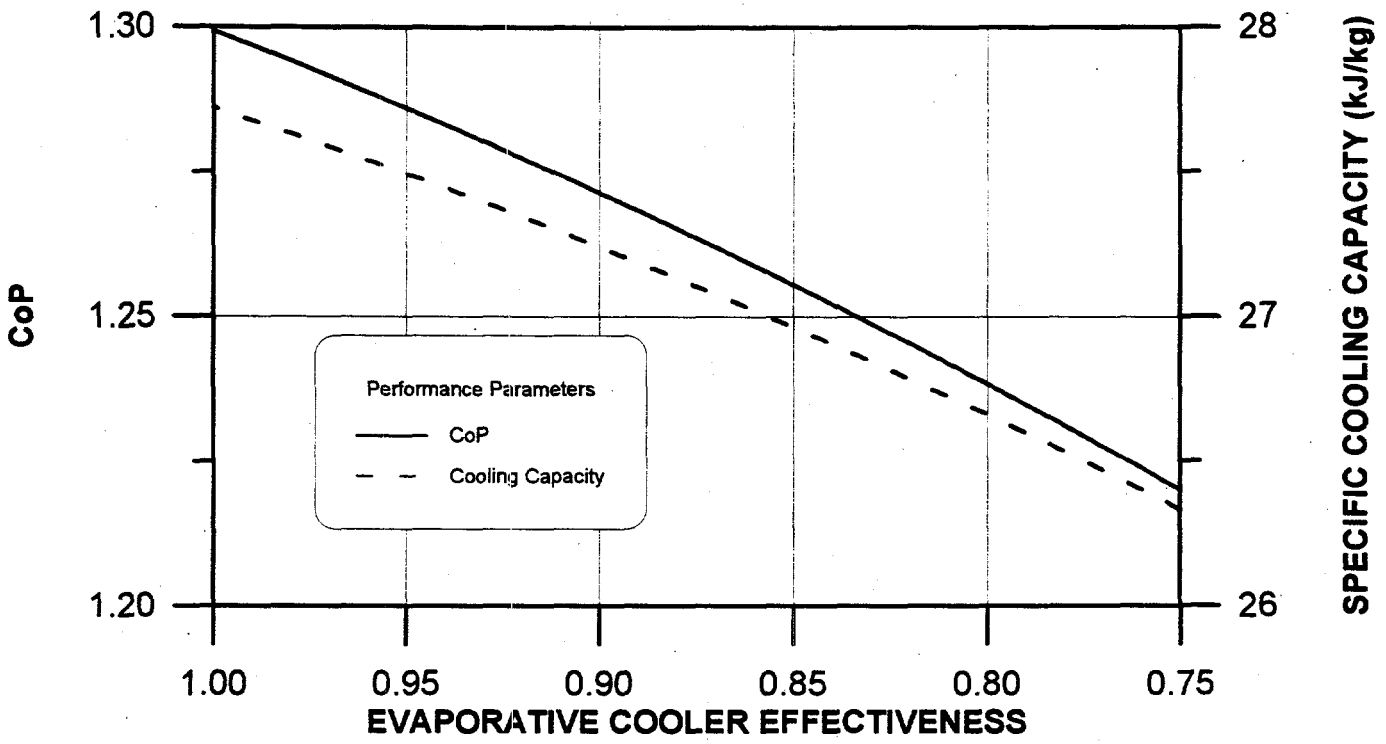

Figure 2-19. Cooling system performance as a function of evaporative cooler effectiveness. Ventilation cycle; 100C regeneration.

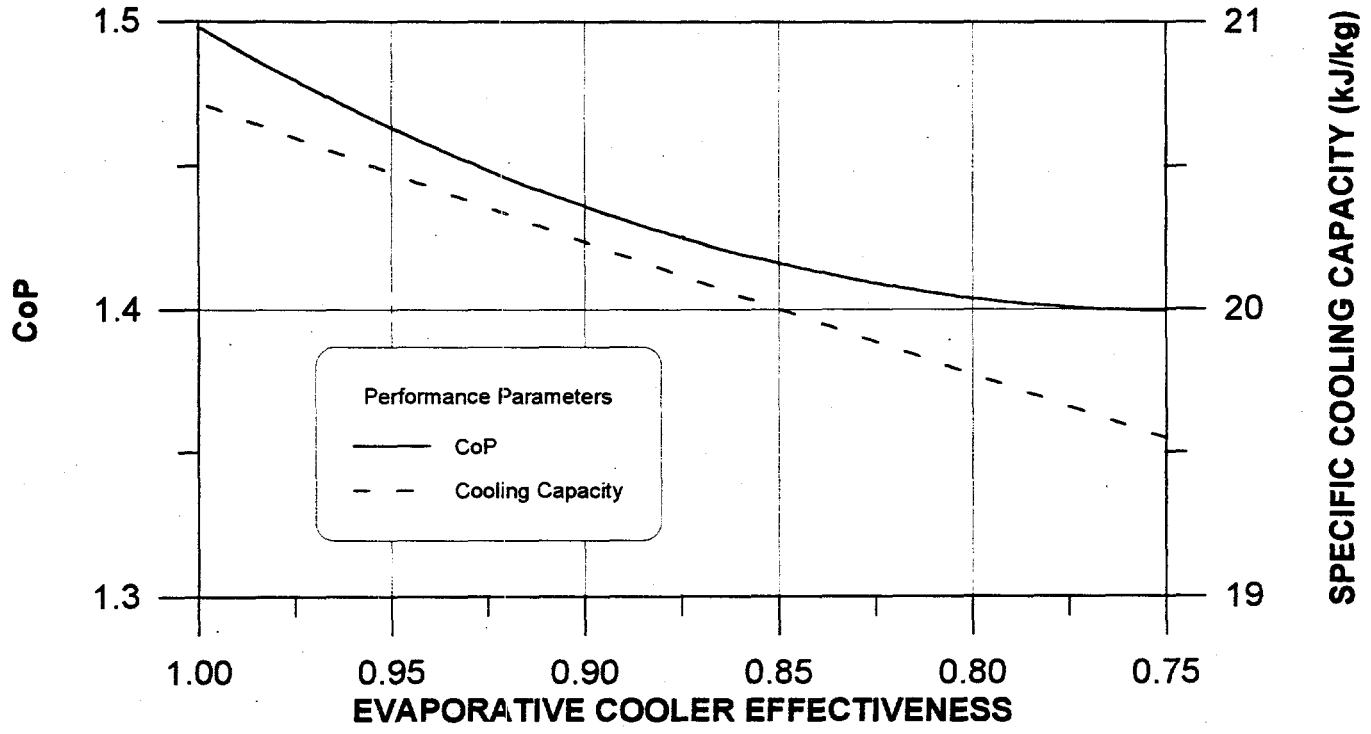

Figure 2-20. Cooling system performance as a function of evaporative cooler effectiveness. Ventilation cycle; 75C regeneration.

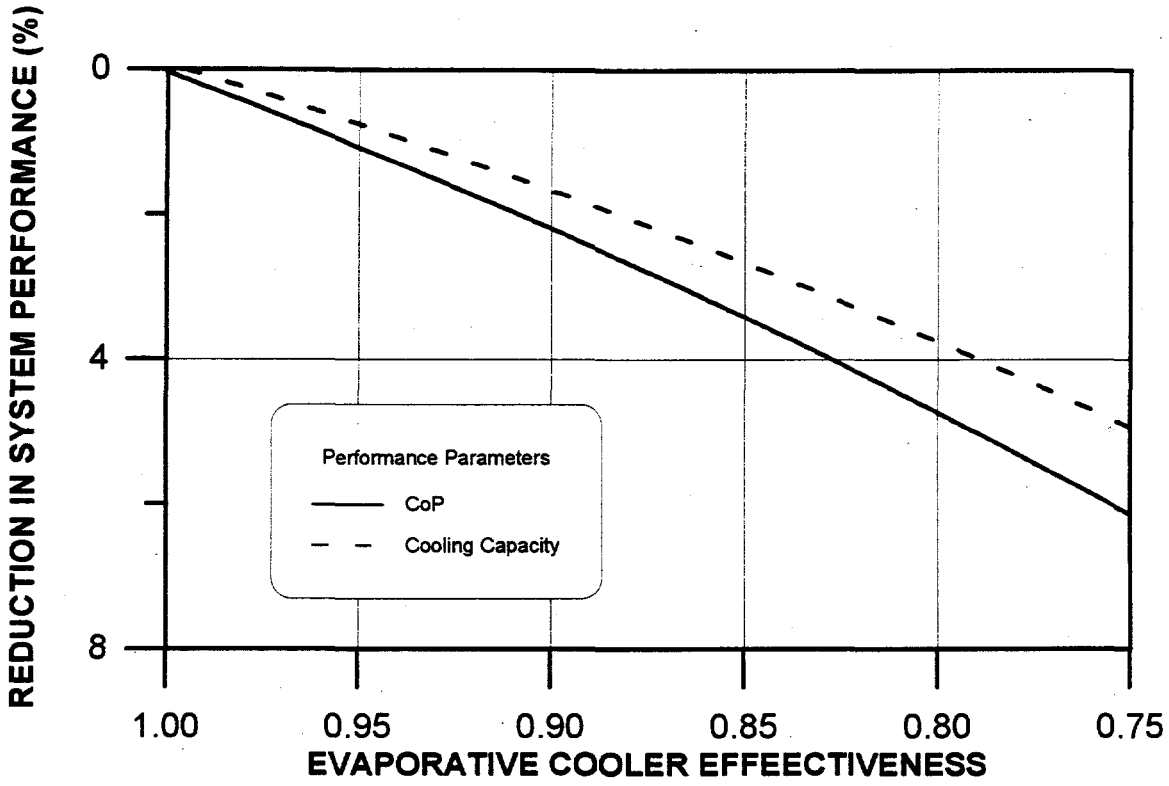

Figure 2-21. Reduction in system performance as a function of evaporative cooler effectiveness. Ventilation cycle; 100C regeneration.

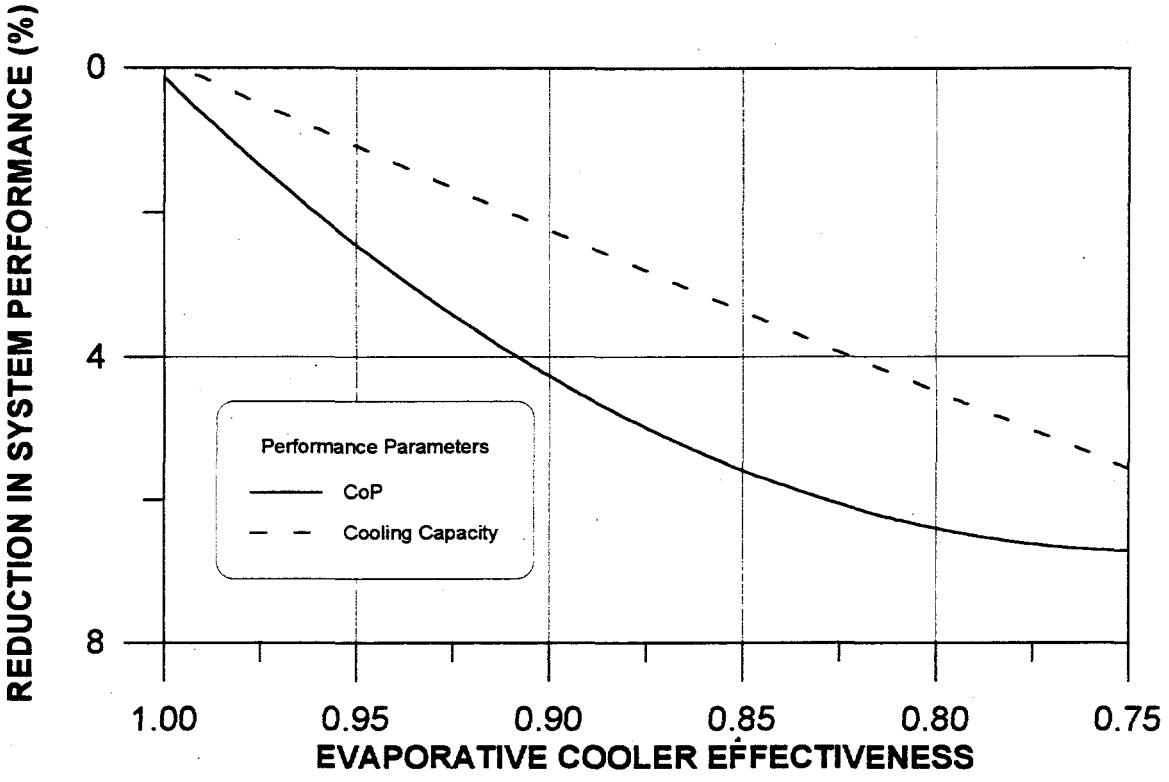

Figure 2-22. Reduction in system performance as a function of evaporative cooer effectiveness. Ventilation cycle; 75C regeneration.

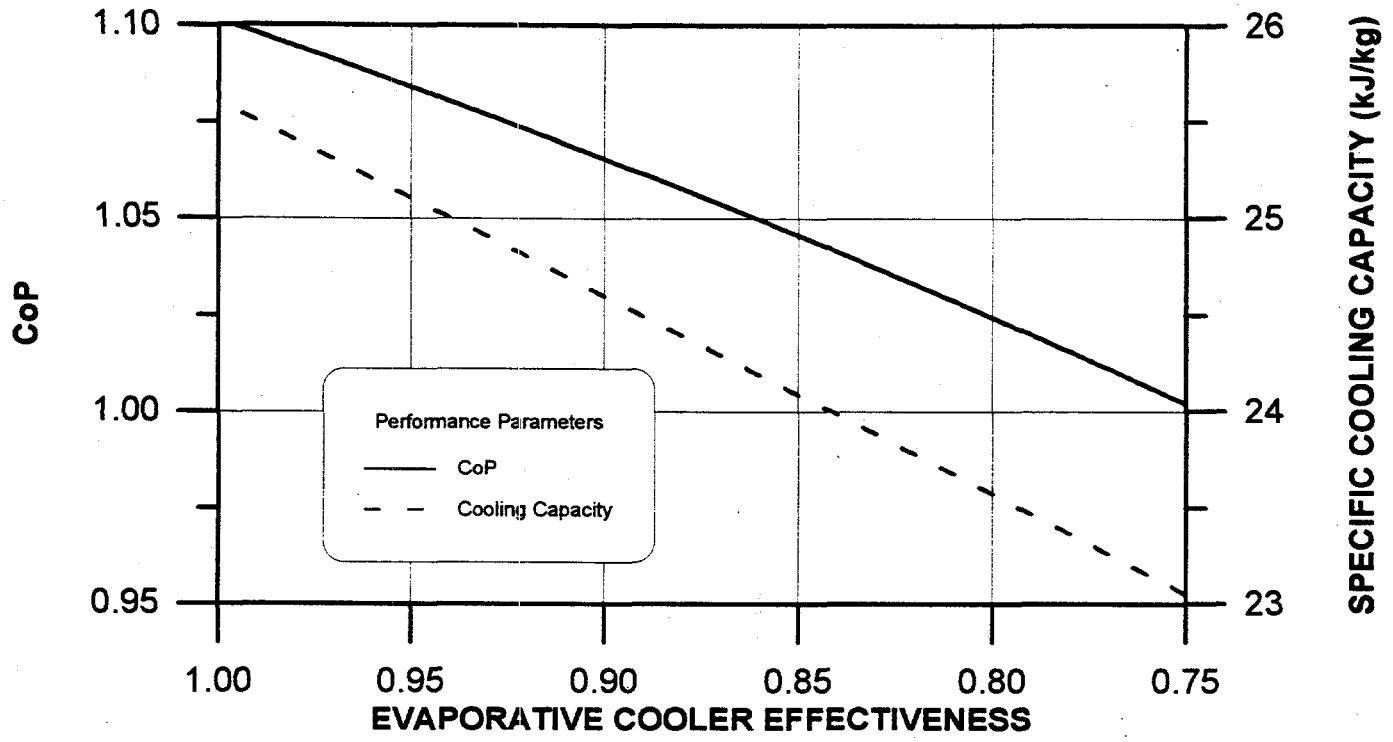

Figure 2-23. Cooling system performance as a function of evaporative cooler effectiveness. Recirculation cycle; 100C regeneration.

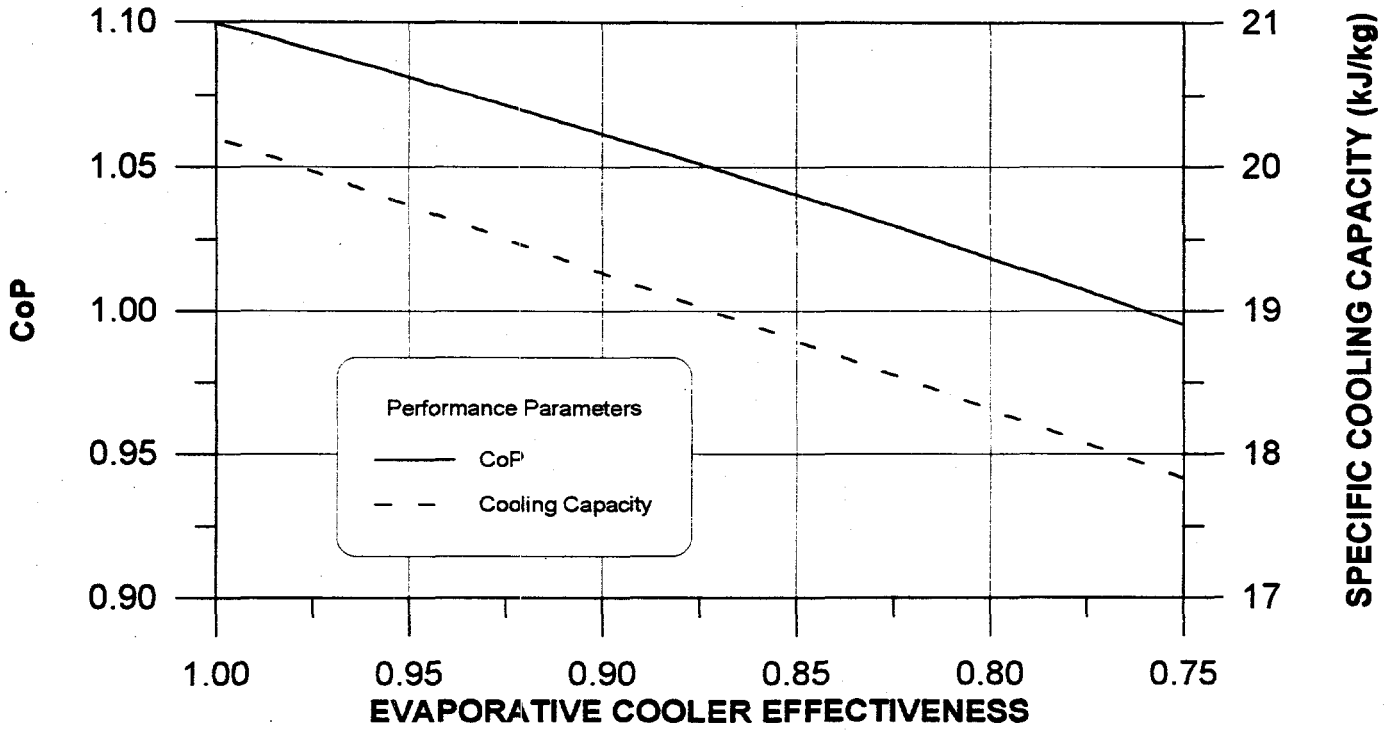

Figure 2-24. Cooling system performance as a function of evaporative cooler effectiveness. Recirculation cycle; 75C regeneration.

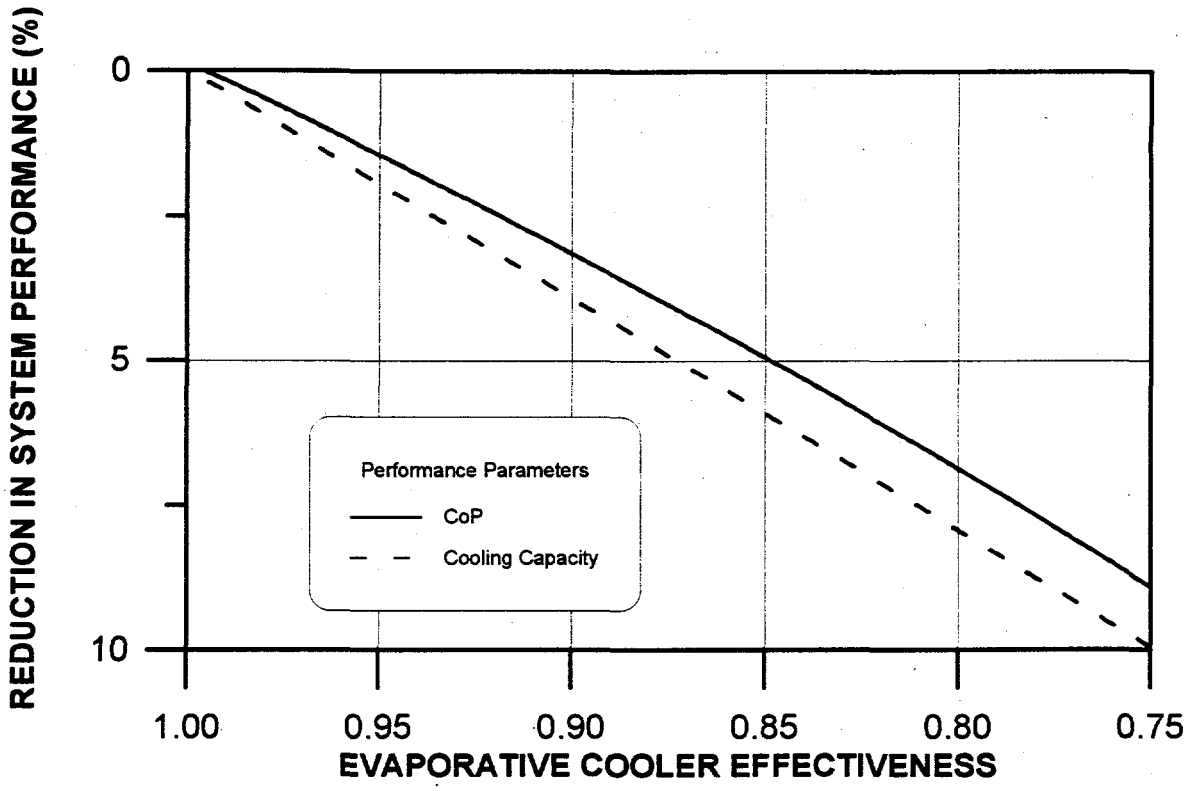

Figure 2-25. Reduction in system performance as a function of evaporative cooler effectiveness. Recirculation cycle; 100C regeneration.

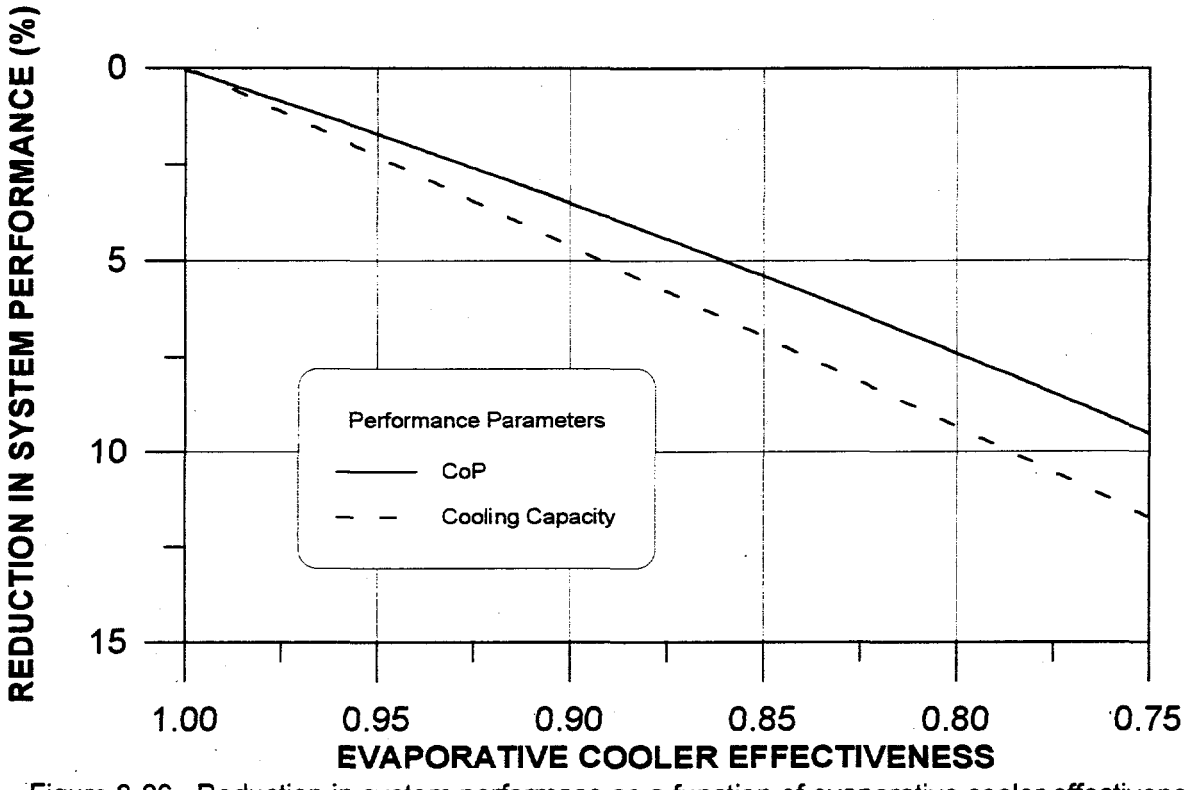

Figure 2-26. Reduction in system performace as a function of evaporative cooler effectiveness. Recirculation cycle; 75C regeneration.

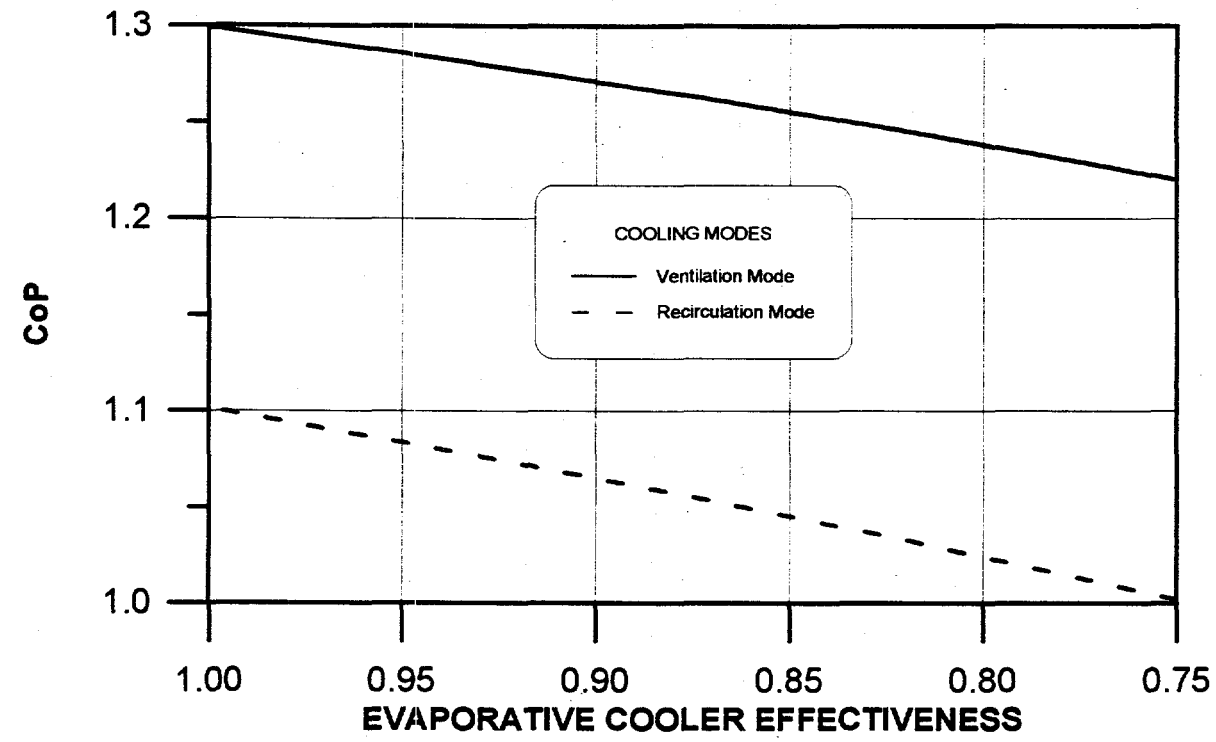

Figure 2-27. CoP comparisons for two cooling modes as a function of evaporative cooler effectiveness; 100C regeneration.

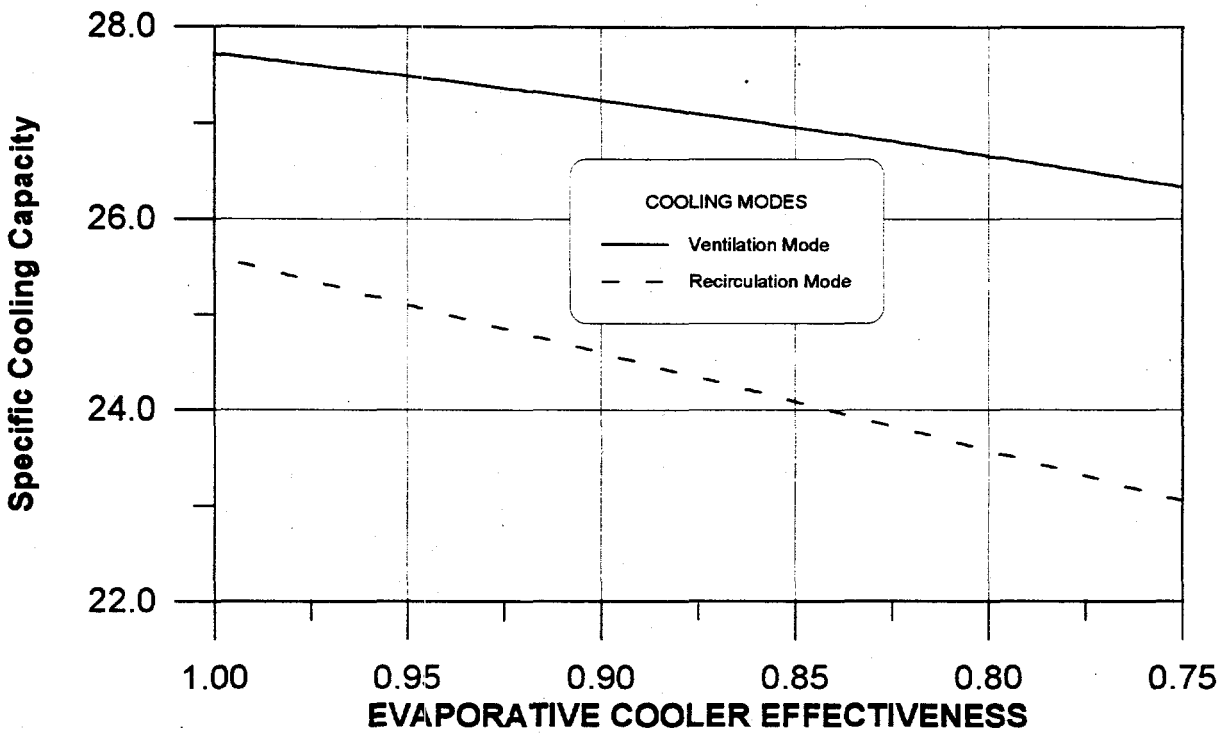

Figure 2-28. Specific Cooling Capacity comparisons for two cooling modees as a function of evaporative cooler effectiveness; 100C regeneration.

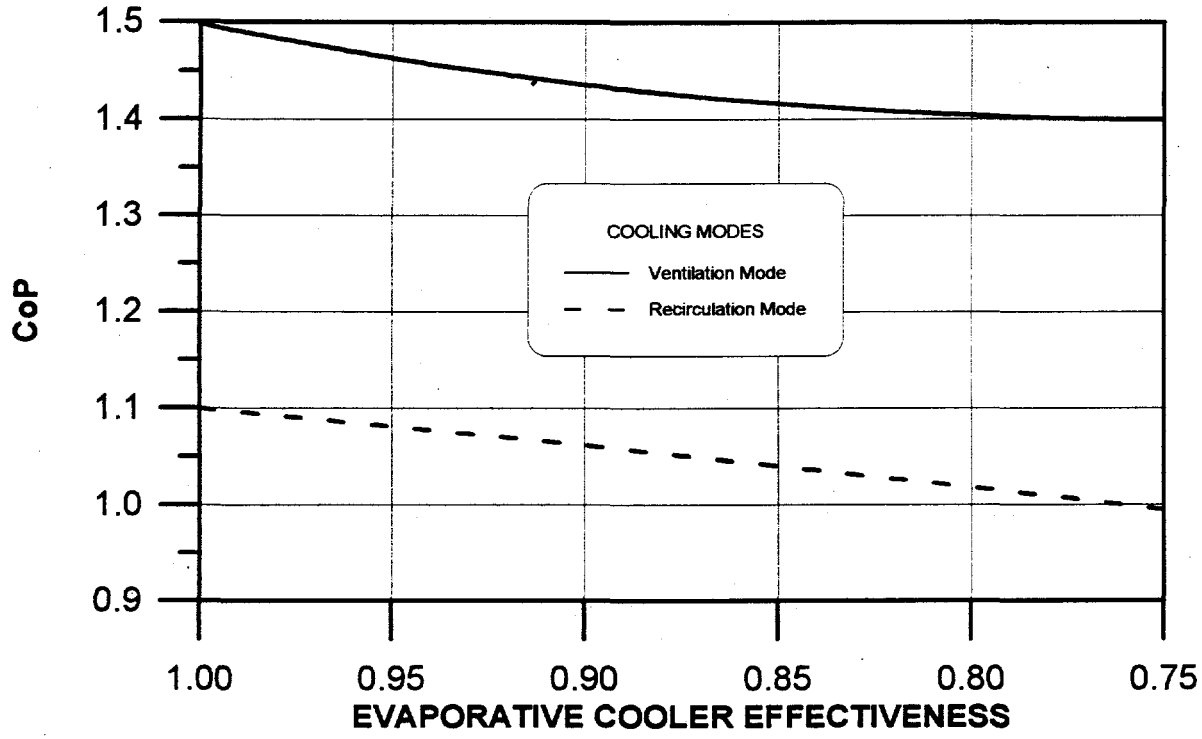

Figure 2-29. CoP comparisons for two cooling modes as a function of evaporative cooler effectiveness; 75C regeneration.

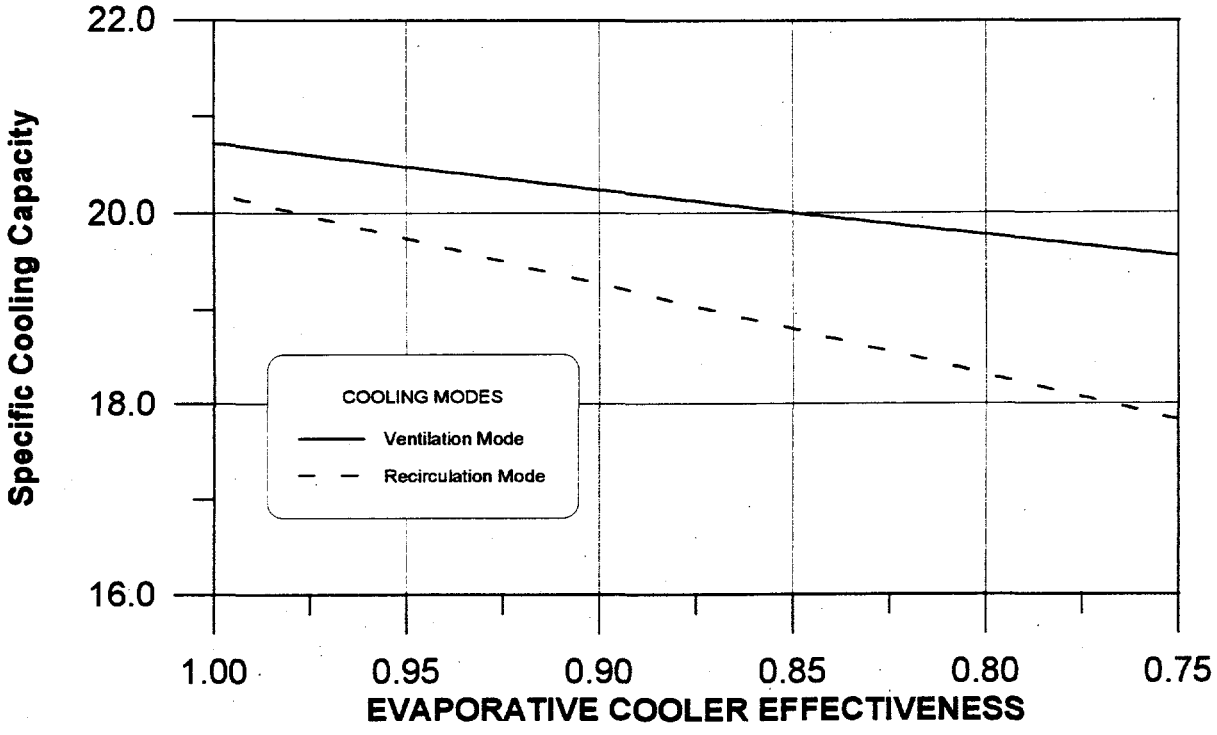

Figure 2-30. Specific Cooling Capacity comparisons for two cooing modes as a function of evaporative cooler effectiveness; 75C regeneration.

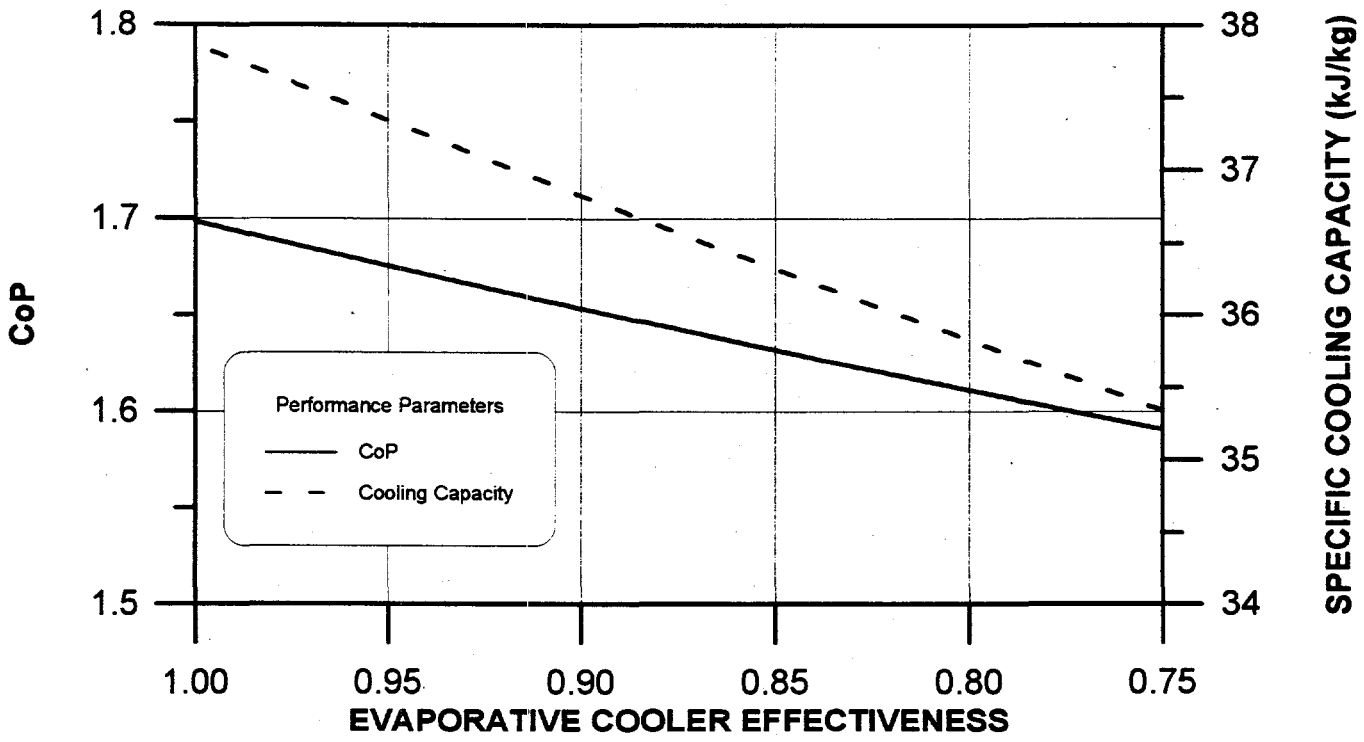

Figure 2-31. CoP and Specific Cooling Capacity as a function of evaporative cooler effectiveness. Vent-vent cycle; 100 C regeneration

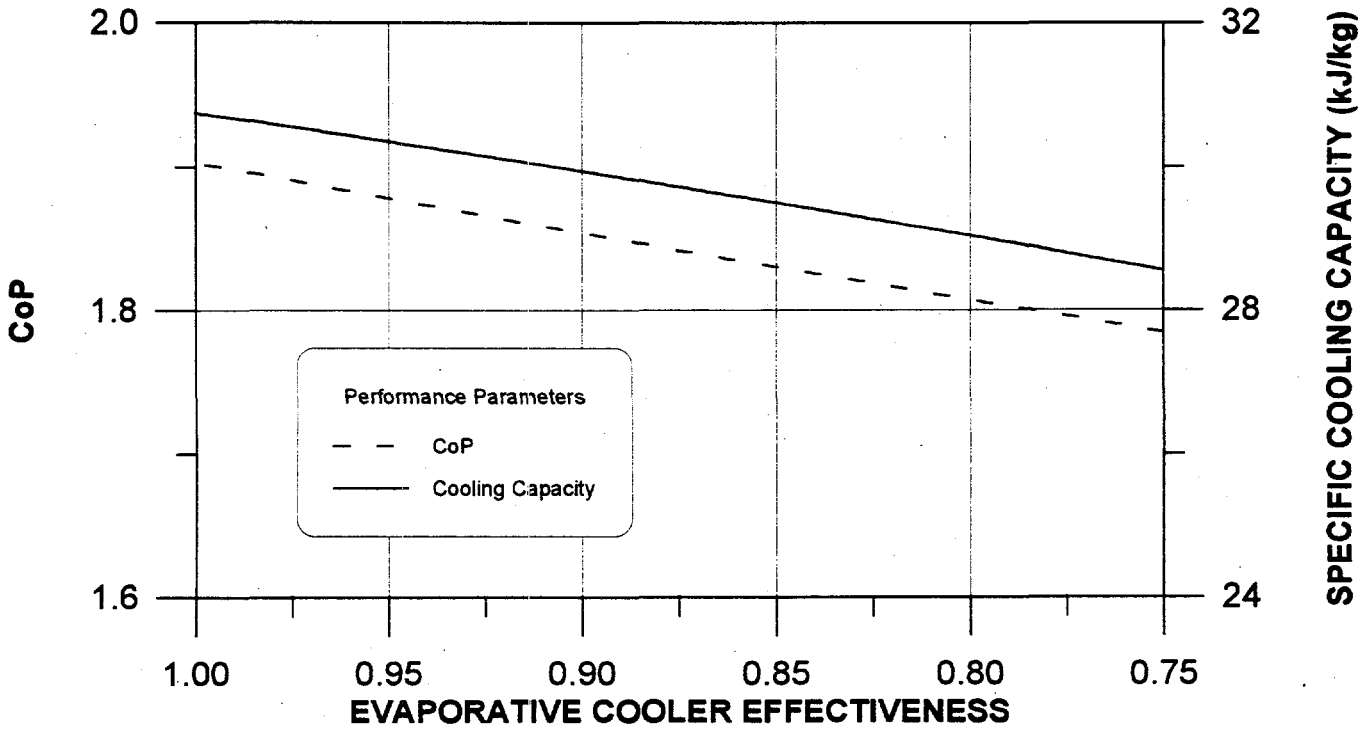

Figure 2-32. CoP and Specific Cooling Capacity as a function of evaporative cooler effectiveness. Vent-vent cycle; 75 C regeneration

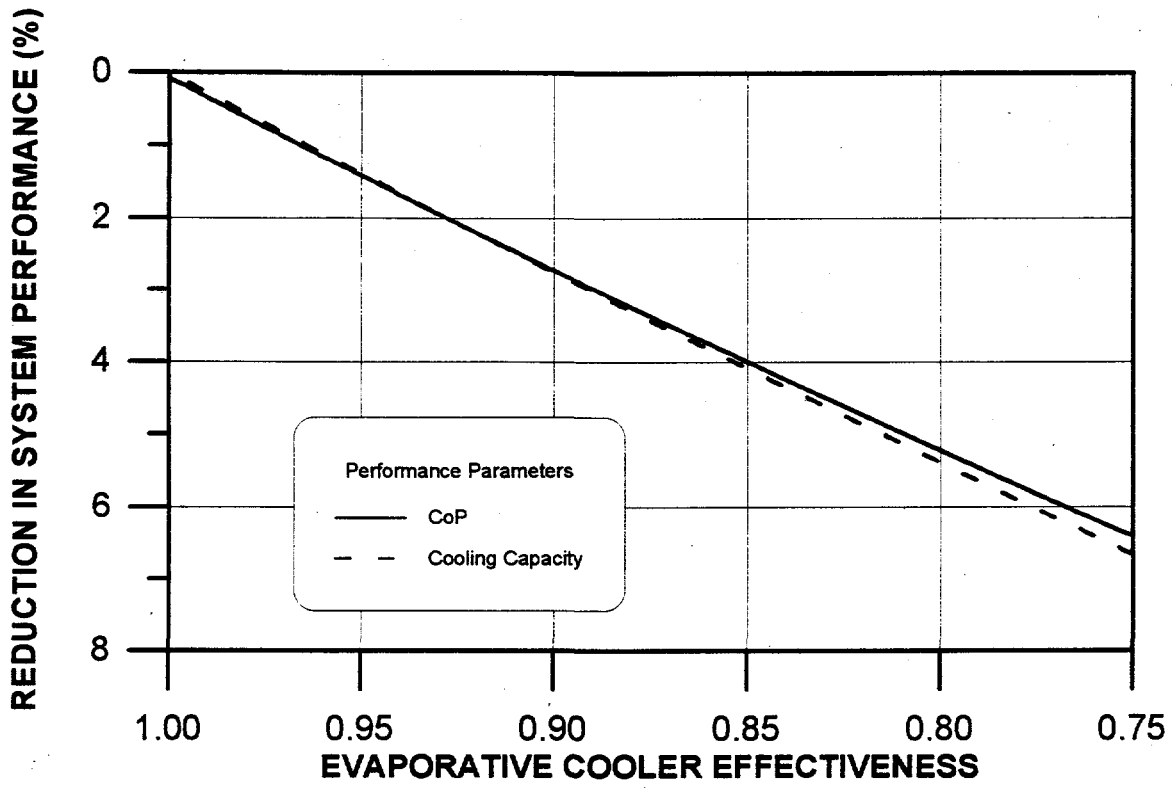

Figure 2-33. Relative reduction in system performance vs. evaporative cooler effectiveness Vent-Vent Cycle; 100C regeneration.

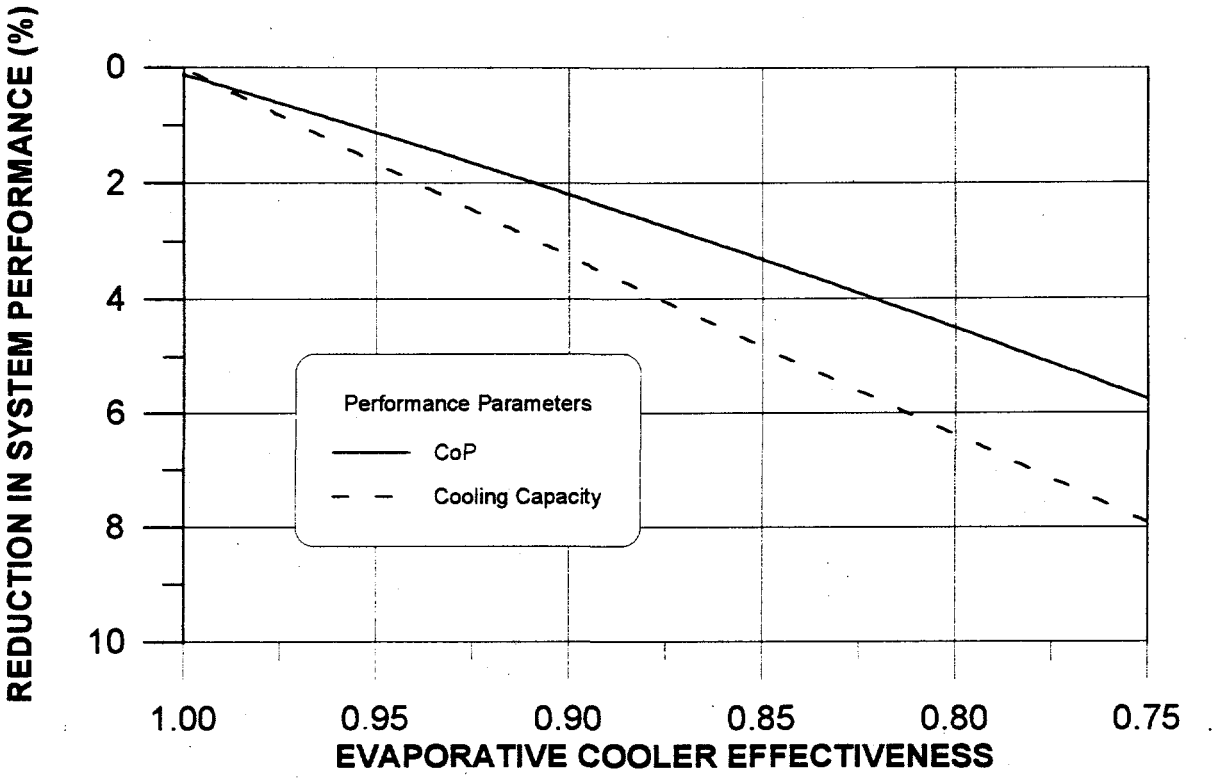

Figure 2-34. Relative reduction in system performance vs. evaporative cooler effectiveness Vent-Vent Cycle; 75C regeneration.

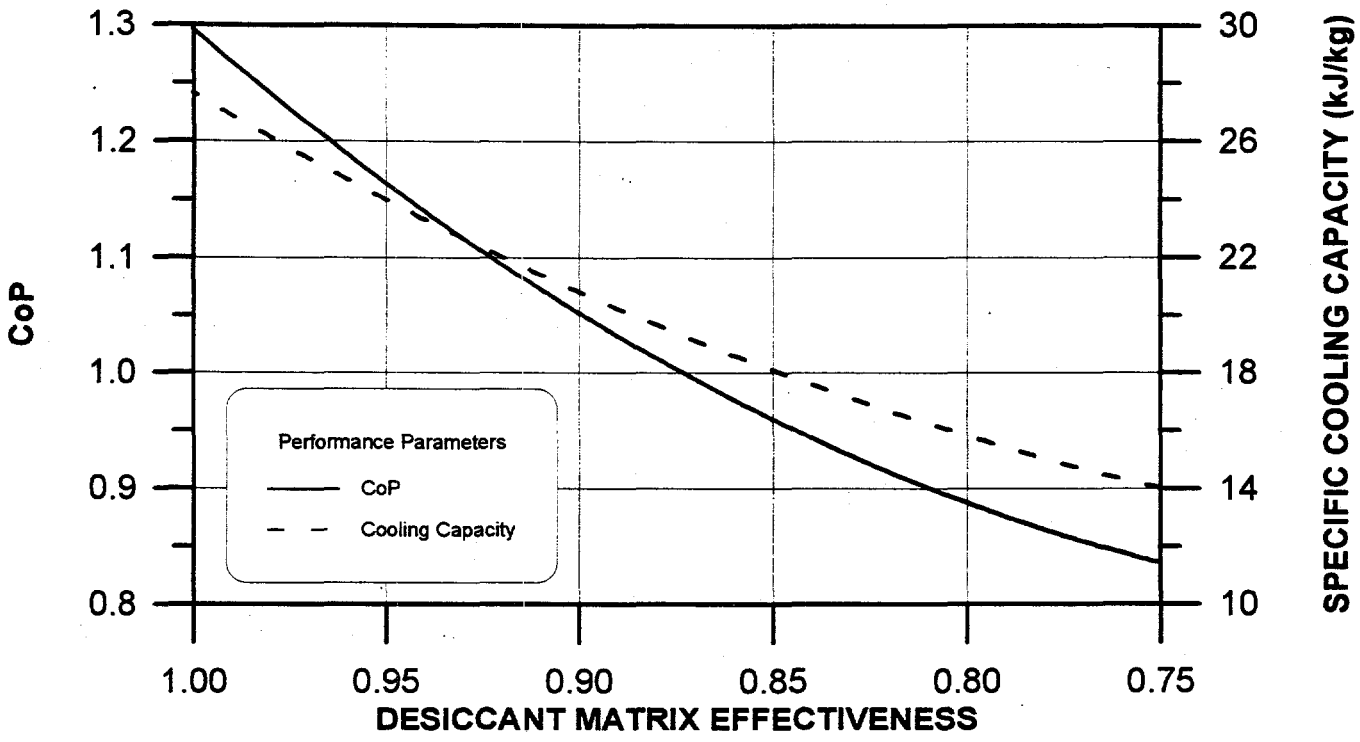

Figure 2-40. Cooling system performance as a function of desiccant matrix effectiveness. Ventilation cycle; 100C regeneration.

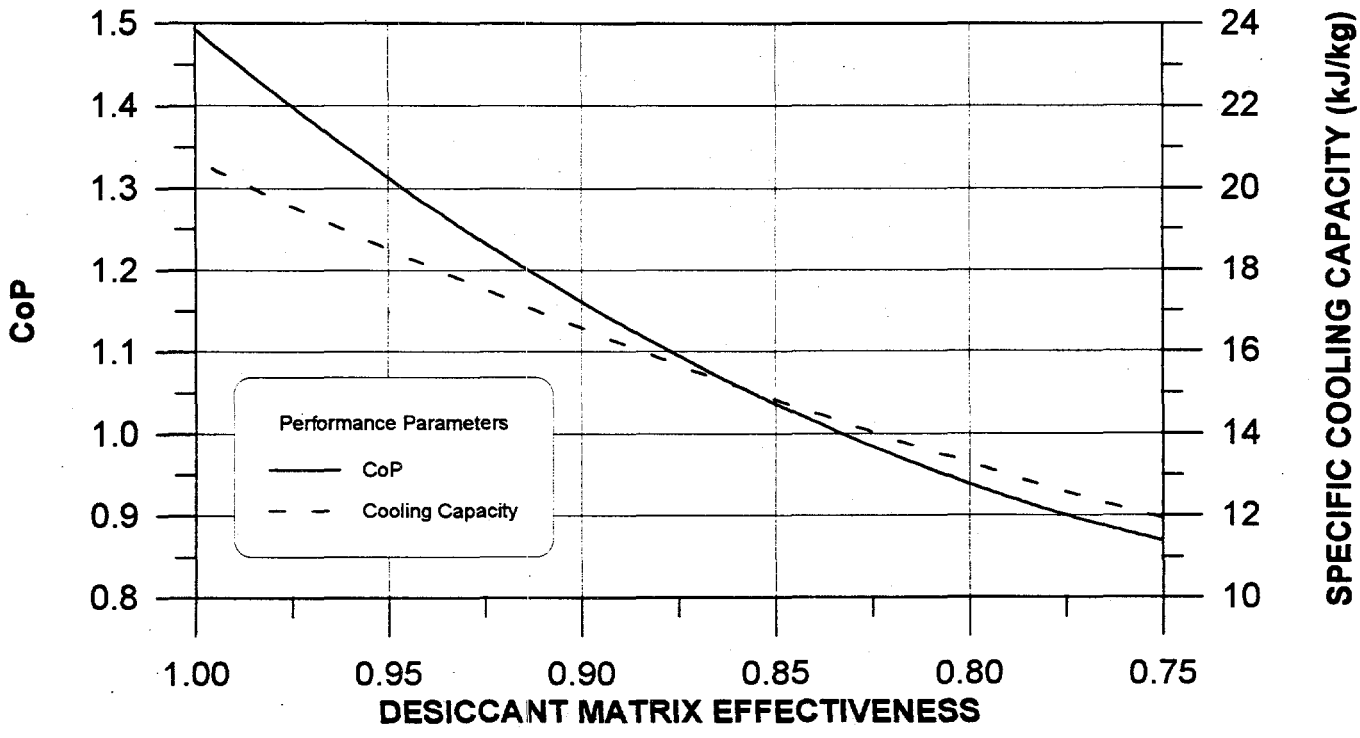

Figure 2-41. Cooling system performance as a function of desiccant matrix effectiveness. Ventilation cycle; 75C regeneration.

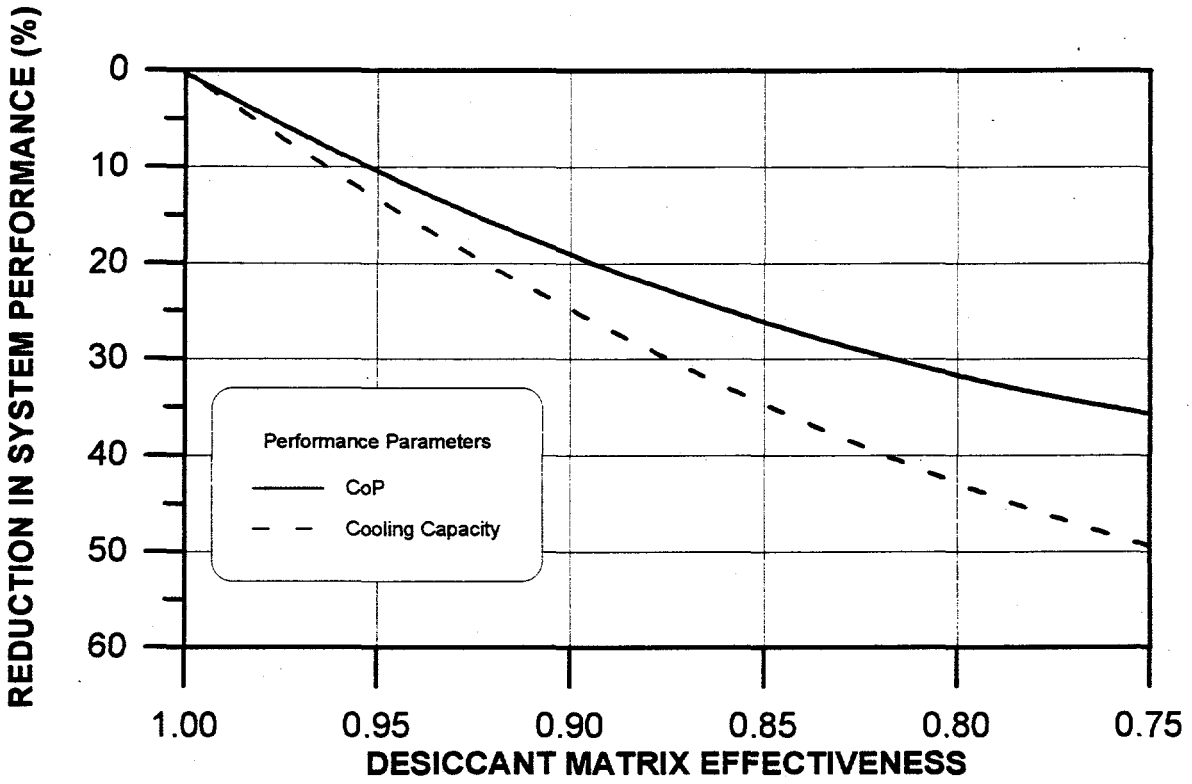

Figure 2-42. Reduction in system performance as a function of desiccant matrix effectiveness. Ventilation cycle; 100C regeneration.

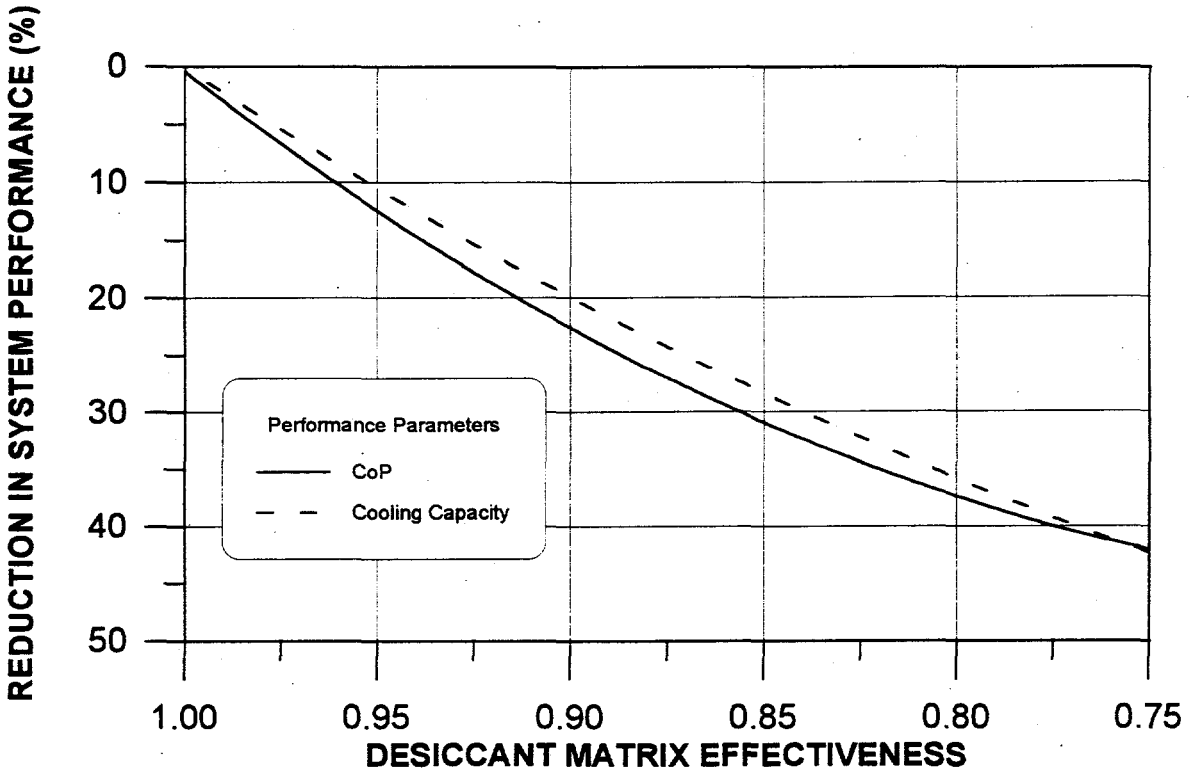

Figure 2-43. Reduction in system performance as a function of desiccant matrix effectiveness. Ventilation cycle; 75C regeneration.

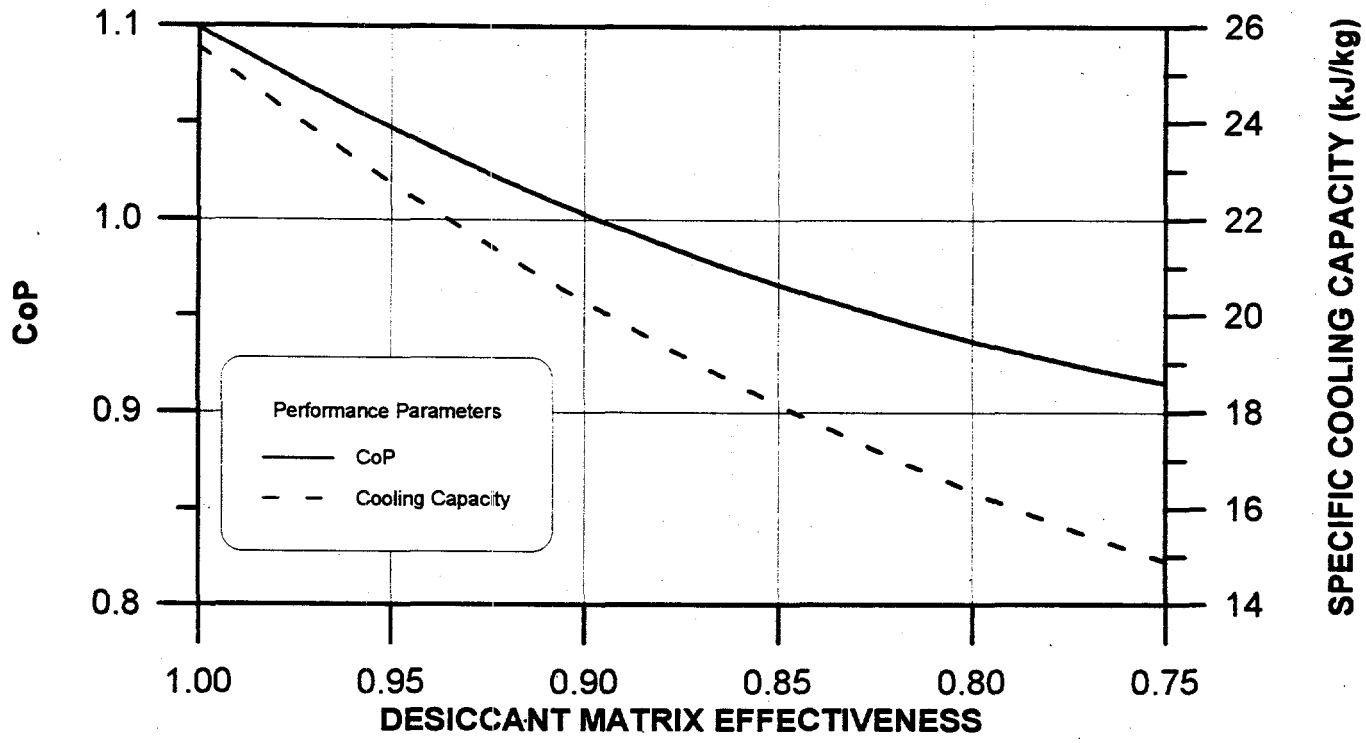

Figure 2-44. Cooling system performance as a function of desiccant matrix effectiveness. Recirculation cycle; 100C regeneration.

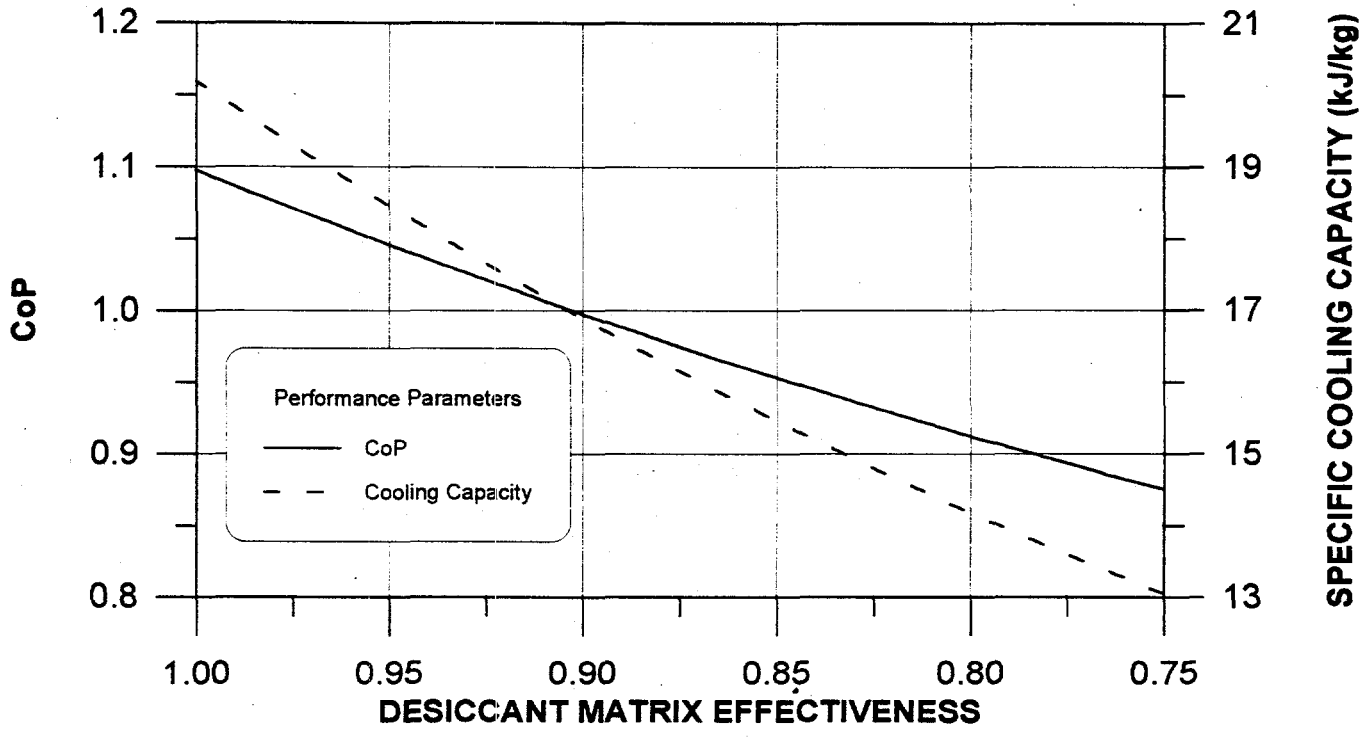

Figure 2-45. Cooling system performance as a function of desiccant matrix effeectiveness. Recirculation cycle; 75C regeneration.

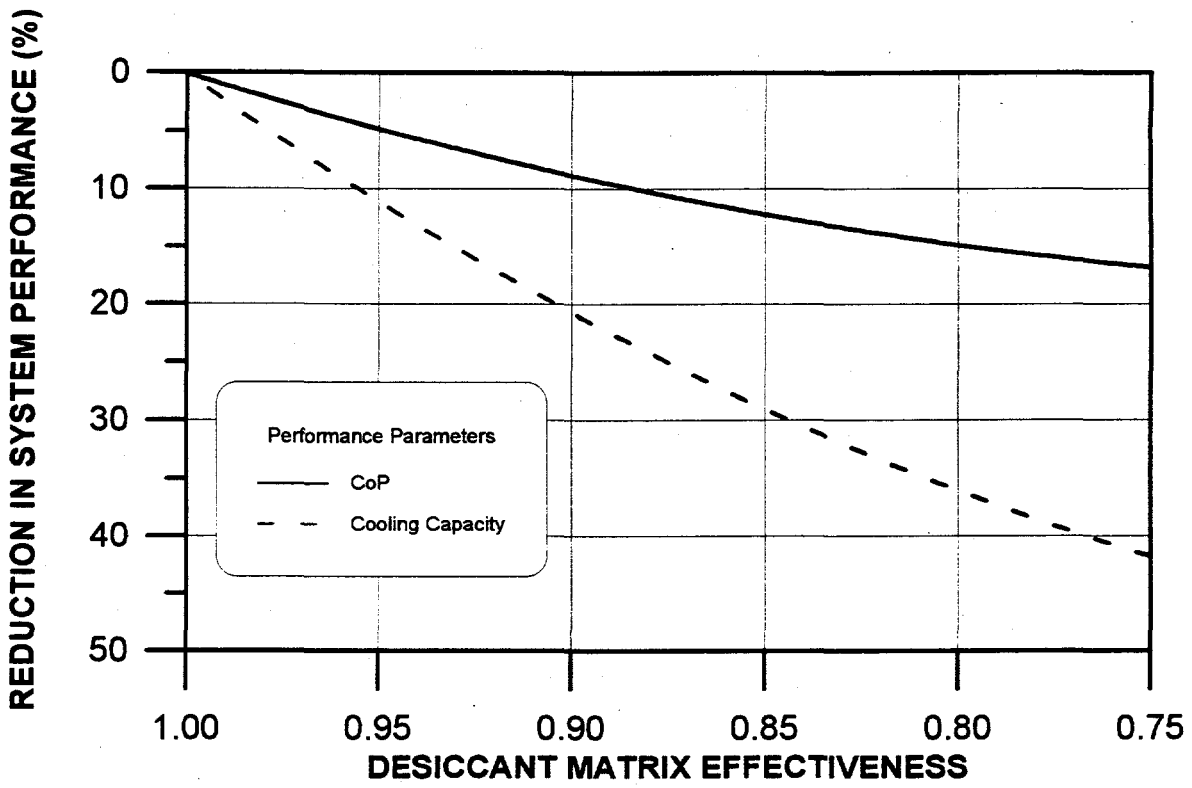

Figure 2-46. Reduction in system performance as a function of desiccant matrix effectiveness. Recirculation cycle; 100C regeneration.

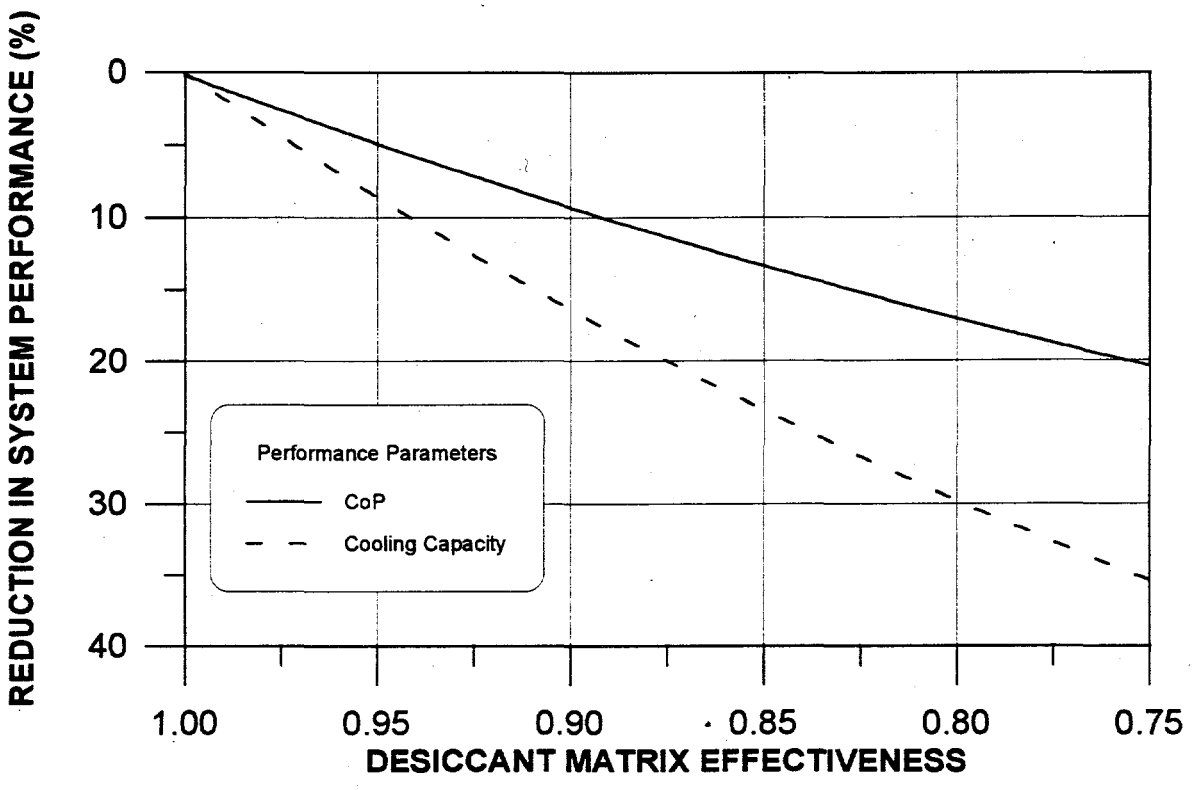

Figure 2-47. Reduction in system performance as a function of desiccant matrix effectiveness. Recirculation cycle; 75C regeneration.

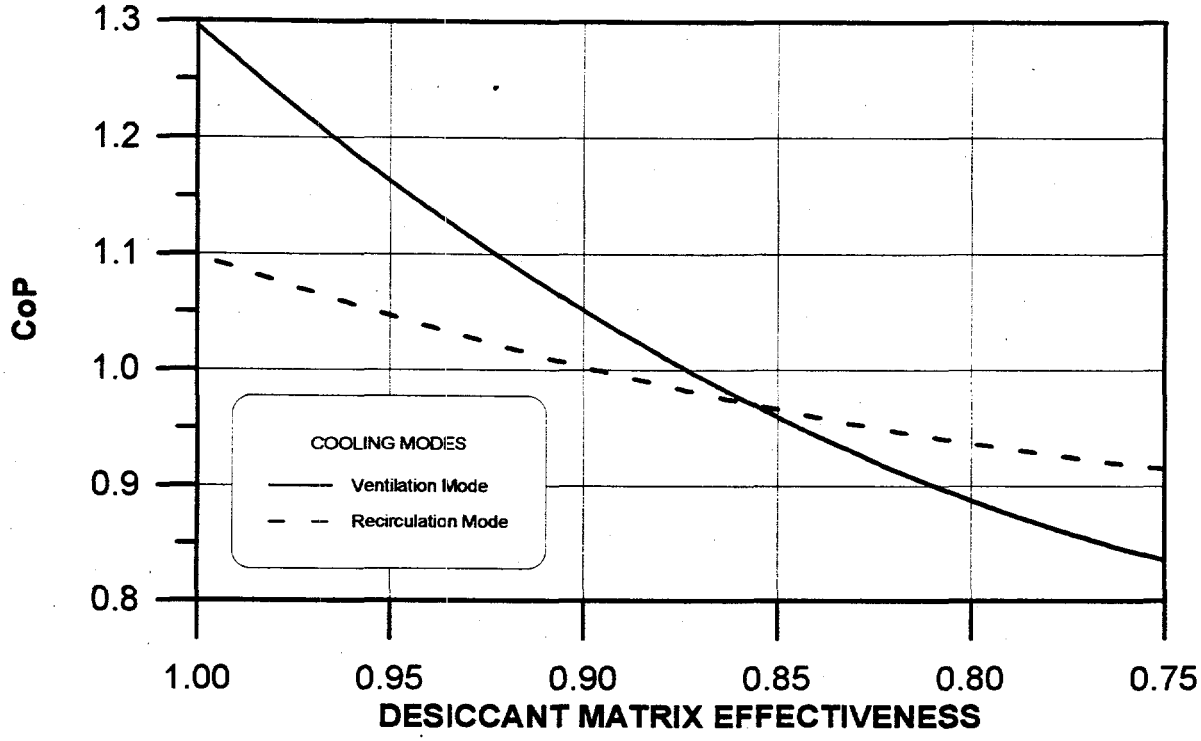

Figure 2-48. CoP comparisons for two cooling modes as a function of desiccant matrix effectiveness; 100C regeneration.

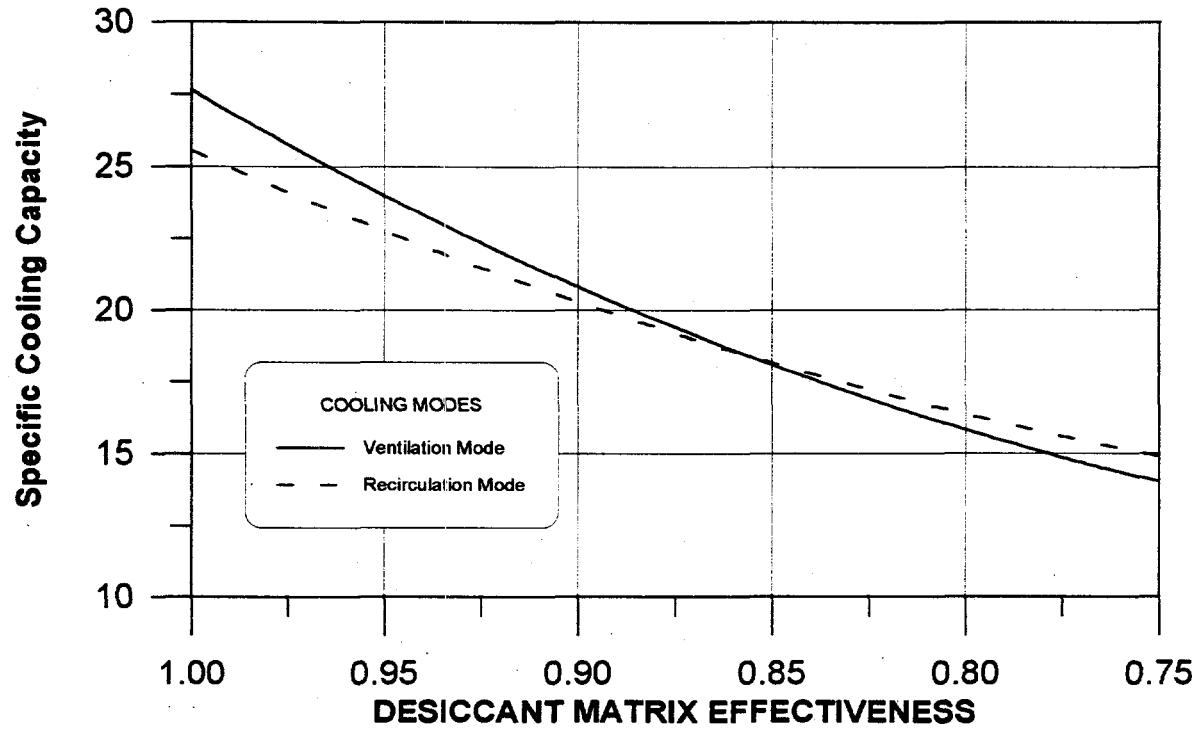

Figure 2-49. Specific Cooling Capacity comparisond for two cooling modes as a function of desiccant matrix effectiveness; 100C regeneration.

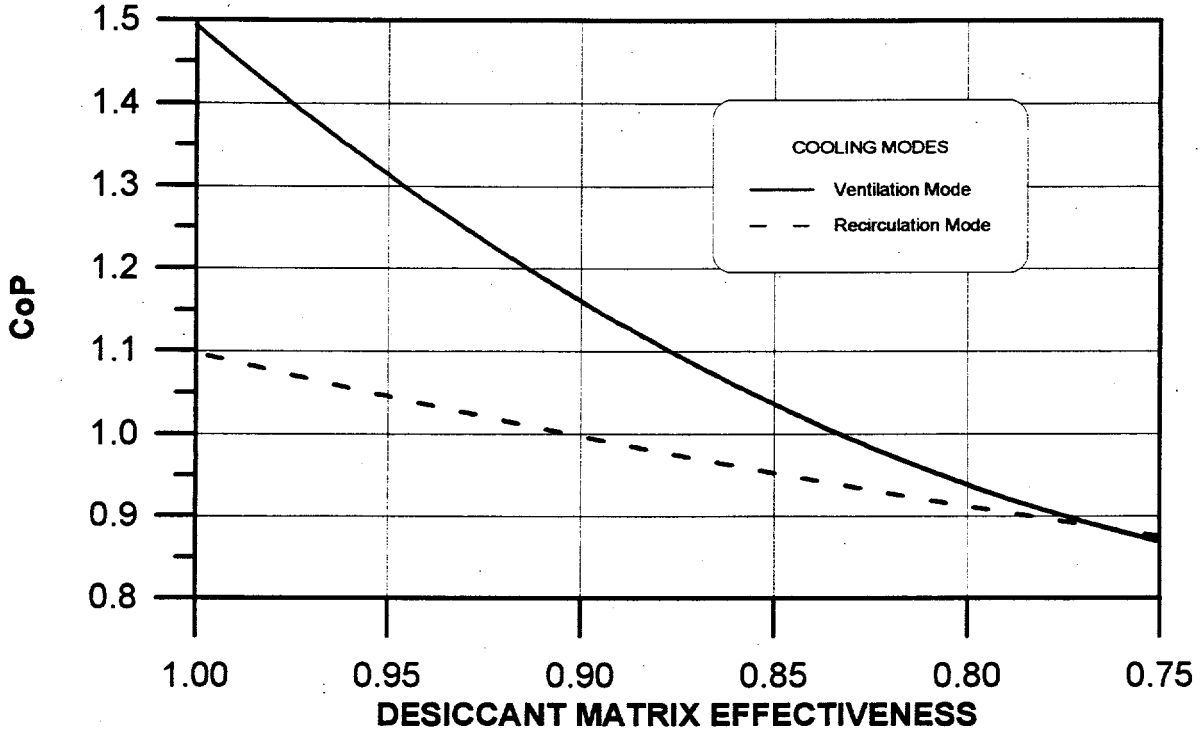

Figure 2-50. CoP comparisons for two cooling modes as a function of desiccant matrix effectiveness; 75C regeneration.

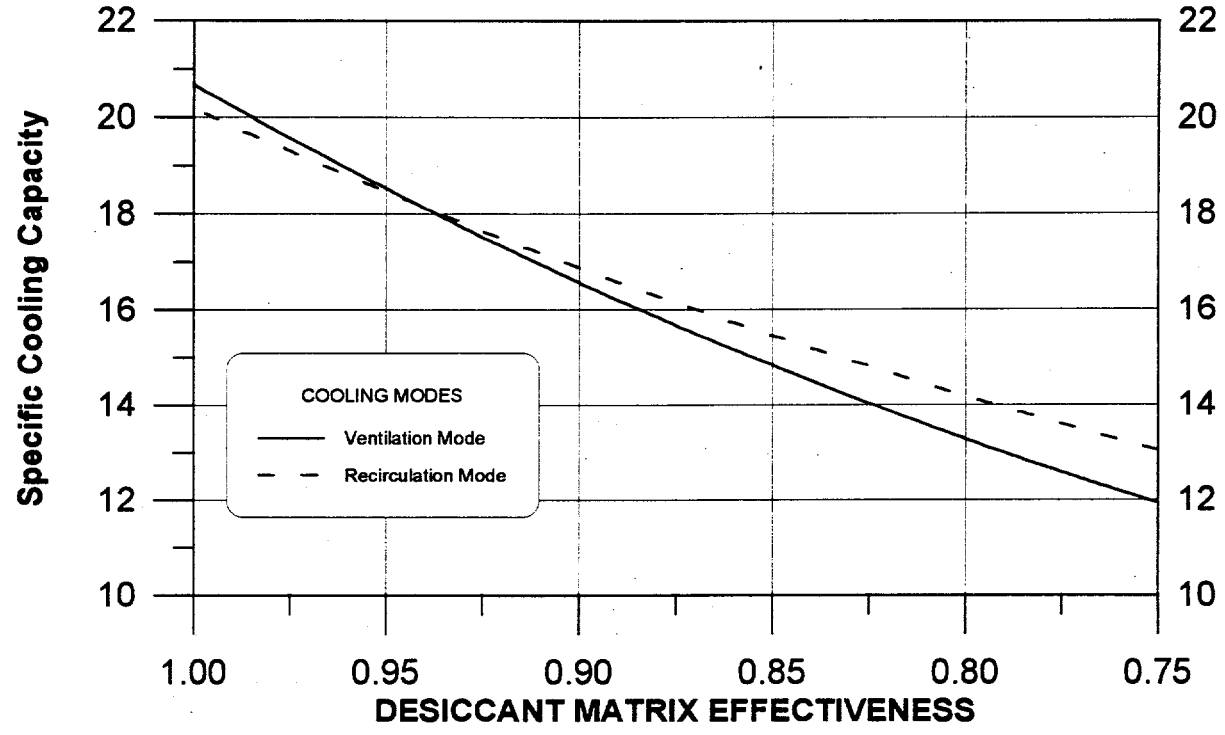

Figure 2-51. Specific Cooling Capacity comparisons for two cooling modes as a function of desiccant matrix effectiveness; 75C regeneration.

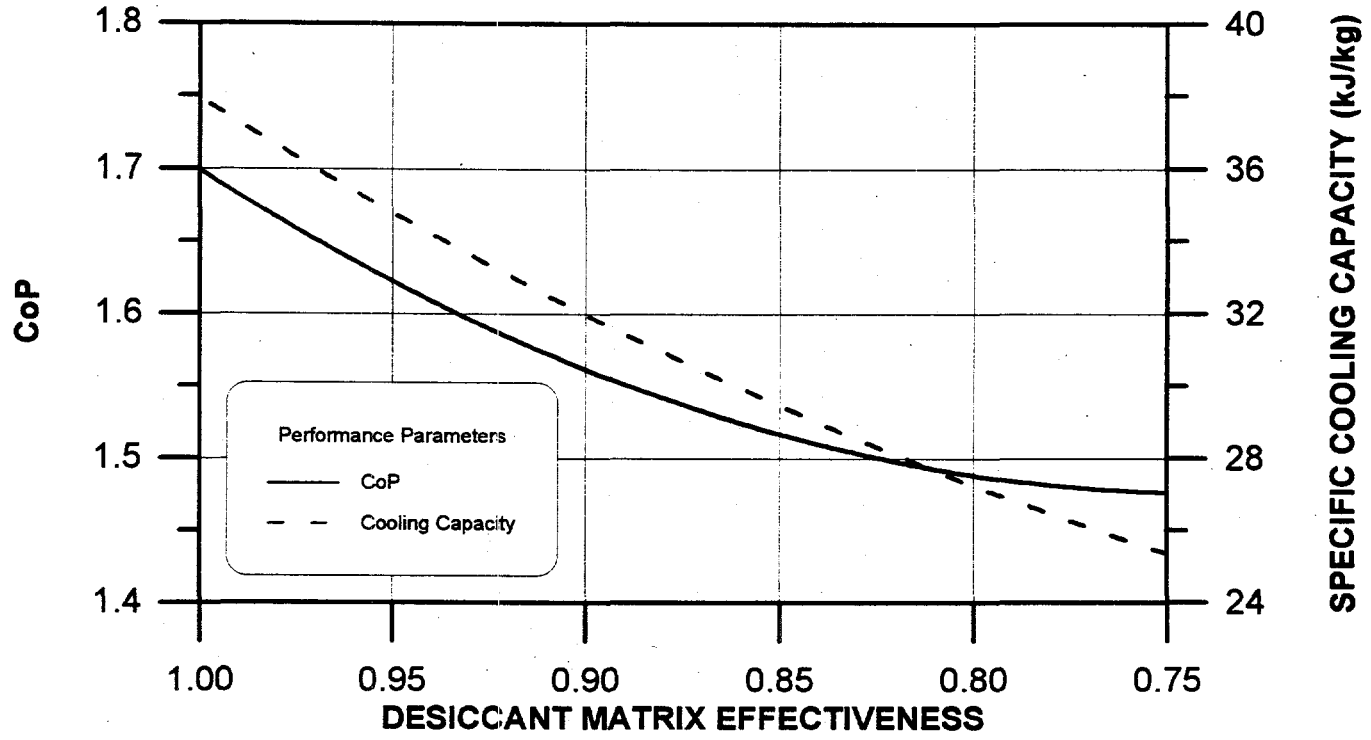

Figure 2-52. CoP and Specific Cooling Capacity as a function of desiccant matrix effectiveness. Vent-vent cycle; 100 C regeneration

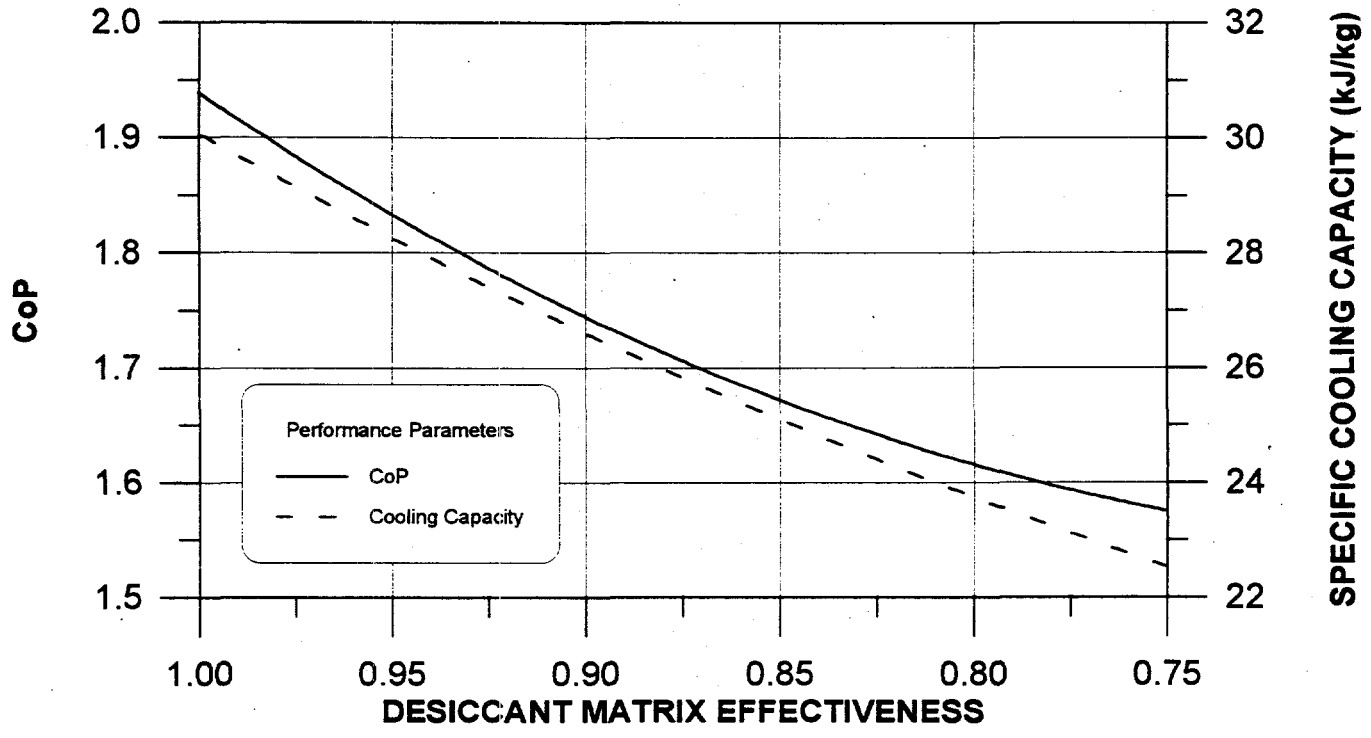

Figure 2-53. CoP and Specific Cooling Capacity as a function of desiccant matrix effectiveness. Vent-vent cycle; 75C regeneration.

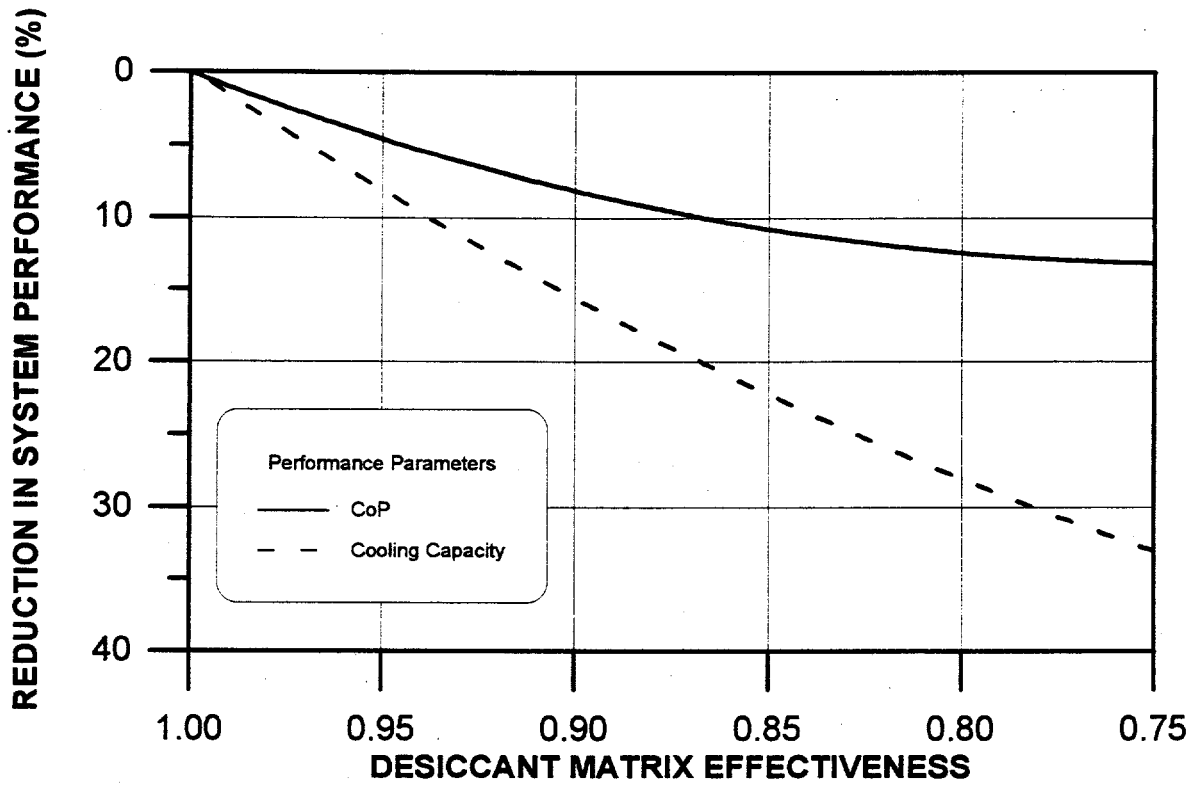

Figure 2-54. Relative reduction in system performance vs. desiccant matrix effectiveness Vent-Vent Cycle; 100C regeneration.

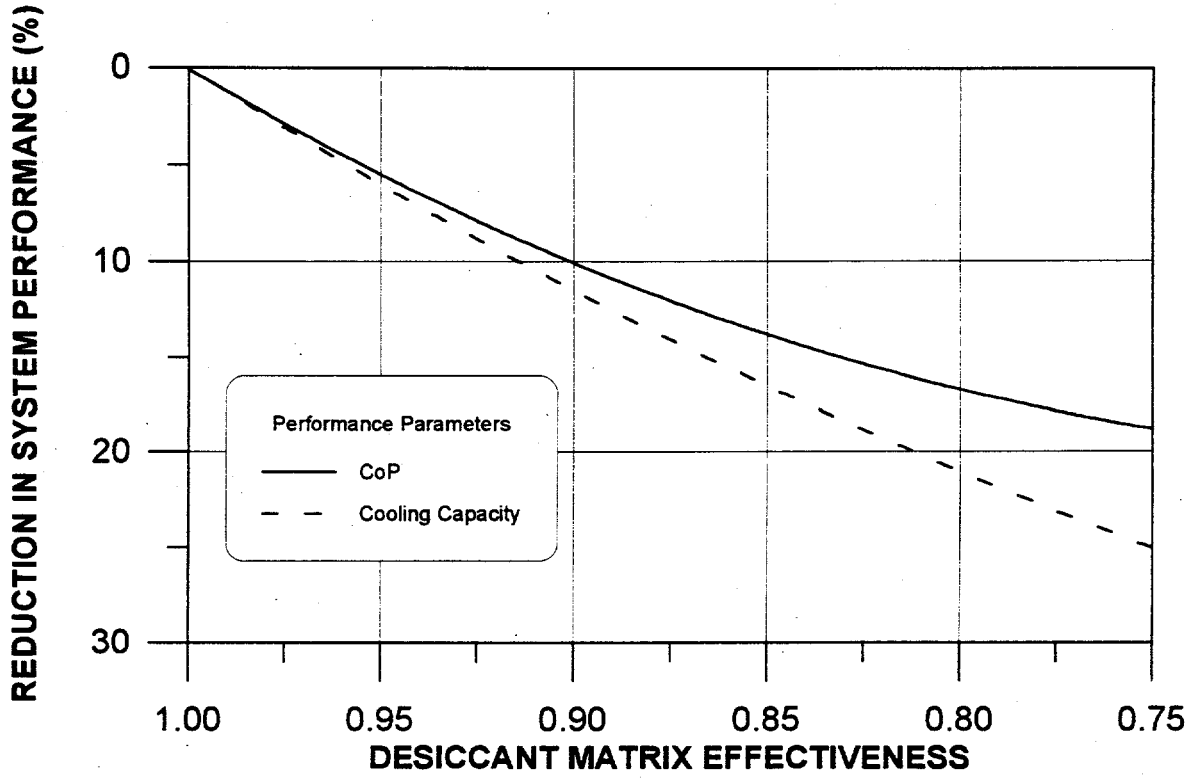

Figure 2-55. Relative reduction in system performance vs. desiccant matrix effectiveness Vent-Vent Cycle; 75C regeneration.

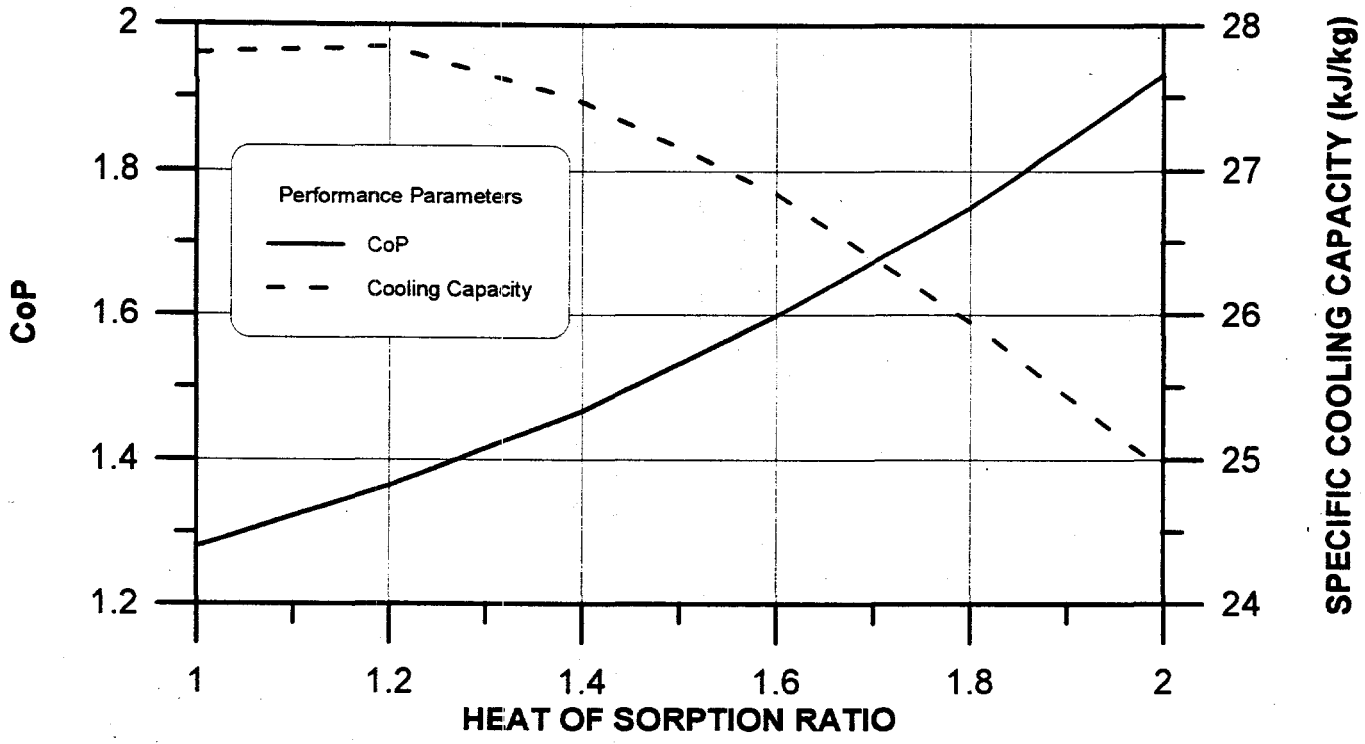

Figure 2-61. Cooling system performance as a function of desiccant heat of sorption ratio. Ventilation cycle; 100C regeneration

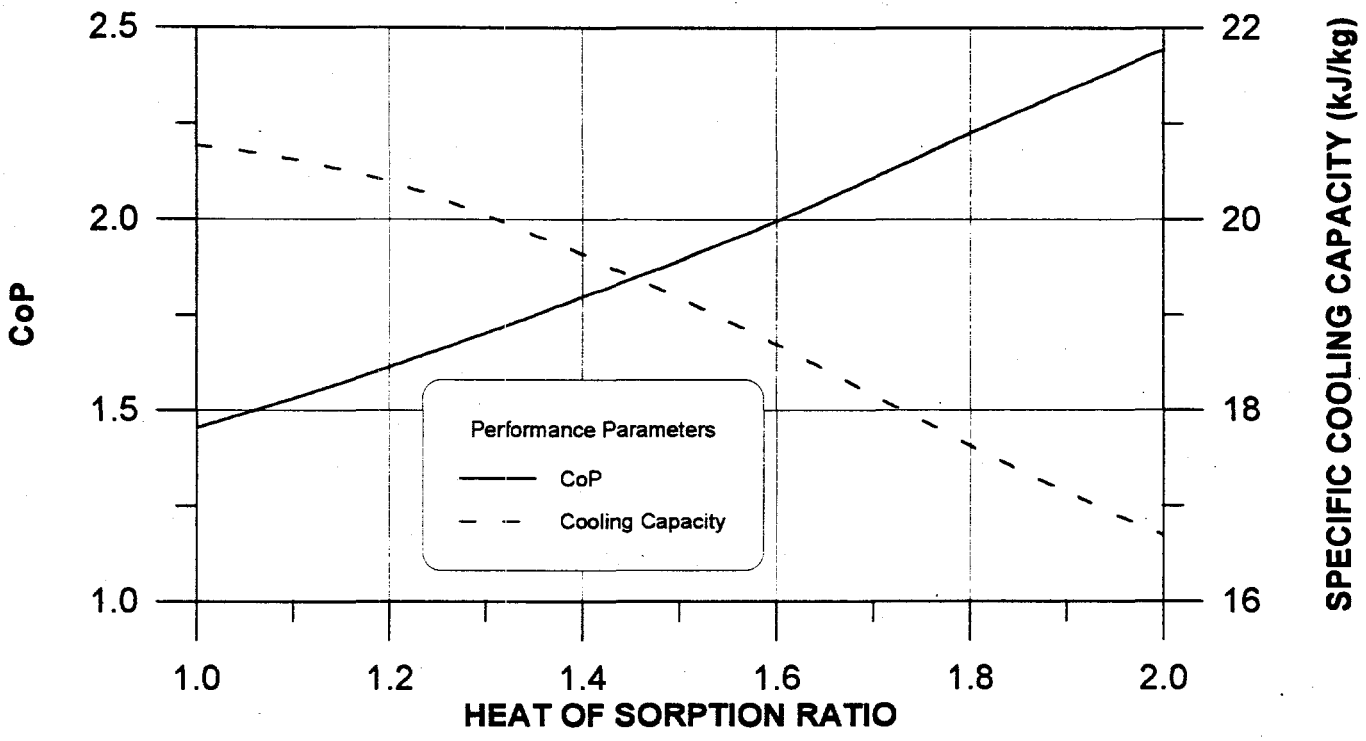

Figure 2-62. Cooling system performance as a function of desiccant heat of sorption ratio. Ventilation cycle; 75C regeneration.

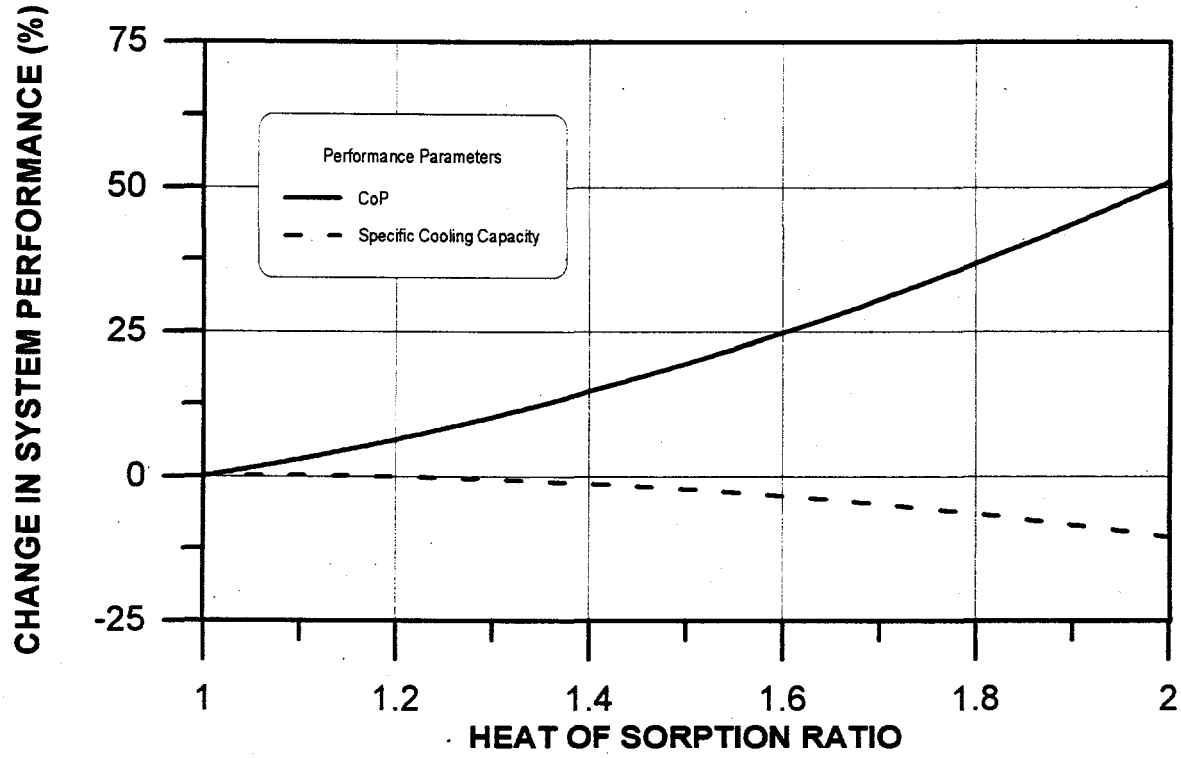

Figure 2-63. Change in system performance as a function of desiccant heat of sorption ratio. Ventilation cycle; 100C regeneration.

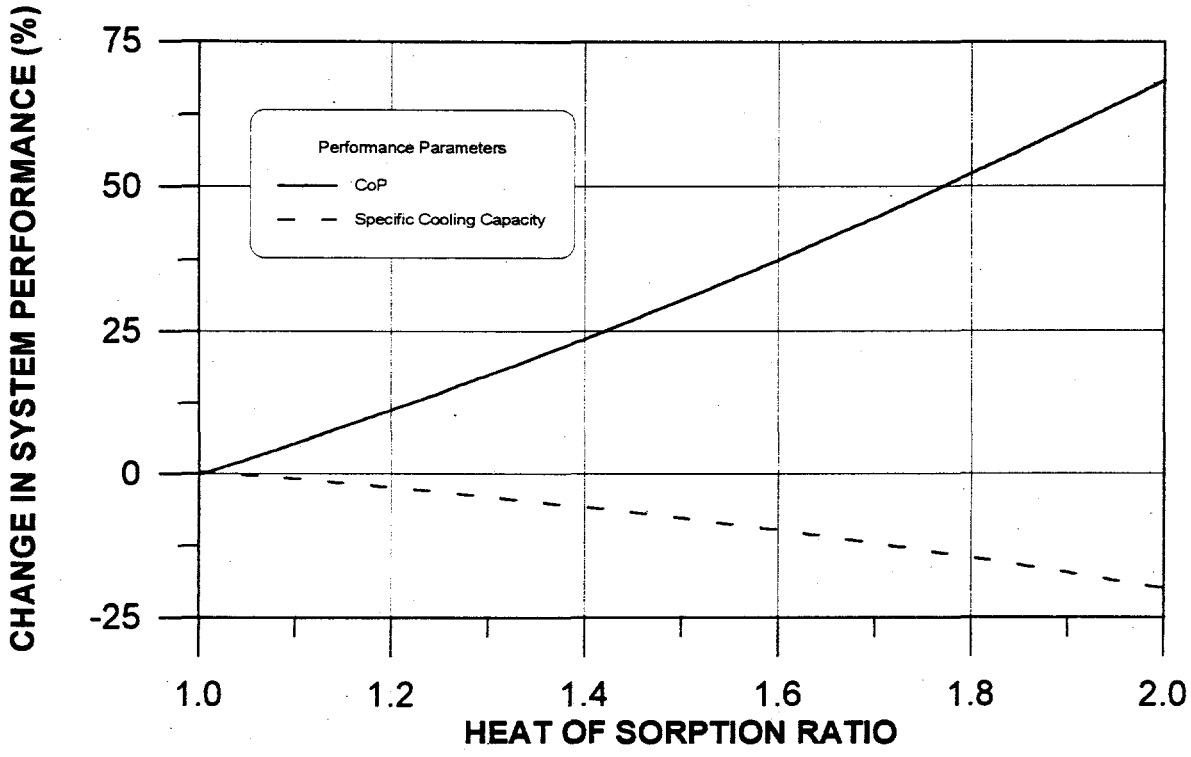

Figure 2-64. Change in system performance as a function of desiccant heat of sorption ratio. Ventilation cycle; 75C regeneration.

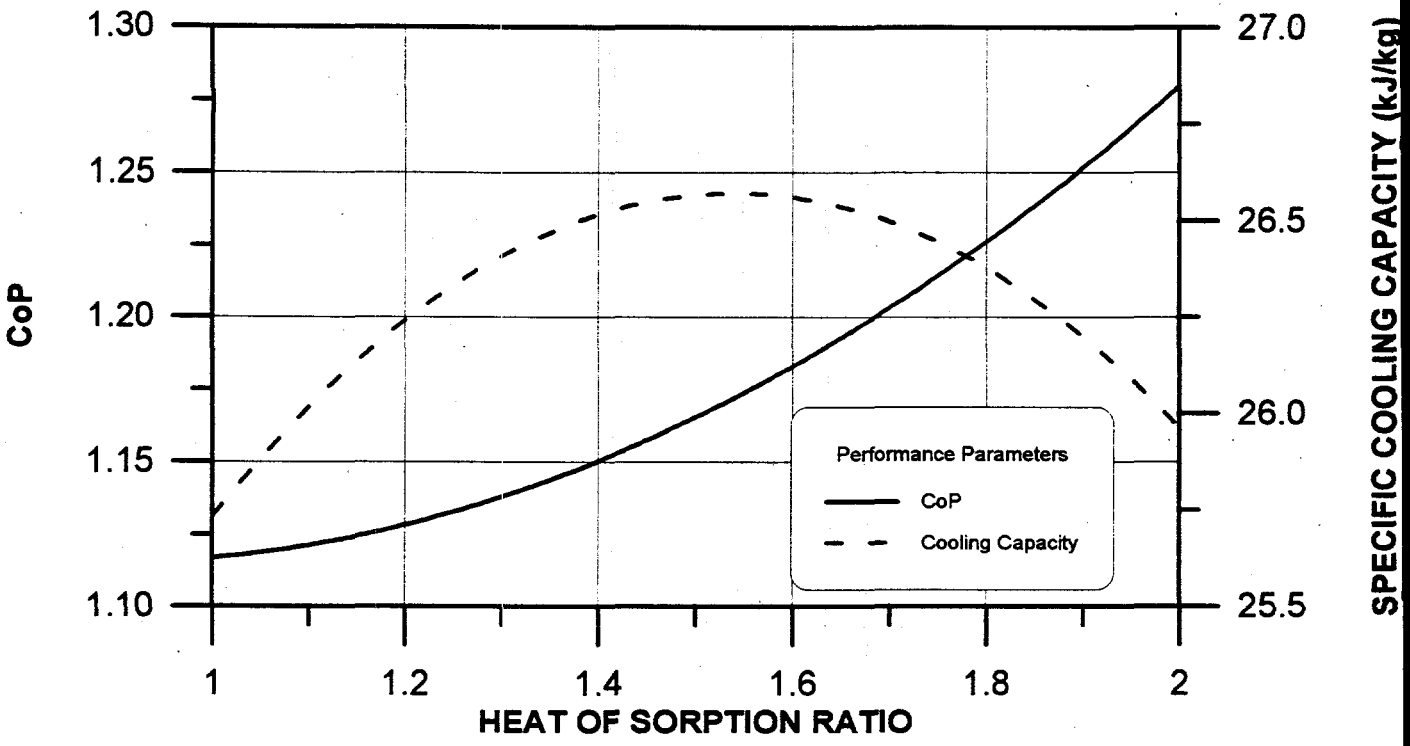

Figure 2-65. Cooling system performance as a function of desiccant heat of sorption ratio. Recirculation cycle; 100C regeneration.

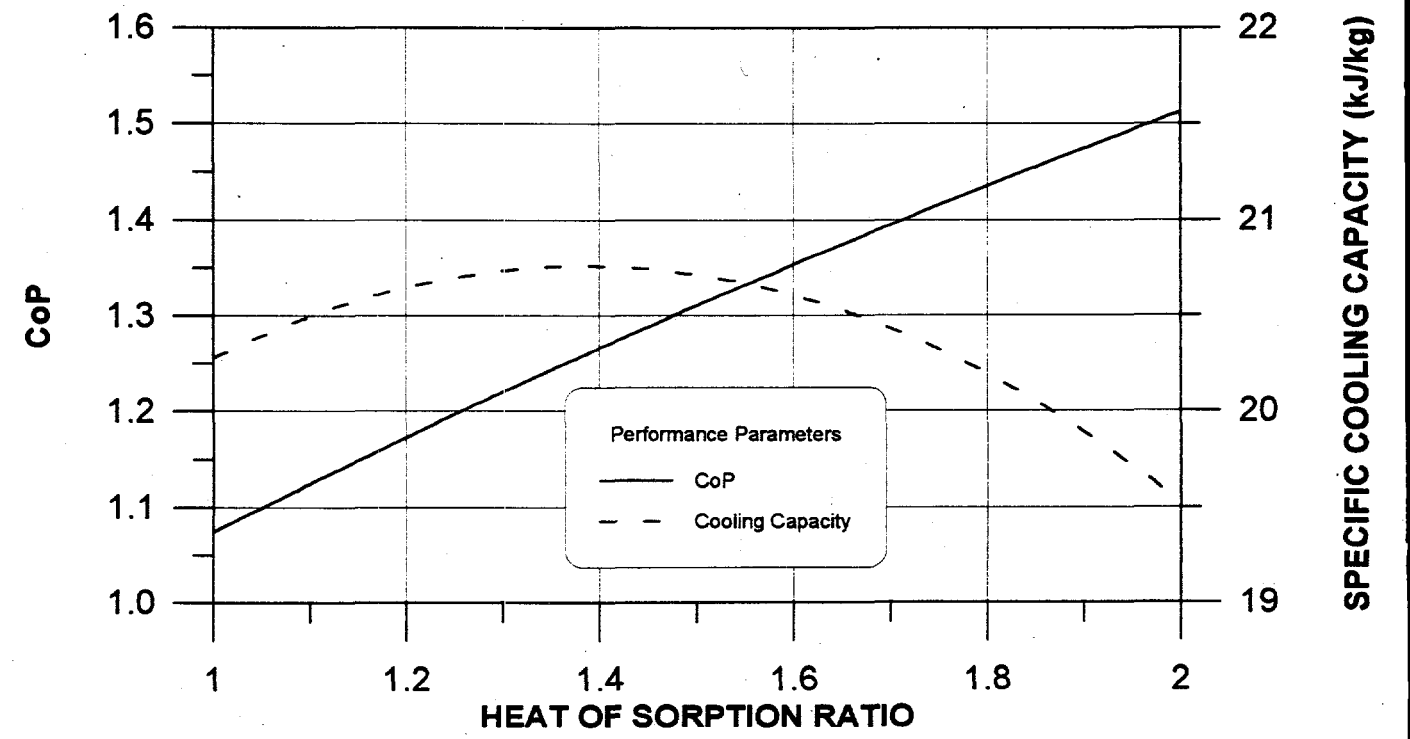

Figure 2-66. Cooling system performance as a function of desiccant heat of sorption ratio. Recirculation cycle; 75C regeneration.

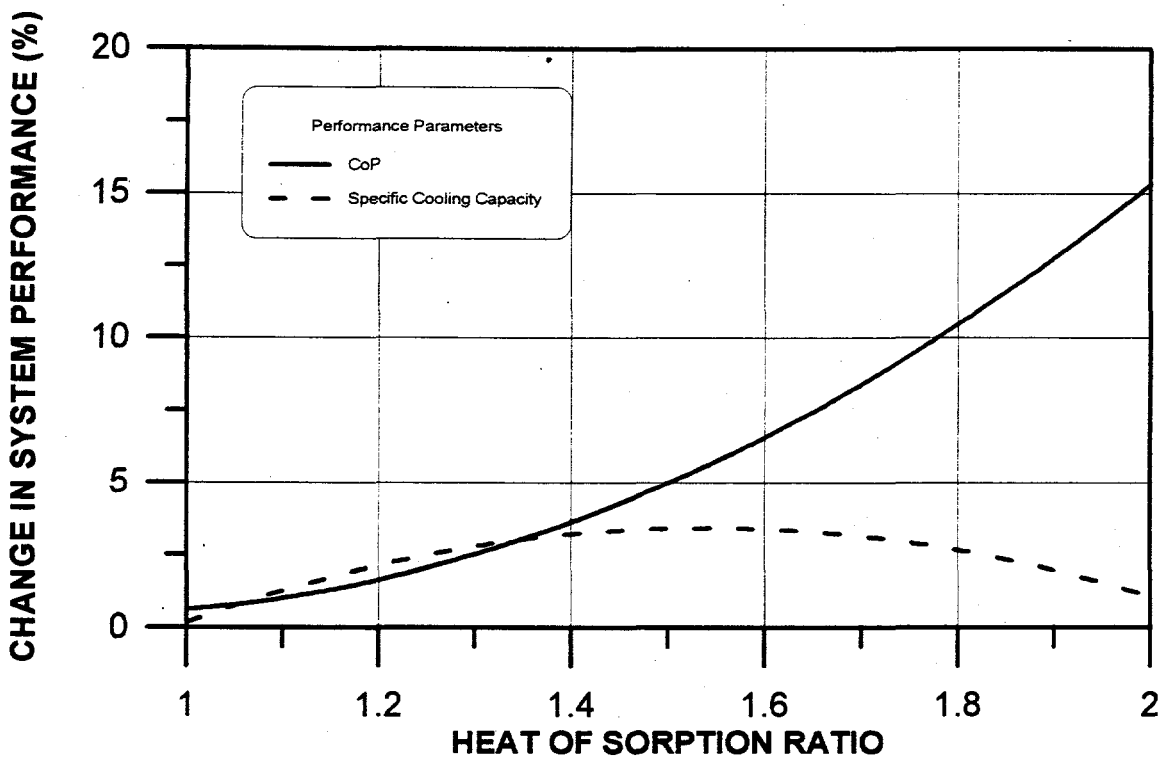

Figure 2-67. Change in system performance as a function of desiccant heat of sorption ratio. Recirculation cycle; 100C regeneration.

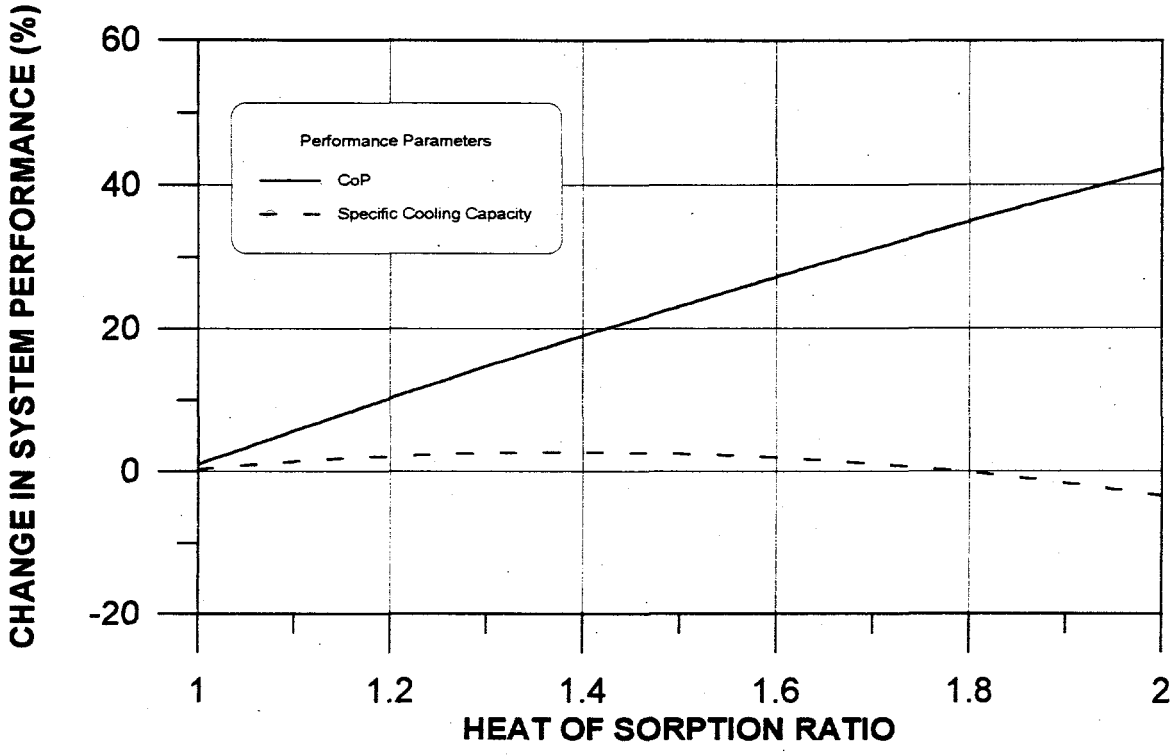

Figure 2-68. Change in system performance as a function of desiccant heat of sorption ratio. Ricirculation cycle; 75C regeneration.

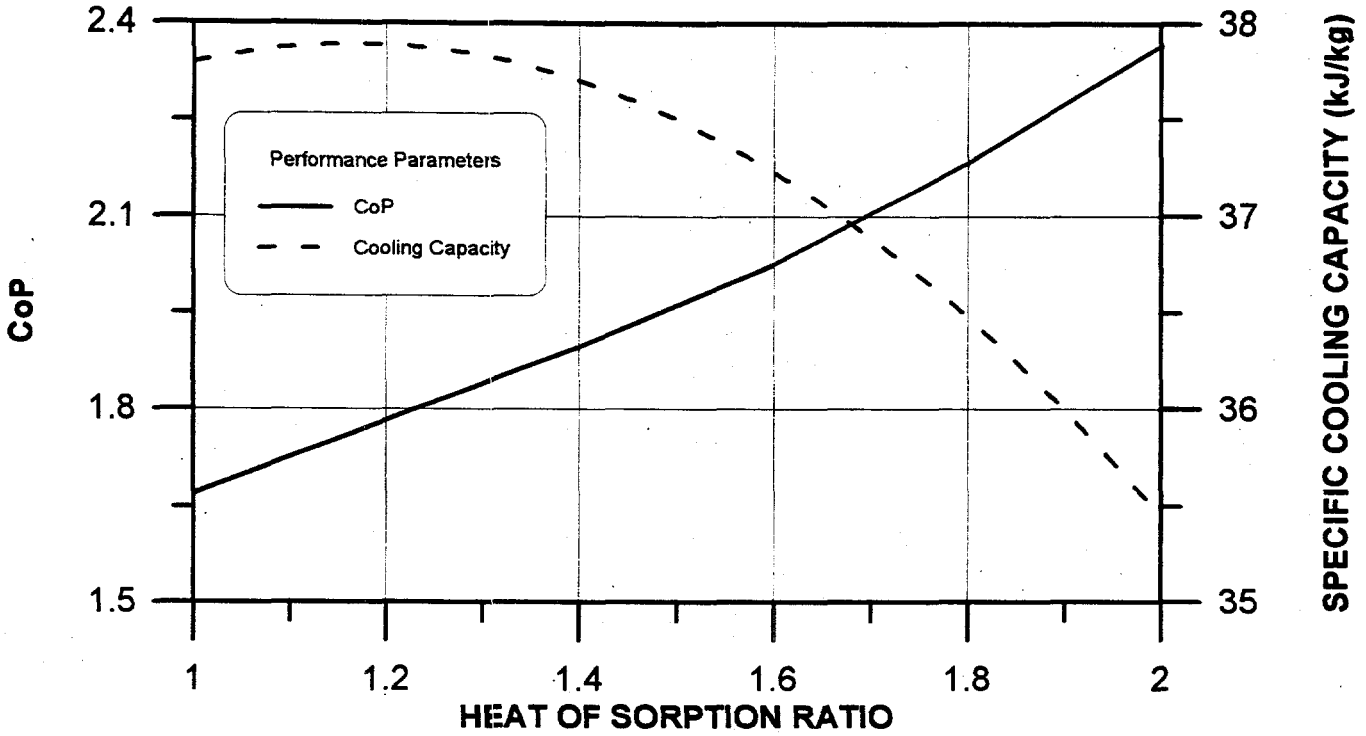

Figure 2-69. Cooling system performance as a function of desiccant heat of sorption ratio. Vent-vent cycle; 100C regeneration.

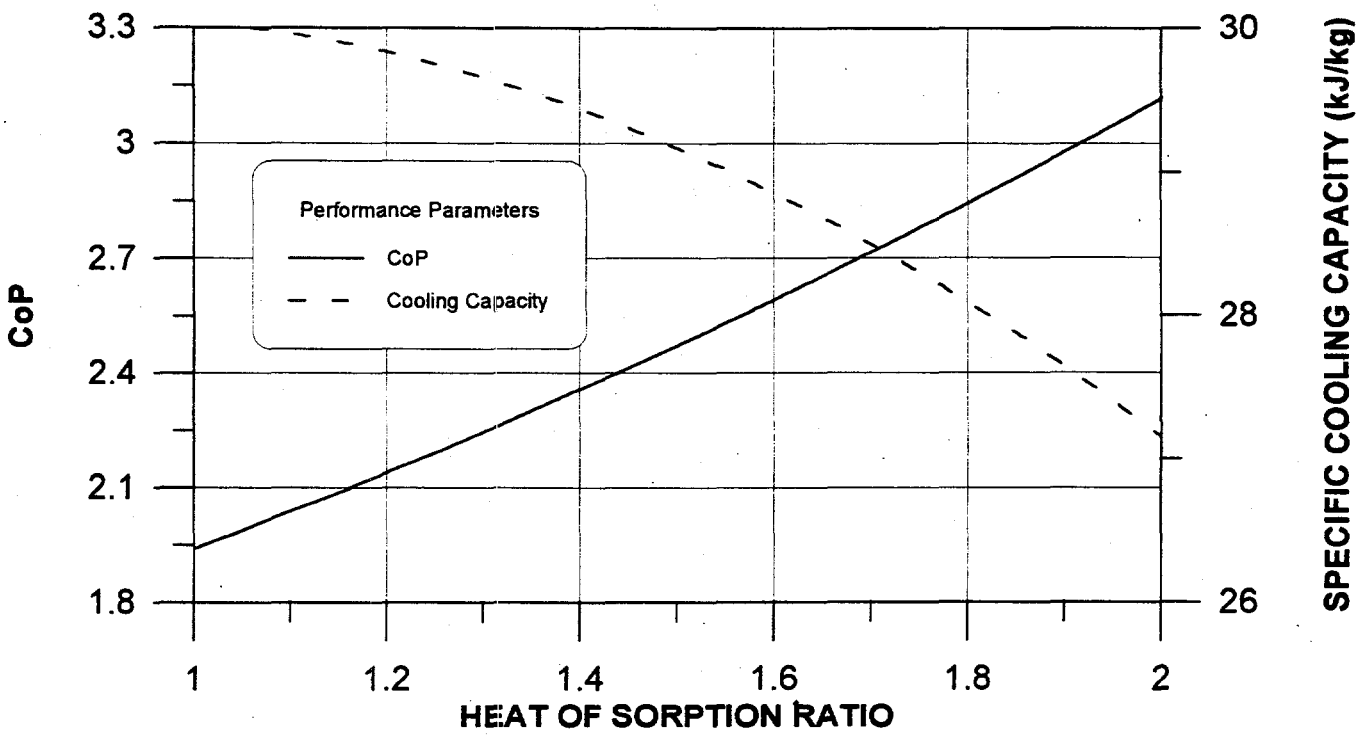

Figure 2-70. Cooling system performance as a function of desiccant heat of sorption ratio. Vent-vent cycle; 75C regeneration.

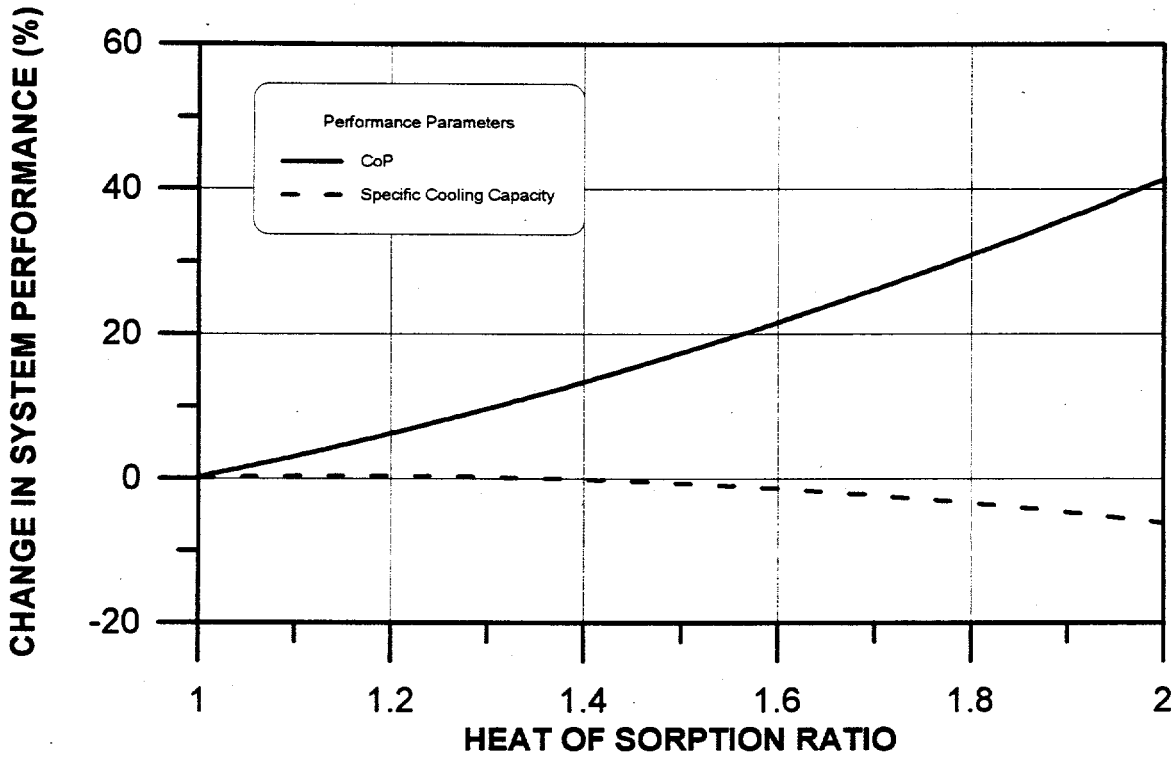

Figure 2-71. Change in system performance as a function of desiccant heat of sorption ratio. Vent-vent cycle; 100C regeneration.

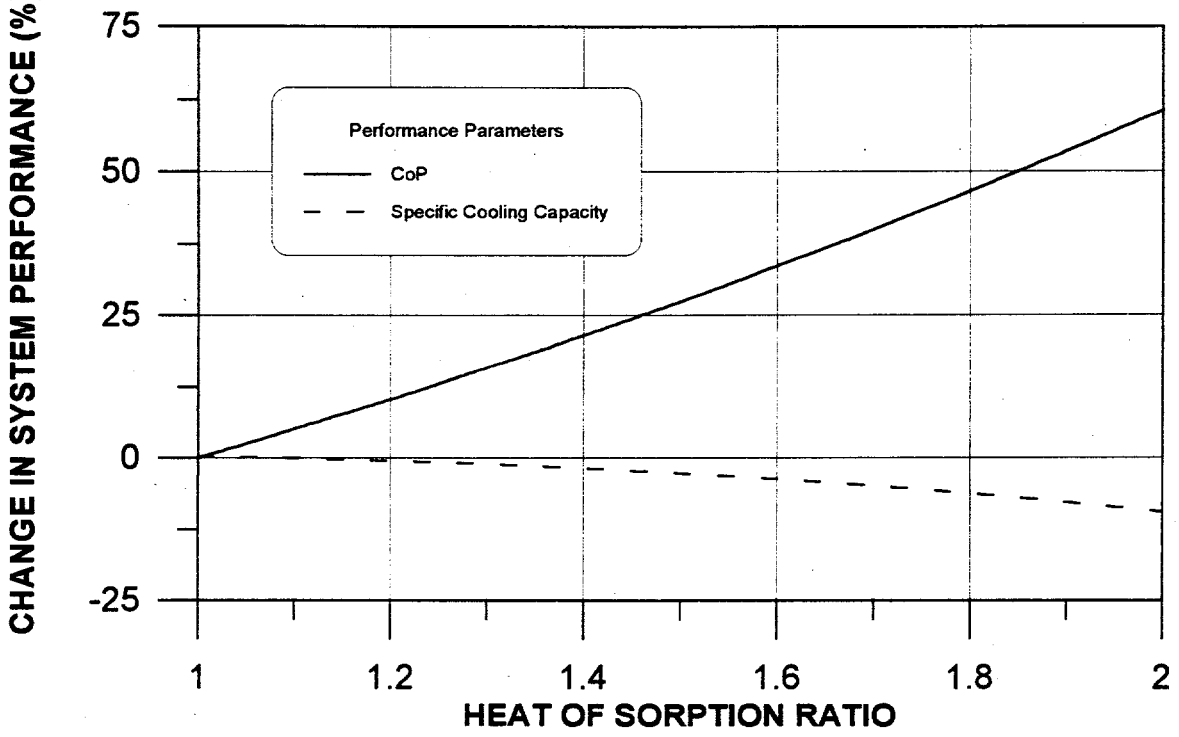

Figure 2-72. Change in system performance as a function of desiccant heat of sorption ratio. Vent-vent cycle; 75C regeneration.

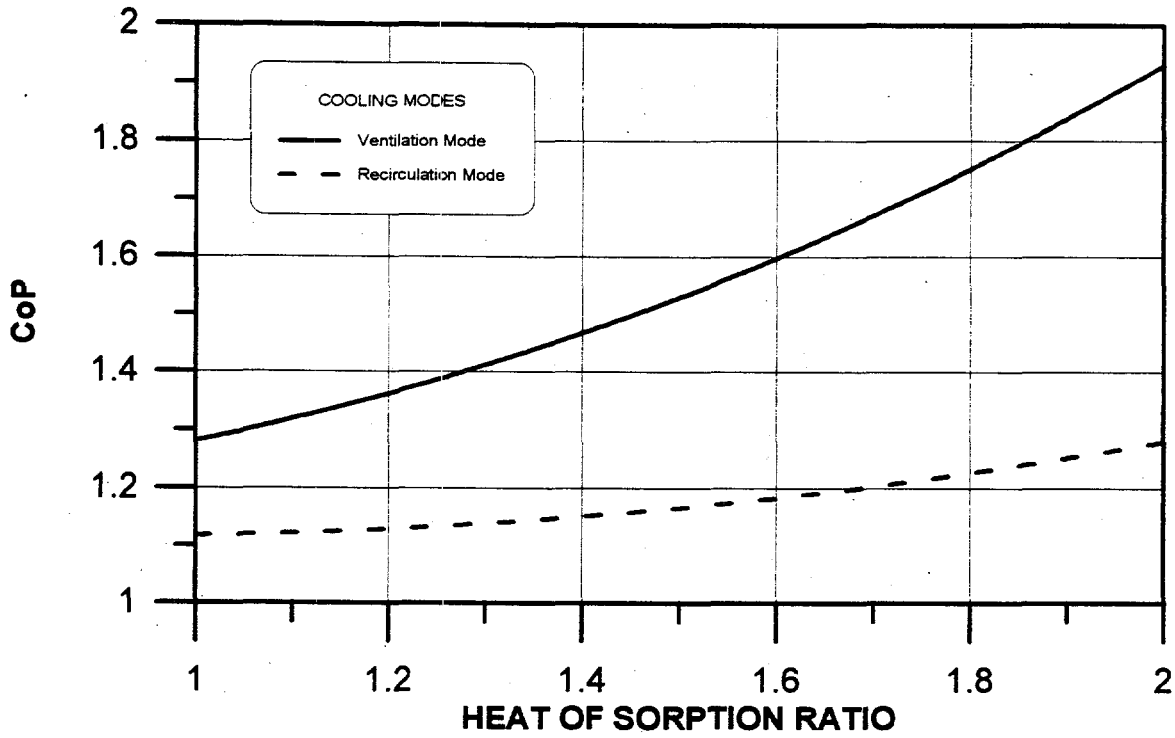

Figure 2-73. CoP comparisons for two cooling modes as a function of desiccant heat of sorption ratio; 100C regeneration.

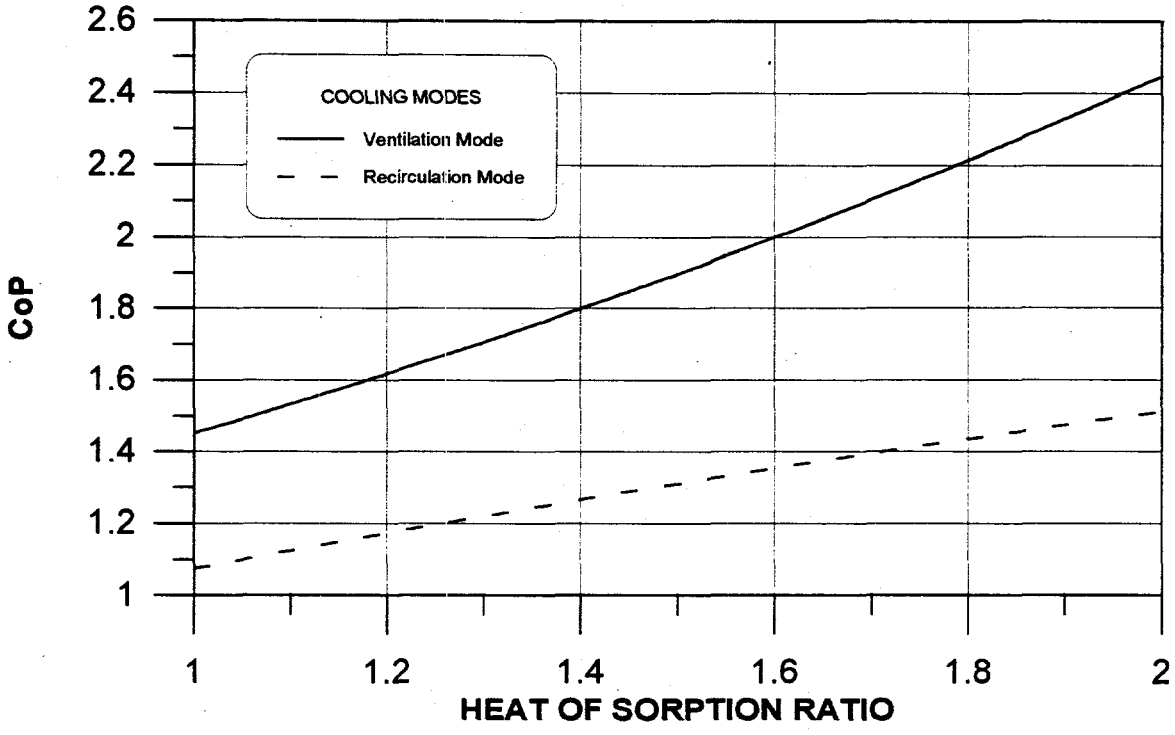

Figure 2-74. CoP comparisons for two cooling modes as a function of desiccant heat of sorption ratio; 75C regeneration.

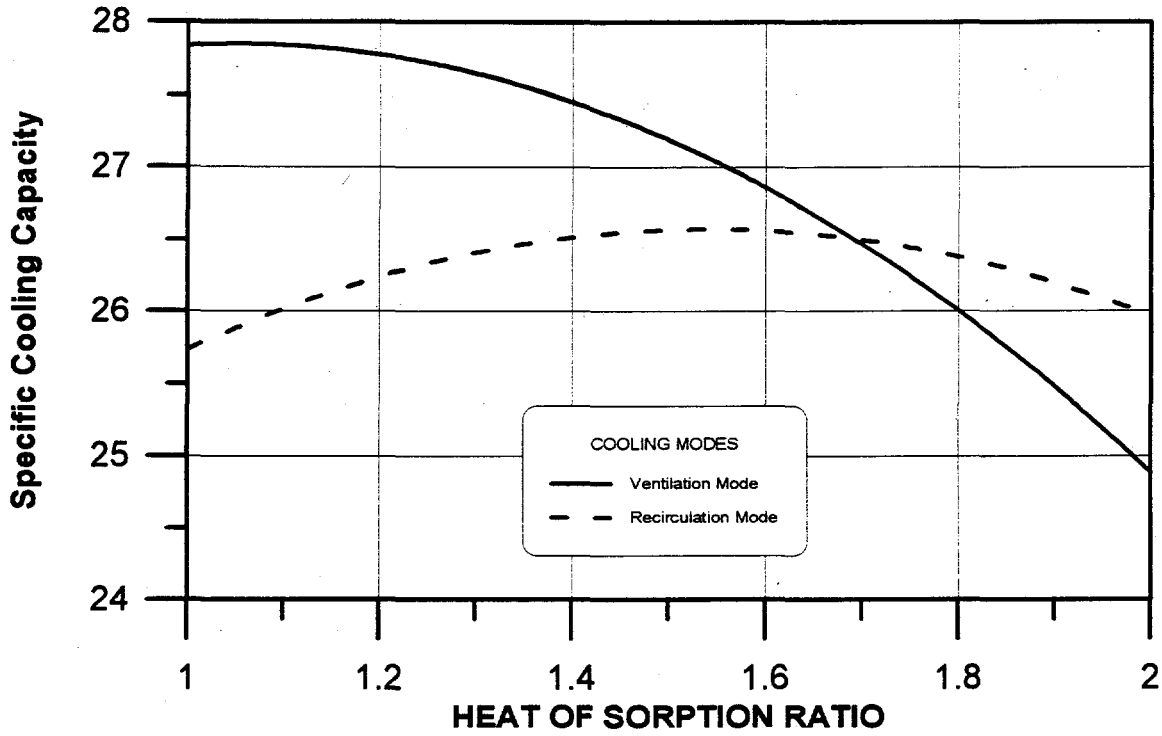

Figure 2-75. Specific Cooling Capacity comparisons for two cooling modes as a function of desiccant heat of sorption ratio; 100C regeneration.

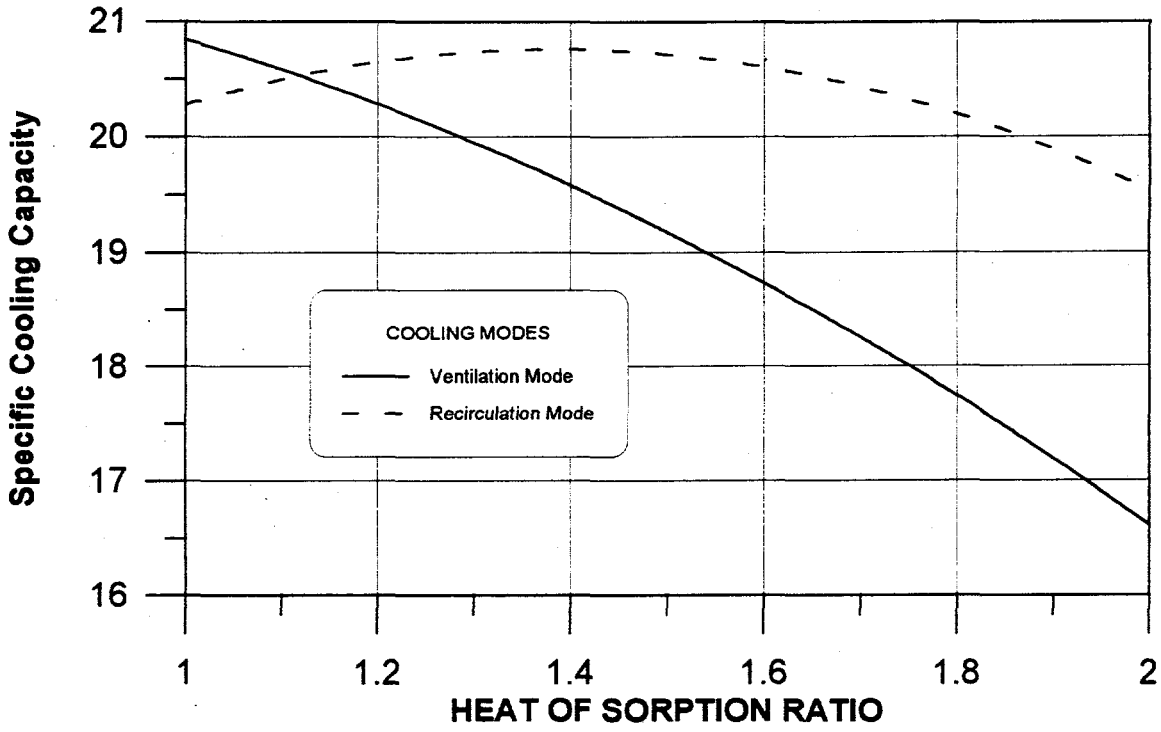

Figure 2-76. Specific cooling capacity comparisons for two cooling modes as a function of desiccant heat of sorption ratio; 75C regeneration.

Appendix C

TABLE 3-2: Modified Ventilation Cycle Seasonal Simulation Results for Variable Heat Exchanger Effectiveness. Regeneration Temperature Constant (T_{reg} = 70°C), ε_{EC} = 1, $\varepsilon_{DW,RH}$ = 1, h_{in}/h_{out} = 1, Atlanta GA.

HX effectiveness	SEASONAL CoP	Average SHR	Average System SCC (kJ/kgda)
1	1.94	.53	25.4
.95	1.71	.54	24.1
.9	1.52	.54	22.8
.85	1.35	.55	21.6
.8	1.21	.56	20.3

TABLE 3-3: Modified Ventilation Cycle Seasonal Simulation Results for Variable Heat Exchanger Effectiveness. Regeneration Temperature Varied ($T_{reg,max}$ = 70°C), ε_{EC} = 1, $\varepsilon_{DW,RH}$ = 1, h_{in}/h_{out} = 1, Atlanta GA.

HX effectiveness	SEASONAL CoP	Average SHR	Average System SCC (kJ/kgda)
1	2.47	.7	11.9
.95	2.11	.71	11.6
.9	1.83	.71	11.3
.85	1.57	.71	11.0
.8	1.37	.72	10.7

TABLE 3-4: Modified Ventilation Cycle Seasonal Simulation Results for Variable Heat Exchanger Effectiveness. Regeneration Temperature Constant (T_{reg} = 70°C), ε_{EC} = 1, $\varepsilon_{DW,RH}$ = 1, h_{in}/h_{out} = 1, Central Park NY.

HX effectiveness	SEASONAL CoP	Average SHR	Average System SCC (kJ/kgda)
1	1.9	.62	22.8
.95	1.66	.63	21.6
.9	1.48	.63	20.5
.85	1.32	.64	19.4
.8	1.18	.66	18.2

TABLE 3-5: Modified Ventilation Cycle Seasonal Simulation Results for Variable Heat Exchanger Effectiveness. Regeneration Temperature Varied ($T_{reg,max}$ = 70°C), ε_{EC} = 1, $\varepsilon_{DW,RH}$ = 1, h_{in}/h_{out} = 1, Central Park NY.

HX effectiveness	SEASONAL CoP	Average SHR	Average System SCC (kJ/kgda)
1	2.56	.76	12.5
.95	2.12	.77	11.9
.9	1.84	.78	11.4
.85	1.63	.78	10.9
.8	1.38	.79	10.4

TABLE 3-6: Modified Ventilation Cycle Seasonal Simulation Results for Variable Heat Exchanger Effectiveness. Regeneration Temperature Constant (T_{reg} = 70°C), ε_{EC} = 1, $\varepsilon_{DW,RH}$ = 1, h_{in}/h_{out} = 1, Chicago IL.

HX effectiveness	SEASONAL CoP	Average SHR	Average System SCC (kJ/kgda)
1	1.92	.65	23.4
.95	1.71	.65	22.3
.9	1.52	.66	21.1
.85	1.36	.68	19.9
.8	1.21	.69	18.7

TABLE 3-7: Modified Ventilation Cycle Seasonal Simulation Results for Variable Heat Exchanger Effectiveness. Regeneration Temperature Varied ($T_{reg,max}$ = 70°C), ε_{EC} = 1, $\varepsilon_{DW,RH}$ = 1, h_{in}/h_{out} = 1, Chicago IL.

HX effectiveness	SEASONAL CoP	Average SHR	Average System SCC (kJ/kgda)
1	2.71	.8	12.8
.95	2.28	.81	12.3
.9	1.97	.82	11.8
.85	1.61	.83	11.3
.8	1.42	.86	10.8

TABLE 3-8: Modified Ventilation Cycle Seasonal Simulation Results for Variable Heat Exchanger Effectiveness. Regeneration Temperature Constant (T_{reg} = 70°C), ε_{EC} = 1, $\varepsilon_{DW,RH}$ = 1, h_{in}/h_{out} = 1, Houston TX.

HX effectiveness	SEASONAL CoP	Average SHR	Average System SCC (kJ/kgda)
1	2.06	.52	26.9
.95	1.82	.52	25.5
.9	1.61	.53	24.2
.85	1.43	.54	22.8
.8	1.27	.55	21.5

TABLE 3-9: Modified Ventilation Cycle Seasonal Simulation Results for Variable Heat Exchanger Effectiveness. Regeneration Temperature Varied ($T_{reg,max}$ = 70°C), ε_{EC} = 1, $\varepsilon_{DW,RH}$ = 1, h_{in}/h_{out} = 1, Houston TX.

HX effectiveness	SEASONAL CoP	Average SHR	Average System SCC (kJ/kgda)
1	2.43	.64	15.8
.95	2.08	.64	15.7
.9	1.79	.64	15.5
.85	1.54	.64	15.4
.8	1.35	.64	15.1

TABLE 3-10: Modified Ventilation Cycle Seasonal Simulation Results for Variable Heat Exchanger Effectiveness. Regeneration Temperature Constant (T_{reg} = 70°C), ε_{EC} = 1, $\varepsilon_{DW,RH}$ = 1, h_{in}/h_{out} = 1, Phoenix AZ.

HX effectiveness	SEASONAL CoP	Average SHR	Average System SCC (kJ/kgda)
1	1.94	.88	23.9
.95	1.73	.89	22.7
.9	1.55	.90	21.5
.85	1.38	.92	20.3
.8	1.23	.93	19.1

TABLE 3-11: Modified Ventilation Cycle Seasonal Simulation Results for Variable Heat

Exchanger Effectiveness. Regeneration Temperature Varied ($T_{reg,max}$ = 70°C), ε_{EC} = 1, $\varepsilon_{DW,RH}$ = 1, h_{in}/h_{out} = 1, Phoenix AZ.

HX effectiveness	SEASONAL CoP	Average SHR	Average System SCC (kJ/kgda)
1	6.08	.98	15.0
.95	4.66	.98	14.4
.9	3.52	.98	13.7
.85	2.94	.98	13.0
.8	2.20	.98	12.4

TABLE 3-12: Modified Ventilation Cycle Seasonal Simulation Results for Variable Desiccant Wheel Enthalpy Ratio. Regeneration Temperature Constant (T_{reg} = 70°C), ε_{EC} = 1, $\varepsilon_{DW,RH}$ = 1, $_{HX}$ = 1, Atlanta GA.

Desiccant Wheel $(h_{in}/h_{out})_{process}$	SEASONAL COP	Average SHR	Average System SCC (kJ/kgda)
1	1.92	.53	25.4
.95	1.87	.53	23.8
.9	1.84	.55	22.0

TABLE 3-13: Modified Ventilation Cycle Seasonal Simulation Results for Variable Desiccant Wheel Enthalpy Ratio. Regeneration Temperature Varied ($T_{reg,max}$ = 70°C), ε_{EC} = 1, $\varepsilon_{DW,RH}$ = 1, $_{HX}$ = 1, Atlanta GA.

Desiccant Wheel $(h_{in}/h_{out})_{process}$	SEASONAL COP	Average SHR	Average System SCC (kJ/kgda)
1	2.50	.7	11.9
.95	2.38	.7	11.3
.9	2.16	.72	10.5

TABLE 3-14: Modified Ventilation Cycle Seasonal Simulation Results for Variable Desiccant Wheel Enthalpy Ratio. Regeneration Temperature Constant (T_{reg} = 70°C), ε_{EC} = 1, $\varepsilon_{DW,RH}$ = 1, $_{HX}$ = 1, Central Park NY.

Desiccant Wheel $(h_{in}/h_{out})_{process}$	SEASONAL COP	Average SHR	Average System SCC (kJ/kgda)
1	1.85	.62	22.8
.95	1.81	.62	21.8
.9	1.78	.63	20.5

TABLE 3-15: Modified Ventilation Cycle Seasonal Simulation Results for Variable Desiccant Wheel Enthalpy Ratio. Regeneration Temperature Varied ($T_{reg,max}$ = 70°C), ε_{EC} = 1, $\varepsilon_{DW,RH}$ = 1, $_{HX}$ = 1, Central Park NY.

Desiccant Wheel $(h_{in}/h_{out})_{process}$	SEASONAL COP	Average SHR	Average System SCC (kJ/kgda)
1	2.56	.76	12.5
.95	2.44	.78	11.5
.9	2.23	.79	10.3

TABLE 3-16: Modified Ventilation Cycle Seasonal Simulation Results for Variable Desiccant Wheel Enthalpy Ratio. Regeneration Temperature Constant (T_{reg} = 70°C), ε_{EC} = 1, $\varepsilon_{DW,RH}$ = 1, $_{HX}$ = 1, Chicago IL.

Desiccant Wheel $(h_{in}/h_{out})_{process}$	SEASONAL COP	Average SHR	Average System SCC (kJ/kgda)
1	1.92	.65	23.4
.95	1.87	.65	22.3
.9	1.84	.67	20.9

TABLE 3-17: Modified Ventilation Cycle Seasonal Simulation Results for Variable Desiccant Wheel Enthalpy Ratio. Regeneration Temperature Varied ($T_{reg,max}$ = 70°C), ε_{EC} = 1, $\varepsilon_{DW,RH}$ = 1, $_{HX}$ = 1, Chicago IL.

Desiccant Wheel $(h_{in}/h_{out})_{process}$	SEASONAL COP	Average SHR	Average System SCC (kJ/kgda)
1	2.71	.8	12.8
.95	2.53	.82	11.9
.9	2.31	.84	10.8

TABLE 3-18: Modified Ventilation Cycle Seasonal Simulation Results for Variable

Desiccant Wheel Enthalpy Ratio. Regeneration Temperature Constant (T_{reg} = 70°C), ε_{EC} = 1, $\varepsilon_{DW,RH}$ = 1, $_{HX}$ = 1, Houston TX.

Desiccant Wheel $(h_{in}/h_{out})_{process}$	SEASONAL COP	Average SHR	Average System SCC (kJ/kgda)
1	2.06	.52	26.9
.95	2.02	.53	24.8
.9	2.00	.54	22.4

TABLE 3-19: Modified Ventilation Cycle Seasonal Simulation Results for Variable Desiccant Wheel Enthalpy Ratio. Regeneration Temperature Varied ($T_{reg,max}$ = 70°C), ε_{EC} = 1, $\varepsilon_{DW,RH}$ = 1, $_{HX}$ = 1, Houston TX.

Desiccant Wheel $(h_{in}/h_{out})_{process}$	SEASONAL COP	Average SHR	Average System SCC (kJ/kgda)
1	2.43	.64	15.8
.95	2.30	.64	15.6
.9	2.19	.65	15.1

TABLE 3-20: Modified Ventilation Cycle Seasonal Simulation Results for Variable Desiccant Wheel Enthalpy Ratio. Regeneration Temperature Constant (T_{reg} = 70°C), ε_{EC} = 1, $\varepsilon_{DW,RH}$ = 1, $_{HX}$ = 1, Phoenix AZ.

Desiccant Wheel $(h_{in}/h_{out})_{process}$	SEASONAL COP	Average SHR	Average System SCC (kJ/kgda)
1	1.94	.88	23.9
.95	1.85	.89	22.7
.9	1.78	.91	21.2

TABLE 3-21: Modified Ventilation Cycle Seasonal Simulation Results for Variable Desiccant Wheel Enthalpy Ratio. Regeneration Temperature Varied ($T_{reg,max}$ = 70°C), ε_{EC} = 1, $\varepsilon_{DW,RH}$ = 1, $_{HX}$ = 1, Phoenix AZ.

Desiccant Wheel $(h_{in}/h_{out})_{process}$	SEASONAL COP	Average SHR	Average System SCC (kJ/kgda)
1	6.08	.98	15.0
.95	5.27	.98	14.5
.9	4.05	.98	13.9

TABLE 3-22: Seasonal CoP Variation with Variable Component Effectiveness. Regeneration Temperature Varied ($T_{reg,max}$ = 70°C), ε_{EC} = 1, $\varepsilon_{DW,RH}$ = 1, Atlanta GA.

Heat Exchanger Effectiveness Desiccant Wheel Enthalpy Ratio	1	.9	.85
1	2.47	1.83	1.57
.95	2.38	1.56	1.31
.9	2.16	1.32	1.07

TABLE 3-23: Average SCC Variation with Variable Component Effectiveness. Regeneration Temperature Varied ($T_{reg,max}$ = 70°C), ε_{EC} = 1, $\varepsilon_{DW,RH}$ = 1, Atlanta GA.

Heat Exchanger Effectiveness Desiccant Wheel Enthalpy Ratio	1	.9	.85
1	11.9	11.3	11.0
.95	11.3	10.6	10.3
.9	10.5	9.65	9.15

TABLE 3-24: Seasonal CoP Variation with Variable Component Effectiveness. Regeneration Temperature Varied ($T_{reg,max}$ = 70°C), ε_{EC} = 1, $\varepsilon_{DW,RH}$ = 1, Central Park NY.

Heat Exchanger Effectiveness Desiccant Wheel Enthalpy Ratio	1	.9	.85
1	2.56	1.84	1.63
.95	2.44	1.59	1.32
.9	2.23	1.28	1.01

TABLE 3-25: Average SCC Variation with Variable Component Effectiveness.

Regeneration Temperature Varied ($T_{reg,max}$ = 70°C), ε_{EC} = 1, $\varepsilon_{DW,RH}$ = 1, Central Park NY.

Heat Exchanger Effectiveness Desiccant Wheel Enthalpy Ratio	1	.9	.85
1	12.5	11.4	10.9
.95	11.6	10.4	9.8
.9	10.3	9.0	8.3

TABLE 3-26: Seasonal CoP Variation with Variable Component Effectiveness. Regeneration Temperature Varied ($T_{reg,max}$ = 70°C), ε_{EC} = 1, $\varepsilon_{DW,RH}$ = 1, Chicago IL.

Heat Exchanger Effectiveness Desiccant Wheel Enthalpy Ratio	1	.9	.85
1	2.71	1.97	1.61
.95	2.53	1.66	1.37
.9	2.31	1.37	1.11

TABLE 3-27: Average SCC Variation with Variable Component Effectiveness. Regeneration Temperature Varied ($T_{reg,max}$ = 70°C), ε_{EC} = 1, $\varepsilon_{DW,RH}$ = 1, Chicago IL.

Heat Exchanger Effectiveness Desiccant Wheel Enthalpy Ratio	1	.9	.85
1	12.8	11.8	11.3
.95	11.9	10.9	10.3
.9	10.8	9.6	8.9

TABLE 3-28: Seasonal CoP Variation with Variable Component Effectiveness. Regeneration Temperature Varied ($T_{reg,max}$ = 70°C), ε_{EC} = 1, $\varepsilon_{DW,RH}$ = 1, Houston TX.

Heat Exchanger Effectiveness Desiccant Wheel Enthalpy Ratio	1	.9	.85
1	2.43	1.79	1.54
.95	2.30	1.59	1.34
.9	2.19	1.41	1.15

TABLE 3-29: Average SCC Variation with Variable Component Effectiveness. Regeneration Temperature Varied ($T_{reg,max}$ = 70°C), ε_{EC} = 1, $\varepsilon_{DW,RH}$ = 1, Houston TX.

Heat Exchanger Effectiveness Desiccant Wheel Enthalpy Ratio	1	.9	.85
1	15.8	15.5	15.4
.95	15.6	15.2	14.8
.9	15.1	14.2	13.6

TABLE 3-30: Seasonal CoP Variation with Variable Component Effectiveness. Regeneration Temperature Varied ($T_{reg,max}$ = 70°C), ε_{EC} = 1, $\varepsilon_{DW,RH}$ = 1, Phoenix AZ.

Heat Exchanger Effectiveness Desiccant Wheel Enthalpy Ratio	1	.9	.85
1	6.08	3.52	2.94
.95	5.27	2.76	2.26
.9	4.05	1.97	1.42

TABLE 3-31: Average SCC Variation with Variable Component Effectiveness. Regeneration Temperature Varied ($T_{reg,max}$ = 70°C), ε_{EC} = 1, $\varepsilon_{DW,RH}$ = 1, Phoenix AZ.

Heat Exchanger Effectiveness Desiccant Wheel Enthalpy Ratio	1	.9	.85
1	15.0	13.7	13.0
.95	14.5	13.2	12.5
.9	13.9	12.4	11.6

TABLE 3-32: Seasonal CoP Variation with Variable Component Effectiveness. Regeneration Temperature Varied ($T_{reg,max}$ = 70°C), ε_{EC} = 1, $\varepsilon_{DW,RH}$ = .9, Atlanta GA.

Heat Exchanger Effectiveness Desiccant Wheel Enthalpy Ratio	1	.9	.85
1	2.03	1.54	1.36
.95	1.70	1.21	1.04
.9	1.37	.94	.77

TABLE 3-33: Average SCC Variation with Variable Component Effectiveness. Regeneration Temperature Varied ($T_{reg,max}$ = 70°C), ε_{EC} = 1, $\varepsilon_{DW,RH}$ = .9, Atlanta GA.

Heat Exchanger Effectiveness Desiccant Wheel Enthalpy Ratio	1	.9	.85
1	11.3	10.7	10.4
.95	10.7	9.9	9.5
.9	9.6	8.7	8.1

TABLE 3-34: Seasonal CoP Variation with Variable Component Effectiveness. Regeneration Temperature Varied ($T_{reg,max}$ = 70°C), ε_{EC} = 1, $\varepsilon_{DW,RH}$ = .9, Central Park NY.

Heat Exchanger Effectiveness Desiccant Wheel Enthalpy Ratio	1	.9	.85
1	2.16	1.61	1.42
.95	1.76	1.24	1.05
.9	1.39	.90	.75

TABLE 3-35: Average SCC Variation with Variable Component Effectiveness. Regeneration Temperature Varied ($T_{reg,max}$ = 70°C), ε_{EC} = 1, $\varepsilon_{DW,RH}$ = .9, Central Park NY.

Heat Exchanger Effectiveness Desiccant Wheel Enthalpy Ratio	1	.9	.85
1	11.5	10.5	10.0
.95	10.5	9.4	8.9
.9	9.2	7.9	7.2

TABLE 3-36: Seasonal CoP Variation with Variable Component Effectiveness. Regeneration Temperature Varied ($T_{reg,max}$ = 70°C), ε_{EC} = 1, $\varepsilon_{DW,RH}$ = .9, Chicago IL.

Heat Exchanger Effectiveness Desiccant Wheel Enthalpy Ratio	1	.9	.85
1	2.30	1.72	1.47
.95	1.92	1.34	1.14
.9	1.54	1.03	.85

TABLE 3-37: Average SCC Variation with Variable Component Effectiveness. Regeneration Temperature Varied ($T_{reg,max}$ = 70°C), ε_{EC} = 1, $\varepsilon_{DW,RH}$ = .9, Chicago IL.

Heat Exchanger Effectiveness Desiccant Wheel Enthalpy Ratio	1	.9	.85
1	12.0	11.1	10.6
.95	11.2	10.1	9.5
.9	9.8	8.6	7.9

TABLE 3-38: Seasonal CoP Variation with Variable Component Effectiveness. Regeneration Temperature Varied ($T_{reg,max}$ = 70°C), ε_{EC} = 1, $\varepsilon_{DW,RH}$ = .9, Houston TX.

Heat Exchanger Effectiveness Desiccant Wheel Enthalpy Ratio	1	.9	.85
1	1.88	1.46	1.29
.95	1.61	1.21	1.05
.9	1.37	.98	.83

TABLE 3-39: Average SCC Variation with Variable Component Effectiveness. Regeneration Temperature Varied ($T_{reg,max}$ = 70°C), ε_{EC} = 1, $\varepsilon_{DW,RH}$ = .9, Houston TX.

Heat Exchanger Effectiveness Desiccant Wheel Enthalpy Ratio	1	.9	.85
1	15.5	15.0	14.7
.95	15.0	14.0	13.4
.9	13.6	12.0	11.1

TABLE 3-40: Seasonal CoP Variation with Variable Component Effectiveness. Regeneration Temperature Varied ($T_{reg,max}$ = 70°C), ε_{EC} = 1, $\varepsilon_{DW,RH}$ = .9, Phoenix AZ.

Heat Exchanger Effectiveness Desiccant Wheel Enthalpy Ratio	1	.9	.85
1	5.55	3.38	2.74
.95	4.44	2.48	2.05
.9	2.88	1.67	1.22

TABLE 3-41: Average SCC Variation with Variable Component Effectiveness. Regeneration Temperature Varied ($T_{reg,max}$ = 70°C), ε_{EC} = 1, $\varepsilon_{DW,RH}$ = .9, Phoenix AZ.

Heat Exchanger Effectiveness Desiccant Wheel Enthalpy Ratio	1	.9	.85
1	14.9	13.5	12.9
.95	14.4	13.0	12.3
.9	13.7	12.2	11.4

Appendix D

Table 4-4. Modified Ventilation Cycle Seasonal Performance: Variable Regeneration Temperature

Process Flow Rate = 15000 cfm
Regeneration Temperature = 70°C

Location	Cooling Hours	Total Cooling (kBTU)	Face Vel. (fpm)	Total Reg. Energy (kBTU)	εHX	εEC	εRH,proc	εRH,reg	hin/hout	Fan kW	seasonal CoP	SHR	SCC	seasonal EER (BTU/W-hr)
Atlanta GA	925	226225	300	191904	0.91	0.905	0.76	1.10	0.96	3.87	1.18	0.72	8.86	63.2
	925	225711	500	195781	0.89	0.835	0.76	1.07	0.97	6.93	1.15	0.69	8.79	35.2
	925	221954	800	211823	0.87	0.76	0.74	0.93	0.98	13.02	1.05	0.65	8.53	18.4
Central Park NY	400	64037	300	78275	0.91	0.905	0.76	1.10	0.96	3.87	1.22	0.81	8.23	41.4
	400	65935	500	78285	0.89	0.835	0.76	1.07	0.97	6.93	1.19	0.79	8.10	23.8
	400	77285	800	71899	0.87	0.76	0.74	0.93	0.98	13.02	1.08	0.76	7.77	14.8
Chicago IL	470	113180	300	84491	0.91	0.905	0.76	1.10	0.96	3.87	1.34	0.85	9.00	62.2
	470	112676	500	86914	0.89	0.835	0.76	1.07	0.97	6.93	1.3	0.83	8.8	34.6
	470	110557	800	95281	0.87	0.76	0.74	0.93	0.98	13.02	1.16	0.80	8.44	18.1
Houston TX	1280	437875	300	376175	0.91	0.905	0.76	1.10	0.96	3.87	1.16	0.66	11.82	88.4
	1280	436807	500	385597	0.89	0.835	0.76	1.07	0.97	6.93	1.13	0.63	11.74	49.2
	1280	422681	800	407247	0.87	0.76	0.74	0.93	0.98	13.02	1.04	0.60	11.32	25.4
Phoenix AZ	563	143554	300	57769	0.91	0.905	0.76	1.10	0.96	3.87	2.49	0.98	12.10	65.9
	563	143267	500	65755	0.89	0.835	0.76	1.07	0.97	6.93	2.18	0.98	11.27	36.7
	563	142593	800	83033	0.87	0.76	0.74	0.93	0.98	13.02	1.72	0.97	10.45	19.5

Table 4-5. Modified Ventilation Cycle Seasonal Performance: Constant Regeneration Temperature

Process Flow Rate = 15000 cfm
Regeneration Temperature = 70°C

Location	Cooling Hours	Total Cooling (kBTU)	Face Vel. (fpm)	Total Reg. Energy (kBTU)	εHX	εEC	εRH,proc	εRH,reg	hin/hout	Fan kW	seasonal CoP	SHR	SCC	seasonal EER (BTU/W-hr)
Atlanta GA	607	225520	300	210956	0.91	0.905	0.76	1.10	0.96	3.87	1.07	.57	12.9	96.0
	609	225466	500	215245	0.89	0.835	0.76	1.07	0.97	6.93	1.05	.54	12.9	53.4
	625	221536	800	228573	0.87	0.76	0.74	0.93	0.98	13.02	.97	.50	12.3	27.2
Central Park NY	212	78113	300	74145	0.91	0.905	0.76	1.10	0.96	3.87	1.05	.59	12.8	95.2
	213	78196	500	75757	0.89	0.835	0.76	1.07	0.97	6.93	1.03	.56	12.7	53.0
	220	77201	800	80705	0.87	0.76	0.74	0.93	0.98	13.02	.96	.52	12.2	27.0
Chicago IL	284	112925	300	97463	0.91	0.905	0.76	1.10	0.96	3.87	1.16	.68	13.8	102.7
	287	112570	500	100151	0.89	0.835	0.76	1.07	0.97	6.93	1.12	.65	13.6	56.6
	295	110453	800	107059	0.87	0.76	0.74	0.93	0.98	13.02	1.03	.62	13.0	28.8
Houston TX	1139	434954	300	388101	0.91	0.905	0.76	1.10	0.96	3.87	1.21	.59	13.3	98.7
	1140	434436	500	396562	0.89	0.835	0.76	1.07	0.97	6.93	1.10	.56	13.2	55.0
	1150	420498	800	416121	0.87	0.76	0.74	0.93	0.98	13.02	1.01	.52	12.7	28.1
Phoenix AZ	307	143580	300	101350	0.91	0.905	0.76	1.10	0.96	3.87	1.42	.92	16.2	120.8
	317	143461	500	106653	0.89	0.835	0.76	1.07	0.97	6.93	1.35	.90	15.7	65.3
	335	142755	800	118051	0.87	0.76	0.74	0.93	0.98	13.02	1.21	.89	14.8	32.7

Table 4-6: Primary Energy Consumption and Thermal CoP for both operational modes

	Variable Regeneration Temperature				Constant Regeneration Temperature			
	Face Velocity (fpm)	Plant Primary Energy kBTU	Total Primary Energy (kBTU)	Primary Energy CoP	Face Velocity (fpm)	Plant Primary Energy kBTU	Total Primary Energy (kBTU)	Primary Energy CoP
Atlanta GA	300	43647	235551	0.96	300	28642	239598	0.94
	500	78159	273940	0.82	500	51458	266703	0.85
	800	146845	358668	0.62	800	99219	327792	0.68
Central Park NY	300	18875	97150	0.66	300	10004	84149	0.93
	500	33799	112084	0.59	500	17998	93755	0.83
	800	63500	135399	0.57	800	34925	115630	0.67
Chicago IL	300	22178	106668	1.06	300	13401	110864	1.02
	500	39713	126627	0.89	500	24251	124402	0.90
	800	74613	169894	0.65	800	46832	153891	0.72
Houston TX	300	60399	436574	1.00	300	53745	441846	0.98
	500	108156	493753	0.88	500	96326	492888	0.88
	800	203201	610448	0.69	800	182564	598685	0.70
Phoeniz AZ	300	26566	84335	1.70	300	14486	115836	1.24
	500	47572	113327	1.26	500	26785	133438	1.08
	800	89377	172410	0.83	800	53182	171233	0.83

Table 4-7. Modified Ventilation Cycle Seasonal Performance: Constant Regeneration Temperature; Advanced Desiccant Material.

Process Flow Rate = 15000 cfm
Regeneration Temperature = 70°C

Location	Cooling Hours	Total Cooling (kBTU)	Face Velocity (fpm)	Total Reg. Energy (kBTU)	εHX	εEC	εRH,proc	εRH,reg	hin/hout	Fan kW	Seasonal CoP	SHR	SCC (kJ/kg)	Seasonal EER (BTU/W-hr)
Atlanta GA	522	240200	300	203751	0.91	0.905	0.86	1.10	0.96	3.87	1.18	.52	16.0	118.9
	526	239821	500	210117	0.89	0.835	0.86	1.07	0.97	6.93	1.14	.49	15.8	65.8
	547	237064	800	228721	0.87	0.76	0.84	0.93	0.98	13.02	1.04	.46	15.1	33.3
Central Park NY	180	82039	300	70927	0.91	0.905	0.86	1.10	0.96	3.87	1.16	.54	15.8	117.8
	181	82022	500	73177	0.89	0.835	0.86	1.07	0.97	6.93	1.12	.51	15.7	65.4
	190	81465	800	79895	0.87	0.76	0.84	0.93	0.98	13.02	1.02	.47	14.9	32.9
Chicago IL	248	118645	300	95470	0.91	0.905	0.86	1.10	0.96	3.87	1.24	.62	16.6	123.6
	252	118497	500	99157	0.89	0.835	0.86	1.07	0.97	6.93	1.20	.59	16.3	67.9
	263	117355	800	108685	0.87	0.76	0.84	0.93	0.98	13.02	1.08	.56	15.5	34.3
Houston TX	1072	503203	300	406886	0.91	0.905	0.86	1.10	0.96	3.87	1.24	.54	16.3	121.3
	1075	501415	500	419497	0.89	0.835	0.86	1.07	0.97	6.93	1.20	.50	16.2	67.3
	1096	486860	800	450272	0.87	0.76	0.84	0.93	0.98	13.02	1.08	.47	15.4	34.1
Phoenix AZ	274	143931	300	101294	0.91	0.905	0.86	1.10	0.96	3.87	1.42	.88	18.2	135.7
	284	143931	500	107176	0.89	0.835	0.86	1.07	0.97	6.93	1.34	.86	17.6	73.1
	301	143887	800	120457	0.87	0.76	0.84	0.93	0.98	13.02	1.20	.85	16.6	36.7

Table 4-8. Primary Energy Consumption and CoP for Advanced Desiccant Material.

	Constant Regeneration Temperature			
	Face Velocity (fpm)	Plant Primary Energy kBTU	Total Primary Energy (kBTU)	Primary Energy CoP
Atlanta GA	300	24632	228383	1.05
	500	44439	254556	0.94
	800	86801	315522	0.75
Central Park NY	300	8491	79418	1.03
	500	15292	88469	0.93
	800	30191	110086	0.74
Chicago IL	300	11704	107174	1.11
	500	21279	120436	0.98
	800	41717	150402	0.78
Houston TX	300	50581	457467	1.10
	500	90842	510339	0.98
	800	174083	624355	0.78
Phoenix AZ	300	12932	114226	1.26
	500	24007	131183	1.10
	800	47804	168261	0.86

Table 4-9. Modified Ventilation Cycle Seasonal Performance: Constant Regeneration Temperature; Advanced Control Strategy

Process Flow Rate = 15000 cfm
Regeneration Temperature = 70°C

Location	Cooling Hours	Total Cooling (kBTU)	Face Velocity (fpm)	Total Reg. Energy (kBTU)	εHX	εEC	εRH,proc	εRH,reg	hin/hout	Fan kW	Seasonal CoP	SHR	SCC (kJ/kg)	Seasonal EER (BTU/W-hr)
Atlanta GA	662	225439	300	199051	0.91	0.905	0.76	1.10	0.96	3.87	1.13	.62	11.8	88.0
	662	225278	500	204356	0.89	0.835	0.76	1.07	0.97	6.93	1.10	.59	11.8	49.1
	673	221444	800	219478	0.87	0.76	0.74	0.93	0.98	13.02	1.01	.55	11.4	25.3
Central Park NY	250	78077	300	67216	0.91	0.905	0.76	1.10	0.96	3.87	1.16	.69	10.8	80.7
	252	78088	500	69403	0.89	0.835	0.76	1.07	0.97	6.93	1.13	.66	10.8	44.7
	254	77147	800	75443	0.87	0.76	0.74	0.93	0.98	13.02	1.02	.62	10.5	23.3
Chicago IL	328	112757	300	86344	0.91	0.905	0.76	1.10	0.96	3.87	1.31	.75	11.9	88.8
	328	112503	500	91063	0.89	0.835	0.76	1.07	0.97	6.93	1.24	.72	11.9	49.5
	338	110328	800	98229	0.87	0.76	0.74	0.93	0.98	13.02	1.12	.69	11.3	25.1
Houston TX	1170	434880	300	380036	0.91	0.905	0.76	1.10	0.96	3.87	1.14	.61	12.9	96.0
	1171	434329	500	389666	0.89	0.835	0.76	1.07	0.97	6.93	1.12	.57	12.9	53.5
	1180	420271	800	409867	0.87	0.76	0.74	0.93	0.98	13.02	1.03	.54	12.3	27.4
Phoenix AZ	386	142994	300	51208	0.91	0.905	0.76	1.10	0.96	3.87	2.79	.94	12.9	95.7
	399	142626	500	61774	0.89	0.835	0.76	1.07	0.97	6.93	2.31	.93	12.4	51.6
	412	141713	800	77123	0.87	0.76	0.74	0.93	0.98	13.02	1.84	.92	11.9	26.4

Table 4-10: Primary Energy Consumption and CoP for Advanced Control Strategy

	Constant Regeneration Temperature			
	Face Velocity (fpm)	Plant Primary Energy kBTU	Total Primary Energy (kBTU)	Primary Energy CoP
Atlanta GA	300	31236	230287	0.98
	500	55943	260299	0.87
	800	106721	326199	0.68
Central Park NY	300	11797	79013	0.99
	500	21300	90703	0.86
	800	40371	115814	0.67
Chicago IL	300	15482	101826	1.11
	500	27712	118775	0.95
	800	53594	151823	0.73
Houston TX	300	55234	435270	1.00
	500	98985	488651	0.89
	800	187018	596885	0.70
Phoenix AZ	300	18218	69426	2.06
	500	33702	95476	1.49
	800	65450	142573	0.99

Table 4-11. Modified Ventilation Cycle Seasonal Performance: Constant Regeneration temperature; Advanced Control Strategy, Advanced Desiccant Material

Process Flow Rate = 15000 cfm
Regeneration Temperature = 70°C

Location	Cooling Hours	Total Cooling (kBTU)	Face Velocity (fpm)	Total Reg. Energy (kBTU)	εHX	εEC	εRH,proc	εRH,reg	hin/hout	Fan kW	Seasonal CoP	SHR	SCC (kJ/kg)	Seasonal EER (BTU/W-hr)
Atlanta GA	582	240105	300	192264	0.91	0.905	0.86	1.10	0.96	3.87	1.25	.58	14.3	106.6
	584	239628	500	199528	0.89	0.835	0.86	1.07	0.97	6.93	1.20	.55	14.2	59.2
	599	236970	800	219769	0.87	0.76	0.84	0.93	0.98	13.02	1.08	.51	13.7	30.4
Central Park NY	221	81992	300	64305	0.91	0.905	0.86	1.10	0.96	3.87	1.28	.66	12.9	95.9
	223	81907	500	67064	0.89	0.835	0.86	1.07	0.97	6.93	1.22	.63	12.8	53.0
	226	81397	800	74750	0.87	0.76	0.84	0.93	0.98	13.02	1.09	.59	12.5	27.7
Chicago IL	297	118465	300	84663	0.91	0.905	0.86	1.10	0.96	3.87	1.40	.71	13.9	103.1
	297	118420	500	90279	0.89	0.835	0.86	1.07	0.97	6.93	1.31	.68	13.8	57.5
	309	117235	800	99957	0.87	0.76	0.84	0.93	0.98	13.02	1.17	.65	13.2	29.1
Houston TX	1107	503110	300	399025	0.91	0.905	0.86	1.10	0.96	3.87	1.26	.56	15.8	117.4
	1109	501311	500	412745	0.89	0.835	0.86	1.07	0.97	6.93	1.22	.52	15.7	65.2
	1127	486602	800	444053	0.87	0.76	0.84	0.93	0.98	13.02	1.10	.49	15.0	33.2
Phoenix AZ	367	143347	300	49880	0.91	0.905	0.86	1.10	0.96	3.87	2.87	.92	13.6	100.9
	377	143102	500	61006	0.89	0.835	0.86	1.07	0.97	6.93	2.35	.91	13.2	54.8
	388	142845	800	77942	0.87	0.76	0.84	0.93	0.98	13.02	1.83	.89	12.8	28.3

Table 4-12: Primary Energy Consumption and CoP for Advanced Control Strategy and Advanced Desiccant Material

	Constant Regeneration Temperature			
	Face Velocity (fpm)	Plant Primary Energy kBTU	Total Primary Energy (kBTU)	Primary Energy CoP
Atlanta GA	300	27463	219727	1.09
	500	49354	248882	0.96
	800	95044	314813	0.75
Central Park NY	300	10425	74730	1.10
	500	18843	85907	0.95
	800	35829	110579	0.74
Chicago IL	300	14010	98673	1.20
	500	25111	115390	1.03
	800	49121	149078	0.79
Houston TX	300	52252	451277	1.11
	500	93749	506494	0.99
	800	178707	622760	0.78
Phoenix AZ	300	17322	67202	2.13
	500	31840	92846	1.54
	800	61544	139486	1.02

Table 4-13. Modified Ventilation Cycle Seasonal Performance: Constant Regeneration Temperature; Enthalpy Exchange of Ventilation Air.

Process Flow Rate = 15000 cfm
Regeneration Temperature = 70°C

Location	Cooling Hours	Total Cooling (kBTU)	Face Velocity (fpm)	Total Reg. Energy (kBTU)	εHX	εEC	εRH,proc	εRH,reg	hin/hout	Fan kW	Seasonal CoP	SHR	SCC	Seasonal EER (BTU/W-hr)
Atlanta GA	925	228229	300	N/A	N/A	N/A	N/A	N/A	N/A	N/A	N/A	0.14	8.64	246.7
	925	212840	500	N/A	N/A	N/A	N/A	N/A	N/A	N/A	N/A	0.14	8.06	76.7
	925	196844	800	N/A	N/A	N/A	N/A	N/A	N/A	N/A	N/A	0.14	7.46	42.6
Central Park NY	400	75806	300	N/A	N/A	N/A	N/A	N/A	N/A	N/A	N/A	0.11	6.64	189.5
	400	70695	500	N/A	N/A	N/A	N/A	N/A	N/A	N/A	N/A	0.11	6.19	58.9
	400	65382	800	N/A	N/A	N/A	N/A	N/A	N/A	N/A	N/A	0.11	5.73	32.7
Chicago IL	470	109908	300	N/A	N/A	N/A	N/A	N/A	N/A	N/A	N/A	0.27	8.20	233.8
	470	102497	500	N/A	N/A	N/A	N/A	N/A	N/A	N/A	N/A	0.27	7.64	72.7
	470	94794	800	N/A	N/A	N/A	N/A	N/A	N/A	N/A	N/A	0.27	7.07	40.3
Houston TX	1280	516511	300	N/A	N/A	N/A	N/A	N/A	N/A	N/A	N/A	0.18	14.14	403.5
	1280	481686	500	N/A	N/A	N/A	N/A	N/A	N/A	N/A	N/A	0.18	13.19	125.4
	1280	445486	800	N/A	N/A	N/A	N/A	N/A	N/A	N/A	N/A	0.18	12.20	69.6
Phoenix AZ	563	130226	300	N/A	N/A	N/A	N/A	N/A	N/A	N/A	N/A	1.0	8.11	231.3
	563	121446	500	N/A	N/A	N/A	N/A	N/A	N/A	N/A	N/A	1.0	7.56	71.9
	563	112319	800	N/A	N/A	N/A	N/A	N/A	N/A	N/A	N/A	1.0	6.99	39.9

Table 4-14. Full Ventilation Cycle Seasonal Performance: Constant Regeneration Temperature

Process Flow Rate = 15000 cfm
Regeneration Temperature = 70°C

Location	Cooling Hours	Total Cooling (kBTU)	Face Velocity (fpm)	Total Reg. Energy (kBTU)	εHX	εEC	εRH,proc	εRH,reg	hin/hout	Fan kW	Seasonal CoP	SHR	SCC (kJ/kg)	Seasonal EER (BTU/W-hr)
Atlanta GA	530	245375	300	181735	0.91	0.905	0.76	1.10	0.96	3.87	1.35	.54	16.1	119.6
	537	244872	500	187861	0.89	0.835	0.76	1.07	0.97	6.93	1.30	.51	15.8	65.8
	560	242532	800	202783	0.87	0.76	0.74	0.93	0.98	13.02	1.20	.49	15.0	33.3
Central Park NY	188	82404	300	65346	0.91	0.905	0.76	1.10	0.96	3.87	1.26	.56	15.2	113.3
	191	82299	500	67372	0.89	0.835	0.76	1.07	0.97	6.93	1.22	.54	15.0	62.2
	199	81609	800	72569	0.87	0.76	0.74	0.93	0.98	13.02	1.13	.51	14.2	31.5
Chicago IL	247	119741	300	83893	0.91	0.905	0.76	1.10	0.96	3.87	1.43	.63	16.8	125.3
	251	119613	500	86967	0.89	0.835	0.76	1.07	0.97	6.93	1.38	.61	16.5	68.8
	262	118871	800	94208	0.87	0.76	0.74	0.93	0.98	13.02	1.26	.59	15.8	34.8
Houston TX	1072	523574	300	359897	0.91	0.905	0.76	1.10	0.96	3.87	1.46	.54	17.0	126.2
	1079	521265	500	370805	0.89	0.835	0.76	1.07	0.97	6.93	1.41	.52	16.8	69.7
	1101	508290	800	393647	0.87	0.76	0.74	0.93	0.98	13.02	1.29	.50	16.0	35.5
Phoenix AZ	241	143931	300	77984	0.91	0.905	0.76	1.10	0.96	3.87	1.85	.85	20.7	154.3
	246	143931	500	81845	0.89	0.835	0.76	1.07	0.97	6.93	1.76	.84	20.3	84.4
	257	143931	800	89975	0.87	0.76	0.74	0.93	0.98	13.02	1.60	.83	19.4	43.0

Table 4-15: Primary Energy Consumption and CoP for Enthalpy Exchange of Ventilation Air.

	Constant Regeneration Temperature			
	Face Velocity (fpm)	Plant Primary Energy kBTU	Total Primary Energy (kBTU)	Primary Energy CoP
Atlanta GA	300	11280	11280	20.2
	500	33835	33835	6.3
	800	56340	56340	3.5
Central Park NY	300	4878	4878	15.5
	500	14635	14635	4.8
	800	24379	24379	2.7
Chicago IL	300	5732	5732	19.2
	500	17190	17190	6.0
	800	28680	28680	3.3
Houston TX	300	15608	15608	33.1
	500	46835	46835	10.3
	800	78042	78042	5.7
Phoenix AZ	300	6865	6865	19.0
	500	20595	20595	5.9
	800	34323	34323	3.3

Table 4-16: Primary Energy Consumption and CoP for Full Ventilation Cycle.

	Constant Regeneration Temperature			
	Face Velocity (fpm)	Plant Primary Energy kBTU	Total Primary Energy (kBTU)	Primary Energy CoP
Atlanta GA	300	25015	206750	1.19
	500	45375	233236	1.05
	800	124325	327108	0.74
Central Park NY	300	8868	74214	1.11
	500	16133	83505	0.99
	800	31589	104158	0.78
Chicago IL	300	11652	95545	1.25
	500	21198	108165	1.11
	800	41649	135857	0.87
Houston TX	300	50585	410482	1.28
	500	91187	461992	1.13
	800	174578	568225	0.89
Phoenix AZ	300	11373	89357	1.61
	500	20793	102638	1.40
	800	40812	130787	1.10

Table 4-17. Ventilation Air Requirements For Commercial Buildings by Principal Building Activity

Building Use	Total Number (thousands)	Typical Space	Total Floorspace (million ft²)	Minimum Outside Air For Ventilation						Total Outside Air For Ventilation		
				62-1981			62-1989			62-1981	62-1989	Increase
				cfm / person	x persons /1000 ft²	=cfm /ft²	cfm / person	x persons /1000 ft²	=cfm /ft²	(million cfm)		
Assembly	278	Auditorium	4,556	20	100	2.00	15	150	2.25	9,112	10,251	1,139
Education	301	Classroom	8,470	10	50	0.50	15	50	0.75	4,235	6,353	2,118
Food Sales	130	Supermarket	757	5	20	0.10	8	15	0.12	76	91	15
Food Service	260	Restaurant	1,491	10	100	1.00	20	100	2.00	1,491	2,982	1,491
Health Care	63	Nursing Areas	1,763	15	10	0.15	25	10	0.25	264	441	176
Mercantile and Services	1,272	Retail Floors	12,402	5	10	0.05	20	10	0.20	620	2,480	1,860
Office	749	Office Space	12,319	5	10	0.05	20	10	0.20	616	2,464	1,848
Public Order & Safety	60	Office Space	820	5	10	0.05	20	10	0.20	41	164	123
Religious Worship	366	Chapel	3,747	20	100	2.00	15	150	2.25	7,494	8,431	937
Total	**3,479**		**46,325**							**23,949**	**33,656**	**9,707**

References:

Energy Information Administration, 1994. "Commercial Buildings Characteristics 1992", Office of Energy Markets and End Use, U.S. Department of Energy, Washington, D.C., Report DOE-EIA-0246-92

ASHRAE, 1989. ASHRAE Standard 62-1989, Ventilation for Acceptable Indoor Air Quality, American Society of Heating Refrigerating and Air Conditioning Engineers, Inc. Atlanta, Georgia.

ASHRAE 1981. ASHRAE Standard 62-1981, Ventilation for Acceptable Indoor Air Quality, American Society of Heating Refrigerating and Air Conditioning Engineers, Inc. Atlanta, Georgia.

Note: The building categories lodging, warehouse and storage, and other were not included in this study due to the insignificant impact of the revised ventilation standard on these buildings.